SD 67-621-4

FINAL REPORT

TECHNOLOGICAL REQUIREMENTS COMMON TO MANNED PLANETARY MISSIONS

(Contract NAS2-3918)

APPENDIX C

Subsystem Synthesis and Parametric Analysis

SPACE DIVISION
NORTH AMERICAN ROCKWELL CORPORATION

ERRATA

Technological Requirements Common to Manned Planetary Missions

Final Report - Appendix C, SD67-621-4

1. Page 4 - first paragraph: Second-to-last sentence should read as follows:

"At 297 K (75F) the sensible load for 166 watts (13,600 BTU/man-day) becomes 77 watts (6300 BTU/man-day) and a latent heat load of 89 watts (7300 BTU/man-day).

SD 67-621-4

TECHNOLOGICAL REQUIREMENTS COMMON TO MANNED PLANETARY MISSIONS NAS2-3918

Appendix C - Subsystem Synthesis and Parametric Analysis

January 1968

Prepared by

R. D. Meston
Project Engineer

Approved by

A. Codik
Project Manager

SPACE DIVISION
NORTH AMERICAN ROCKWELL CORPORATION

FOREWORD

This report contains the final results of the studies conducted under Contract NAS2-3918, Technological Requirements Common to Manned Planetary Missions. This report consists of five volumes. The first volume (SD 67-621-1) summarizes the study results. The detailed descriptions of the study are presented in the following volumes:

Appendix A -	Mission Requirements	(SD 67-621-2)
Appendix B -	Environments	(SD 67-621-3)
Appendix C -	Subsystem Synthesis and Parametric Analysis	(SD 67-621-4)
Appendix D -	System Synthesis and Parametric Analysis	(SD 67-621-5)

CONTENTS

ILLUSTRATIONS

Figure

Page

TABLES

INTRODUCTION

The environmental control and life support subsystem, communications subsystem, electrical power subsystem, and propulsion subsystem analyses which were conducted during the study are reported in this volume. Candidate environmental control and life support subsystems are defined in terms of weight, volume, and electrical power requirements for all manned modules. This includes the Earth reentry module, mission module, and both ascent and descent stages of the planetary excursion module. Several types of communications techniques are compared parametrically, and the range of power requirements is established. Propulsion subsystem weight scaling equations are developed and the characteristics of candidate propellants established. All promising power generation (including nuclear reactor, radioisotope, and solar) and conversion system combinations are compared. Weights, volumes, and areas are provided along with qualitative analyses of the integration factors.

LIFE SUPPORT SUBSYSTEM PARAMETRIC ANALYSIS

Scaling equations were established for weight synthesis and for testing the sensitivity of the spacecraft modules to the type of environmental control and life support subsystem (EC/LSS) used in their design. Equations for weight, volume, and power requirements were developed for Earth reentry modules (ERM), planetary excursion modules (PEM) ascent and descent stages, and for mission modules (MM). These equations are valid for crew sizes from 2 to 16 for the PEM's and for crew sizes from 4 through 20 for MM's and ERM's. These equations are suitable for mission durations up to 24 hours for ERM's and PEM ascent stages, up to 90 days for PEM descent stages, and up to 1500 days for MM's.

The equations represent three degrees of closure: open; water recovery only; and water and oxygen recovery. The production of food was investigated but rejected for reasons explained below. Separate equations were established for the various elements of the environmental control and life support system as follows: crew and crew support; furniture and housekeeping; food management; water supply or recovery; waste management temperature and humidity control; atmospheric purification; atmospheric supply or recovery; and instruments and controls. The detailed elements that comprise each of these major categories are defined later. The

equations discussed in this report, in general, were developed earlier for other programs; therefore, only changes and the rationale for these changes are discussed in this report. The basic equations for the ERM's and PEM ascent stages and the open system and the water and oxygen recovery system for the MM's and PEM descent stages were generated by NASA, Mission Analysis Division, and were either modified by mutual agreement or corroborated by parametric data used by NR for other studies. The long-duration (over 90 days) open system and the water recovery only system were generated during this study.

REQUIREMENTS

This section discusses the requirements, ground rules, and assumptions upon which the equations are based. They are presented so that the equations may be applied correctly.

Operational Duration

It was assumed that the ERM's and the PEM ascent stages will be occupied for no more than 24 hours, and will therefore use open-type life support subsystems. The PEM descent stages, which include the living quarters while on the planetary surface, are assumed to be occupied by a crew of up to 16 men for durations up to 90 days. Mission module occupancy times vary from approximately 300 days to 1500 days.

Man's Daily Balance

Two factors significantly effect the input and output quantities for man's daily balance: metabolic load and wash water. Metabolic rates in the ranges discussed in this report are assumed to effect only the perspired water since studies have shown that the food and oxygen intake quantities vary only slightly with changes in the metabolic rate. Table 1 shows man's daily balance which reflects the ground rules for metabolic rate and wash water discussed in the following paragraphs. The more fully closed ecological systems also use the same metabolic rate and wash water requirements established for the open system for mission durations greater than 90 days.

Metabolic Rate

Two levels of metabolic rate were established; 136 watts (11,200 Btu/man-day) for missions of less than 90 days where crew members are relatively restrained in their motions, and 166 watts (13,600 Btu/man-day) for missions longer than 90 days where larger free volume permits higher crew activities. In recent studies, such as the Mars/Venus Flyby (Reference 1), a metabolic load of 166 watts (13,600 Btu/man-day) was used. This may be

Table 1. Life Support Daily Balance

Man's Daily Balance	Open System				Water and Oxygen Recovery		Water Recovery Only	
	< 90 Days		> 90 Days					
	Pounds	Kilogram	Pounds	Kilogram	Pounds	Kilogram	Pounds	Kilogram
Input:								
Food	1.40	0.64	1.40	0.64	1.40	0.64	1.40	0.64
Oxygen	2.00	0.91	2.00	0.91	2.00	0.91	2.00	0.91
Water:								
Drinking	4.00	1.82	7.70	3.50	7.70	3.50	7.70	3.50
Reconstituting Food	2.00	0.91	2.00	0.91	2.00	0.91	2.00	0.91
Washing	3.00	1.36	10.00	4.54	10.00	4.54	10.00	4.54
Total	12.40	5.64	23.10	10.50	23.10	10.50	23.10	10.50
Output:								
Feces	0.30	0.14	0.30	0.14	0.30	0.14	0.30	0.14
Urine	3.25	1.48	3.25	1.48	3.25	1.48	3.25	1.48
Carbon Dioxide	2.25	1.02	2.25	1.02	2.25	1.02	2.25	1.02
Water:								
Exhaled and	2.00	0.91	2.00	0.91	2.00	0.91	2.00	0.91
Perspired	1.60	0.73	5.30	2.41	5.30	2.41	5.30	2.41
Washing	3.00	1.36	10.00	4.54	10.00	4.54	10.00	4.54
Total	12.40	5.63	23.10	10.50	23.10	10.50	23.10	10.50
Recovery System Daily Balance								
Input:	Not Applicable		Not Applicable					
Carbon Dioxide					2.25	1.02		
Water: Urine					3.25	1.48	3.25	1.48
Exhaled and perspired					7.30	3.32	7.30	3.32
Wash					10.00	4.54	10.00	4.54
Total					22.80	10.36	20.55	9.34
Output:								
Oxygen:								
Carbon Dioxide					1.64	0.74		
Water					0.36	0.16		
Water:								
Urine					2.92	1.33	2.92	1.33
Exhaled and perspired					6.94	3.16	7.22	3.28
Wash					9.80	4.45	9.93	4.51
Wastes:								
Urine					0.33	0.15	0.33	0.15
Exhaled and perspired water					0.08	0.04	0.08	0.04
Wash water					0.07	0.03	0.07	0.03
Hydrogen					0.05	0.02		
Carbon					0.61	0.28		
Total					22.80	10.36	20.55	9.34

representative of the activity in the MM where a free volume of 750 cubic feet per man was established as the nominal value for this study. This metabolic rate allows for the exercise and equipment maintenance required for long-duration missions. It is representative of an activity level of slightly above sitting effort or light factory bench work and slightly lower than light work or standing, whereas the 136 watts (11,200 Btu/man-day) is typical of that experienced in Gemini flights and expected in Apollo flights. At 297 K (75 F) the sensible load for 166 watts (13,600 Btu/man-day) becomes 73.2 watts (600 Btu/man-day) and a latent heat load of 88 watts (720 Btu/man-day). This increased latent load would increase man's drinking water input over that required for the Gemini and Apollo type missions by about 50 percent.

Wash Water

Wash water quantity is generally an arbitrary value and almost any value can be selected, depending on usage requirements such as personal hygiene, type and amount of clothing and associated laundry requirements (if any) and general psychological well being of the crew. For mission durations up to 90 days, the wash water requirement has been established as 1.36 kilograms/man-day (3 lbs/man-day) and for missions over 90 days 4.53 kilograms/man-day (10 lbs/man-day) was selected as being more representative of the long duration missions.

Emergency Supply Requirements

The requirement for an emergency supply of oxygen and water was assumed. This requirement was satisfied for oxygen by providing a separate oxygen supply for 30 days. This includes tankage, piping, and controls. This supply can be used while the main system is being serviced or repaired, or during other similar emergencies. As for water, an emergency supply of water (metabolic only) for 10 days was provided. This water can also be used during short periods when the recovery system is not in operation or to account for a reduction in recovery efficiency. The reserve water supply is normally an arbitrary value selected on the basis of the degree of protection that is desired. Ten days was selected as representative of typical planetary missions. This could provide for deactivation of the water recovery system during the high crew activity period at planet encounter, reducing somewhat the high peak demand from the electrical power system.

Leakage

The number of times airlocks are utilized and the amount of air leaking through the cabin walls, seals, and throughputs, affect the life support subsystem requirements. The frequency of which the cabin may be repressurized also affects the subsystem. The atmosphere is assumed to be a 50-50 mixture

of oxygen and nitrogen at 7 psi total pressure. The leak rate and cabin repressurization criteria are as follows:

Oxygen:	6.82×10^{-4} kilograms/meter^2-day (1.4×10^{-4} pound/square foot-day)
Nitrogen:	7.80×10^{-4} kilograms/meter^2-day (1.6×10^{-4} pound/square foot-day)
Airlocks:	2 refills per day
Repressurization:	Refill cabin volume each 180 days

These leak rates are considerably lower than the rates presently being measured for the Gemini and Apollo modules. However, they are of the same order of magnitude as those in current laboratory vacuum systems, and it is anticipated that similar leakage characteristics may be obtained by careful design and manufacturing procedures. The leakage rates are based on molecular diffusion of O_2 and N_2. As for the airlock makeup, it was assumed that at least 50 percent of the gas in the airlock can be recovered by pumping it back into the system.

Feces

The requirement was assumed that the feces be either stored on the spacecraft or processed and ejected from the spacecraft in such a way that it will not impact nor contaminate any of the planetary bodies. The scaling laws presented herein are based on the storage of the processed (e.g., vacuum dried) feces in empty food canisters.

Storage

The scaling laws for the atmospheric supply are based on storage of gases in a cryogenic state.

Electrical Power Requirements

Electrical power demands for the environmental control and life support elements are provided, but weights and volume penalties for the power subsystem to furnish this power has not been included in the scaling laws. These weights are included in the power subsystem scaling laws discussed in a subsequent section of this Appendix.

ENVIRONMENTAL CONTROL/LIFE SUPPORT SUBSYSTEM COMPONENTS

Table 2 shows the components that were included in the scaling laws. The values used are sufficient to account for small items not specifically itemized in this table.

EC/LSS for ERM and PEM Ascent Stage

The environmental control and life support subsystem for the ERM and PEM ascent stage is divided into two categories for simplicity, "crew and seats" and "life support." Weights and volumes for these elements are shown parametrically in Figures 1 and 2 which are valid for occupancy times of no more than 24 hours. Power requirements are assumed to be negligible and are therefore not isolated from other loads. Both the weight and volume for the life support subsystem increase linearly with increased crew size, as does the weight for the crew and seats. Volume for crew and seats is shown as zero because it is provided inherently in the mission module free volume.

EC/LSS for MM and PEM Descent Stage

The scaling laws for the MM and PEM descent stage are shown in Tables 3 through 5 for weight, volume and power, respectively. The four different systems are shown on each chart for comparison. For purposes of simplicity, the open life support system for durations of less than 90 days is shown as the baseline system; only the differences from the baseline system are shown for the other systems.

As can be seen in Tables 3 through 5 the scaling equations are divided into four factors representing: the fixed elements; those elements which vary as a function of the crew size; those elements which vary as a function of the mission duration but not a function of crew size; and those elements which vary as a function of the product of the mission duration and the crew size. It should be noted that all elements of the EC/LSS do not have values in all four of these categories. Those that do not are so indicated by a dash. (Refer to Table 2 for a breakdown of the components included in each of these categories.)

Open System for Durations Less Than 90 Days

This open system concept is similar to that used in the present Apollo Command/Service Module. The daily requirements criteria for a crew member in this system are given in the first Section of Table 1. All of the crews daily needs and the waste products thereof are carried and stored onboard the spacecraft. The weight scaling laws for this system are shown

Table 2. Environmental Control and Life Support Subsystem Components

Subsystem	Components
1. Crew and crew support	95-percentile man (> 197 pounds) Shoes Undergarments Coveralls Bedding Personal property Personal hygiene kit Space suit Space helmet Space boots and gloves Space back pack Space suit 14-day O_2 supply Fire fighting equipment Medical equipment and supplies Puncture sealant
2. Furniture and housekeeping	Two airlocks Sleeping compartment Furniture Clothes laundry Janitorial equipment Cleaning and janitor supplies
3. Food management	Kitchenette Culinary equipment Water heater and stove Initial water supply Food Meal containers Refrigeration Repackaging supplies
4. Water supply	Drinking water Cooking water Wash water Containers
5. Waste management	Toilet room Feces collector - commode, dehydrator, and supplies Urine collector - adapter, pump, holding tank, and water in system Wash water collector - filter unit, pump, filter supplies, holding tanks, and water in system Personal hygiene - filter unit, suction pump, and supplies
6. Temperature and humidity control	Main condensing coil Spare condensing coil Heating coils Spare heating coils Fan Controls Ducting Coolant in system Coolant pump Electronic heat conduction plates Condensed water separator Condensed water pump Condensed water tank Plumbing

Subsystem	Components
7. Atmospheric purification	Charcoal filters Fiberglass filters Diverter valves Heater Cooling coils Ducting Trap Ultra-violet lamp Silica-Gel Zeolite Blowers Chromatograph Catalytic burner
8. Atmospheric supply	Oxygen Oxygen tankage Emergency oxygen supply Emergency oxygen tankage Pressure control Valves and piping
9. Instruments and controls	Panel board Instruments Controls Digitizing equipment

Note: If the oxygen is recovered by the Bosch process, then the above subsystem functions of numbers 7 and 8 are combined into the following subsystem:

Atmospheric purification and supply	Charcoal filters Fiberglass filters Ducting Diverter valves Heater Cooling coils Trap Ultra-violet lamp Chromatograph Silica-gel Zeolite Blower Valving Bosch process unit Electrolysis unit Oxygen pumps Hydrogen pumps Tankage Catalytic burner

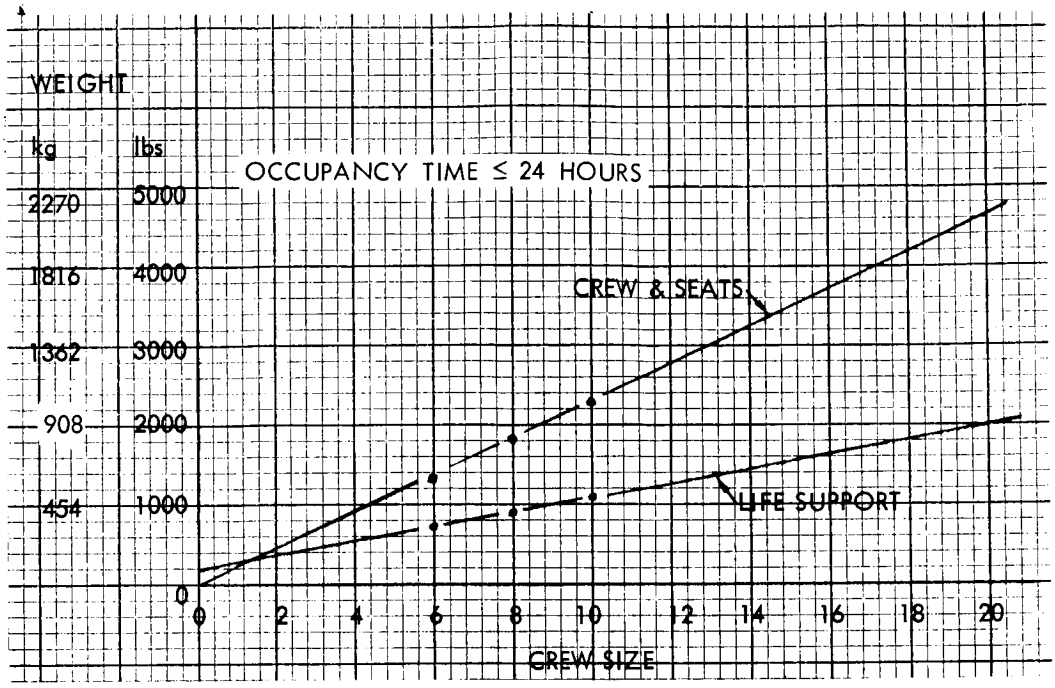

Figure 1. ERM and PEM Ascent Stage Environmental Control and Life Support Subsystem Weights

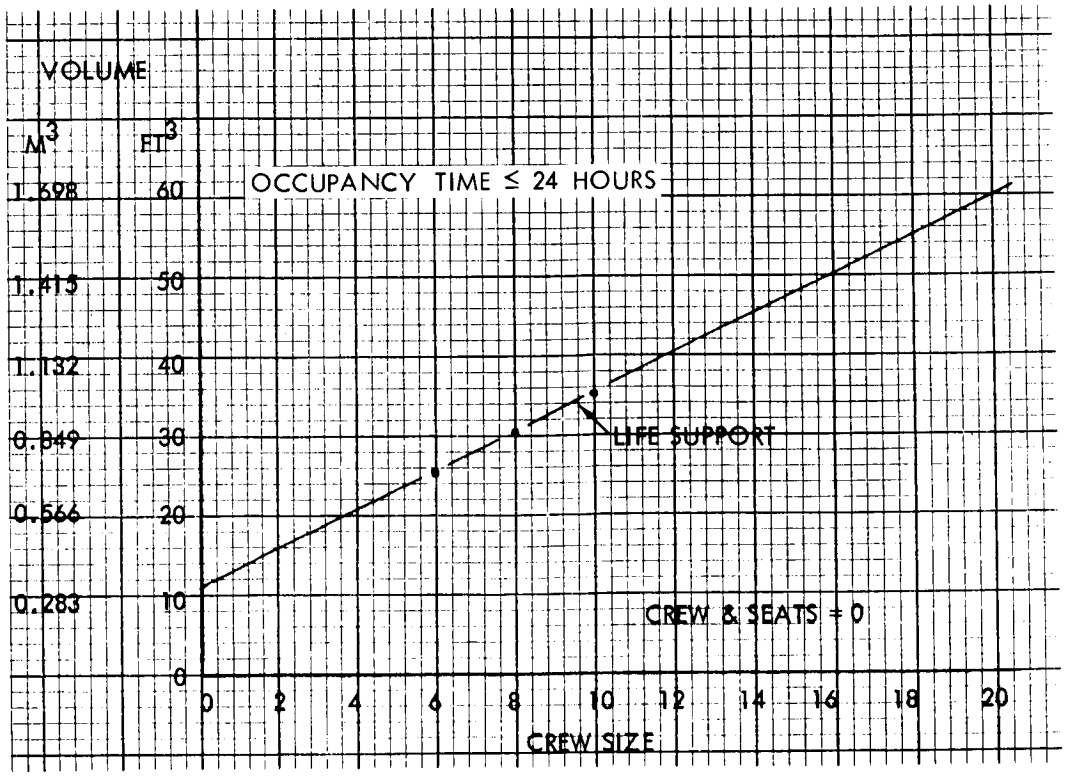

Figure 2. ERM and PEM Ascent Stage Environmental Control and Life Support Subsystem Volumes

Environmental Control/ Life Support System Elements	Open < 90 Days				Op	
	Pounds	Pounds/ Man	Pounds/ Day	Pounds/ M-D	Pounds	Pounds/ Man
Crew and crew support	65 (29)	360 (164)	— —	0.140 (0.064)	←	
Furniture and housekeeping	295 (134)	65 (30)	— —	0.025 (0.011)	←	
Food management	50 (23)	25 (11)	0.05 (0.02)	1.640 (0.745)	←	
Water supply or recovery	— —	— —	— —	9.450 (4.297)	— —	— —
Water management	72 (33)	14 (6)	0.15 (0.07)	0.100 (0.045)	←	
Temperature and humidity control	225 (102)	54 (25)	— —	— —	←	
Atmospheric purification	52 (24)	47 (21)	— —	0.053 (0.024)	← Same as C	
Atmosphere supply	40 (18)	161 (73)	— —	2.240 (1.018)	← Same as C	
Instruments and Controls	100 (45)	— —	— —	— —	← Same as C	
Total pounds (kilogram)	899 (408)	726 (330)	0.20 (0.09)	13.648 (6.204)	899 (408)	726 (330)

Note: Metric equivalents (kilograms, kilograms/man, kilograms/day, and kilograms

FOLDOUT FRAME

Table 3. Environmental Control and Life Support Subsystem Weights

...en > 90 Days		Water and Oxygen Recovery				Water Recovery Only			
Pounds/ Day	Pounds/ M-D	Pounds	Pounds/ Man	Pounds/ Day	Pounds/ M-D	Pounds	Pounds/ Man	Pounds/ Day	Pounds/ M-D
← Same as Open < 90 Days →									
← Same as Open < 90 Days →									
← Same as Open < 90 Days →									
—	20.700	80	80	—	0.140	80	80	—	(0.074)
—	(9.410)	(37)	(37)	—	(0.064).	(37)	(37)	—	0.160
← Same as Open < 90 Days →									
← Same as Open < 90 Days →									
...pen < 90 Days →		100	110		0.150	← Same as Open < 90 Days →			
		(45)	(50)		(0.068)				
...pen < 90 Days →		← Combined with ATM Purification →				← Same as Open < 90 Days →			
...pen < 90 Days →		150	—	—	—	← Same as Water and Oxygen Recovery System →			
		(68)	—	—	—				
0.20	24.898	1037	708	0.20	2.195	1029	806	0.20	4.358
(0.09)	(11.317)	(471)	(323)	(0.09)	(0.997)	(468)	(367)	(0.09)	(1.981)

.../man day) are given in parentheses.

FOLDOUT FRAME

Environmental Control/ Life Support System Elements	Open < 90 Days				
	Feet^3	Feet^3/ Man	Feet^3/ Day	Feet^3/ M-D	Feet^3
Crew and crew support	2.0 (0.1)	5.05 (0.14)	— —	0.0089 (0.00025)	←
Furniture and housekeeping	132.0 (3.7)	110.0 (3.08)	— —	0.015 (0.00042)	←
Food management	52.0 (1.5)	0.50 (0.02)	— —	0.2000 (0.00567)	←
Water supply or recovery	— —	— —	— —	0.1800 (0.00510)	— —
Waste management	55.8 (1.6)	1.00 (0.03)	0.015 (0.001)	0.0100 (0.00028)	←
Temperature and humidity control	20.0 (0.6)	2.50 (0.07)	— —	— —	←
Atmospheric purification	2.6 (0.1)	— —	— —	0.1330 (0.00377)	← Sa
Atmosphere supply	0.50 (0.014)	20.25 (0.57)	— —	0.1500 (0.00425)	← Sa
Instruments and controls	2.5 (0.1)	— —	— —	— —	← Sa
Total	267.4 (7.6)	139.30 (3.93)	0.015 (0.001)	0.6969 (0.0197)	267.4 (7.6)

Note: Metric equivalents (meters^3, meters^3/man, meters^3/day, and met

FOLDOUT FRAME

Table 4. Environmental Control and Life Support Subsystem Volumes

Open > 90 Days			Water and Oxygen Recovery				Water Recovery Only			
$Feet^3$/ Man	$Feet^3$/ Day	$Feet^3$ M-D	$Feet^3$	$Feet^3$/ Man	$Feet^3$/ Day	$Feet^3$/ M-D	$Feet^3$	$Feet^3$/ Man	$Feet^3$/ Day	$Feet^3$/ M-D
Same as Open < 90 Days →										
Same as Open < 90 Days →										
Same as Open < 90 Days →										
—	—	0.4000 (0.01133)	2.00 (0.06)	0.25 (0.009)	—	—	2.00 (0.06)	0.25 (0.009)	—	0.008 (0.0002)
—	—									
Same as Open < 90 Days →										
Same as Open < 90 Days →										
ne as Open < 90 Days →			4.00 (0.11)	0.5 (0.014)	0.010 (0.0003)		← Same as Open < 90 Days →			
ne as Open < 90 Days →			← Combined with Atmospheric purification →				← Same as Open < 90 Days →			
ne as Open < 90 Days →			3.50 (0.10)				← Same as Water and Oxygen Recovery System →			
9.30 (3.93)	0.015 (0.001)	0.9169 (0.02597)	271.3 (7.7)	119.80 (3.39)	0.025 (0.0007)	0.2339 (0.0066)	270.9 (7.7)	139.55 (3.95)	0.015 (0.001)	0.5177 (0.01466)

rs^3/man day) are given in parentheses)

FOLDOUT FRAME

Environmental Control/Life Support System Elements	Open < 90 Days				
	Watts	Watts/ Man	Watts/ Day	Watts/ M-D	W
Crew and crew support	←				
Furniture and housekeeping	←				
Food management	200	10	—	—	←
Water supply or recovery	←				Nor
Waste management	85	—	—	—	←
Temperature and humidity control	25	40	—	—	
Atmospheric purification	125	55	—	—	
Atmospheric supply	300	—	—	—	
Instrumentation and control	100	—	—	—	
Total	835	105	—	—	8

FOLDOUT FRAME

Table 5. Environmental Control and Life Support Subsystem Power Requirements

Open > 90 Days				Water and Oxygen Recovery				Water Recovery Only			
atts	Watts/ Man	Watts/ Day	Watts/ M-D	Watts	Watts/ Man	Watts/ Day	Watts/ M-D	Watts	Watts/ Man	Watts/ Day	Watts/ M-D
None											
None											
Same as Open < 90 Days											
e				50	100	—	—	50	100	—	—
Same as Open < 90 Days											
Same as Open < 90 Days											
Same as Open < 90 Days				300	250	—	—	Same as Open < 90 Days			
Same as Open < 90 Days				Combined with Atmospheric purification				Same as Open < 90 Days			
Same as Open < 90 Days				200	—	—	—	Same as Water and Oxygen Recovery System			
35	105	—	—	860	400	—	—	985	205	—	—

FOLDOUT FRAME

in the first section of Table 3. As noted above, the open system is divided into less than and greater than 90-day missions because of the need for additional wash water and perspiration water for the longer missions. The volume and power requirements for the open system, less than 90 days, are shown in Tables 4 and 5 respectively.

Open System for Durations Greater than 90 Days

The open system, greater than 90 days, differs from the open system less than 90 days, only in the weight of the water supply. This is also reflected in the volume on Table 4. The power requirements for the two open life support subsystems are identical.

Water and Oxygen Recovery

The difference between this system and the baseline system is in the water supply and atmosphere purification and supply. In the case of the water supply, the fixed weight and weight per man has increased to account for the water processing equipment, and the weight as a function of the product of mission duration and crew size has dropped drastically. It represents only the expendables required in the processing of water, such as filters. In the case of the atmospheric purification and supply, these two functions are combined into one equation. Note that the weight factor for atmospheric purification and supply which is a function of the product of the mission duration and crew size has dropped to only about 5 percent of the former value. The weight of the instruments and controls has increased approximately 50 percent to account for the additional controls for water and oxygen recovery.

Water Recovery Only

This system is an intermediate ecological closure between the open system and the water and oxygen recovery systems discussed above. Therefore, the weights, volumes, and power requirements are essentially those represented by these two systems for the appropriate type of closure. Note from Table 1 however, that in this system more water is produced than is required for water balance. Equations for weight and volume reflect the provisions for storage of this excess water. This excess water can be used for many purposes such as evaporative cooling, hence the weight for the storage of this water is justified.

FOOD PRODUCING SYSTEMS

A study was made of food producing systems to determine if they were attractive for the missions under consideration in this study. The primary

evaluation criterion was weight in Earth orbit, but the potential reliability was also considered qualitatively in the evaluation.

Figure 3 compares the weight* contributed by the three most significant consumables of the life support system: water, oxygen, and food. It can be seen that the potential weight saving for food is small compared to that for water and oxygen. Figure 3 also shows the combined weight of water and oxygen for the water and oxygen recovery system to illustrate the benefit of recovering these items. The shaded area of Figure 3 represents the most probable conditions for most missions (one to two years duration and 4 to 10 men). This again reduces the significance of the food weight compared to the overall vehicle weight. In the boundary case (5, 000 man-days), the stored food weight is about 8, 000 pounds, only part of which can be saved at best.

The savings of stored food weight will be offset to some degree by the hardware and electrical power required for regeneration. For short duration missions, the food producing hardware exceeds the weight of stored food. Several of the most promising systems were compared on a gross basis with the stored food weight to determine at what point the production of food starts to become attractive from a weight standpoint. The fixed weight plus the required increase in the electrical power system weight is shown in Figure 4 for three typical systems for a crew size of 20 men. For realistic systems studied to date, stored food is required to supplement the nutrients from the produced food. It is not unreasonable to add 10 to 50 percent stored food as a supplement. The amount is not known because the nutritional value of produced food has not been established. Long term development tests are required for this purpose. The Physico-Chemical System B with Glycerol (Reference 2) is shown with 30 percent stored food as a typical example. This produces a crossover at about one year. The Hydrogenomonas System and the Duckweed System have different crossover points as noted. A similar evaluation made for a three-man system produced the same crossover points.

The results summarized in Figure 4 are not intended to be exact but are sufficiently accurate to indicate the trend. They are based on: (1) 1.64 pounds/man-day for stored food, which includes an allowance for containers; (2) 500 pounds/kilowatt for electrical power; (3) adjustments to account for weights of water regeneration, etc., which should not be charged to the production of food; (4) the assumption that the food producing systems can be scaled linearly between crew sizes of three and twenty men using the points designs of Reference 2 which are for a crew size of ten men. Although these assumptions may not be strictly true, it is believed the results are sufficiently accurate to conclude that food producing systems did not warrant

*Fixed weight and weight as function of crew size only were omitted for simplicity.

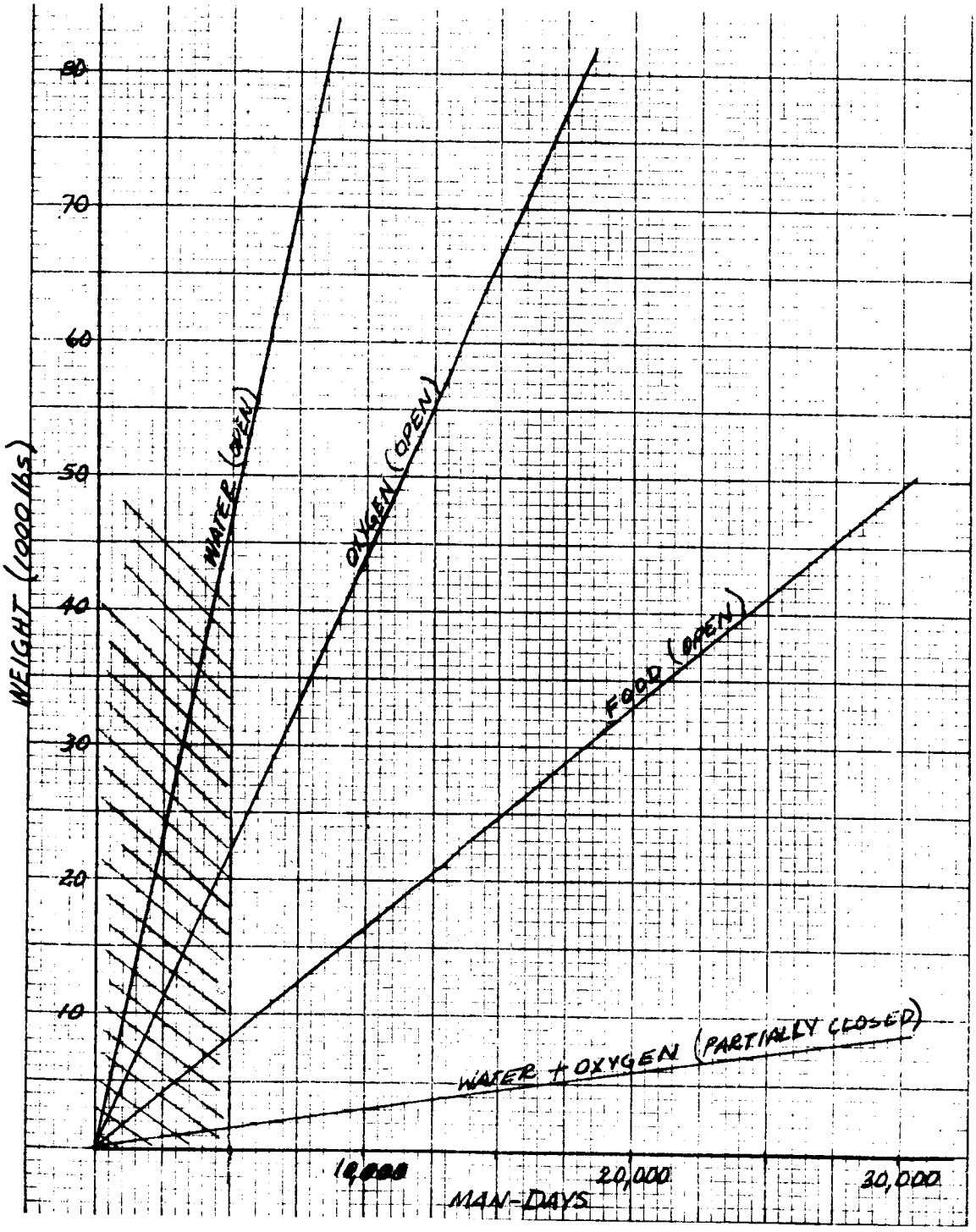

Figure 3. Life Support System Weight Comparison

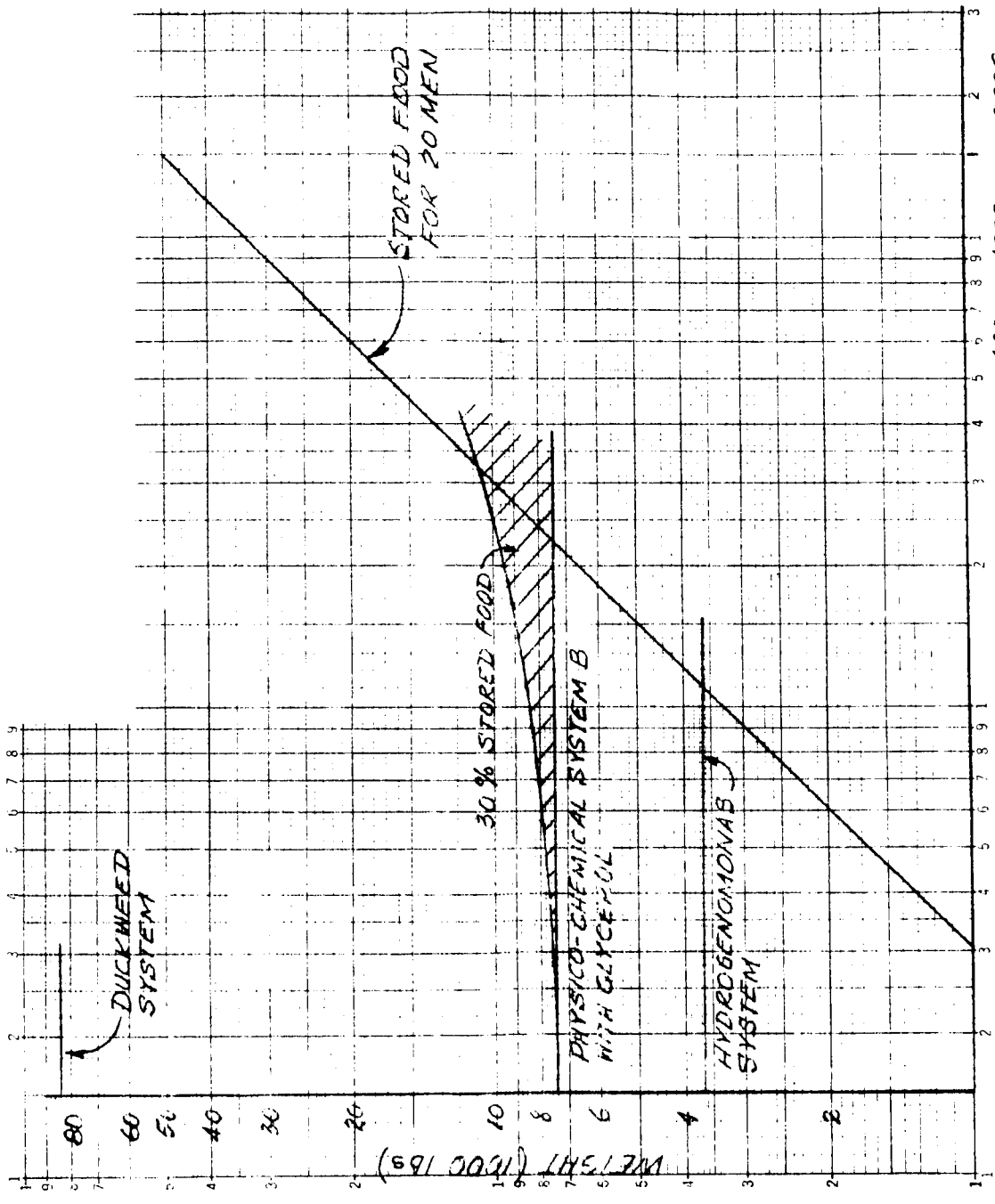

Figure 4. Stored Food Versus Produced Food for 20 Men

inclusion in the weight synthesis and sensitivity evaluation. It is questionable whether there is adequate incentive to develop these systems for the 1980 to 2000 time period.

CONCLUSIONS

Due to the short occupancy times (no more than 24 hours), the open system was assumed for use in the ERM and the PEM ascent stage during subsequent analyses. The open system was also used in the PEM descent stages. Although there would be a mass advantage if a partially closed system were used for the longer occupancy times, the magnitude of the savings did not warrant the additional system complexity.

The mass requirements of the three systems considered in detail for use in the mission module are shown in Figure 5 (as a function of mission duration) for crew sizes of 8 and 20 men. As can be seen from the figure, the mass requirements of the open system are excessive for the mission durations applicable to the study—300 to 1500 days. Therefore, this system was not considered further. The mass requirements of the system with oxygen recovery only is approximately 50 percent heavier than the system with both water and oxygen recovery for a mission duration of 300 days. As the mission duration increases to 1500 days, the system with water recovery only is approximately 80 percent heavier than the more fully closed system. This mass penalty was considered to be excessive for these missions. In order to utilize a system which is compatible with the requirements of all of the missions considered in this study, the water and oxygen recovery system was utilized during the module and system synthesis analyses discussed in Appendix D. The system will not necessitate major technological advancements and could be readily available for all missions during the time period being considered.

Because of the low weight of the communications subsystem relative to the remainder of the total spacecraft, it is not necessary to select a particular type of subsystem for the subsequent weight synthesis analyses. However, in choosing a power subsystem (whose weight is not insignificant) the power required by the communications subsystem must be known. Therefore, a communications subsystem power requirement of 2,000 watts has been assumed.

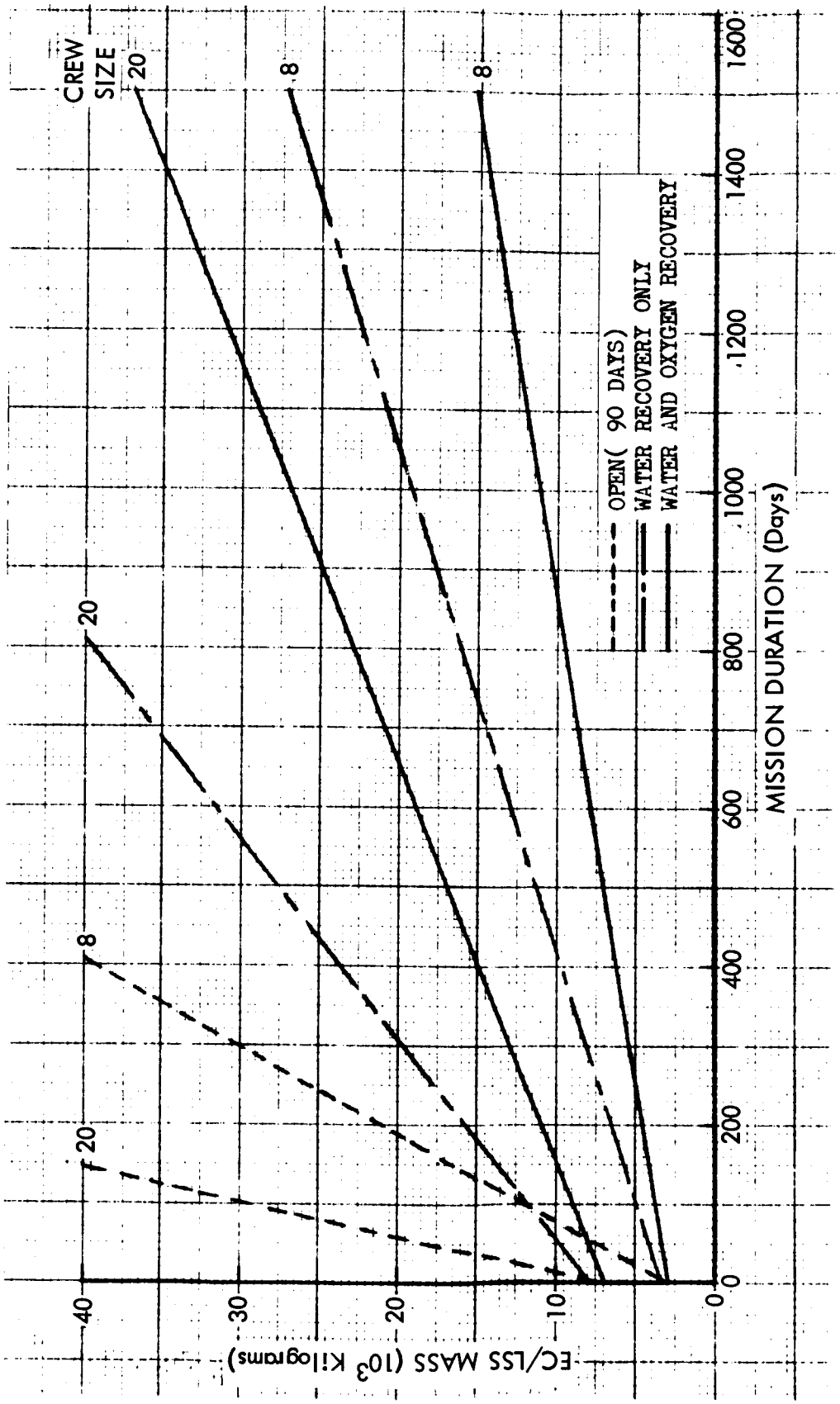

Figure 5. Mission Module EC/LSS Mass Comparison

COMMUNICATIONS PARAMETRIC ANALYSIS

The economics of planetary exploration missions dictate that a maximum amount of data be obtained and transmitted back to Earth. In particular, some form of color television or color picture transmission would be desirable. Due to the extremely high number of data bits in a high resolution picture or TV frame, a high bit rate is required to accomplish transmission in a reasonable time, even with low frame rates and compaction. This problem is aggravated by the extremely long communicating distances, which range from 0.42×10^8 kilometers (0.28 A.U.) to 9.30×10^8 kilometers (6.2 A.U.). Thus the communications subsystem is a critical element of interplanetary spacecraft design. It will represent compromises and/or penalties in the areas of power requirements, antenna sizes, pointing and tracking requirements, transmission duty cycle, data rate, etc. Much work must be done to develop communication technology and spacecraft hardware, and perhaps even the replacement of the existing ground communications network, to be compatible with the new spacecraft equipment.

The scope of this study was limited to the spacecraft-to-ground communication link. The other communication links, which include the ground to spacecraft (up-link), spacecraft to/from planetary excursion module (PEM) and exploration crew to/from PEM or orbiting spacecraft, have unique problems which have not yet been completely resolved, but they are not considered critical for the purposes of this study.

STUDY APPROACH

The study results insofar as is practical are presented parametrically. This is because of the sensitivity of the system to various requirements that have not been fully established. Examples, which represent typical requirements, are presented to illustrate the use of the parametric data, but these should not be considered as final or recommended design points. For example, one might select a certain data rate, duty cycle, beam width or tracking capability, etc., and find that the requirements for power, size, weight, etc., were very moderate, while on the other hand another set of input requirements would change the power, weight, and size by several orders of magnitude.

The critical parameter in the communications study was assumed to be input power because the weight of the various communication elements are not as sensitive to changes in the input requirements as is the weight penalty for the changes in the power requirement. For example, the transmitter and receiver elements probably will not exceed 500 pounds, and even the largest practical antenna (≈15.2 meters) would not weigh more than 500 pounds, while the weight penalty for input power may well exceed 5,000 pounds. Therefore, input power was used as a measure of the communication subsystem, i.e., all other things being equal, the system requiring the least input power for a given bit rate range squared product (BR^2) is considered the best system.

There are a large number of parameters which effect the capability of any specific communication subsystem. In order to simplify this study and still obtain meaningful results, certain assumptions were made regarding the performance parameters of the ground receiving station, modulation efficiency, performance margin, type of modulation, efficiencies, etc., expected in the 1980 to 2000 time period. The values selected for these parameters and the rationale are discussed below. The significant factors for comparing different types of communication systems are transmitted power of the spacecraft terminal, spacecraft antenna gain, and efficiency.

Various constraints or limitations, either theoretical or projected state-of-the-art, tend to make one system better than another. For example, some systems are power limited while others are bandwidth limited. The parameter BR^2 was used for comparing candidate communication subsystems because bit rate can be traded off equally with the square of the communicating range. Additional factors are included in the parametric data for developing the characteristics of the communication subsystem for any particular set of input requirements. These include such items as the number of bits of information to be transmitted, such as in a photograph or TV frame, the rate at which this information must be transmitted, various beamwidths which must be selected to be compatible with tracking and pointing capability, and the transmission duty cycle.

Four different types of communication subsystems were selected for comparison: S-band, millimeter, carbon dioxide (CO_2) gaseous laser, and galium arsenide (GaAs) injection laser. These were selected to represent the complete spectrum of available systems. Although only four subsystems were investigated in depth, these systems represent the inherent advantages and problems of many other systems and are considered to be those most likely to be considered for future applications. The characteristics used for each of these systems were those that could be postulated for 1980 to 2000 time period, assuming active development and funding during the interim time period.

Earth atmospheric transmissability, transmission dispersion, and spreading losses were considered but other planetary atmospheric losses were omitted in considering the spacecraft-to-Earth link by assuming that the spacecraft operates outside the influence of the planet atmosphere or radiation belts. Occultation, solar corona effects, and trapped radiation belts were not included in the values computed for each system.

It was found convenient, for the purposes of applying the parametric data to the missions of the study, to consider three mission groups. Mercury, Venus, and Mars were considered in one group; the asteroids Ceres and Vesta in a second group; and Jupiter/Ganymede as a third group. The mission groupings were selected on the basis of communicating distances.

BASIC COMMUNICATIONS SUBSYSTEM REQUIREMENTS

The requirements for a deep space communication subsystem in support of manned planetary missions are very severe because of the primary considerations of distance, length of mission, and planetary/interplanetary environment. The communication subsystem must also satisfy many other requirements.

Down-data transmissions should be maximized because scientific justifications of the mission may require that high-resolution pictures be transmitted in reasonable time. For digital modulation techniques, 10^6 to 10^7 bits per frame are normally required. Bandwidth requirements will vary with frame-rate, compaction, and modulation techniques. Down-data link television or picture transmission may also have medical uses for monitoring the astronaut's health.

Interplanetary missions defined by this study result in propagation distances for a direct link from a planetary orbiting spacecraft to Earth ranging from 0.28 A.U. (0.42×10^8 kilometers) to 6.2 A.U. (9.3×10^8 kilometers). The inverse square law as it relates to received energy places high demands on whatever system is to be used.

Mission times for interplanetary travel will range up to several years in duration; therefore, the communications subsystem must be extremely reliable. Assuming the need for a 0.99 probability of crew safety and using the Apollo apportionment criteria (one percent of allowable numbers of mission failures), the required communications reliability is 0.9999.

Crew considerations require that communication coverage be continuous although lower bandwidth capabilities, and some sacrifice in overall reliability, may be required during periods when occultation by the sun or the planet occurs.

Monitoring of spacecraft progress and the requirement to correctly point highly directive Earth-based and spacecraft-based antenna (or lens) systems make it necessary that the communications subsystem have an automatic tracking system which can acquire and lock-on narrow beam transmissions.

CANDIDATE SUBSYSTEMS

Four subsystems, which span the frequency range of 2.3 gigahertz through 357,000 gigahertz (S-band to near infrared light) are compared in this study as follows:

System	Frequency Range
S-band	2.3 GHz - 13.05 cm
Millimeter waves	94 GHz - 3.19 mm
Carbon dioxide laser (coherent detection)	28,300 GHz - 10.6 micron
Galuim arsenide laser (non-coherent detection)	357,000 GHz - 0.84 micron

S-Band Systems

S-band was selected as the baseline system for the purposes of comparison during the communications subsystem analyses because of the state of development and large investment in the Earth terminal network. All current planetary spacecraft use this network but continued development is still required of both the Earth based systems and the spacecraft systems. Larger spacecraft antennae may be required with diameters up to 15.2 meters (50 ft). The development of the deployment and steering mechanisms for these antennae would also be required. Large, high gain, phased arrays may be more desirable and also require further development.

Millimeter

The 3.19-millimeter wavelength (94 GHz) system was selected for analysis since millimeter frequencies are the next logical development of the radio-frequency type communication systems, and large investments are being made annually in this area for a wide variety of applications. The millimeter-wave systems have an advantage over S-band for spacecraft applications because high gain antennas and components can be much smaller, and the higher frequency inherent with millimeter systems permits higher data rates, provided transmitted power level is commensurate with the required range.

Optical Systems

The field of optical communications is such a fast moving area that a single clear cut program is difficult to define and many areas of further work are required. The areas requiring further work are shown in Table 6 which summarizes the accomplishments necessary to bring the various types of laser sources and their detectors to practical usage for space applications. Solid lasers (e.g., ruby) are not covered in this table because they are inherently best adapted to high peak powers at low repetition rates. Ideally, a laser and its detector should have the following characteristics:

High efficiency

High cw power output

Capable of internal modulation at high frequencies

Compact, rugged package

Stable area, narrow line (single mode), lasing

No cooling requirements

Highly sensitive detectors

High frequency response in the detector

As indicated by Table 6, much work must be done in the area of basic components. The present "workhorse", the CO_2 laser, must be rugged and compact, capable of internal modulation, and easily cooled in the space environment. The corresponding detector presently lacks high sensitivity and frequency response.

Internal modulation of gas lasers is very limited, whereas the semiconductor laser can be easily modulated internally. To achieve high performance under background noise limited conditions, a heterodyne receiving system must be developed. In support hereof, wide band FM internal modulation of c.w. coherent injection (semiconductor) and gas lasers is required of the order of 4 GHz. Correspondingly, demodulator mixers capable of mixing the local oscillator laser with the incoming signal and demodulating information bandwidths up to 100 GHz are required. This area is very difficult but highly important. Local oscillators must compensate for doppler shift and maintain spatial and temporal coherence with the incoming signal.

Table 6. R&D Objectives for Laser Sources and Detectors

Parameter	Argon Gas 0.4880 microns		HeNe Gas 0.6328 microns		CO_2 Gas 10.6 microns		GaAs Semiconductor 0.8400 microns	
	Existing	R&D	Existing	R&D	Existing	R&D	Existing	R&D
Laser Sources								
Power output (c.w.)	10-50 watts	Improve	0.2 watts	Improve	1 kilowatt Size limited	Small pack	10 watts (4 K)	10 watts (77 K)
Efficiency (percent)	0.01	Improve	0.1	Improve	10 to 40	Improve	50	Improve
Single-mode lasing	Yes		Yes		Yes		No	Required
Stable lasing area	Yes		Yes		Yes		No	Required
Internal modulation	Low frequency limited	Improvement desirable	Low frequency limited	Improvement desirable	No	Desirable	Exist	
Cooling requirements	Heat exchanger		Heat exchanger		Heat exchanger	Space radiation	4 K or 77 K	Minimize
Detector	S-20 PMT		S-20 PMT		Ge: Hg Semiconductor (SBRC)**		S-1 PMT	
1. Quantum efficienty (percent)	15 to 30	Improve	8 to 16	Improve	20	Improve	0.36 to 1	Greatly improve
2. Frequency response	1 GHz	Increase	16 Hz	Increase	16 Hz	Increase	1GHz	Increase
3. Detectivity (D*)	10^{15}	Increase	5×10^{14}	Increase	10 inches	Improve	10^{12}	Increase
4. Cooling Requirements	Yes-for response		Yes-for response		30 K	No problem on ground	Yes-for response	

**Santa Barbara Research Center

Further work in the optics area is required to achieve the following:

Spacecraft optics systems up to 1 meter aperture diameter whose performance achieves diffraction limited beamwidth.

Common transmit-receives optics with provisions for lead angle generation, wide-beam acquisition, and provision for automatic tracking.

Non-degradation of performance due to launch and interplanetary environment.

Narrow-band filters (doppler-shift limited).

Adaptive (self correcting) control systems.

Carbon dioxide (CO_2) was selected as the most promising continuous-wave (c.w.) laser being developed at the present time. Liquid lasers may eventually be developed and supersede the gaseous lasers due to inherent higher power capability (better cooling) but they cannot be considered as a competitive system for the operational time period for this study (1980 to 2000). Heterodyne detection was assumed which permits a theoretical 40- to 60-decibel increase in the signal-to-noise ratio over background limited detection.

Galium arsenide (GaAs) was selected as being typical of semiconductor injection lasers. Although maximum transmitted power capability is very low, total performance is competitive with other communication subsystems because efficiencies are high and the wavelength is compatible with photo-multiplier (photoemissive) detectors with high sensitivity. Since they transmit in the near infrared spectrum, the advantages and problems common to other systems with similar frequencies are represented. Non-coherent detection was assumed because atmospheric distortion of the wave front limits receiver diameter.

Helium neon lasers were considered initially but not used in the comparison because they have very low efficiency (about 0.1 percent) and are limited to about 0.1 watt output.

GROUND RULES AND ASSUMPTIONS

In order to simplify the study, as many parameters as possible were established and held constant. The values for these parameters are shown in Table 7. They represent the postulated post-1980 technology. The bases for these values are discussed in the following paragraphs.

Table 7. Fixed Parameters for Comparison Optical and Radio Space Communication

Parameter	S-Band	Millimeter	CO_2 (heterodyne)	GaAs (non-coherent)
Frequency	2.3 GHz	94 GHz	28,300 GHz	357,000 GHz
Wavelength	13.05 cm	3.19 mm	10.6 microns	0.8400 microns
Spacecraft antenna diameter (m)	4.88 15.2	0.304 0.67 4.58	0.014 0.178 1	0.10 1 m
Spacecraft antenna gain (db) ([A])	38.8 48.7	47 53.8 70	73.22 94.8 109.6	111.5 131.5
Beam angle (arc-sec) ([B])	6750 2150	2640 1200 165	180 15 2.67	2.12 0.21
Ground antenna diameter, D_R (m)	64 (210 ft)	4.58 (15 ft)	2	10
Ground antenna gain (db)	61	70	NA ([F])	NA ([F])
Ground antenna area (effective) A_R ($-dbm^2$)	32.5	9.56	4.96	18.9
Modulation efficiency, ξ - (db) ([C])	10	10	10	10
Performance margin, M (db) ([D])	10	10	20	20
Receiver system noise temperature (°K)	35	400	NA	NA
Noise spectral density				
$\psi = KT$ (radio spectrum)	4.83×10^{-22}	5.52×10^{-21}	NA	NA
$\psi = KT$(db)	-213	-203	NA	NA
$\psi = hf$ (optical spectrum)	NA	NA	1.88×10^{-20}	
$\psi = hf$ (db)	NA	NA	-197.3 dbw-cps^{-1}	
Detector responsivity, ρ	NA	NA		0.002 amp-watt^{-1}
Quantum efficiency, η	NA	NA	0.20	
Modulation	PCM/PSK/PM	PCM/PSK/PM	PCM/PL	PCM/PL
Range equation ([E])	$P_T G_T = \frac{BR^2(\xi)M\,4\pi\psi}{A_R}$	$P_T G_T = \frac{BR^2(\xi)M\,4\pi\psi}{A_R}$	$P_T G_T = \frac{R^2 B\, hf(16)\, M(\xi)}{D_R^2\, \eta}$	$P_T G_T = \frac{BR^2\, 32M(\xi)\, e}{D_R^2\, \rho}$
Efficiency (percent)	50	40	40	50

Footnotes to Table of Fixed Parameters

([A]) Gain of optics assumes uniform density within limits of beam

([B]) Diffraction limit assumed for optical beams

$\theta = 1.22 \frac{\lambda}{D}$

Beam angle for radio frequency based on 3-decibel points

$\theta = \frac{252{,}000\lambda}{D}$ arc-seconds

([C]) Modulation efficiency for digital systems:

$(\xi) = \frac{S\,T}{N/B} = 10$ decibels for all systems

where:

ξ = modulation efficiency in cycles per sec per bit per second
S = signal power in watts
T = time in seconds per bit
N = Noise power in watts
B = bit rate in bits per second

Example of bit error rate (BER):
For 10 cps/bit sec.
S-band BER 5×10^{-6}
Optical BER 4×10^{-3}

([D]) Performance margin

For S-band and 3 mm, includes transmission line and atmospheric losses

For Optics, includes following transmissivities:

	GaAs		CO_2	
Transmitter optics	$T_T = 0.50$	-3 db	$T_t = 0.50$	-3 db
Atmospheric	$T_a = 0.80$	-1 db	$T_a = 0.36$	-4.5 db
Filter	$T_f = 0.20$	-7 db	$T_f = 0.90$	-0.5 db
Diffraction (farfield)	$T_d = 0.50$	-3 db	$T_d = 0.50$	-3 db
Receiving optics	$T_r = 0.50$	-3 db	$T_r = 0.50$	-3 db
Modulation	$T_m = 0.50$	NA	$T_m = 0.50$	-3 db
Subtotal		-17 db		-17 db
Tolerance		-3 db		-3 db
Total		-20 db		-20 db

([E]) The terms in the range equations are as follows:

B = bits per second
R = range (meters)
ξ = modulation efficiency
M = performance margin
ψ = noise spectral density
A_R = antenna area (effective)
D_R = diameter of optical aperture
e = electronic charge
η = quantum efficiency
ρ = detector responsivity

([F]) Not applicable because ground aperture used as collector of photons only.

The radio and optical frequencies shown in Table 7 coincide with known atmospheric "windows" and cover the spectrum from microwaves through millimeter waves to near infrared. The ground station portion of the link was assumed to be near optimum without the constraints of cost or size, although recognized technical limits were taken into account.

Spacecraft antenna diameters were chosen to cover a full range of physical sizes and beam angles. They are tabulated in Table 8 for ready comparison. The pointing accuracy must be no less than one-half the beam angle and in some cases (depending on modulation and detection methods used) must be much less. Spacecraft antenna gains corresponding to the various antenna or aperture diameters are also tabulated in Table 7 and range from 38.3 decibel for the 16-foot (4.88-meter) S-band antenna to 131.5 decibels for the 1-meter GaAs aperture.

The ground antenna for S-band was taken equivalent to the present 64-meter (210-feet) diameter Goldstone antenna, as this equipment is considered to be near optimum economically for the period of interest.

The ground antenna for the millimeter waves was assumed to net 70 decibels with a diameter of 4.58 meters (15 feet). This is considered to be a maximum realizable gain for a parabolic antenna.

The ground optics for the galium arsenide non-coherent laser system is assumed to be a large segmented reflector with an effective diameter of 10 meters. This system will be essentially a photon collector and can be constructed of many individual reflectors.

The CO_2 heterodyne system is based on an f.3 telescope with an effective diameter of 2 meters.

A modulation efficiency of 10 decibels is assumed for all systems, which is equivalent to a ratio of bandwidth to bit rate of 10. The performance margin for the radio frequency systems is taken as 10 decibels and for the optical systems as 20 decibels, due to the losses in the optics. (See Table 6, footnotes). The performance margin makes allowance for various losses in the transmission lines, optics, and atmosphere, and the losses due to pointing error, polarization, and modulation.

The S-band receiving system noise temperature of 35 K is based on a 30 K sky temperature and a 5 K receiving system temperature. For millimeter waves, the system noise temperature is assumed to be 215 K sky noise, 85 K line noise, and 100 K receiver noise for an overall system temperature of 400 K. Relay satellites could be used to receive in the millimeter spectrum and relay in the S-band to reduce the effective millimeter background noise, but data rates would be essentially those of S-band.

Table 8. Spacecraft Antenna Diameters and Beam Angles

System	Spacecraft Antenna Diameter		Beam Angle* (arc-seconds)
	Meters	Feet	
GaAs	1	3.28	0.21
GaAs	0.1	2-3/4 inches	2.12
CO_2	1	3.28	2.67
CO_2	0.178	4.8	15
CO_2	0.014	0.38 inches	180
94 GHz	4.58	15	165
94 GHz	0.67	2.2	1200
S-band	15.2	50	2150
94 GHz	0.304	1	2640
S-band	4.88	16	6750

*Between 3-decibel points for radio frequency
Diffraction limit for optical apertures

The detector responsivity for the galium arsenide system is based on the S-1 Photocathode detecting surface. The quantum efficiency for the CO_2 laser system is based on current work being conducted at the Hughes Santa Barbara Research Center.

Digital modulation is assumed for all systems, due to the inherent advantages of being able to handle many data channels on a time shared basis and the direct data reduction by computer. The range equations are formulated on the basis that both the bit rate and the range are variables which are fixed by the mission requirements and thereby establish the required spacecraft power and gain product ($P_T G_T$).

The comparison of the systems which follows is very sensitive to the values for the fixed parameters shown in Table 7 and must be interpreted

within the framework of the above ground rules and assumptions. For example, the maximum antenna sizes and/or gains affect the power requirement significantly and could slant the comparison to one system or another. Another example is the tracking/pointing capabilities. If developments in these areas make the use of narrower beams possible, the higher frequency systems would become more attractive.

SUBSYSTEM COMPARISON

The candidate communication subsystems are compared in Figure 6 by plotting transmitting capability (BR^2) versus transmitter output power with antenna size as a parameter. It is believed that, for the purpose of this study, the differences in the candidate communication subsystems in the areas of performance, integration, and weight of transmitter, receiver, and antenna (aperture) are so small as to be insignificant compared to the input power weight penalty. For example, in the area of performance, both modulation efficiency and performance margin are specified so that error rate and signal-to-noise ratio are equal for the candidate subsystems. The only integration factors which might be significant are in the areas of antenna size and tracking/pointing requirements. In the first case, it is assumed that the largest antenna required, 15.2 meters for S-band, can be accommodated. Thus the rating factor is qualitative. In the case of pointing/tracking, beam-angle effects reflect into the input power requirements and are shown parametrically.

The galium arsenide non-coherent laser requires least power for a given bit rate range squared product (BR^2) and would normally be rated as best. However, this rating is based on a beam width of 0.21 arc-seconds (Table 8) which is believed to be a tracking/pointing accuracy requirement that cannot be met within the time period under consideration.* Widening the beam to 2.12 arc-seconds by using a 0.1 meter aperture increases the power requirement by about 100 times so that it becomes worse than S-band with a small antenna.

The next best system is the CO_2 laser with a 1.0 meter aperture. This system has only a 2.67 arc-second beam, which also presents a serious pointing/tracking problem.

The S-band looks very attractive if an antenna of 15.2 meters (50 feet) can be provided. Tracking/pointing is not expected to be a problem with S-band. Although the S-band system with a 4.88-meter (16-foot) antenna

*Laboratory devices have demonstrated 1/50 arc-second tracking/pointing capability based on boresighting. However, boresighting cannot be used to advantage at planetary distances because Earth lead angles must be computed from navigational data. The GaAs laser beam represents a spot size an order of magnitude smaller than the Earth diameter from Jupiter (about 550 miles) and it is considered unreasonable to expect calculated pointing capability of one half the beam width (about 275 miles) from those distances.

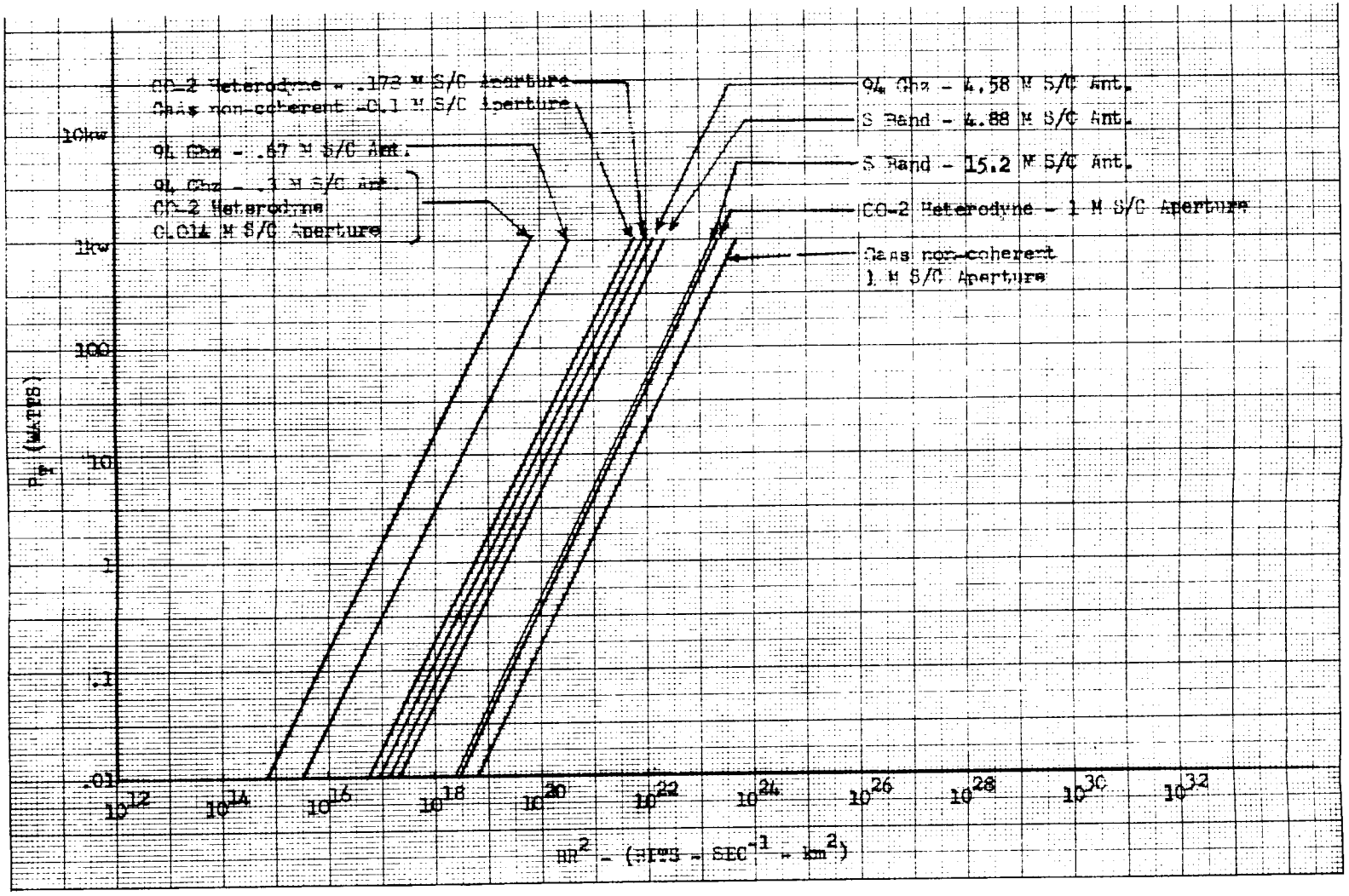

Figure 6. Interplanetary Communications System Comparison—
Transmitted Power Versus (Bit Rate - Range^2) Product

requires an order of magnitude more power, it is still next best to the 15.2 M S-band system and will handle most of the data rate requirements at ranges up to 6.0 A.U. (Jupiter)

The values for BR^2 for color TV from Mars to Jupiter varies from about 10^{21} to 10^{23}. Typical low values are of the order of 10^{19} to 10^{20} for telemetry and voice at these ranges. Thus, the transmitter output requirements vary from 0.01 watts with GaAs to over 1 megawatt for the millimeter system with a 0.3-meter antenna. It can be seen that the power penalty is very sensitive to the range, data rate requirements, and system selected.

Although, the power penalty varies with the square of the range, the difference between the inner planets and the outer planets is only 15 decibels. The variation in the antenna gains between S-band with a 4.88-meter antenna and the GaAs with a 1-meter aperture is over 90 decibels. Thus, it can be seen that the antenna gain overshadows the range problem by a large factor.

The 15-decibel variation in the range can be achieved by simply enlarging the antenna size. For the S-band, two thirds of this can be achieved by changing from a 4.88-meter antenna to a 15.2-meter antenna. For GaAs, 20 decibel gain can be achieved by changing the aperture from 10 centimeter to 1 meter.

It can also be seen that the power-weight penalty is directly proportional to the data rate. Reducing the amount of data to be transmitted by a factor of ten by compaction reduces the power penalty by the same factor. (Compaction ratios of 4:1 to 6:1 are within the current state-of-the-art.) This also illustrates how important data management is in reducing spacecraft weight. Care should obviously be used in selecting the type and quantity of data to be transmitted. For example, if transmitting compacted TV from Jupiter at one frame per five seconds requires 400 watts, increasing this rate to the standard 30 frames per second for commercial TV would increase the required power to 60,000 watts.

The parametric data of Figure 6 represent specific antenna sizes so as to permit a ready comparison of the candidate systems. Figure 7 is more universal and can be used when other antenna gains are desired. Thus, knowing or specifying any three of the four parameters, P_T, G_T, B, and R, allows the fourth parameter to be determined readily. For example, if we select S-band and specify the power as 100 watts, antenna gain as 50 decibels, and range as 10^8 kilometers ($R^2 = 10^{16}$), it can be seen that 10^7 (representing 10^2 watts x 10^5 gain) intersects the S-band line at approximately 3×10^{22} or a bit rate of 3×10^6 bits/second. (3×10^{22} 10^{16}.)

Care should be exercised when using Figure 7 for specific systems. Maximum transmitted power capability for the post-1980 time period

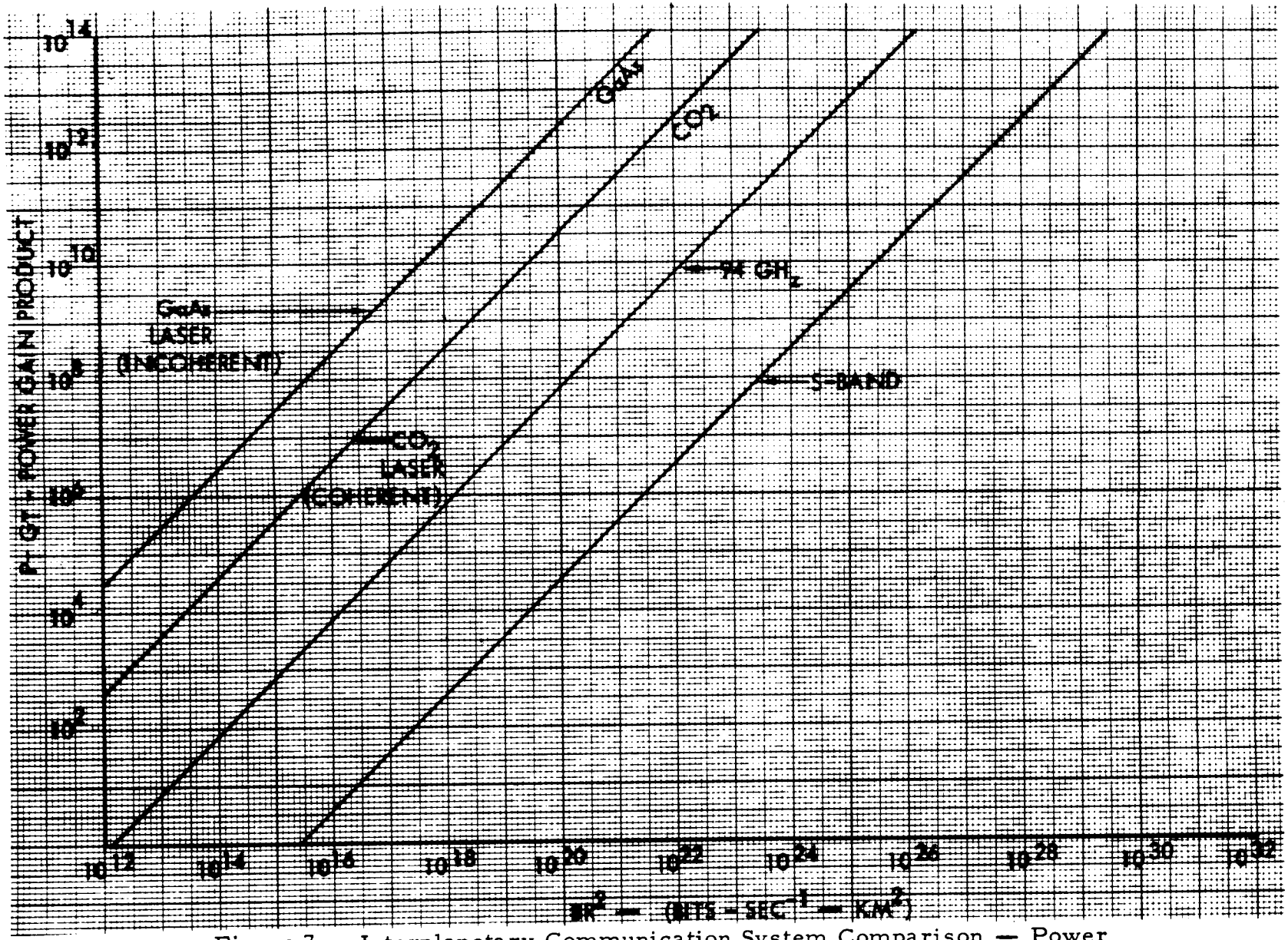

Figure 7. Interplanetary Communication System Comparison — Power Gain Product Versus (Bit Rate - Range^2) Product

is expected to be 1 kilowatt for S-band and millimeter systems, 40 kilowatts for CO_2 lasers, and 10 watts for GaAs lasers.* Also, each frequency has a theoretical maximum data-rate capability. In general, it may be assumed that the data rate is approximately one percent of the carrier frequency or 2.3×10^7 for S-band, 9.4×10^8 for millimeter, 2.8×10^{11} for CO_2, and 3.6×10^{12} for GaAs. From this it can be seen that the GaAs has 10^5 the data rate capability, but it should be noted that S-band can accommodate the projected requirements (up to $BR^2 = 10^{23}$ bits-km/sec).

Figure 8 presents typical data requirements for color TV—both present commercial type and a postulated compacted type (compaction ratio 10:1)—and for voice—again both current and postulated types. This chart can be used to determine bit rate (B) by selecting the time to transmit the data. For example, compacted color TV transmitted at the rate of one frame each five seconds produces a bit rate of 4.5×10^4 bits/second.

Figures 9 through 12 show the bit rate as a function of transmitted power and input power for various antennae and ranges for S-band, millimeter, CO_2 and GaAs lasers, respectively. The same limitations on power and data rate presented for Figure 7 must be observed for these figures. Efficiencies for the various systems have been estimated for 1980 time period and entered in Table 6. The same efficiencies form the basis of the power input scales of Figures 9 through 12. Required transmitted power and the corresponding input power for specified bit rate, range, spacecraft system, and antennae diameter, can be determined by the use of these figures. The parametric lines are a function of the range in astronomical unit and antenna diameter. The distances represent approximate nominal communications ranges for Mercury, Venus, and Mars - about 1 AU; Ceres and Vesta - about 3.5 AU; and Jupiter/Ganymede - about 6 AU. It can be seen from Figures 9 through 12 that, for the systems which would probably be selected for reasonable data rates, the power requirements are of the order of 100 to 1000 watts. It probably would not be worthwhile to develop an exotic system to reduce the power below these values, and higher bit rates won't be specified (or required if compaction techniques are developed) because of the rapid increase of power penalty. Perhaps, however, the peak demand may be as much as two orders of magnitude higher for short periods. For example, it might be feasible to operate a CO_2 laser at 8 kilowatts output, which would represent a peak input demand of 20 kilowatts. If the transmitter were used for only four hours per day the average power would be only 3.3 kilowatts, as seen from Figure 13.

*These maximum transmitter power ratings are estimated on the basis of the status of laboratory or developmental models of each of these devices being operated today projected to the 1980 period. For example, experimental 100-watt traveling-wave tubes have been demonstrated in the laboratory, and 1000 watts seems to be reasonable by 1980. The power limit shown for the gaseous laser is based on physical size limitations. The GaAs lasers are based on the use of an array and a reasonable projection of output power per unit.

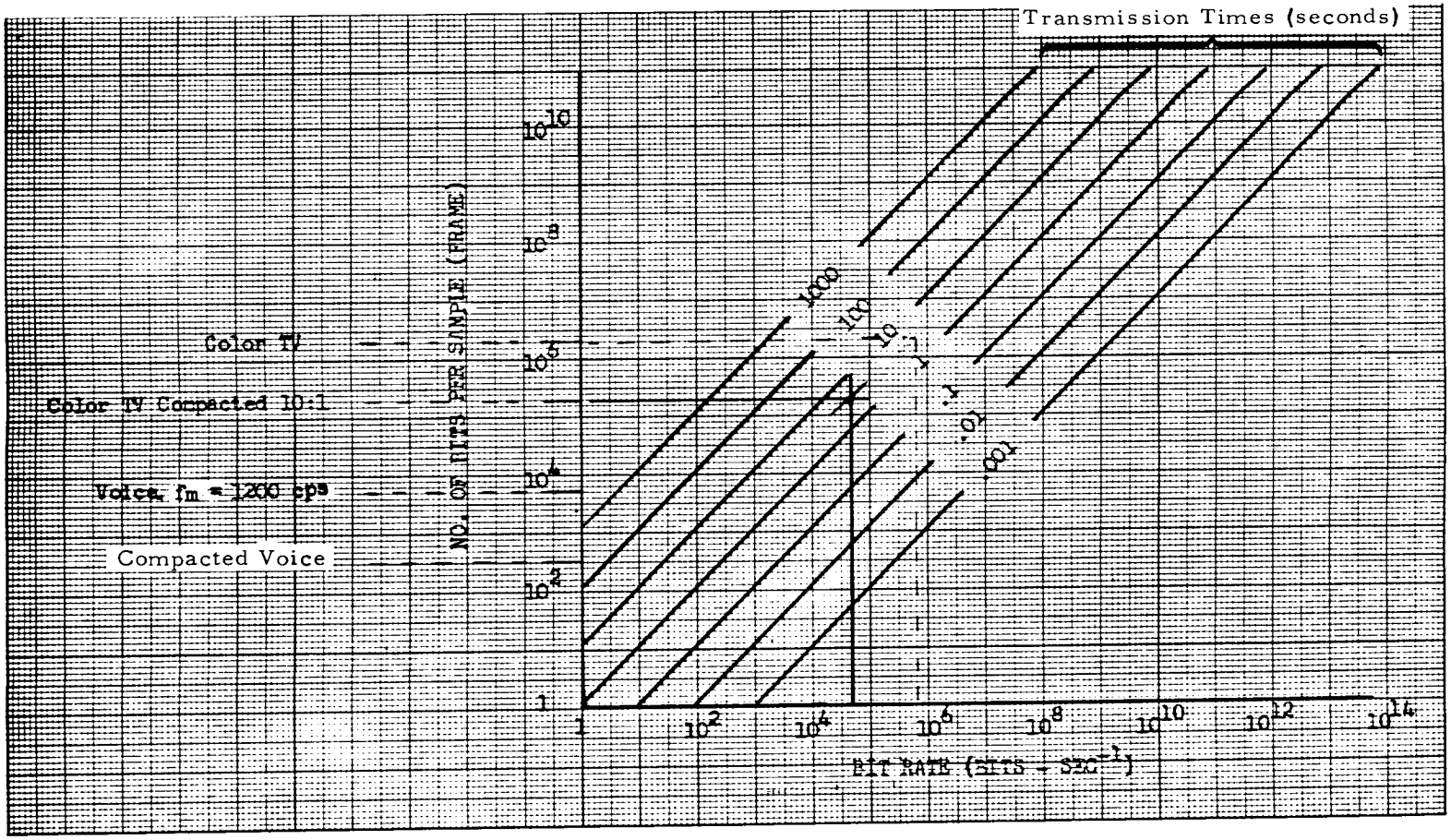

Figure 8. Required Bit Rate Versus Types of Quantized Data for Various Transmission Times in Seconds

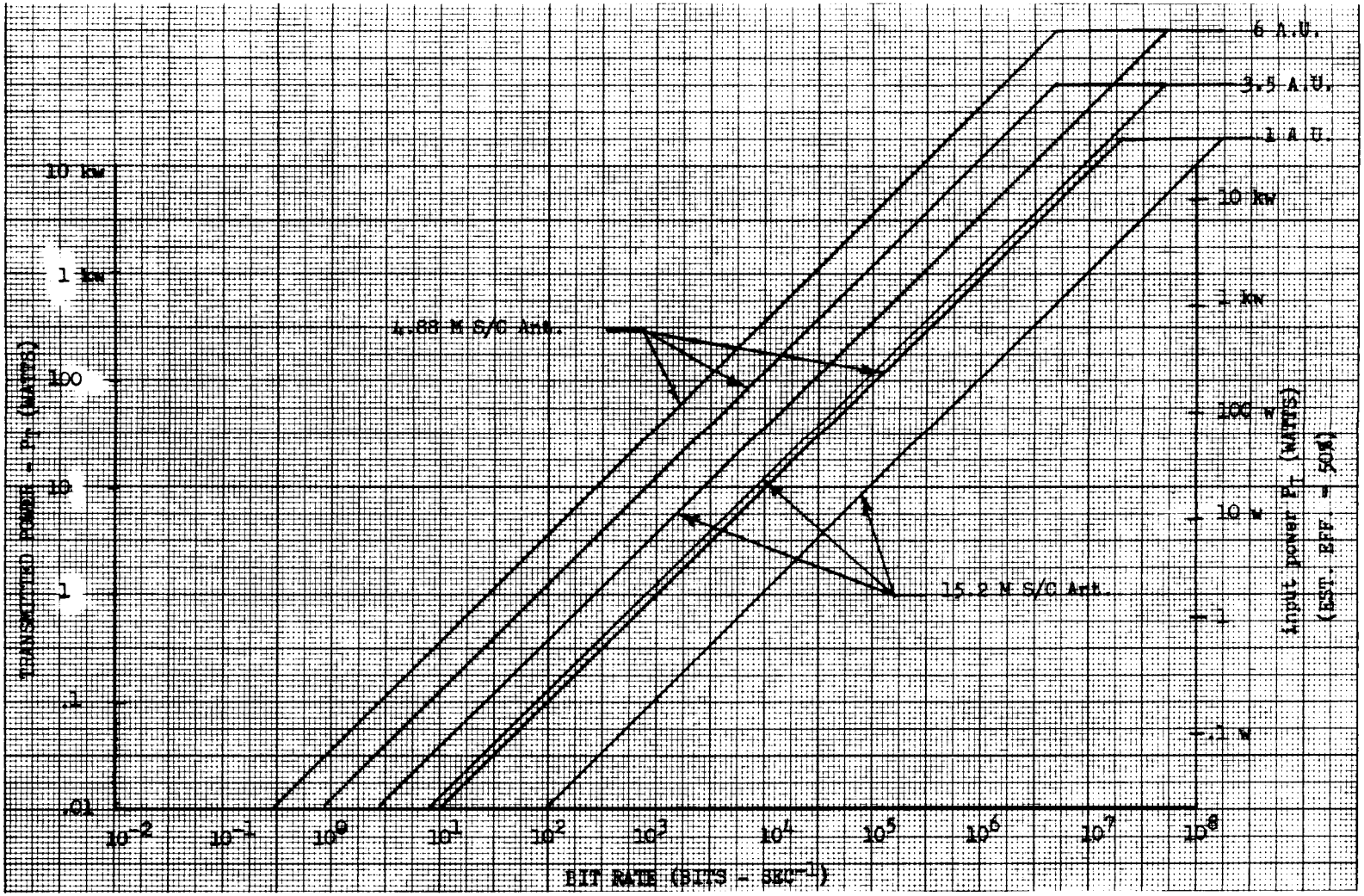

Figure 9. Interplanetary Communication System Comparison—
Power Versus Bit Rate, S-Band

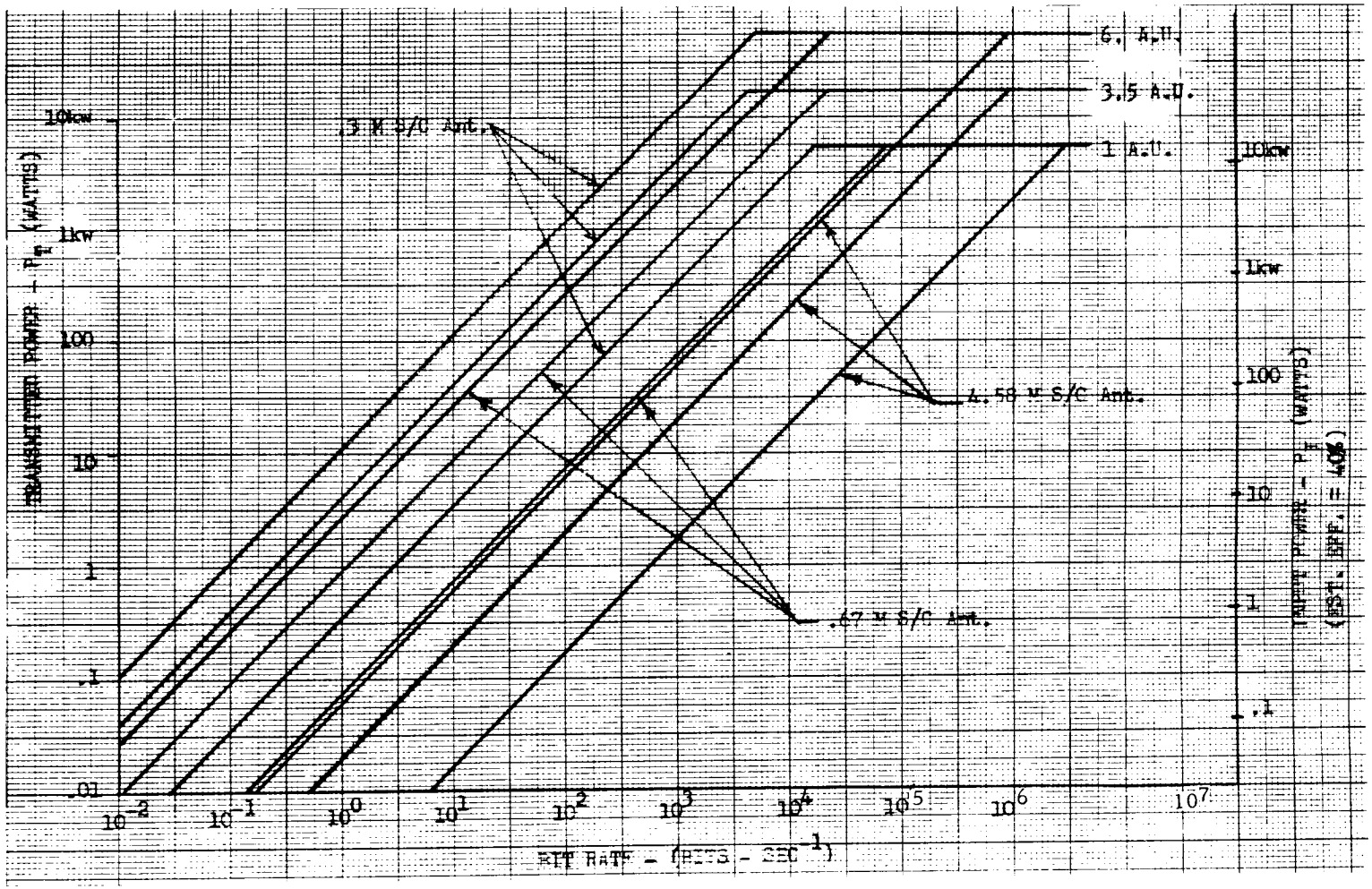

Figure 10. Interplanetary Communication System Comparison— Power Versus Bit Rate, 94 Gigahertz

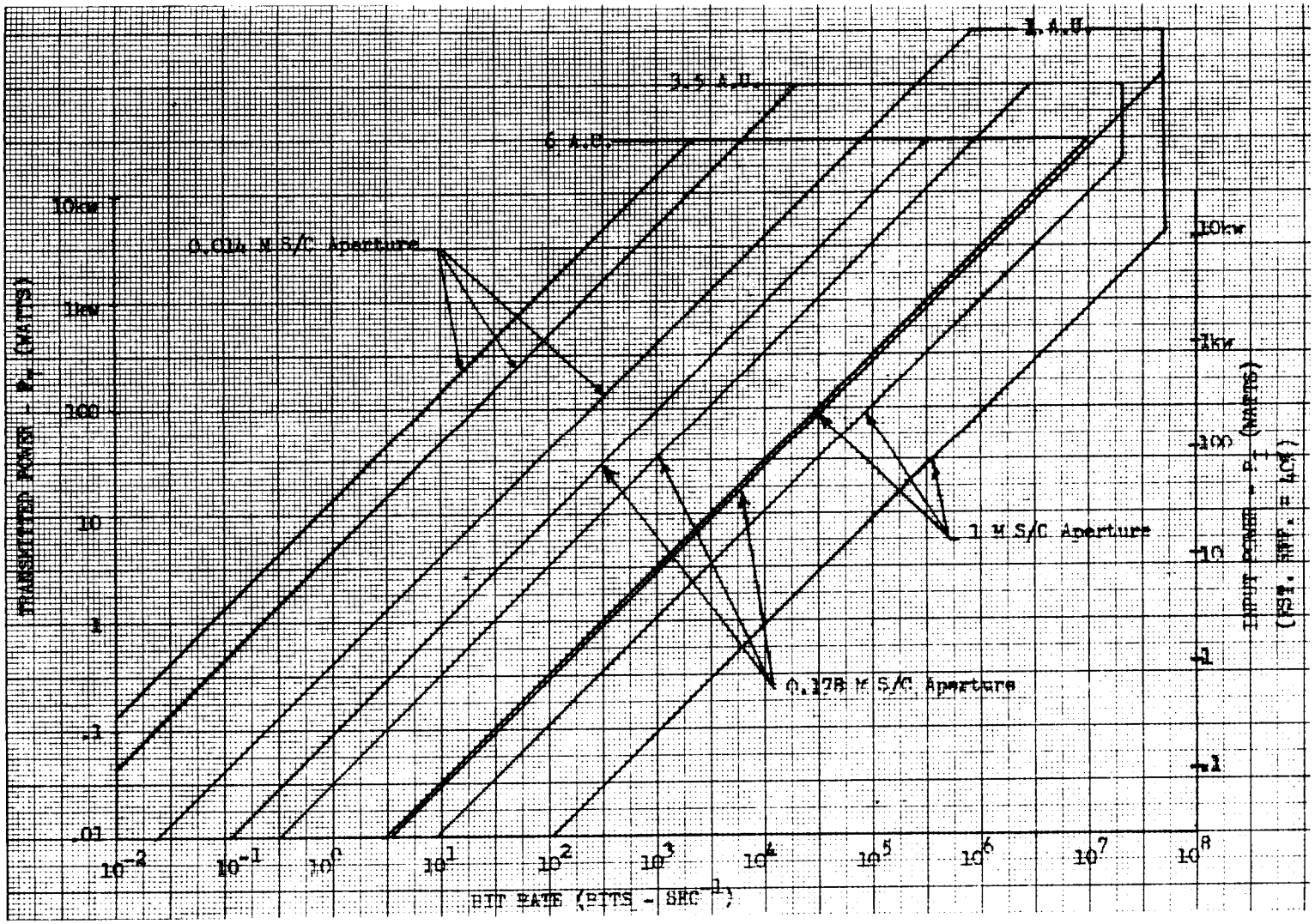

Figure 11. Interplanetary Communication System Comparison—
Power Versus Bit Rate, CO_2 Heterodyne

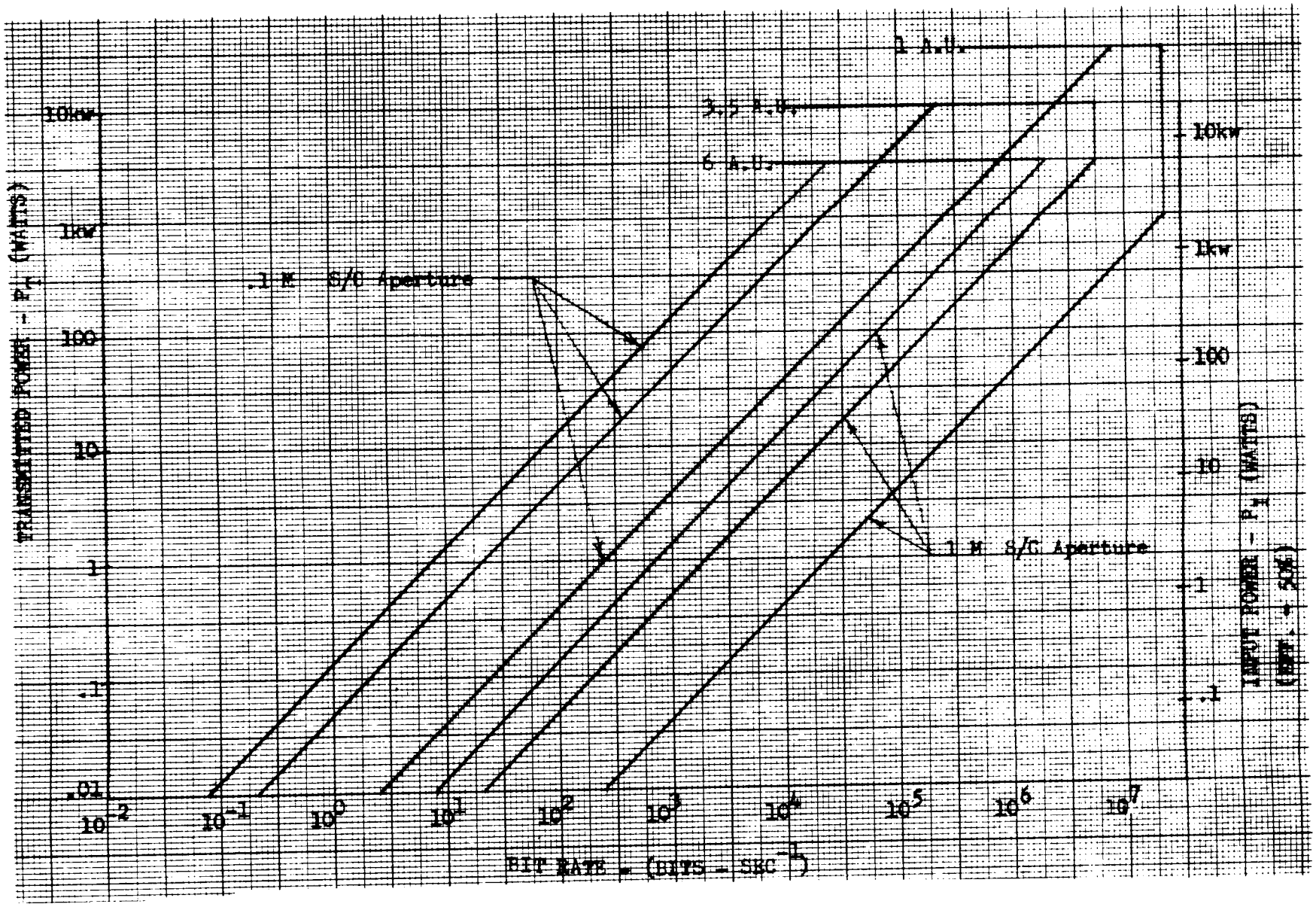

Figure 12. Interplanetary Communication System Comparison - Power Versus Bit Rate, GaAs Non-Coherent

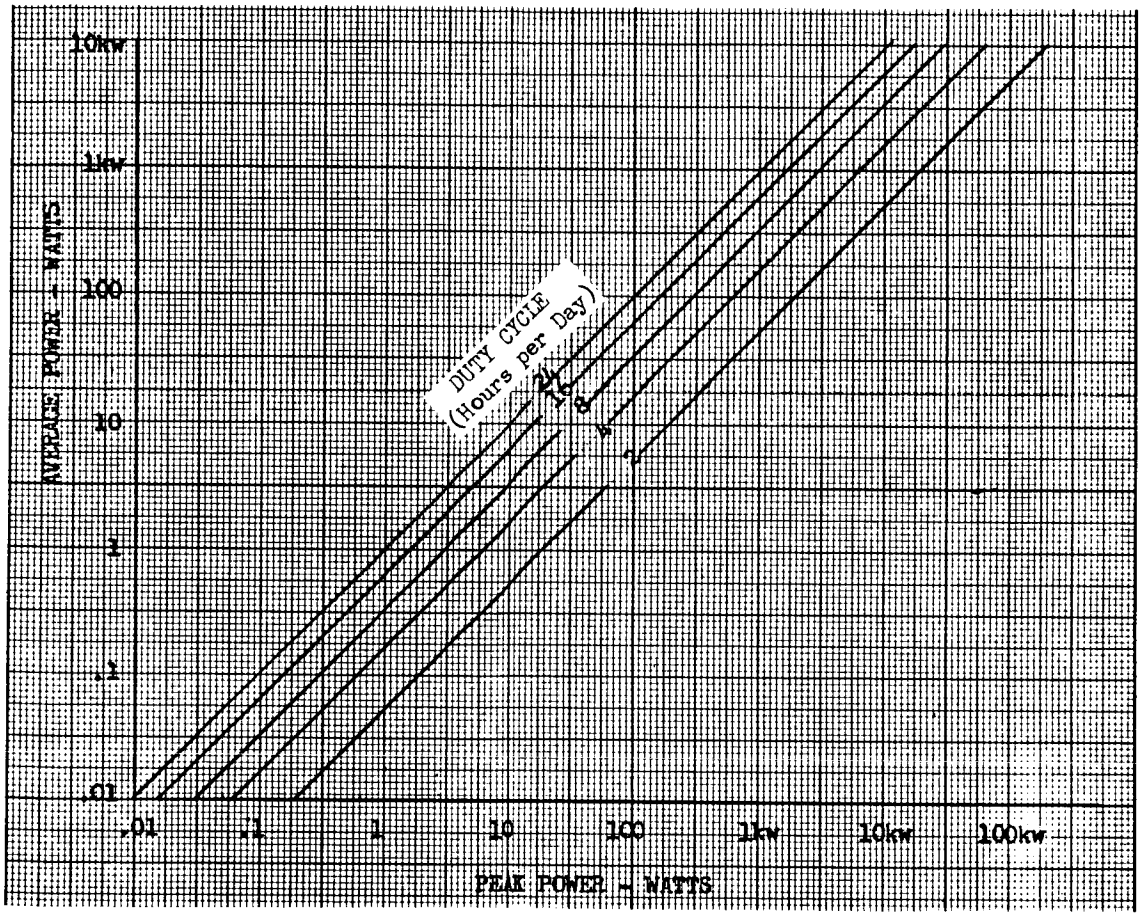

Figure 13. Average Power Versus Peak Power

Table 9. Interplanetary Communication System Comparison for a Mars Mission

Parameter	S-Band	Millimeter Waves	CO_2 Laser	GaAs Laser
Frequency	2.3 GHz	94 GHz	28,300 GHz	357,000 GHz
Spacecraft antenna diameter (meters)	15.2	4.58	1	1
BR^2 product (bps-km^2)	1.03×10^{21}	1.03×10^{21}	1.03×10^{21}	1.03×10^{21}
Transmitted power from (Figure 5) (watts)	5.3 W	75	4	1.8
Estimated efficiency (percent)	50	40	40	50
Input power - peak (watts)	10.6 (from Figure 8)	188 (from Figure 9)	10 (from Figure 10)	3.6 (from Figure 11)
Duty cycle (hours)	4	4	4	4
Average daily power requirements (from Figure 12) (watts)	1.8	31.3	1.66	0.6

Notes: Range = 1.5×10^8 kilometers
Bit rate = 4.6×10^4 bits per second

Table 10. Interplanetary Communication System Comparison for a Ceres Mission

Parameter	S-Band	Millimeter Waves	CO_2 Laser	GaAs Laser
Frequency	2.3 GHz	94 GHz	28,300 GHz	357,000 GHz
Spacecraft antenna diameter (meter)	15.2	4.58	1	1
BR^2 product (bps-km^2)	1.24×10^{22}	1.24×10^{22}	1.24×10^{22}	1.24×10^{22}
Transmitted power (from Figure 5) (watts)	66 w.	900 w	50	22.2
Estimated efficiency (percent)	50	40	40	50
Input power-peak (watts)	132 w (from Figure 8)	2250 w (from Figure 9)	125 (from Figure 10)	44.6 (from Figure 11)
Duty cycle (hours)	4	4	4	4
Average daily power requirements (from Figure 12) (watts)	22	375	20.8	7.4

Notes: Range = 5.2×10^8 kilometers
Bit rate = 4.6×10^4 bits per second

Table 11. Interplanetary Communication System Comparison for a Jupiter Mission

Parameter	S-Band	Millimeter Waves	CO_2 Laser	GaAs Laser
Frequency	2.3 GHz	94 GHz	28,300 GHz	357,000 GHz
Spacecraft antenna diameter (meters)	15.2	4.58	1	1
BR^2 product (bps-km^2)	3.67×10^{22}	3.67×10^{22}	3.67×10^{22}	3.67×10^{22}
Transmitted power (from Figure 5) (watts)	200	2,800	160	70
Estimated efficiency (percent)	50	40	40	50
Input power-peak (watts)	400 (from Figure 8)	7000 (from Figure 9)	400 (from Figure 10)	140 (from Figure 11)
Duty cycle (hours	4	4	4	4
Average daily power requirements (from Figure 12) (watts)	67	1165	67	23

Notes: Range = 8.94×10^8 kilometers
Bit rate = 4.6×10^4 bits per second

TYPICAL APPLICATIONS

Typical missions to Mars, Ceres, and Jupiter are analyzed to illustrate the use of the parametric data. Tables 9 through 11 show the significant parameters for each of the four candidate systems for these three missions. In all cases, compacted color TV was assumed to be transmitted at one frame each five seconds and that transmission occurs at the rate of four hours per day. Figure 8 indicates the bit rate would be 4.6×10^4 bits/second. This bit rate, when multiplied by the range squared, produces a BR^2 value for Mars of 1.03×10^{21}. The transmitted power for the various systems can be obtained from Figure 6. In the case of S-band it was assumed that a 15.2-meter (50-foot) unfurlable spacecraft antenna is used. This produces a transmitted power requirement of 5.3 watts. For the millimeter system, a 4.58-meter spacecraft antenna is used which approaches the upper limit of 70 decibels gain for a parabolic antenna. The comparable power for this system is 75 watts. The optical systems were analyzed on the basis of diffraction limited optics. The largest practical size is considered to be a 1-meter aperture. This size aperture is assumed for both the CO_2 laser and the GaAs laser. This results in 4 watts for the CO_2 laser and 1.8 watts for the GaAs laser.

The input power requirements for the four systems being analyzed have been determined and the data are entered in Table 9. Using the peak input power values so calculated and the arbitrary duty cycle of 4 hours, the average power on a 24-hour basis can be determined using Figure 13. The average power for S-band, millimeter, CO_2, and GaAs for the Mars case is 1.8, 31.3, 1.66, and 0.6, respectively.

Missions to Ceres and Jupiter (Tables 10 and 11) require higher power. The highest peak input power is 7,000 watts for Jupiter, using the millimeter system. This is only slightly more than 1 kw at the 4 hour/day duty cycle. It was assumed that the tracking problem could be solved for all these systems for purposes of illustration.

SUBSYSTEM ANALYSIS

As S-band is not significantly affected by weather and because pointing and tracking is considerably less restrictive, it appears that S-band will hold a significant position in post-1980 communications. The assumed unfurlable, 15.2-meter (48.7-decibel gain) parabolic antenna is considered to be about as large as is practical to deploy and retract, and thus better antenna efficiency is desirable. The only significant drawback of S-band is the limited bandwidth. If compaction ratios of 10:1 or more are not achieved, the higher frequency systems may be selected over S-band.

Millimeter waves require power an order of magnitude higher than required for S-band, but the antennas and other equipment required are much smaller. For spacecraft applications where the craft is spun to produce artificial gravity, a small retractable antenna or an array former on the surface of the vehicle is attractive. The millimeter systems would be more competitive if antenna arrays could be developed that would greatly exceed the 70-db figure assumed for both the spacecraft and ground terminals. Also, system noise temperature may be decreased, although only a 3-db gain can be achieved in this area as the sky temperature contributes 215 degrees of the 400 K system noise temperature assumed. The millimeter system is an attractive successor to S-band because the equipment can be co-located at the S-band stations and much of the existing electronics and physical facilities can be shared or used to reduce costs.

Due to high antenna gains possible with lasers, wide band, high data-rate communications can be achieved with significantly smaller power requirements. The transition from today's components and devices to space-qualified hardware, however, will require significant breakthroughs in many areas and a heavy expenditure in research and development dollars. Also, the present investment of the ground-based network will have to be increased with optical receiving stations located in areas having a low probability of rain, snow, cloud cover, or fog (e.g., certain mountain peaks). An alternative to special ground stations for laser systems is the use of satellite relays where lower frequency is used to penetrate cloud cover. Tracking would still be a serious problem. In fact, it would probably be more difficult to acquire and track satellites than to acquire and track Earth based stations. The special stable platform and optical telescope required for lasers and the difficulty of computing lead angles tend to offset the advantages offered by laser systems.

Ultimately, any system becomes limited by power and data rate. Optical systems are inherently capable of transmitting wide bandwidths due to the high frequency of the light source. They can also transmit high data rates for less power, provided tracking/pointing problems are solved. Therefore, optical systems must ultimately be developed if high resolution, live motion, real time color television becomes a requirement. The state-of-the-art is such today that only the feasibility of using optics for such purposes can be visualized. There is much research and development to be done in basic components, system techniques, and supporting hardware before a highly reliable, workable system can replace the present microwave spacecraft and ground terminals.

CONCLUSIONS

A parallel research and development approach appears desirable for the continued development of communication subsystems. S-band should be

developed to its full capability, since it probably will fulfill many interplanetary requirements for the next 20 to 30 years. On the other hand, smaller, lighter, and higher data-rate systems will be required eventually and research must be continually applied. A gradual transition from S-band to either millimeter or optical systems should be developed to take advantage of their favorable system characteristics.

PROPULSION SUBSYSTEM PARAMETRIC ANALYSIS

Propulsion subsystem scaling equations were developed which define the engine and pressurization system weights as a function of the engine characteristics. The basic scaling equations defining engine weights were provided by the NASA/MAD and were modified to reflect the effects of engine type. The characteristics of candidate chemical propellant combinations were established and representative propellants selected on the basis of performance and storability considerations.

PROPULSION SUBSYSTEM SCALING EQUATIONS

Investigations were undertaken to verify the form of the NASA/MAD furnished rocket engine weight scaling equation and to determine appropriate coefficients for use with these equations for various engine types. Both chemical and nuclear engines were considered.

Chemical Engine Weights

The equation provided has the following form:

$$W_c = \left(\frac{T}{\tau} + Z\right) n$$

where

W_c = weight of chemical engine cluster, kg

T = thrust of each engine, kg

τ = engine thrust-to-weight ratio

Z = constant (nominal value = 45)

n = number of engines in cluster

To develop propulsion and engine thrust-to-weight trend predictions, liquid propellant rocket engines have been investigated, accounting for past developments, scheduled future developments, and projected rocket engine capabilities during the next quarter century. Figure 14 presents engine thrust-to-weight ratio trends. It will be noted that there is, and will continue to be, a distinct difference in engine weight between engines employing

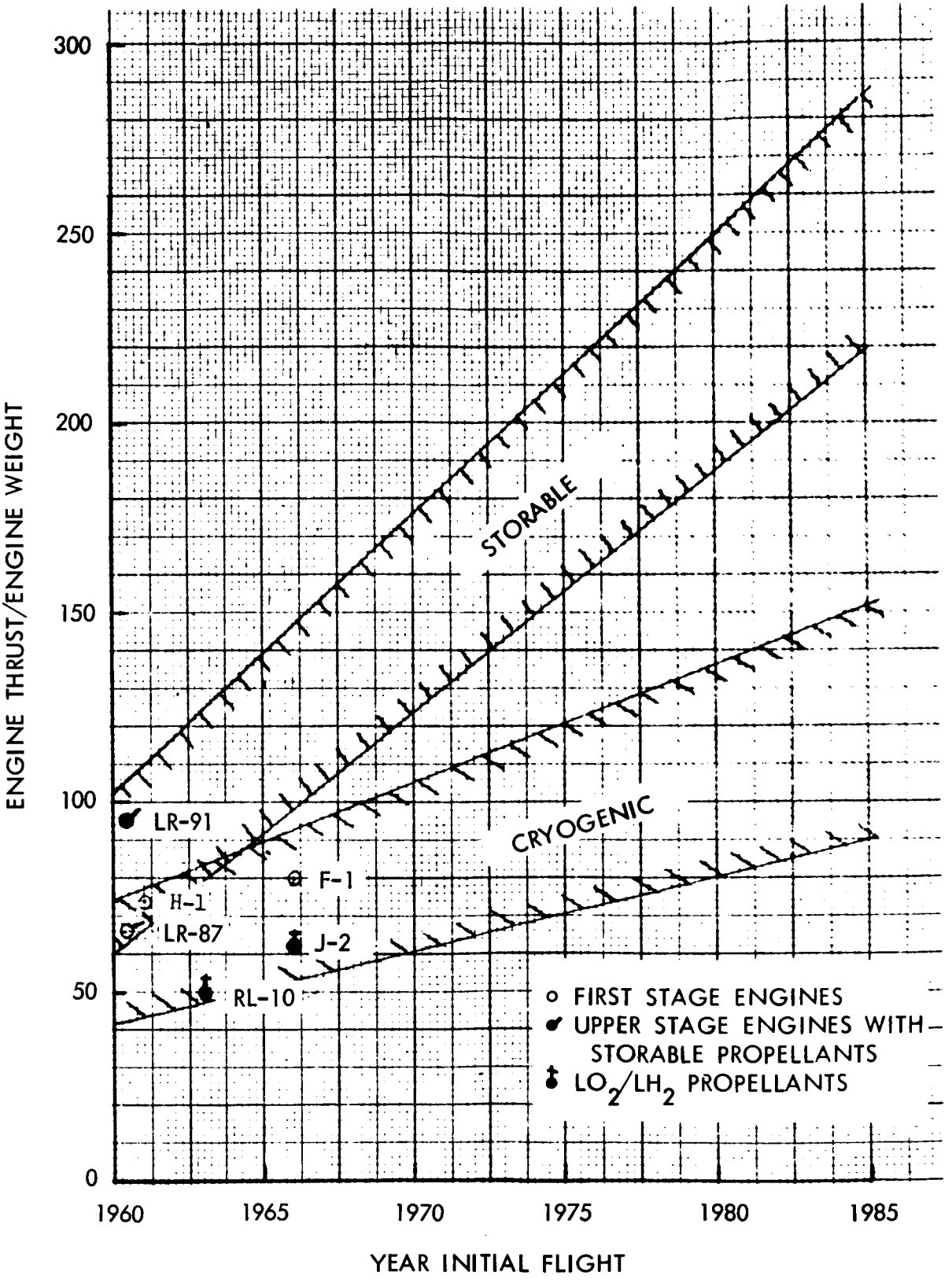

Figure 14. Engine Thrust/Engine Weight Versus Year of Initial Flight

cryogenic propellants and those using the storable propellants. This difference is due primarily to the relatively high density exhibited by the storable propellant combinations and the resulting reduction in turbomachinery and thrust chamber weight. The predicted thrust-to-weight ratio trends are based on the assumption that progress in future years will be at the same rate as has been evidenced during the past 15 years.

Engine thrust-to-weight ratios as a function of engine thrust level were examined for various types of liquid propellant engine designs. These data were correlated with the NASA/MAD chemical engine weight scaling equation and an appropriate coefficient for use with these engine types derived. The engine thrust-to-weight ratios are based on current engine designs projected to higher thrust levels.

Figure 15 indicates the thrust-to-weight relationship exhibited by the conventional nominal chamber pressure (500 - 1000) psia pump-fed engine designs. The projected trend curves shown on Figure 15 were established and scaling equation coefficients estimated for these engines. The value of the coefficient (K) is shown in Figure 16 as a function of vacuum thrust. Similar data regarding pressure fed storable liquid propellant engines of conventional design are shown in Figures 17 and 18.

Investigations of the engine thrust-to-weight relationship as a function of thrust magnitude have also been conducted for the more advanced engine design concepts. These include the current high chamber pressure (2000 - 3000 psia) engine development and the proposed aerospike nozzle configuration engines. Figure 19 shows the trend indicated for high chamber pressure engine concepts. The data points shown on the figure for the storable propellant engines are based on the Aerojet-General Ares studies. The data points for the LO_2/LH_2 propellants are based on Pratt & Whitney design data. Figure 20 provides the estimated coefficient for these engine types for use in the chemical engine weight scaling equation. In Figures 21 and 22, engine thrust-to-weight data estimates and the appropriate scaling equation coefficients are provided for the aerospike engine design concepts.

These data indicate that the NASA/MAD chemical engine weight-scaling equation that was furnished is in good general agreement with rocket engine design data; and that by the employment of an appropriate numerical coefficient, the equation will provide realistic weight estimates for a large variety of liquid propellant engine designs and thrust levels.

Nuclear Engine Weights

The solid core nuclear engine weight equation was given by the NASA/MAD in the following form:

$$W_N = (\alpha T + \beta)\, n$$

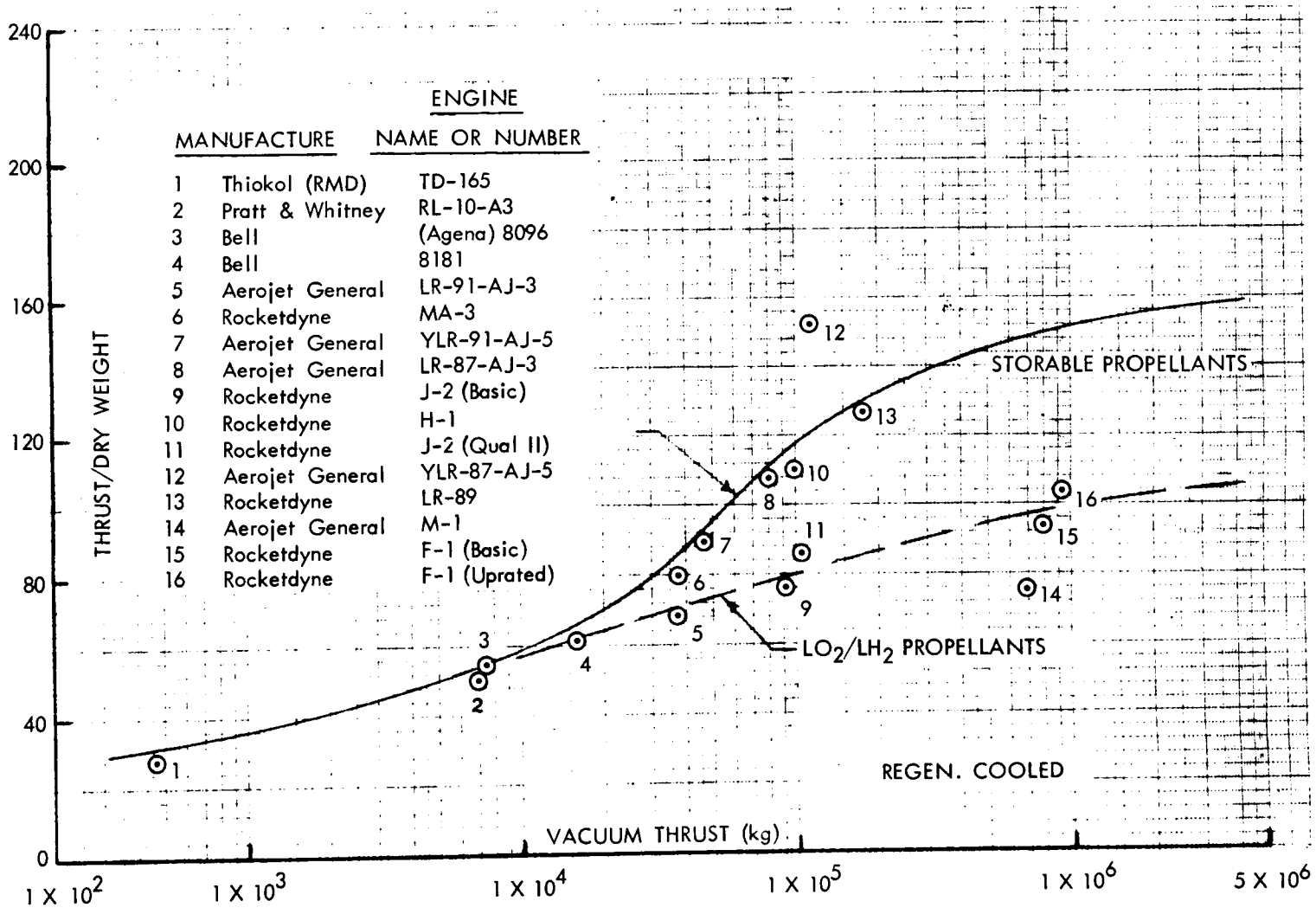

Figure 15. Nominal Pump-Fed Engine Thrust-to-Weight Ratio

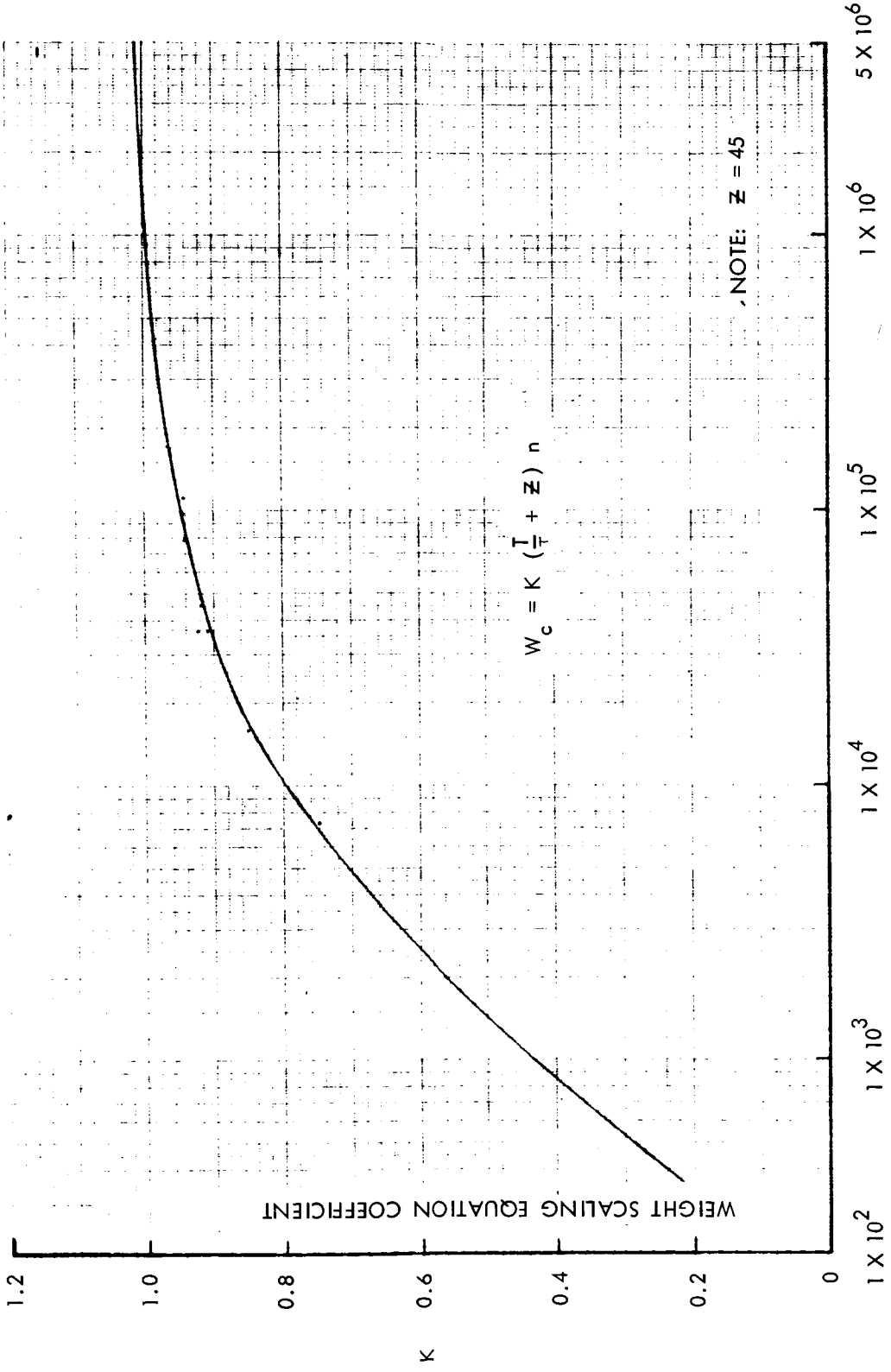

Figure 16. Nominal Pump-Fed Engine Weight Scaling Coefficient

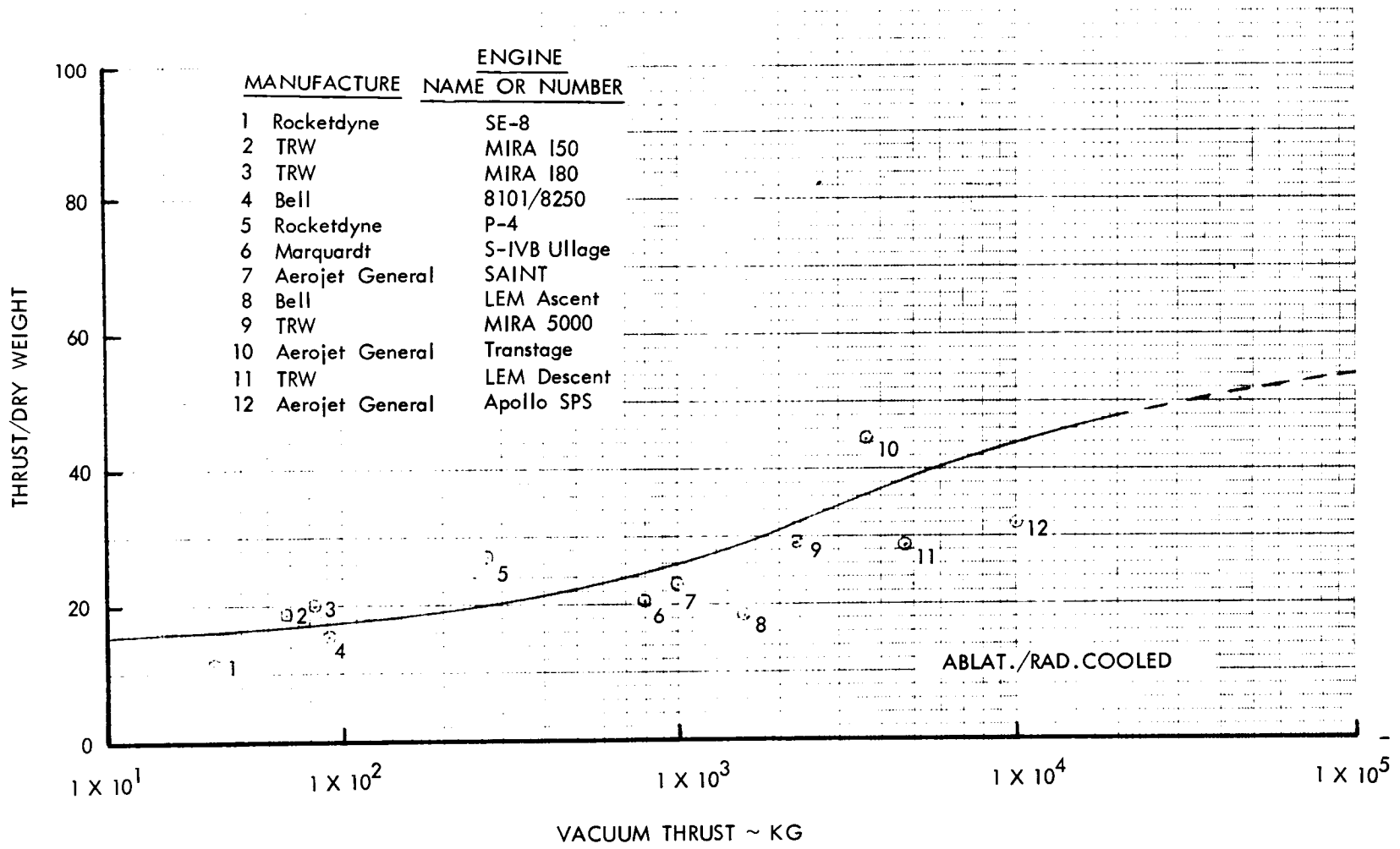

Figure 17. Pressure-Fed Storable Propellant Engine Thrust-to-Weight Ratio

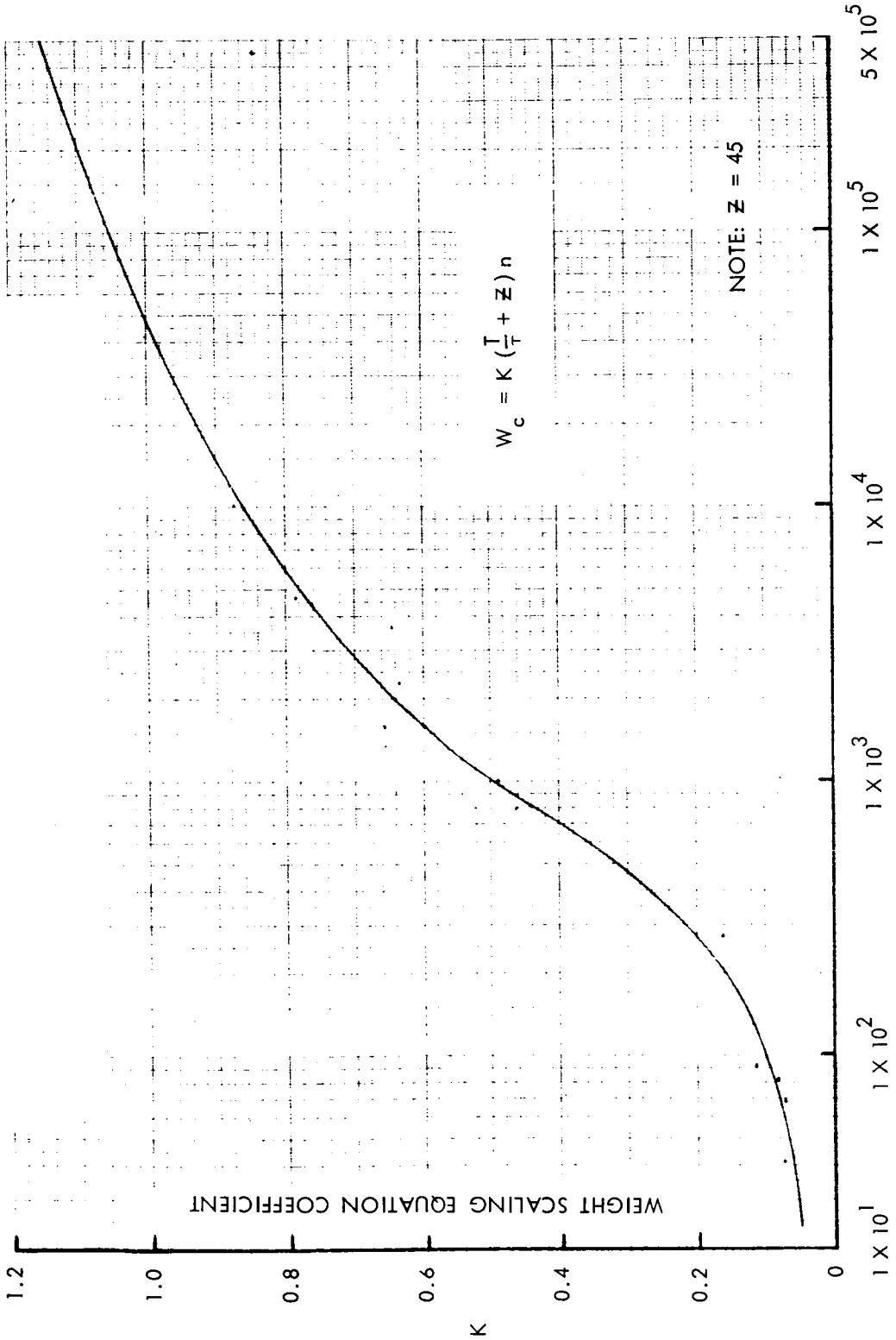

Figure 18. Storable Propellant Pressure-Fed Engine Weight Scaling Coefficient (Ablat/Rad. Thrust Chamber)

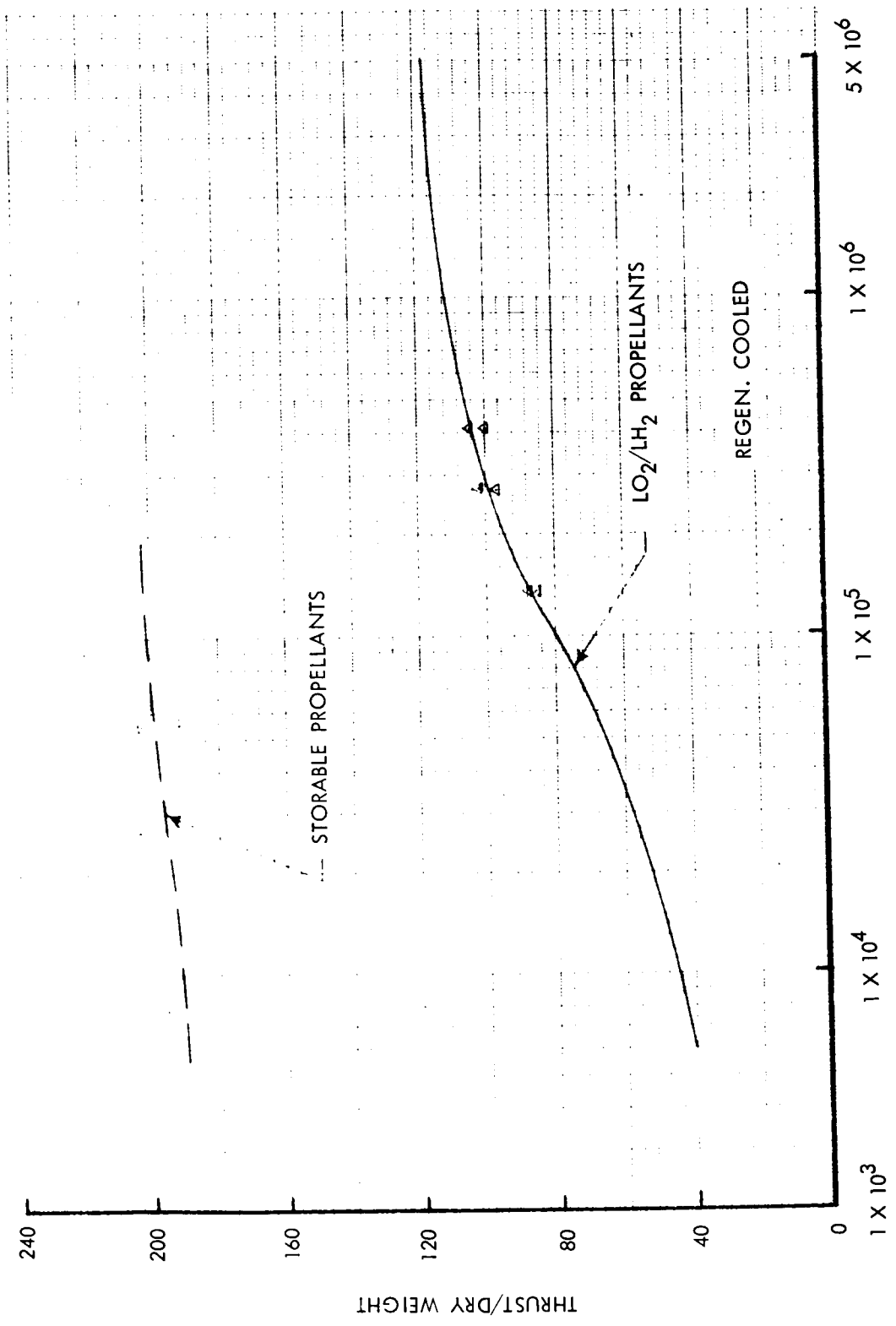

Figure 19. Representative High Chamber Pressure Engine (Pump-Fed) Thrust-to-Weight Ratio

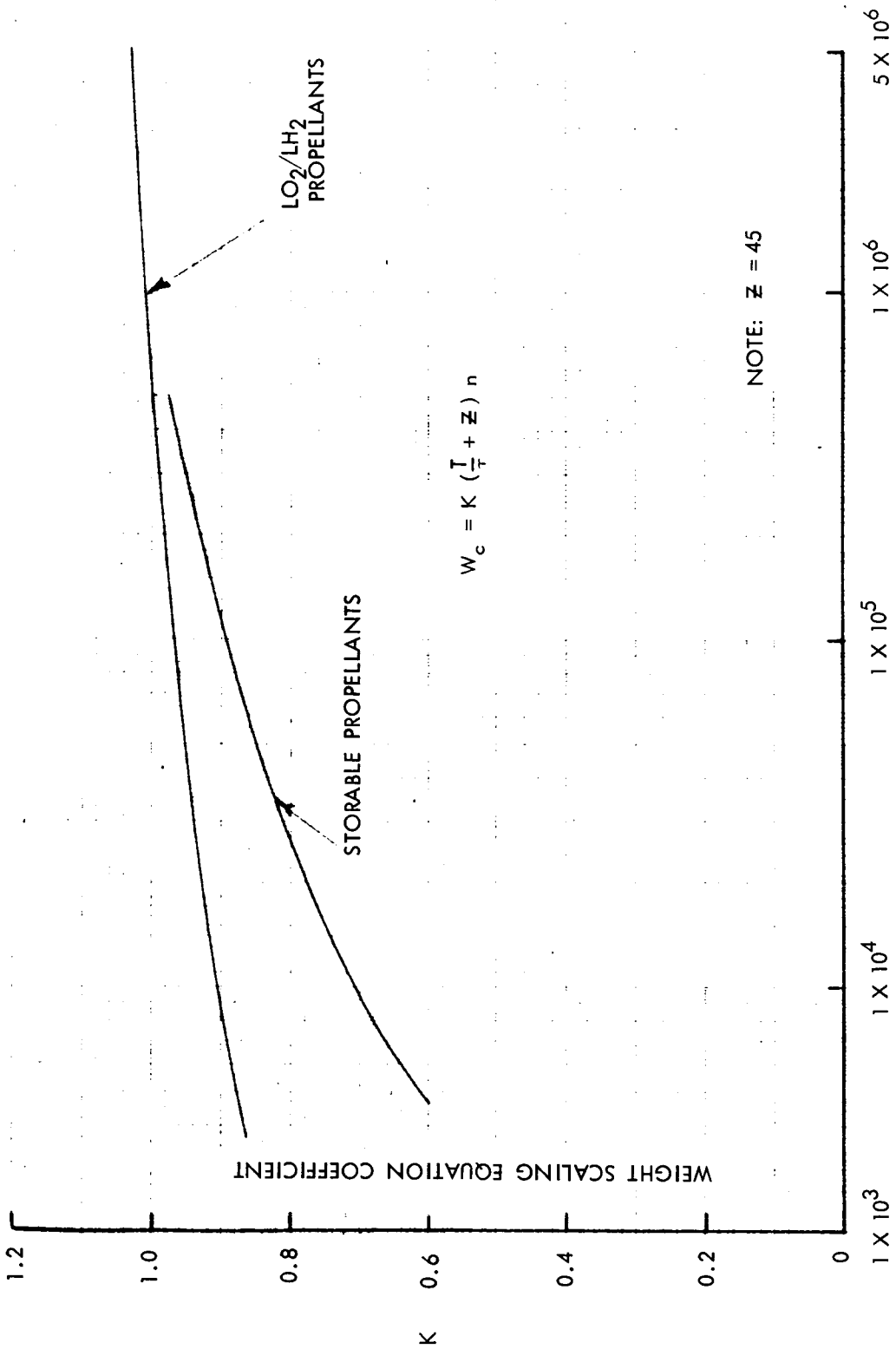

Figure 20. High Chamber Pressure Engine (Pump-Fed) Scaling Coefficient

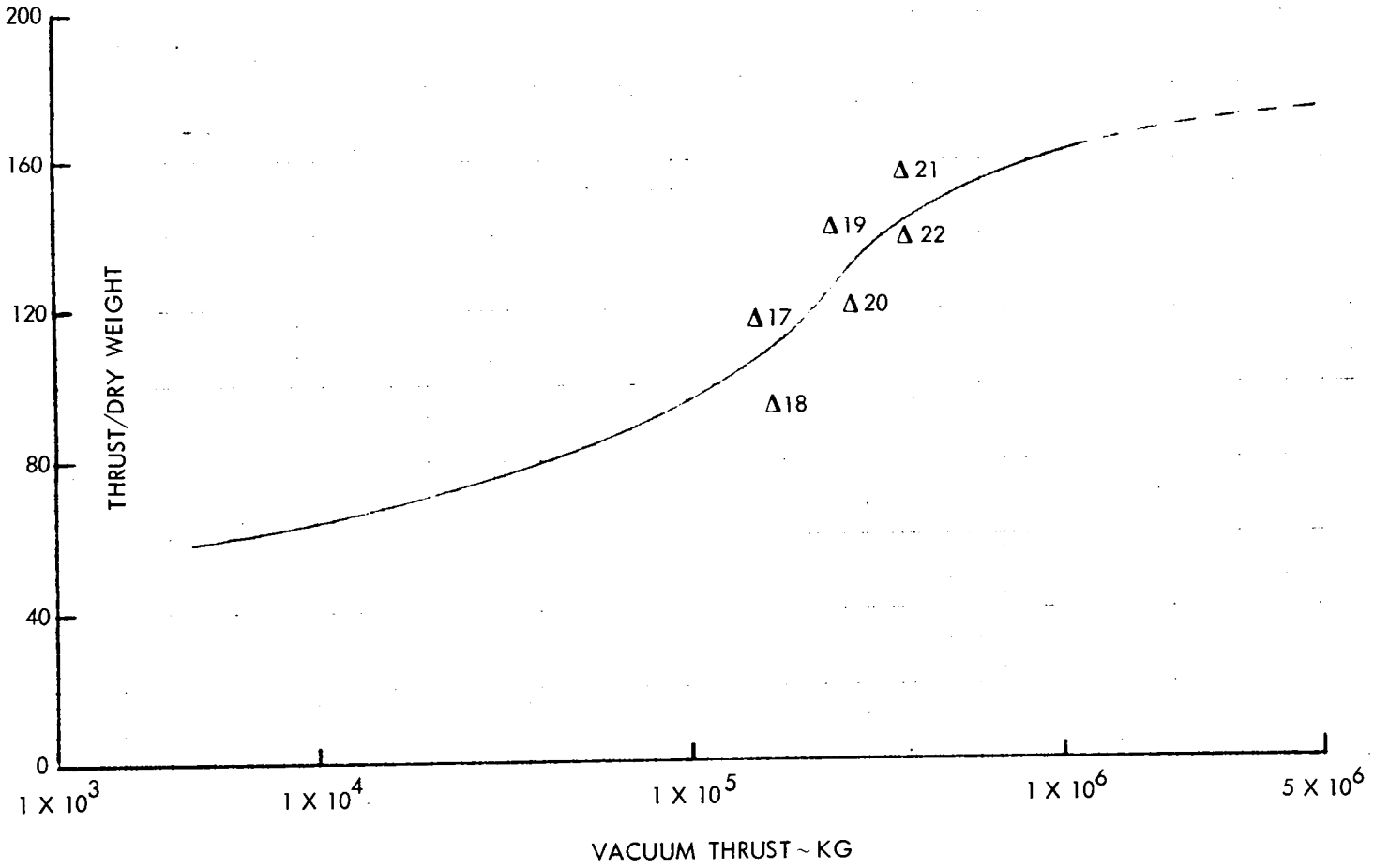

Figure 21. Representative Toroidal Aerospike Engine (Pump-Fed) Thrust-to-Weight Ratio

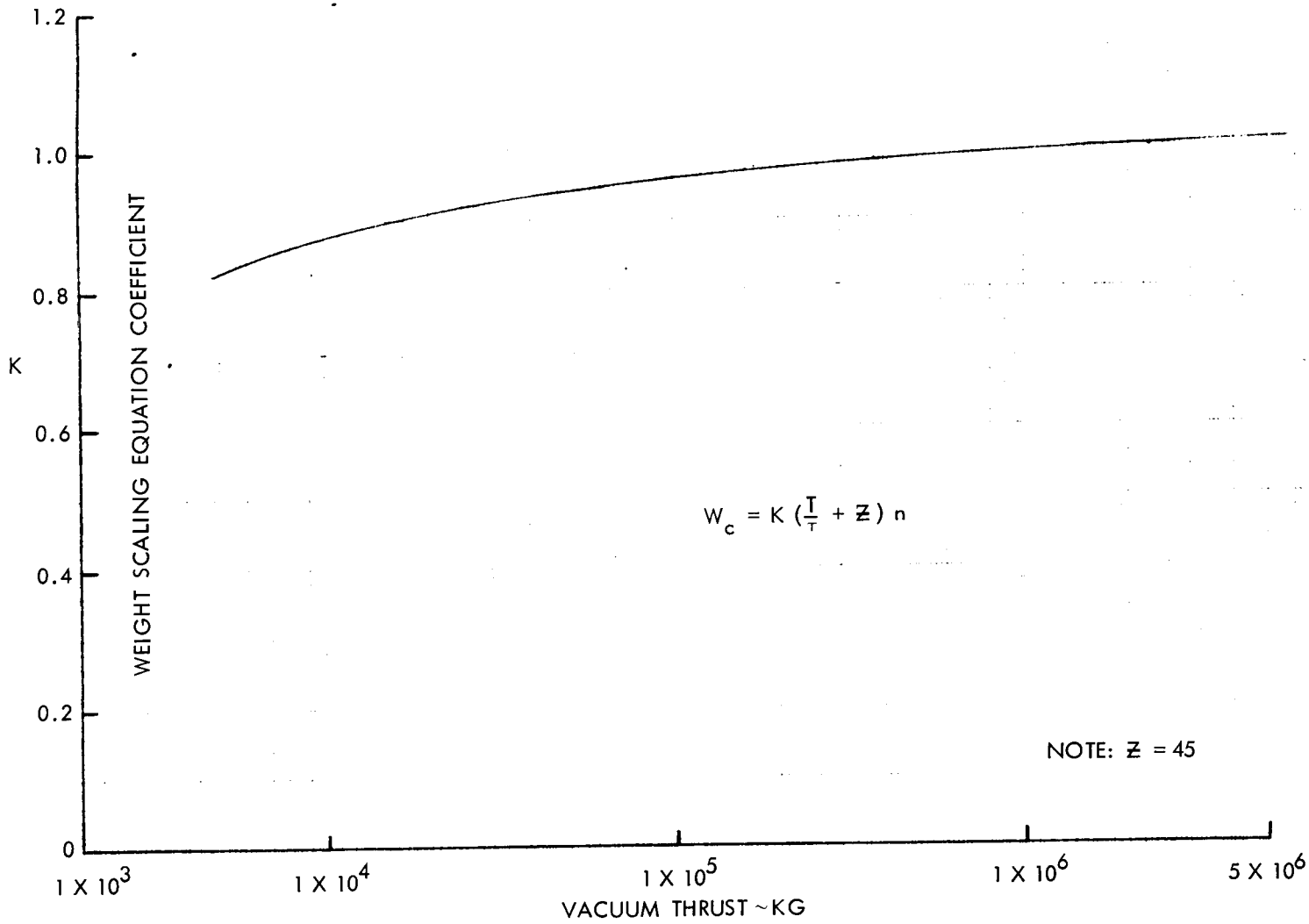

Figure 22. Toroidal Aerospike Engines (Pump-Fed) Weight Scaling Coefficient

where

W_N = weight of nuclear engine cluster including radiation shield, K_g

T = thrust of each engine, Kg

n = number of engines in cluster

α = constant (nominal value = 0.129)

β = constant (nominal value = 3310)

This equation was compared against predicted nuclear engine weight estimates as a function of thrust magnitude. Comparative data were derived from several sources, and it was determined that the proposed equation agrees reasonably well with the most recent estimates of nuclear engine weights.

PROPULSION SUBSYSTEM ANALYSIS

Potential chemical propellants were examined and several combinations selected as being representative of the chemical systems applicable to the missions considered during this study. Tank pressure and propellant temperature ranges were established for several propellant constituents. To generate representative chemical and nuclear propulsion subsystems weight data, parametric tank pressurization systems were generated.

Candidate Propellant Combinations

The propellants considered prior to the selection of propellant combinations representative of the chemical systems are presented in Table 12. This table lists various propellants and their appropriate performance levels, physical characteristics, and thermal properties. Also shown in the table is a criterion which has been developed which is an approximate measure of the in-space storage capability of the various candidate propellant combinations. It is, in effect, the ability of the propellant to absorb heat through bulk temperature increases and evaporative cooling (through venting), divided by the potential heat absorption rate. The heat absorption rate is proportional to the bulk liquid temperature less the environmental temperature. Those combinations which exhibit the higher values have the greater degree of storability.

A criterion for determining the relative cooling capability of these propellant combinations in regenerative rocket engines is also presented in Table 12. This is of particular importance to large propulsive stages, where

Propellants	Opt. Mixture Ratio	Bulk Density (lb/ft^3)	Vacuum Specific Impulse (sec)	Vacuum Density Impulse 1000 lb-sec ft^3	Chamber Temp (°F)	Fre P
F_2/N_2H_4	2.27	81.7	430	35.1	7140	
N_2F_4/N_2H_4	3.24	89.2	390	34.8	6950	
OF_2/MMH	2.42	78.3	416	32.6	6620	
N_2F_4/MMH	3.38	85.5	380	32.5	6600	
87.5% FLOX/MMH	2.75	77.0	421	32.4	7080	
ClF_5/MHF-3[1]	2.60	90.4	358	32.4	6350	
N_2F_4/NH_3	4.50	78.3	381	29.8	6660	
82% FLOX/CH_4	5.75	66.1	424	28.0	7090	-
OF_2/B_2H_6	3.75	62.4	444	27.7	6990	-
O_2/CH_4	3.32	51.2	379	19.4	5370	-
F_2/H_2	11.0	35.0	479	16.8	6660	-
O_2/H_2	4.80	19.8	461	9.1	5070	-

NOTE:

1. MHF-3 = 86 percent MMH + 14 percent N_2H_4

2. 100 psia to vacuum, 100 percent theoretical shifting equilibrium, ϵ = 60

FOLDOUT FRAME

Table 12. Comparison of Candidate Liquid Propellants

Fuel Temp (°F)			Oxidizer Temp (°F)			Chamber Regenerative Cooling Merit Rating	Storability Criterion Temperature at Environmental Temperature of		
	Boiling Point			Boiling Point					
ezing oint	14.7 psia	90 psia	Freezing Point	14.7 psia	90 psia		150°F	0°F	-150°F
35	236	355	-363	-307	-266	1.48	0.0202	0.0126	0.0072
35	236	355	-264	- 99	-23	1.56	0.0218	0.0318	0.0184
·62	189	305	-371	-230	-177	1.11	0.0222	0.0237	0.0255
·62	189	305	-264	-99	-23	1.13	0.0228	0.0398	0.0264
·62	189	305	-363	-306	-264	0.85	0.0202	0.0210	0.0169
·65	194	310	-153	8	104	1.32	0.0302	0.0377	0.0170
·62	189	305	-153	8	104	1.26	0.0305	0.0380	0.0172
:96	-259	-197	-363	-305	-262	0.15	0.0049	0.0079	0.0207
:66	-135	-61	-371	-230	-177	0.18	0.0079	0.0183	0.0410
:96	-259	-197	-362	-297	-258	0.28	0.0068	0.0110	0.0296
435	-423	-408	-363	-307	-266	6.29	0.0040	0.0057	0.0105
435	-423	-408	-362	-297	-258	15.4	0.0067	0.0096	0.0171

FOLDOUT FRAME

it may become impractical to design and develop ablative cooled engines at the required thrust level due to the excessive weight penalties incurred. Those combinations which exhibit the higher values have the greater cooling capacity.

Selected Propellant Combinations

To provide the basis for the propulsion subsystem design data, the following propellant combinations were selected as representative of the chemical systems:

LO_2/LH_2
OF_2/B_2H_6
OF_2/MMH
87.5%FLOX/MMH
82%FLOX/CH_4

The above combinations were selected, in part, on the basis of performance and storage considerations. Some of the thermal properties of the propellant constituents are listed in Table 13.

Table 13. Selected Propellant Constituent Properties

Propellant Constituent	Freezing Point		Normal Boiling Point (1 Atmos)		Critical Temperature	
	°F	°R	°F	°R	°F	°R
O_2	-362	98	-297	163	-182	278
H_2	-435	25	-423	37	-400	60
OF_2	-371	69	-230	230	-73	387
B_2H_6	-266	194	-135	325	53	513
MMH	-62	398	189	649	593	1053
87.5% FLOX	-363	97	-305	155	-203	257
CH_4	-296	164	-259	201	-116	344

Liquid oxygen/liquid hydrogen was selected as the propellant combination representative of the high performance levels and storability characteristics which are consistent with large orbital launch vehicles. There is also a wealth of experience with this propellant combination and the possibility exists that existing (e. g., J-2) engines can be used in upper stages. Also, it may be possible to utilize this propellant combination in the mission module life support subsystem.

The remaining propellant combinations exhibit a reasonable degree of in-space storability when both boiling and freezing characteristics are considered. The OF_2/B_2H_6 and 82%FLOX/CH_4 represent high performance, moderately space-storable combinations. An 87. 5%FLOX/MMH propellant provides a somewhat lower specific impulse with a substantial increase in bulk density. It is a combination that is readily available; however, it does not exhibit the same storability characteristics as does OF_2/MMH. At present, OF_2 is being produced in limited quantities and the costs of establishing the production rates required for the missions considered in this study may preclude its use. Both 87. 5%FLOX/MMH and OF_2/MMH are somewhat more storable overall than either OF_2/B_2H_6 or 82%FLOX/CH_4 at the expense of performance potential. The 82%FLOX/CH_4 is inexpensive, has a moderate density, high specific impulse, but it has the lowest regenerative cooling capability. The OF_2/MMH provides the greatest potential for use in large regenerative cooled engines since it has an 11 percent margin over that required.

During subsequent propulsion module and system analyses, LO_2/LH_2 and 87. 5%FLOX/MMH were assumed as the nominal cryogenic and storable propellants, respectively. A bulk density of 317 kg/m^3 (19. 8 lb/ft^3), a mixture ratio of 4. 80, and a specific impulse of 450 seconds were used during the sizing of LO_2/LH_2 propulsion modules. The corresponding values for 87. 5%FLOX/MMH were 1233 kg/m^3 (77. 0 lb/ft^3), 2. 75, and 387 seconds, respectively.

Tank Pressure and Propellant Temperature Regimes

To establish the propellant tank pressure and propellant temperature regimes for the selected propellant combinations in this study, representative pump-fed and pressure-fed systems were assumed. Pressure schedules consistent with each type were then calculated, and the allowable temperature rise regime for each was established.

Vapor pressure data as a function of temperature for several propellant constituents are provided in Figures 23 through 27.

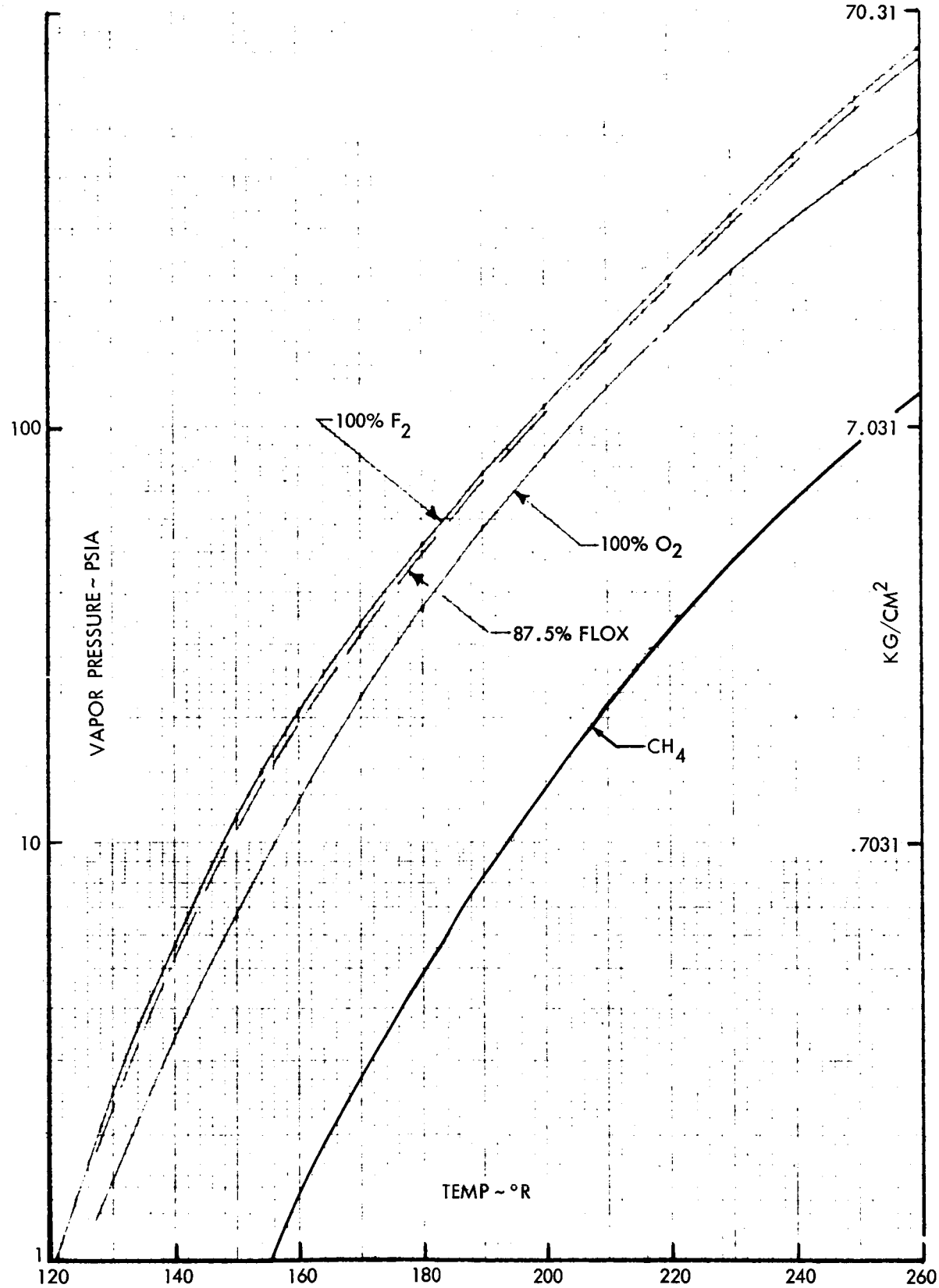

Figure 23. F_2, O_2, CH_4 and FLOX Vapor Pressure Versus Temperature

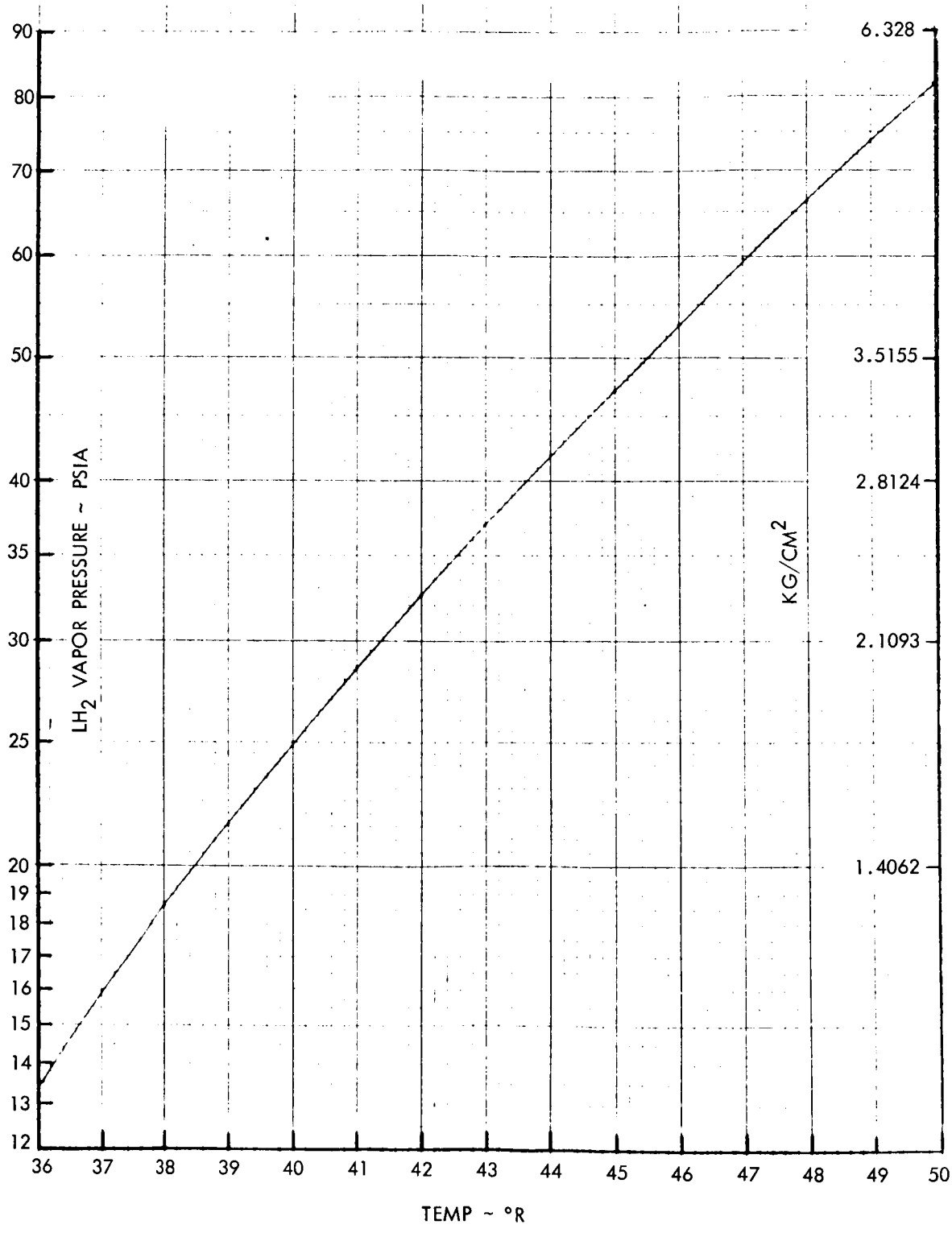

Figure 24. LH_2 Vapor Pressure Versus Temperature

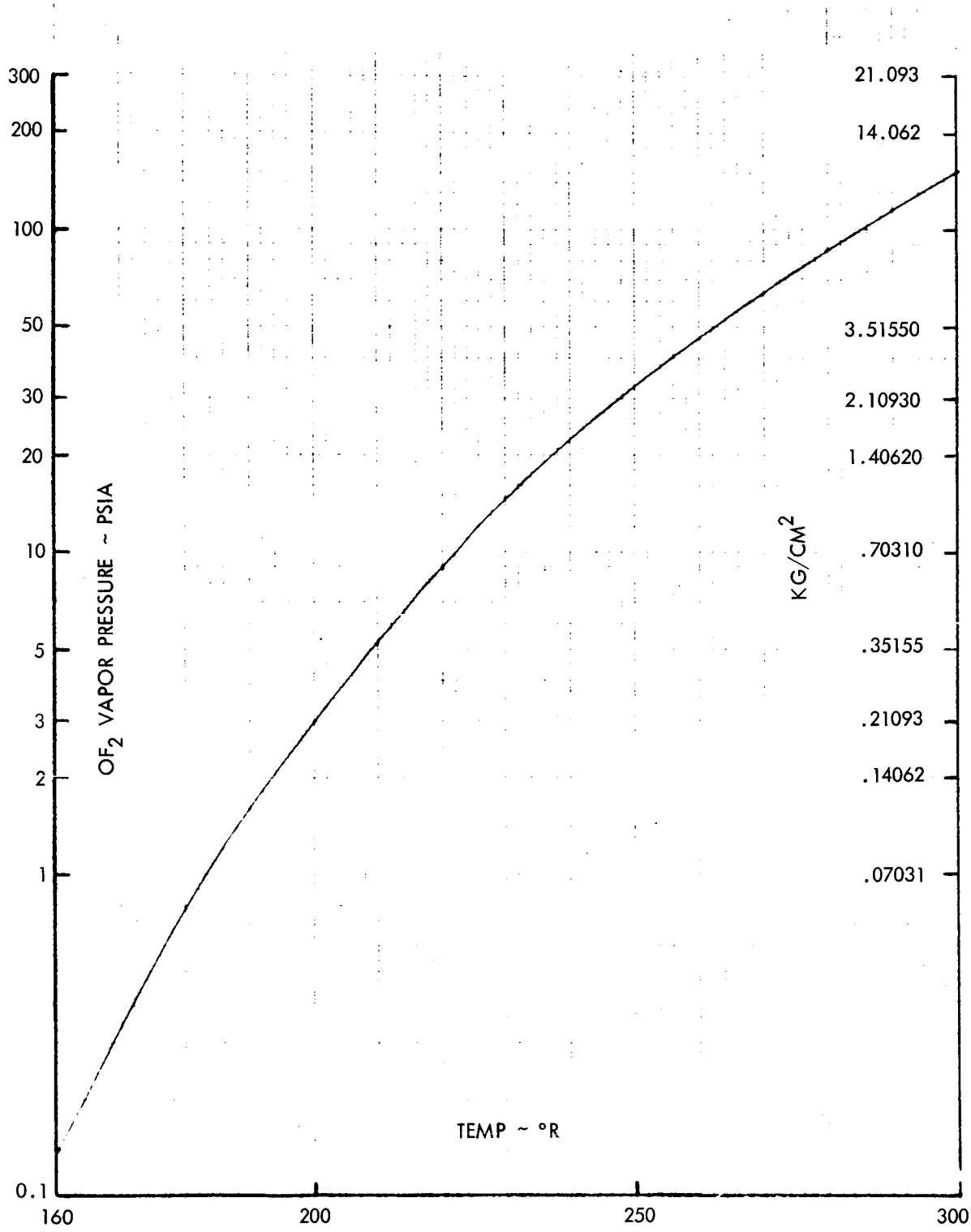

Figure 25. OF_2 Vapor Pressure Versus Temperature

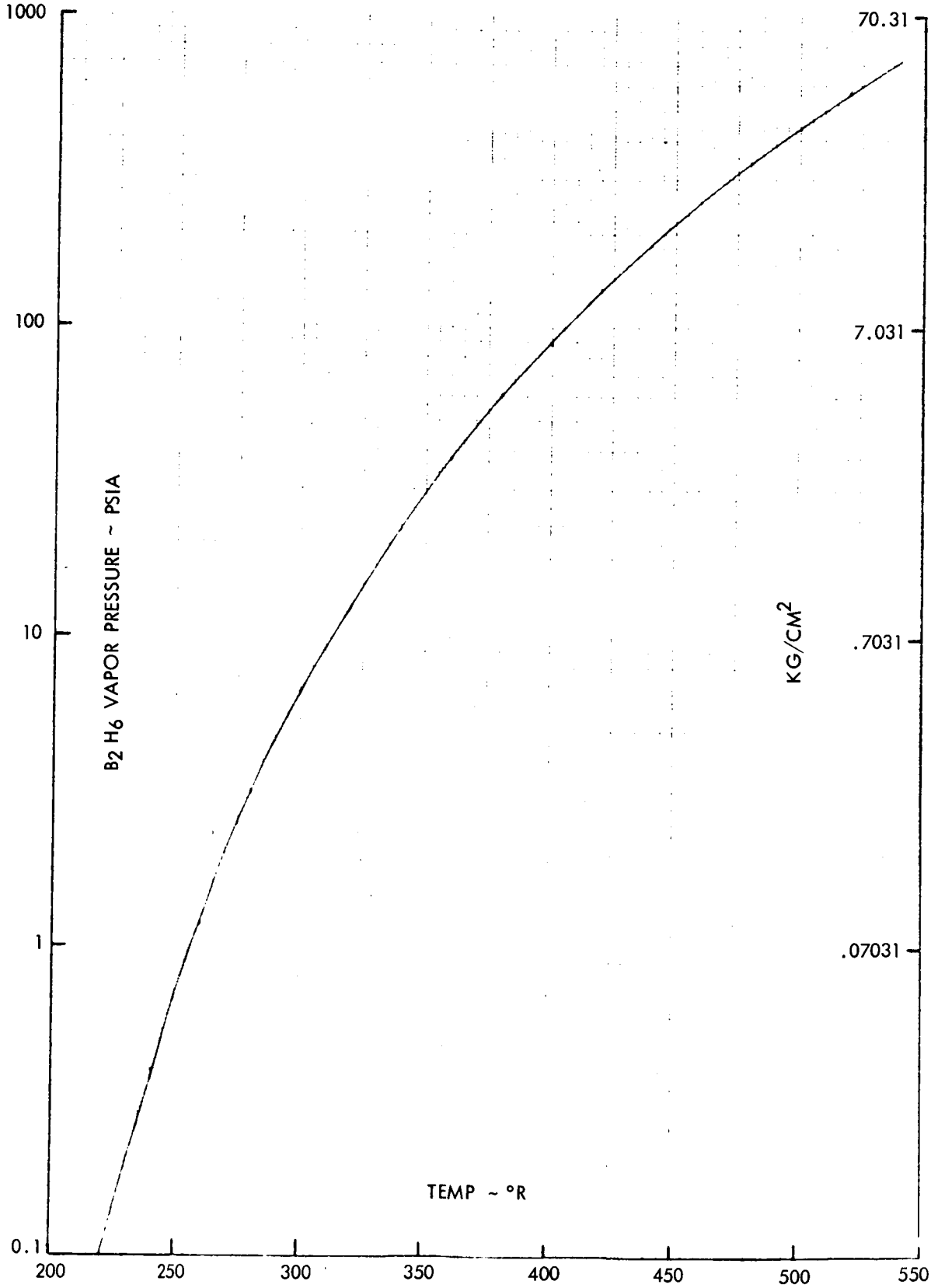

Figure 26. Diborane (B_2H_6) Vapor Pressure Versus Temperature

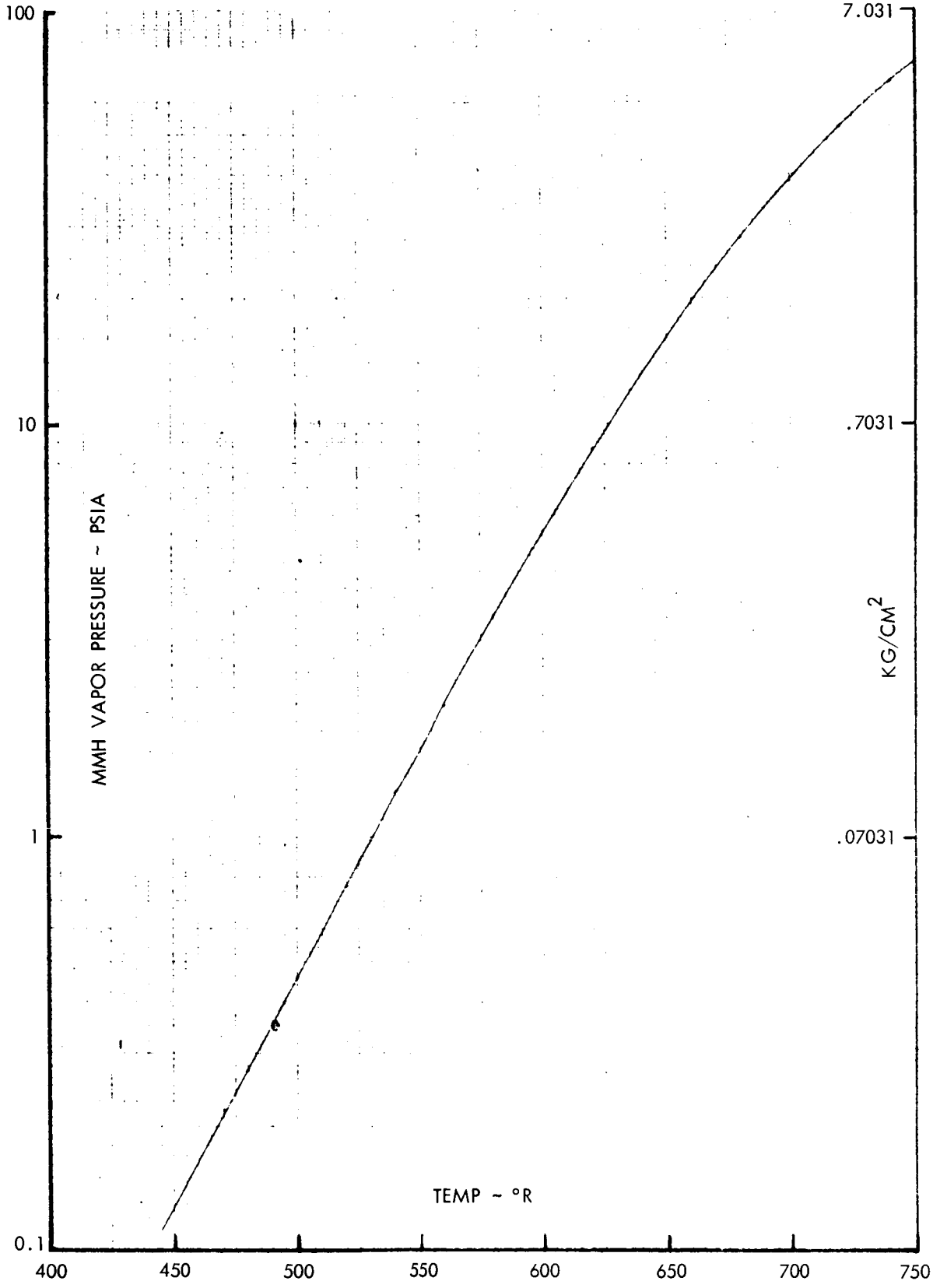

Figure 27. MMH Vapor Pressure Versus Temperature

Pump-fed

A maximum tank operating pressure (vent pressure) of 50 psia (3.52 kg/cm^2) is assumed. The nominal propellant turbopumps net positive suction head (NPSH) inlet requirements have been developed, based on current pump design requirements and the normal boiling point propellant density relationships. Table 14 provides a summary of the pump-fed tank pressure and propellant temperature estimates. These estimates are representative of pump-fed propellant systems, where structural and dynamic load considerations for the vehicle influence vent pressure requirements.

Pressure-fed

A tank operating pressure of 225 psia (15.82 kg/cm^2) has been utilized as representative of pressure-fed propellant feed systems. An engine chamber pressure requirement of 150 psia (10.55 kg/cm^2) is typical of pressure-fed engine systems and has been assumed here. To assure that flashing through the injector system will not occur, a propellant vapor pressure margin of 15 psia (1.05 kg/cm^2) below the chamber pressure has been assured. The selected propellant pressure-temperature estimates for pressure fed systems are summarized in Table 15.

Region of Applicability of Stored Gas and Evaporative Pressurization

Representative stored gas and propellant evaporative pressurization systems weight comparisons have been developed based on vehicle propellant requirements. These data are shown in Figure 28 over a range of propellant weight. The pressurization systems weight in this figure includes: pressurant medium, storage vessel, plumbing and control components, and required brackets and supports. In developing these weights, there was a representative estimate made of the engine thrust level utilized with vehicle propellant quantity to account for the variation in plumbing size and control component weight with propellant flow requirements. Example points of existing systems are shown in Figure 28.

Stored gas (usually helium) pressurization systems are applicable to liquid propellant pressure-fed propulsion systems; evaporative propellant pressurization can be utilized to provide the turbopump NPSH requirements of pump-fed systems if the propellant is a volatile liquid. In most pump-fed applications, a combination propellant bleed and stored gas system is utilized. The stored gas system provides for engine pressure requirements until steady-state operation is accomplished.

SCALING EQUATIONS FOR STORED GAS PRESSURIZATION SYSTEM

Representative cold stored gas propellant pressurization system weight scaling equations and parametric data have been developed for pump-fed and

Table 14. Summary of Pump-Fed Tank Pressure and Temperature Estimates

Item	Propellant Constituent													
	O_2		H_2		OF_2		B_2H_6		MMH		87.5% FLOX		CH_4	
	psia	kg/cm^2	psia	kg/cm^2	psia	kg/cm^2	psia	kg/cm^2	psia	kg/cm^2	psia	kg/cm^2	psia	kg/cm^2
Vapor Pressure at Nominal Boiling Point	14.7	1.03	14.7	1.03	14.7	1.03	14.7	1.03	14.7	1.03	14.7	1.03	14.7	1.03
Est. Nom. Net Positive Suction Head Requirement	20.5	1.44	6.5	0.47	25.5	1.79	11.5	0.81	16.5	1.16	24.5	1.72	12.0	0.84
Est. Feed System Loss	3.0	0.21	3.0	0.21	3.0	0.21	3.0	0.21	3.0	0.21	3.0	0.21	3.0	0.21
Nom. Ullage Requirement	38.2	2.69	24.2	1.70	43.2	3.04	29.2	2.05	34.2	2.40	42.2	2.97	29.7	2.09
Assumed Design Vent Pressure	50.0	3.52	50.0	3.52	50.0	3.52	50.0	3.52	50.0	3.52	50.0	3.52	50.0	3.52
Est. Δ Rise Tank Press.	11.8	0.83	25.8	1.81	6.8	0.48	20.8	1.46	15.8	1.11	7.3	0.55	20.3	1.43
Est. Max. Vapor Pressure	26.5	1.86	40.5	2.85	21.5	1.51	35.5	2.50	30.5	2.14	22.5	1.58	35.0	2.46
Temp. at Max. Vapor Pressure (^oR)	173		43.7		239		357		685		163		223	
Nominal Boiling Point (^oR)	163		37		230		325		649		155		201	
Est. Allow. ΔT (deg)	10		6.7		9		32		36		8		22	

Table 15. Summary of Pressure-Fed Tank Pressure and Temperature Estimates

Item	Propellant Constituent													
	O_2		H_2		OF_2		B_2H_6		MMH		87.5% FLOX		CH_4	
	psia	kg/cm^2	psia	kg/cm^2	psia	kg/cm^2	psia	kg/cm^2	psia	kg/cm^2	psia	kg/cm^2	psia	kg/cm^2
Operating Prop. Tank Pressure	225	15.82	225	15.82	225	15.82	225	15.82	225	15.82	225	15.82	225	15.82
Engine Chamber Pressure	150	10.55	150	10.55	150	10.55	150	10.55	150	10.55	150	10.55	150	10.55
Maximum Prop. Vapor Pressure	135	9.49	135	9.49	135	9.49	135	9.49	135	9.49	135	9.49	135	9.49
Temp. at Max. Vapor Pressure (^oR)	212		56		296		422		803		206		265	
Nominal Boiling Point (^oR)	163		37		230		325		649		155		201	
Est. Allowable ΔT (deg)	49		19		66		97		154		51		65	

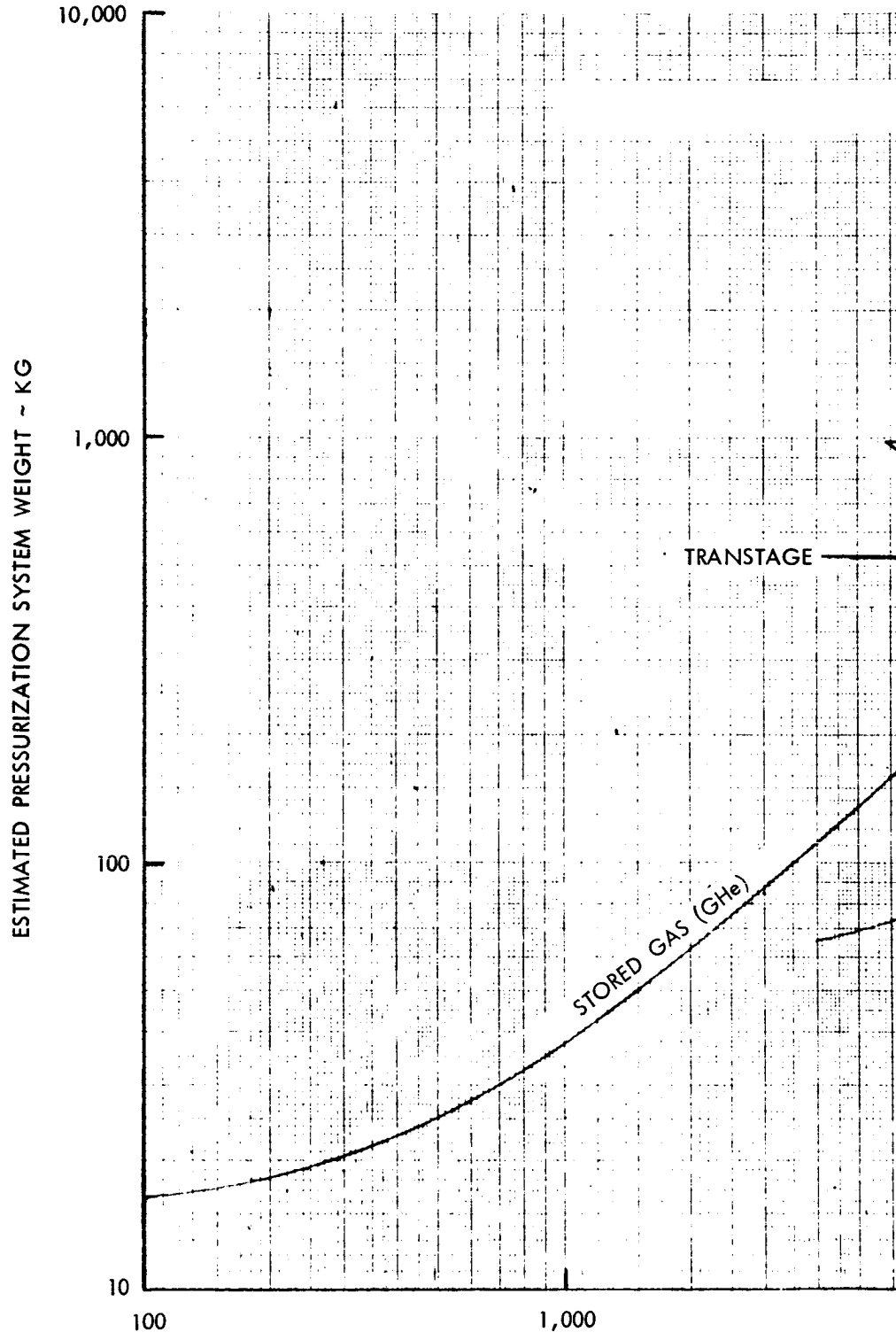

FOLDOUT FRAME

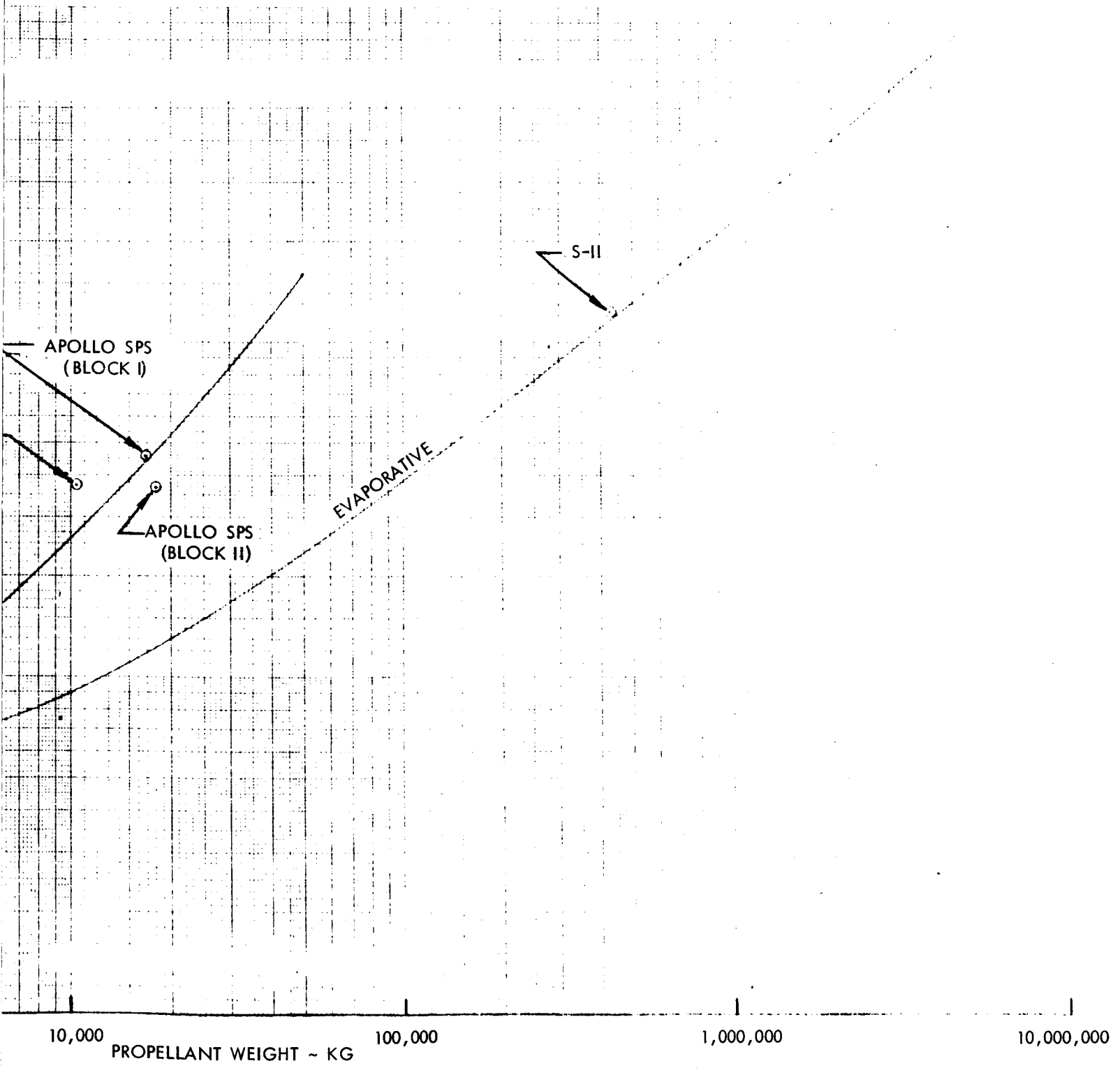

Figure 28. Representative Pressurization System Weight Regimes

pressure-fed liquid propulsion systems. The propellant combination OF_2/MMH was utilized; however, the results are reasonably good for other propellants of interest.

Pump-fed Propulsion Systems

The pressurization system weight scaling data for pump-fed propulsion systems are based on the following:

OF_2/MMH with a mixture ratio of 2.42

Propellant tank maximum operating pressure (P_P) (vent pressure) of (P_P) = 50 psia (3.52 Kg/cm^2), both tanks at same pressure.

Pressurant medium GH_e stored at 530°R and 3000-4000 psi (211-281 kg/cm^2); cutoff pressure = P_P + 100.

Adiabatic system assumed

Ti-6Al-4V titanium pressure storage vessel; safety factor of 2

The pressurization weight scaling equations derived for the pump-fed system under the established assumptions are as follows:

1. Pressurization gas = (0.000815) (total propellant weight)

2. Pressurization storage sphere = (0.00675) (total propellant weight)

3. Plumbing, controls, and associated hardware

$$= (4.85)\ \mathrm{EXP}\left(\frac{\text{ENGINE THRUST}}{46}\right)^{1/8}$$

where

engine thrust is in kilograms.

Pressure-fed Propulsion Systems

The pressurization system weight scaling data for pressure-fed propulsion systems is based on the following:

OF_3/MMH with a mixture ratio of 2.42

Both propellant tanks at same operating pressure (P_P) of 225 psia (15.82 kg/cm^2)

Pressurant medium GHe stored at 530°R and 3000-4000 psi (211-281 kg/cm^2); cutoff pressure = P_P + 100

Adiabatic system assumed

Ti-6Al-4V titanium pressure storage vessel; safety factor of 2

The pressure-fed propulsion system pressurization system weight-scaling equations based on these assumptions are as follows:

1. Pressurization gas = (0.00385) (total propellant weight)

2. Pressurization storage sphere = (0.032) (total propellant weight)

3. Plumbing, controls, and associated hardware

$$= (8.20)\ \mathrm{EXP}\left(\frac{\text{ENGINE THRUST}}{46}\right)^{1/8}$$

where:

engine thrust is in kilograms.

Parametric Data

Parametric data have been developed to provide weight estimating procedures for both the stored gas propellant pressurization system gas and storage vessel. These data are shown in Figures 29 and 30, respectively. A representative range of propellant tank pressures are covered. Propellent tank pressure requirements for pump-fed systems are in the lowest range, while pressure requirements for pressure-fed propulsion are in the higher ranges illustrated. GHe and spherical titanium storage vessels are assumed.

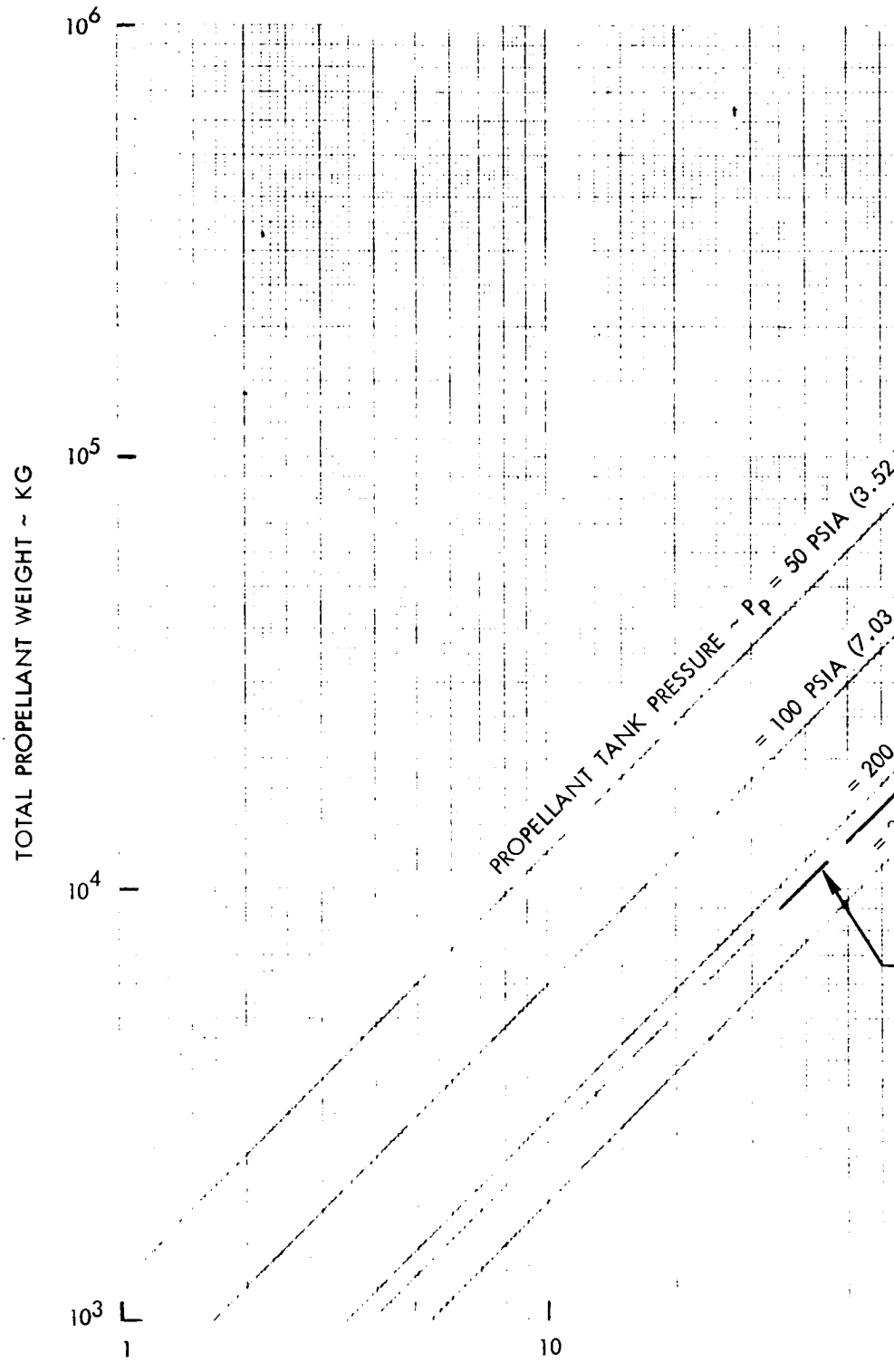

FOLDOUT FRAME

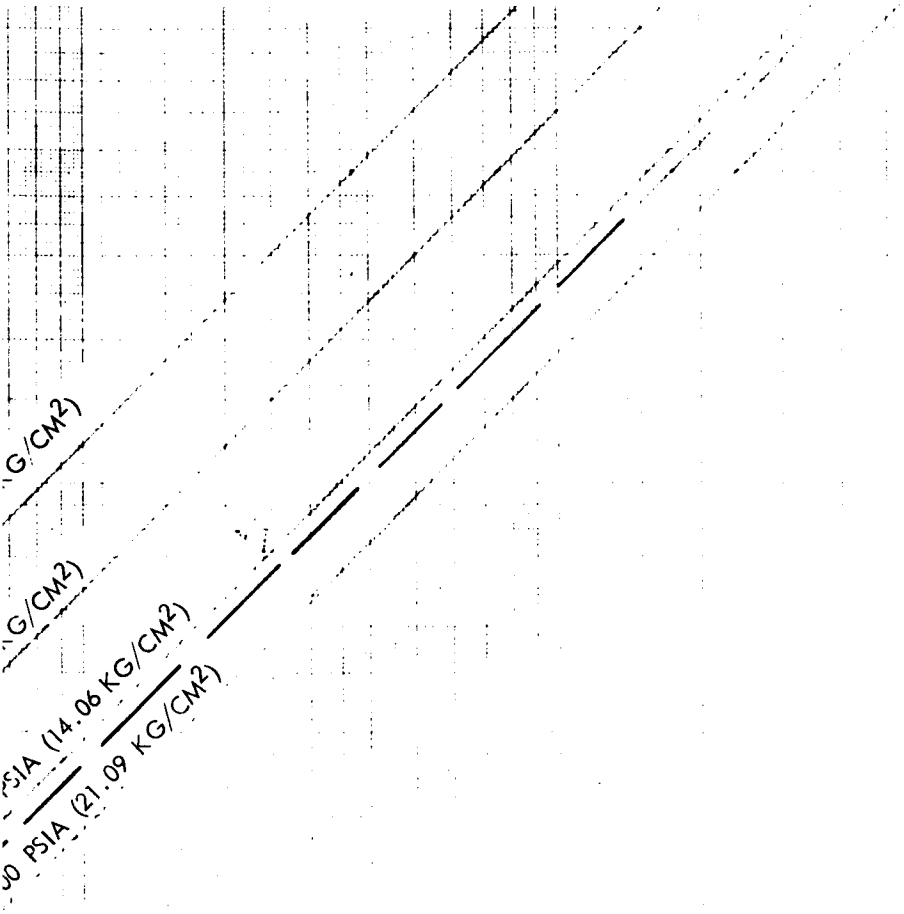

NOTE:
(BASED ON)

OF_2/MMH PROPELLANT
BOTH TANKS AT SAME P_p MIXTURE
RATIO (O/F) = 2.42
GAS STORED AT 530°R & 3000-4000 PSI
(211-281 KG/CM^2)
ADIABATIC SYSTEM ASSUMED

- = 225 PSIA (15.82 KG/CM^2)

100 1,00 10,000

IELIUM PRESSURANT GAS WEIGHT REQUIRED ~ KG

Figure 29. Total Propellant Weight Versus Helium Pressurant Gas Weight Required

FOLDOUT FRAME

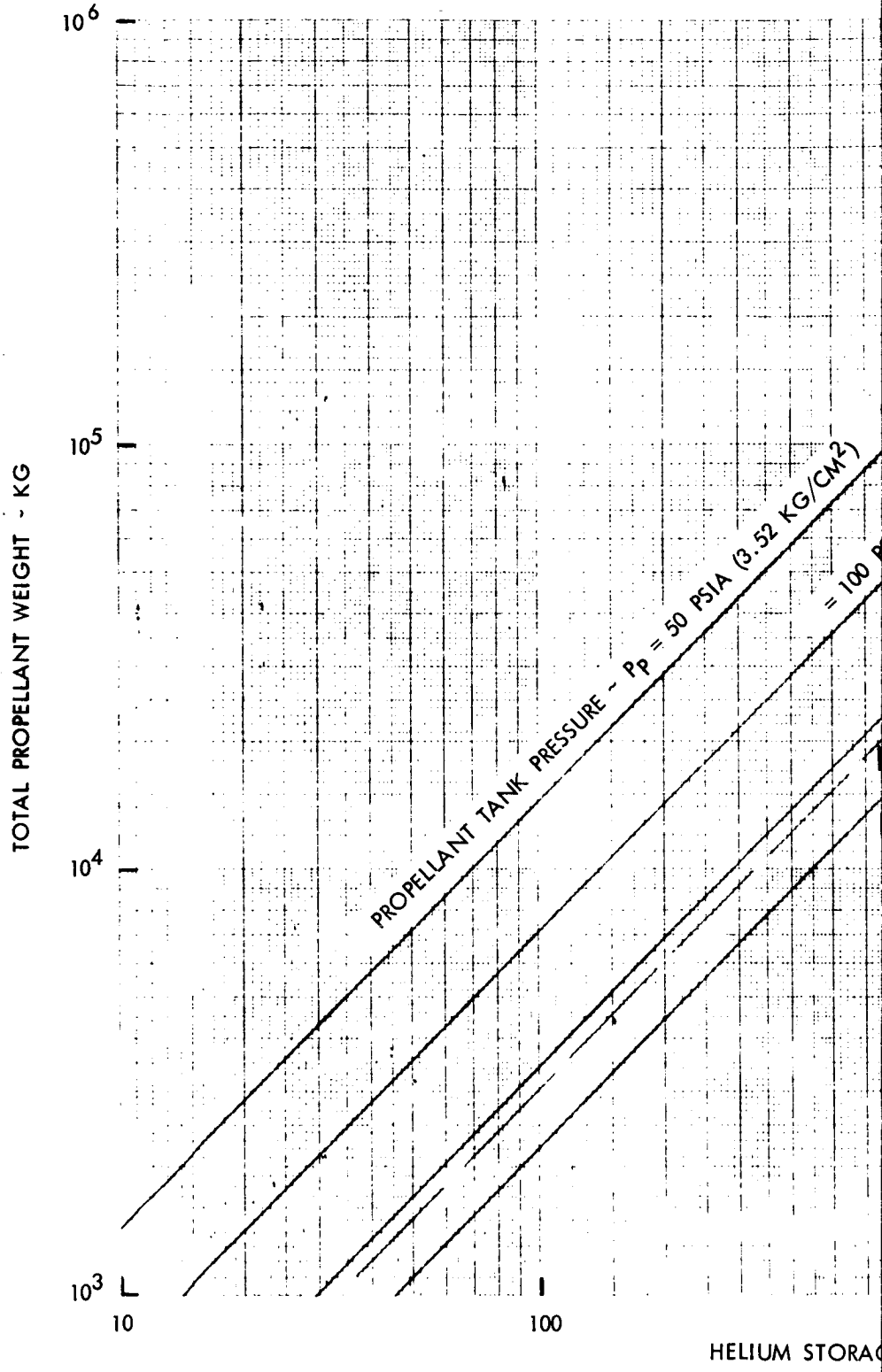

FOLDOUT FRAME

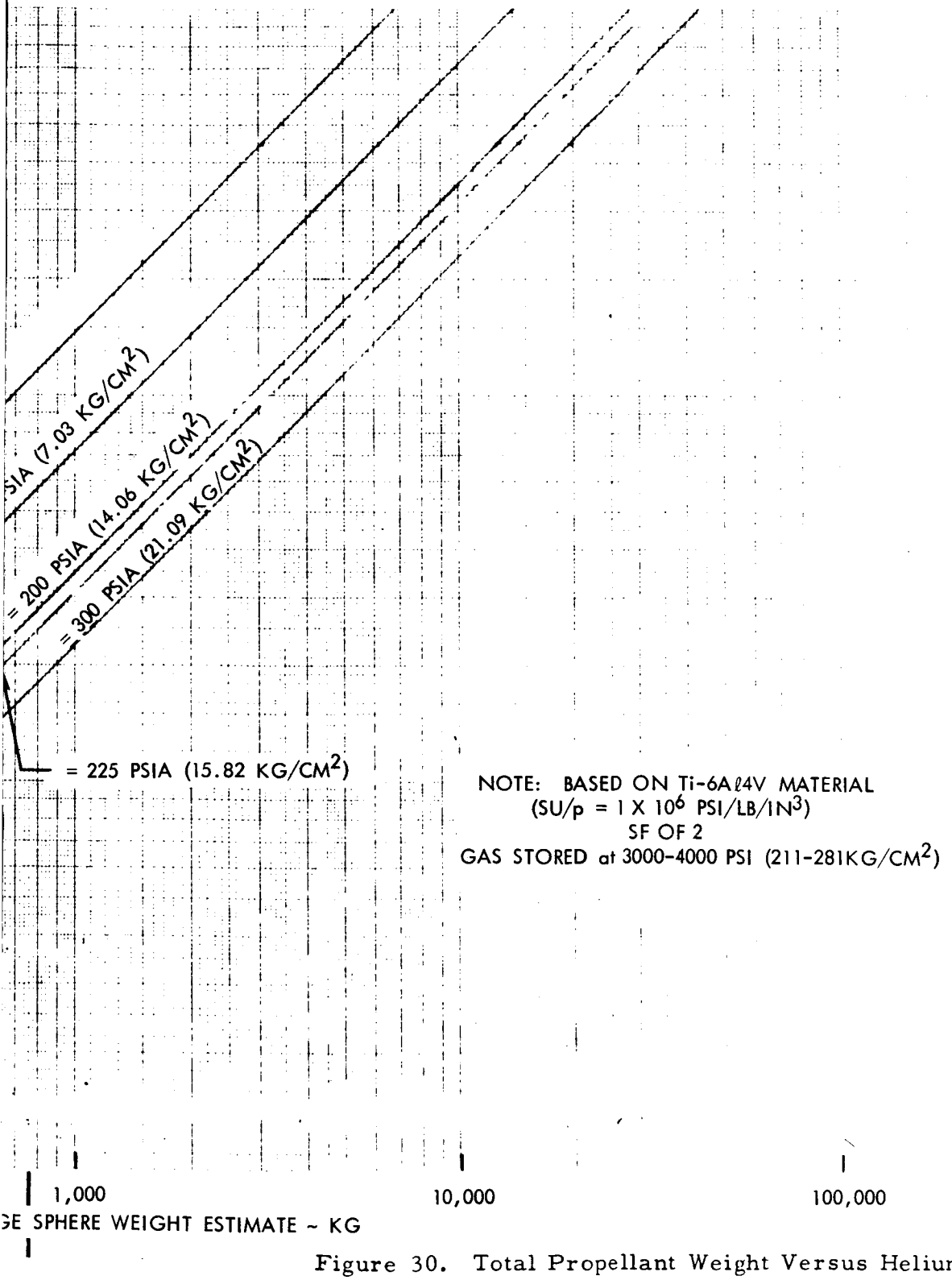

Figure 30. Total Propellant Weight Versus Helium Storage Sphere Weight Estimate

FOLDOUT FRAME

ELECTRICAL POWER SUBSYSTEM PARAMETRIC ANALYSIS

The purpose of the electrical power subsystem analysis was to develop, for a spectrum of candidate systems, relationships between operational power levels, subsystem weight and dimensional requirements, and the heliocentric radius at which a system might be used. These relationships were based on the estimated technology in the 1980 to 2000 time period. Several subsystems appropriate to mission modules (with mission durations between one and four years) and planetary excursion module descent stages (with occupancy times not greater than ninety days) were considered. The Earth reentry module and planetary excursion module ascent stages were assumed to be occupied for no more than 24 hours. Therefore, only batteries were considered for use in these modules during the module and system synthesis analyses discussed in the System Synthesis and Parametric Analysis section (Appendix D).

The spectrum of candidate electrical power subsystems for 1980-2000 application is quite broad when consideration is given to the many possible combinations of power sources and converters. Identification of the most suitable combinations in this study is based on demonstrated capability of developed systems or systems in the process of development, and on projected improvements. Projections must be done with care and on a realistic basis since systems are in various stages of development with technology breakthroughs and/or monetary investments being the pacing items. The electrical power subsystems which are expected to be available through the remainder of this century and the applicable power levels are shown in Figure 31. Also shown in the figure is the expected mission module power requirements. (It should be noted that electric propulsion systems were not considered during this study.)

In order to compare candidate subsystems on a realistic basis, promising combinations of energy sources and power conversion systems were analyzed on an equal basis such that appropriate weight variations were included to compensate for inherent differences in the various combinations. Also, the most advantageous utilization of the candidate subsystems was identified.

In general, the approach taken was to obtain system weights from reference reports describing systems applicable to 1975-1985 interplanetary manned missions. Much of these data were readily available for nuclear and solar photovoltaic systems from NR Space Division and Atomics International studies. Solar dynamic systems data were prepared by assuming the same

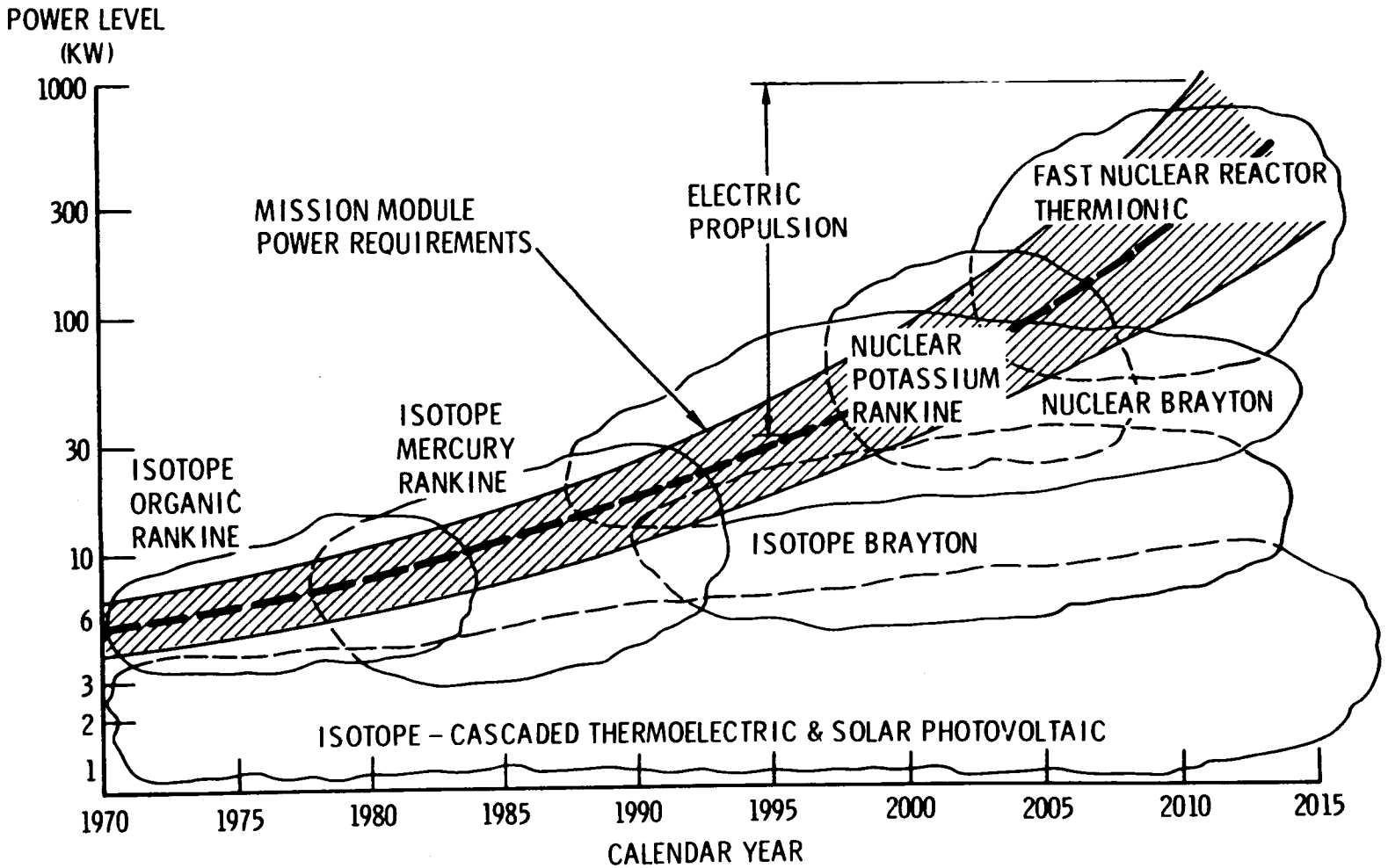

Figure 31. Power Systems Forecast

conversion design as for applicable isotope systems with only the heat source, i.e., solar concentrator-absorber, being different. Chemical systems data were available from the Apollo and Apollo Applications Programs. The accumulated data were examined and an adjustment made for expected system improvements by the 1980-2000 time period. Detailed weights were tabulated and a comparison was made between extrapolated systems and reference design weights.

This section presents a detailed summary of system weights followed by a general discussion of each applicable system (i.e., reference design 1975-1985) and a brief explanation of system improvements and extrapolations to arrive at 1980-2000 weights.

COMPETITIVE POWER SUBSYSTEMS

Competitive subsystems for the mission module[1] and the planetary excursion module descent stage are listed in Tables 16 and 17, respectively. Since the selection of these subsystems cannot be made on weight alone, Tables 18 through 21 discuss qualitatively the other subsystem characteristics which must be considered in a complete evaluation. Many of the same disadvantages apply to all candidate subsystems. To avoid undue repetition, disadvantages were listed only for subsystems that it was felt were most affected; i.e., these are to be taken only as relative measures. Examples of such items are large radiator areas, integration/operation constraints, orbit sensitivity, heliocentric radius sensitivity, and shock sensitivity.

WEIGHT SUMMARY

In order to establish candidate power subsystems, first effort was given to projecting overall subsystem weight as a function of nominal power level. Planetary orbit occultation and heliocentric radius effects on the referenced solar power subsystems were considered but are not included in the projected weights. The weight allowance for occultation effects are described in the Ground Rules section. Radiators have been sized based on a 224 K (440 F) sink and Earth heliocentric radius meteoroid flux.

A breakdown of the component considerations, component weight, and the total subsystem weight and volume of the candidate combinations are presented in Tables 22 through 25. No effort was made to provide individual component weights at 5 and 20 kWe outputs in Tables 22 and 23. Present subsystem definition does not allow scaling in this detail to be very realistic and it was felt that the subsystems could best be scaled on a total weight basis. The gross weight values are presented for all power levels on the assumption that the scaling uncertainty for the components is random and

[1] Thermionics were evaluated but are not considered to be available for the time period of this study.

compensating. The remaining blanks in Tables 22 and 23 are due to a lack of available information in the reference designs; e. g., the unavailability of power conditioning in the reactor power subsystem reference design since the reference is a study only of power sources.

To explain apparent discrepancies in subsystem characteristics with later text material, consider a typical value such as heat source outlet temperature (Table 23). The heat source temperatures for the isotope subsystems were taken to be 83 K (150 F) above the top cycle temperature. For a mercury Rankine cycle, the mercury superheated temperature is presently a maximum of 977 K (1300 F). To account for subsystem improvements, this maximum temperature was increased to 1033 K (1400 F); i. e., see Table 35; the heat source temperature is then taken as 1116 K (1550 F) as shown in Table 23.

Subsystem redundancy for a projected reliability of 0. 999 is shown in Tables 26 and 27. These configurations are reflected in the weights shown in Tables 22 through 25.

Power subsystem gross weights are shown as a function of delivered power on Figures 32 through 36 for various mission durations. Similar data are shown in Figures 37 through 40 for subsystems appropriate to planetary excursion modules for various lifetime requirements.

Table 16. Competitive Auxiliary Power Subsystems for Mission Module

Nominal Power Level (kWe)	Mission Duration (years)	
	≤2.5	≈ 4*
15 to 30	Isotope { Rankine, Brayton, Thermoelectric } Reactor { Rankine, Brayton, Thermoelectric } Solar photovoltaic	Isotope { Rankine, Brayton, Thermoelectric } Reactor { Rankine, Brayton, Thermoelectric }
<15	Isotope { Rankine, Brayton, Thermoelectric } Solar photovoltaic	Isotope { Rankine, Brayton, Thermoelectric }

*Solar photovoltaic systems omitted since longer missions are consistent with heliocentric radius > 2.5 to 3 AU

Table 17. Competitive Auxiliary Power Subsystems for Planetary Excursion Module

Nominal Power Level (kWe)	Operating Time (days)			
	2	10	30	60
20	Fuel cells Solar photovoltaic	Fuel cells Solar photovoltaic Isotope thermoelectric	Solar photovoltaic Isotope thermoelectric	Solar photovoltaic Isotope thermoelectric
10	Fuel cells Solar photovoltaic Chemical dynamic Primary batteries	Fuel cells Solar photovoltaic Isotope thermoelectric	Solar photovoltaic Isotope thermoelectric	Solar photovoltaic Isotope thermoelectric
5	Fuel cells Solar photovoltaic Chemical dynamic Primary batteries	Fuel cells Solar photovoltaic Isotope thermoelectric	Fuel cells Solar photovoltaic Isotope thermoelectric	Fuel cells Solar photovoltaic Isotope thermoelectric
2	Fuel cells Solar photovoltaic Chemical dynamic Primary batteries	Fuel cells Solar photovoltaic Isotope thermoelectric	Fuel cells Solar photovoltaic Isotope thermoelectric	Fuel cells Solar photovoltaic Isotope thermoelectric

Table 18. Nuclear Reactor Auxiliary Power System Considerations

Advantages	Disadvantages
REACTOR	
No attitude control dependence No space radiation degradation Availability of fuel Long life	Operational radiation hazard Handling and storage safety Large shielding weight After shutdown heat removal
POWER CONVERSION SYSTEMS	
Thermoelectric	
High reliability No moving parts Little degradation Long life	Large radiator Low efficiency
Rankine Cycle	
Small radiator Lowest weight for given temperature level	Corrosion problems Zero-G phase separation problems Low reliability, requires redundancy Stop-restart requirements
Brayton Cycle	
High efficiency Considerable existing technology	Large radiator Low reliability, requires redundancy Stop-start requirements High sensitivity to heat sink temperature

Table 19. Isotope Auxiliary Power Source Considerations

Advantages	Disadvantages
ISOTOPE SOURCE	
Low radiation source	Continuous heat and radiation
Light weight	Ground handling and safety problems
High operating temperature	Expensive fuel
No attitude control requirement	Limited availability
Low sensitivity to acceleration and shock	
POWER CONVERSION SYSTEMS	
Rankine Cycle (Mercury)	
Good cycle efficiency	Complex turbine design
Light weight	Toxic working fluid
Low radiator area	High temperature cycle
Excellent development background	Two phase conversion cycle
Rankine Cycle (Organic)	
Good cycle efficiency	Working fluid decomposition
Light weight	Poor growth potential
Low temperature cycle	Large radiator area
Simple turbine design	Poor development background
	Two phase conversion cycle
Brayton Cycle	
No corrosion, inert gas or working fluid	Large radiator area
Single phase conversion cycle	High weight
High cycle efficiency	Large ducts
Low isotope inventory	Requires high temperature isotope
Excellent growth potential	Longer development
Thermoelectric	
Compact	Low efficiency
Static converter	Large radiator area
High inherent reliability	Poor growth potential
Good development	Large isotope inventory

Table 20. Solar Auxiliary Power System Considerations

Advantages	Disadvantages
POWER CONVERSION SYSTEMS	
Dynamic	
Good growth potential	Poor development
Readily available energy source	Orientation requirement
	High weight
Photovoltaic	
Static converter	Large area
Light weight	Environmental sensitivity
Excellent development	Orientation requirement
Proven system	Integration/operation constraints
	Orbit sensitivity
	Heliocentric radius sensitivity
	Shock sensitivity
	Aerodynamic drag

Table 21. Energy-Limited Auxiliary Power System Considerations

Advantages	Disadvantages
FUEL CELLS	
Light weight Delivers drinking water Commonality of reactants with vehicle propellants No electromagnetic interference generated Proven hardware	Hazardous reactants Possible malfunctions due to alkaline electrolyte leakage Large overloads require battery and charger Monitoring required Complicated startup and shutdown
Chemical Dynamic	
Simple startup and shutdown Commonality of reactants with vehicle propellants Intermittent duty possible Compact turboalternator-rectifier	Effectively limited to intermittent duty Turbine materials technology not compatible with higher energy reactants Source of electromagnetic interference
ELECTRIC STORAGE BATTERIES	
Silver-Zinc	
Highest energy density battery qualified to date Long dry shelf life, 5 years + Close voltage regulation Extremely high rate discharge handling capability Dry condition storage at -85°F to +165°F Low internal cell resistance	Life after activation is limited for primary batteries from few hours to weeks For secondary batteries, maximum 6 months Life extension to one year by 1980 Length of life is function of number and depth of discharge Primary batteries require activation immediately before use Operating temperature limited to -20°F to +165°F with optimum performance at 60°F to 80°F
Silver-Cadmium	
High energy density Cycle life two to three years. Five years life by 1980 Long charge retention. As much as 85% of original capacity retained after one year charged wet stand at 70°F Negligible gasing on discharge Dry storage life greater than 3 years Cycle life approaching that of nickel-cadmium batteries by 1980 Low internal cell resistance	50% sacrifice in energy density over silver-zinc Operational temperature limited from -20 to +165°F
Nickel-Cadmium	
Long cycle life Proven in space application Unlimited storage life Relatively less expensive than other space type batteries	Very low energy density About half the energy density of silver-cadmium batteries Competes with silver cadmium batteries only for long missions and this advantage will disappear by 1980; therefore not considered in this study
Isotope Thermoelectric (Table 19)	
Solar Photovoltaic (Table 20)	

Table 22. Auxiliary Power Systems Using Nuclear Reactors (Projected to 1980-2000)

System Characteristic	Thermal Nuclear Reactor with Brayton Cycle				Thermal Nuclear Reactor With Mercury Rankine Cycle				Thermal Nuclear Reactor With Thermoelectric Converter			
Electrical Power Output Level (Kilowatts)	5	10	20	20[1]	5	10	20	15[2]	5	10	20	15[3]
Reactor outlet temperature (°F)		1300		1300		1300		1210		1340		1300
(°K)		978		978		978		928		1000		978
Overall system efficiency (percent)		13.1		13.1		7.0		5.8		5.4		5.4
Reactor weight (lb)		388		755		388		388		388		670
Primary heat loop weight (lb) with heat exchanger		79		157		298		393		153		186
Power conversion weight (lb)		2519		5800		1282		1777		1457		2272
Radiator weight penalty, separate (lb)		885		1769		558		688		1294		2370
Thermal shield weight, including 511-pound disposal system (lb)		1118		1355		921				1581		
Radiation shield weight 125-foot separation, 60-foot diameter (lb)		2980		7064								(2)
Boom and cable weight 125-foot separation (lb) (4)		575		1955		545		630		980		930
Overload battery weight (lb)				1676								
Conditioning equipment weight (lb)		1500		2950		1900				861		
Redundant weight required per year (lb)	650	1242	2435		1062	1611	2751		276	562	1030	
Total weight (lb) 1 year	5900	9044	17189	23481	7062	9107	15800		7551	10214	17750	
2 years	6550	10286	19624		8124	10718	18551		7827	10776	18780	
3 years	7200	11528	22059		9186	12329	21302		8103	11338	19810	
4 years	7850	12770	24489		10248	13940	24053		8379	11900	20840	
5 years	8500	14012	26924		11310	15551	26804		8655	12462	21870	
Radiator temperature (°F) inlet	413	413	413	413	622	622		622	525	525	525	525
(°K)	485	485	485	485	601	601		601	547	547	547	547
Radiator area (feet^2)	287	575	1150	1150	240	360		500	386	772	1410	1185
Total system volume required (feet^3) 1 year		2600			365			765	563			1230

(1)MORL, Reference 3

(2)Reference 4

(3)Reference 5

(4)Retraction mechanism included in boom and cable weights.

Table 23. Auxiliary Power Systems With Radioisotopes (Projected to 1980-2000)

System Characteristic	Radioisotope Pu^{238} Brayton Cycle				Radioisotope Pu^{238} Mercury Rankine				Radioisotope Pu^{238} Cascaded Thermoelectric			
Electrical Power Output, Conditioned (Kilowatts)	10[3]	5	10	20	5	10	20	10[3]	5	10	20	10[3]
Heat source outlet temperature, (°F)[1]	1690		1790			1550		1450		1800		1600
(°K)	1194		1250			1116		1061		1255		1144
Overall system efficiency (percent)	19.8		28.4			14.0		11.4		7.15		5.85
Heat source weight (lb)	530		345			792		990		1425		1855
Primary heat loop weight (lb)	695		450			535		668		452		587
Power conversion weight (lb)	2404		1560			678		849		275		358
Radiator weight penalty, separate (lb)	1150		745			263		329		595		775
Radiation shield weight (lb)	273		175			376		470		750		975
Thermal control apparatus weight (lb)[4]	278		180			322		403		592		770
Conditioning equipment weight (lb)	1040		675			720		900		830		1079
Redundant weight required per year (lb)[2]	1358		880			408		510		505		659
Total weight (lb) 1 Year	6370	2810	4130	5750	2510	3690	5130	4610	3600	4920	8600	6400
2 Years	7730	3400	5010	6950	2790	4100	5730	5120	3970	5430	9500	7060
3 Years	9090	4010	5890	8150	3060	4510	6300	5630	4340	5930	10350	7720
4 Years	10450	4600	6770	9300	3330	4910	6860	6140	4720	6440	11250	8380
5 Years	11800	5170	7650	10500	3610	5320	7450	6650	5100	6940	12150	9040
Radiator temperature, T_{in} (°F)	286						558					510
T_{in} (°K)	414						565					539
T_{out} (°F)	72						400					410
T_{out} (°K)	295						478					483
Radiator area, ft^2 [5]	1090		710			165		204		350		460
Total system volume required, 1 year $(ft)^3$	107	65	70	98	23	40	47	55	39	55	95	70

(1) 150 F above top cycle temperature

(2) 1st year redundancy included in total weight

(3) Interplanetary Flyby Missions of 1975-1985 time period

(4) Includes auxiliary radiator weight penalty

(5) Area requirements are less than shown in Figure 56 since system performance improvements (Table 35, Page 150) have been assumed in this table of summary values.

Table 24. Auxiliary Power Systems With Solar Energy Source

System Characteristic	Solar Cells at 1 AU				Solar Cells		Collector Rankine			Collector Brayton		
					1.5 AU	3.0 AU	1.0 AU	1.5 A.U.	3 AU	1 AU	1.5 AU	3 AU
Electrical Power Output, Conditioned (Kilowatts)	5	10	20	6[4]	10	10	10	10	10	10	10	10
Heat source outlet temperature (°F)	96[2]	96[2]	96[2]	131	-10[2]	-128[2]	1550	1550	1550	1690	1690	1690
(°K)	309	309	309	328	250	185	1116	1116	1116	1194	1194	1194
Overall system efficiency (percent)[3][4]	11.7[4]	11.7[4]	11.7[4]	10.5[4]	11.7[4]	11.7	10.5[3]	10.5[3]	10.5[3]	21.2[3]	21.2[3]	21.2[3]
Array weight (lb)	220	440	885	1912	1000	3960						
Solar collector weight (lb)							304	645	2500	140	306	1200
Primary loop weight (lb)							228	228	228	450	450	450
Orientation penalty per year (lb)[6]	30	60	120	260	140	540	41	91	350	19	42	160
Power Conversion Weight (lb)							685	685	685	1560	1560	1560
Radiator weight penalty, integrated (lb)												
Radiator weight penalty, separate (lb)							263	263	263	745	745	745
Power conditioning equip. weight (lb)	415	660	920	700	660	660	720	720	720	675	675	675
Backup battery weight (lb)				195								
Occultation battery weight (lb)				580								
Occultation heat sink weight (lb)												
Redundant weight required per year (lb)	33	58	96		83	230	425	485	865	685	700	790
Total Weight (lb) 1 year	675	1210	1980	3650	1800	5165	2240	2630	4750	3590	3780	4790
2 years	705	1290	2080		1885	5395	2670	3120	5610	4270	4480	5580
3 years	740	1330	2170		1965	5615	3090	3540	6040	4960	5180	6370
4 years	725	1380	2270		2045	5855	3520	3970	6460	5640	5880	7160
5 years	805	1440	2360		2135	6085	3940	4390	6890	6330	6580	7950
Solar collector area (ft^2)							1060	2380	9490	660	1480	5900
Solar array area, 1 year (ft^2)	495	990	1980	1650	1840	7250[7]						
Radiator area (ft^2)							165	165	165	710	710	710
Radiator temperature, T_{in} (°F)							558	558	558	286	286	286
(°K)							565	565	565	414	414	414
Total system volume, 1 year (ft^3)	14	26	49	38	42	110	32	37	68	72	75	90

(1) Interplanetary Flyby Missions (Earth Orbit Phase) 1975-1985 time period, 262 nautical miles

(2) Solar array equilibrium temperature

(3) Includes concentrator-absorber ($_{conc\text{-}ABS}$ = 75%)

(4) Solar cell efficiency AMO at standard temperature (overall efficiency less because of temperature effects, packing factor, etc.)

(5) Includes shadow (occultation) allowance since this is Earth Orbit. This case is presented only for comparison to show effects of occultation

(6) Total orientation penalty for first year shown, with five percent added for each additional year included in array weight.

(7) Drastic increase in area due to low solar intensity, i.e. area requirements, should be in the order of nine times that at 1.0 AU due to difference in solar constant.

Table 25. Auxiliary Power Systems—Energy Limited

System Characteristics	Primary Battery Ag-Zn Batteries				Chemical Dynamic (1) Turbine Alternator				H_2O_2 Fuel Cell			
Operating Time (days)	2	10	30	60	2	10	30	60	2	10	30	60
Power conversion weight (lb/kW)	-	-	-	-	27	27	27	27	220	220	220	220
Reactant (fuel) weight (lb/kW)	-	-	-	-	524	2620	7860	15720	43	216	648	1296
Tankage weight (lb/kW)	-	-	-	-	77	383	1150	2300	21	103	309	618
Startup equipment weight (lb/kW)	-	-	-	-	5	5	5	5	10	10	10	10
Conditioning equipment weight (lb/kW)	-	-	-	-	3	3	3	3	0	0	0	0
Total weight (lb/kW)	535	2670	8020	16000	636	3038	9045	18055	294	549	1187	2144
Total volume (ft^3/kW)	3.5	17.0	51	102	13	53	153	303	7.5	15.5	35.5	65.5

(1) Aerozine-50, N_2O_4 (O/F = 1.6)

Table 26. Power System Redundancy to Achieve 0.999 Reliability for Mission Module (Based on 10 kwe System)*

Power System	First Year		Each Additional Year	
	Active PCS	Redundant PCS	Redundant PCS	Redundant Power Conditioning (percent)
Reactor				
Rankine	2**	1	1	5
Brayton	1	2	1	5
Thermoelectric	1	-	5% Converter	5
Isotope				
Rankine	1	2	1	5
Brayton	1	2	1	5
Thermoelectric	1	-	5% Converter	5
Solar				
Rankine	1	2	1 + 20% Concentrator Area	5
Brayton	1	2	1 + 20% Concentrator Area	5
Solar photovoltaic	1	-	5% Area	5

*Number of systems vary with power level; see text.

**5 kWe module.

Table 27. Power System Redundancy to Achieve 0.999 Reliability for Planetary Excursion Module

Power System	Active Modules	Redundant Modules	
		Active	Inactive
Fuel cell	2	1	1
Chemical dynamic	1	0	0
Battery	1	0	0
Isotope thermoelectric	1	0	0
Solar photovoltaic	1	0	0

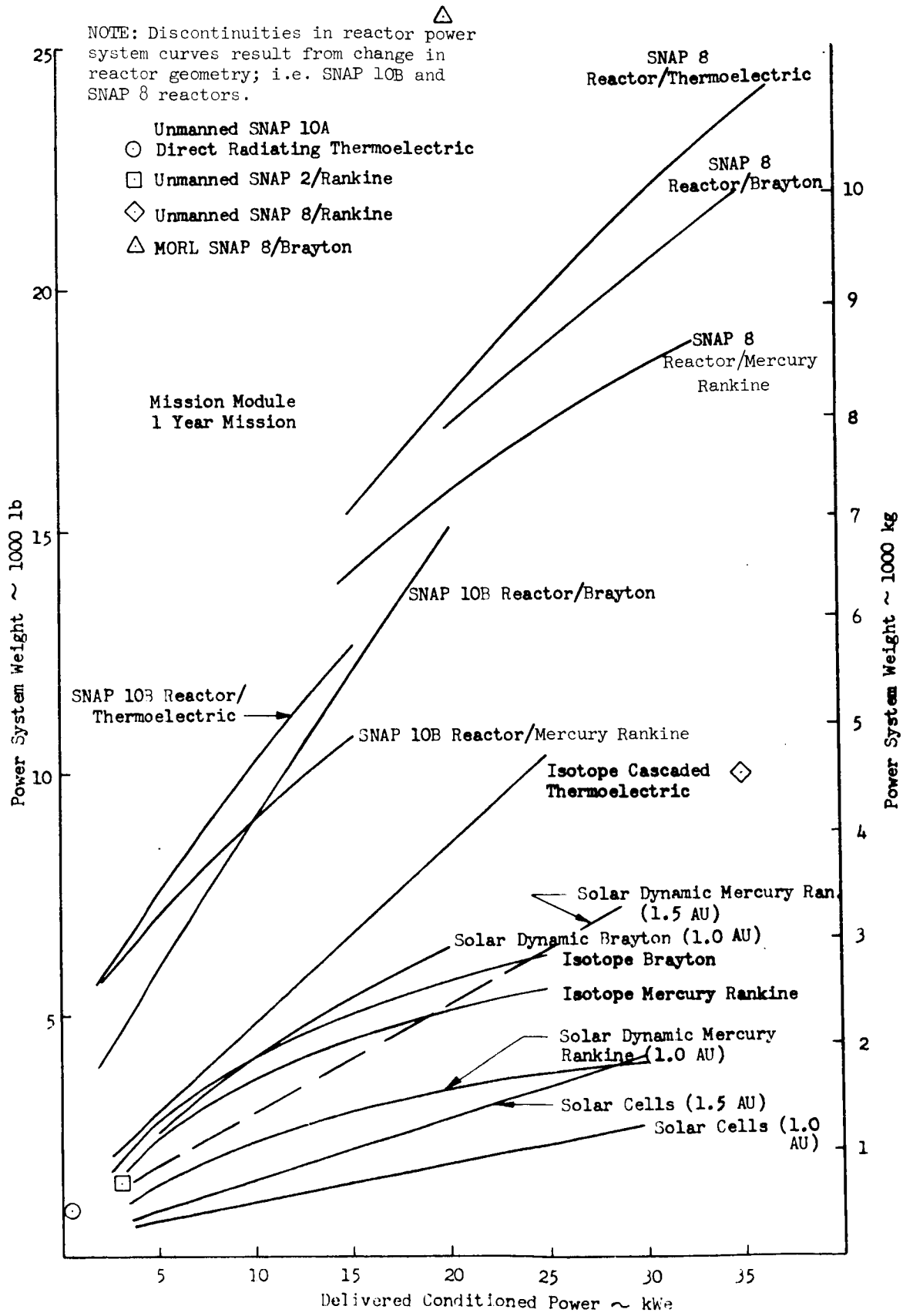

Figure 32. Power System Weight for Mission Module, 1-Year Mission

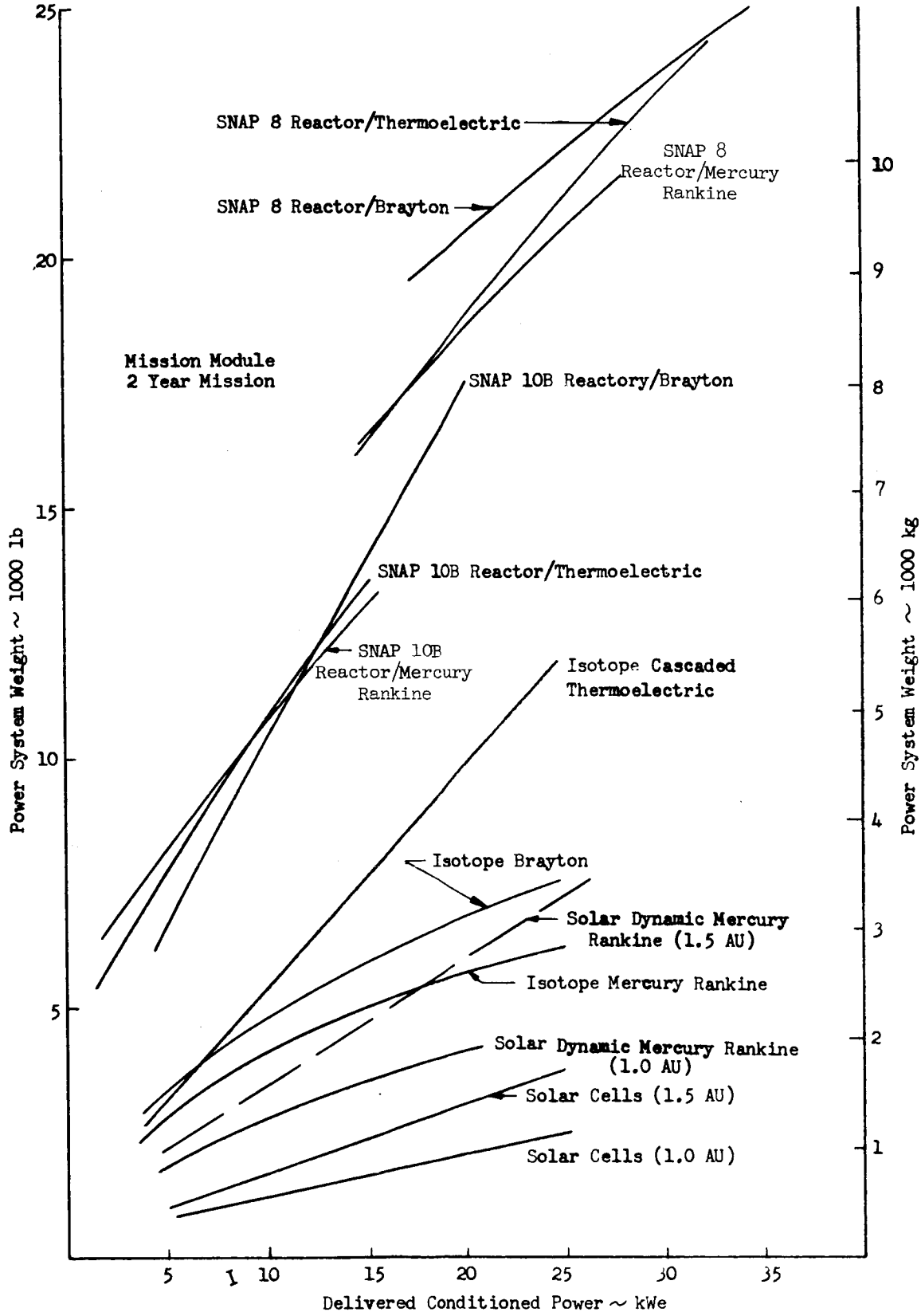

Figure 33. Power System Weight for Mission Module, 2-Year Mission

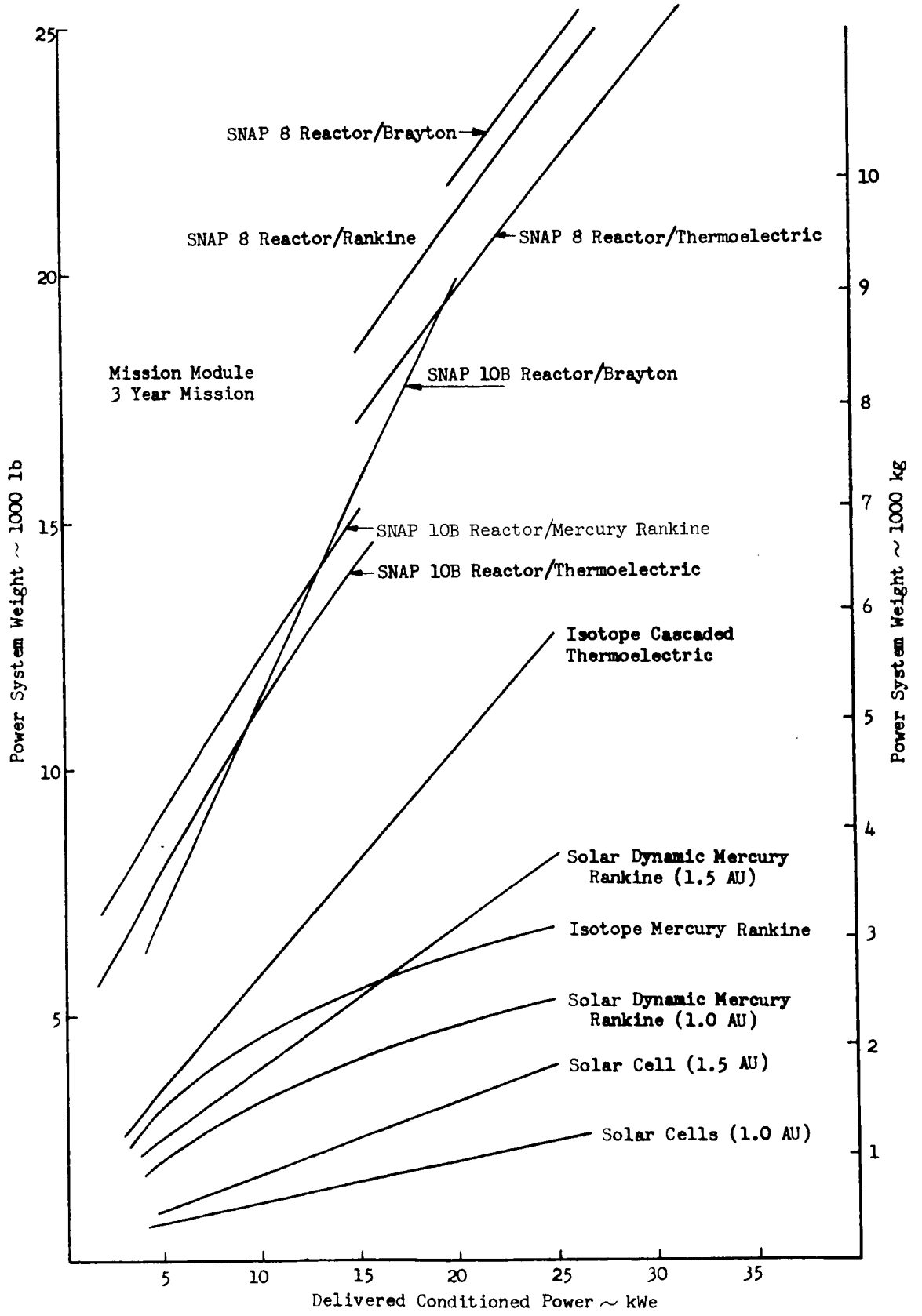

Figure 34. Power System Weight for Mission Module, 3-Year Mission

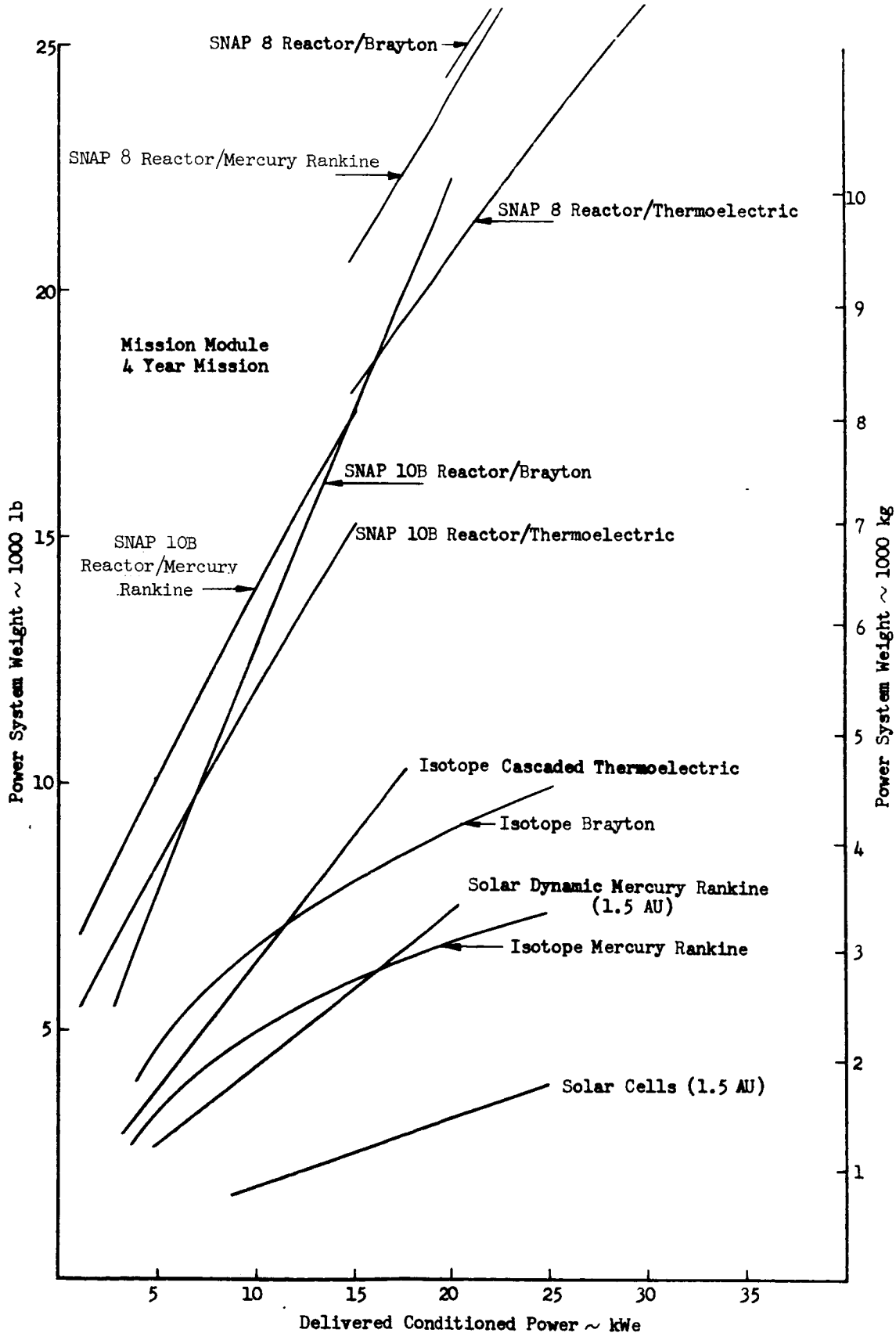

Figure 35. Power System Weight for Mission Module, 4-Year Mission

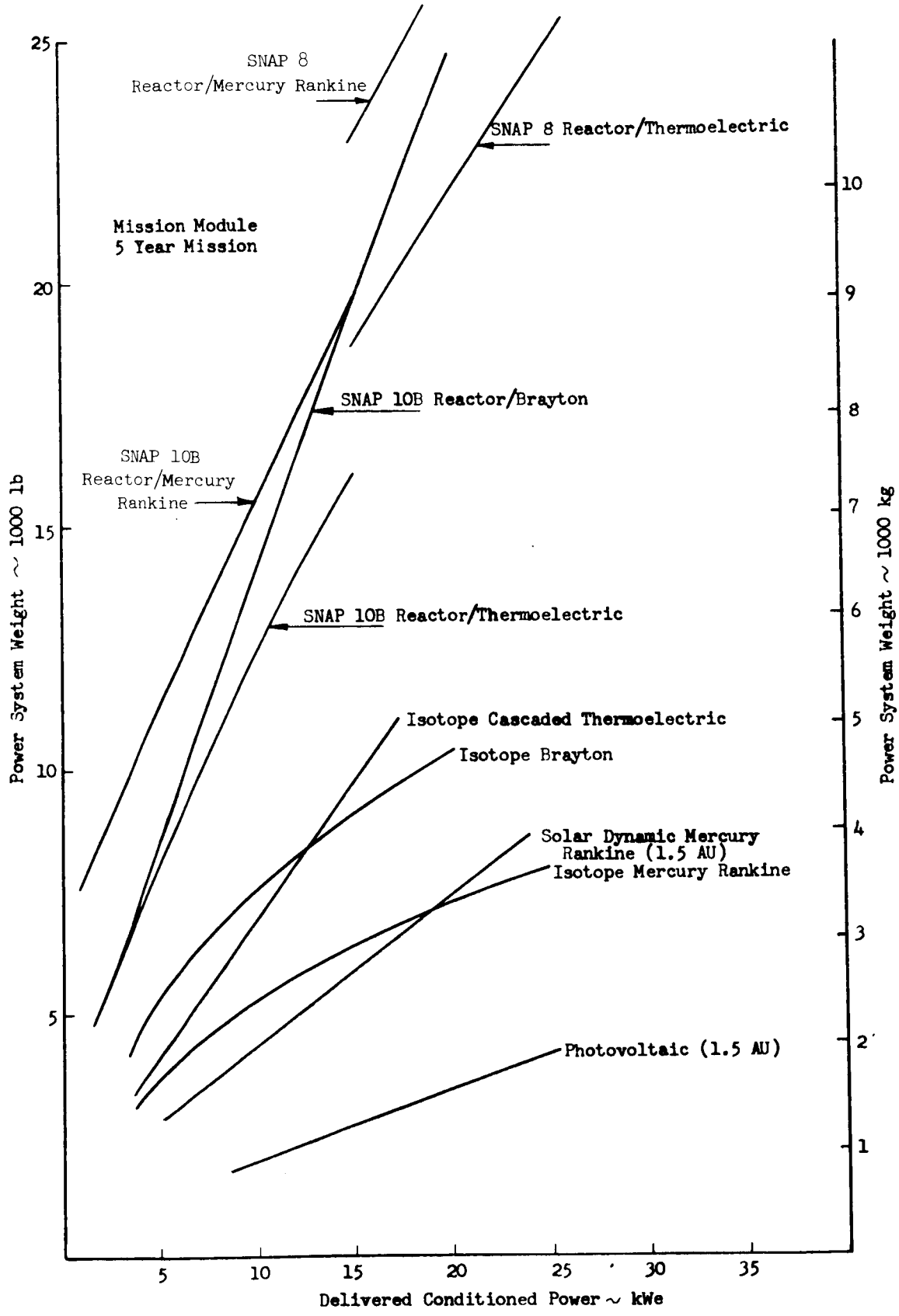

Figure 36. Power System Weight for Mission Module, 5-Year Mission

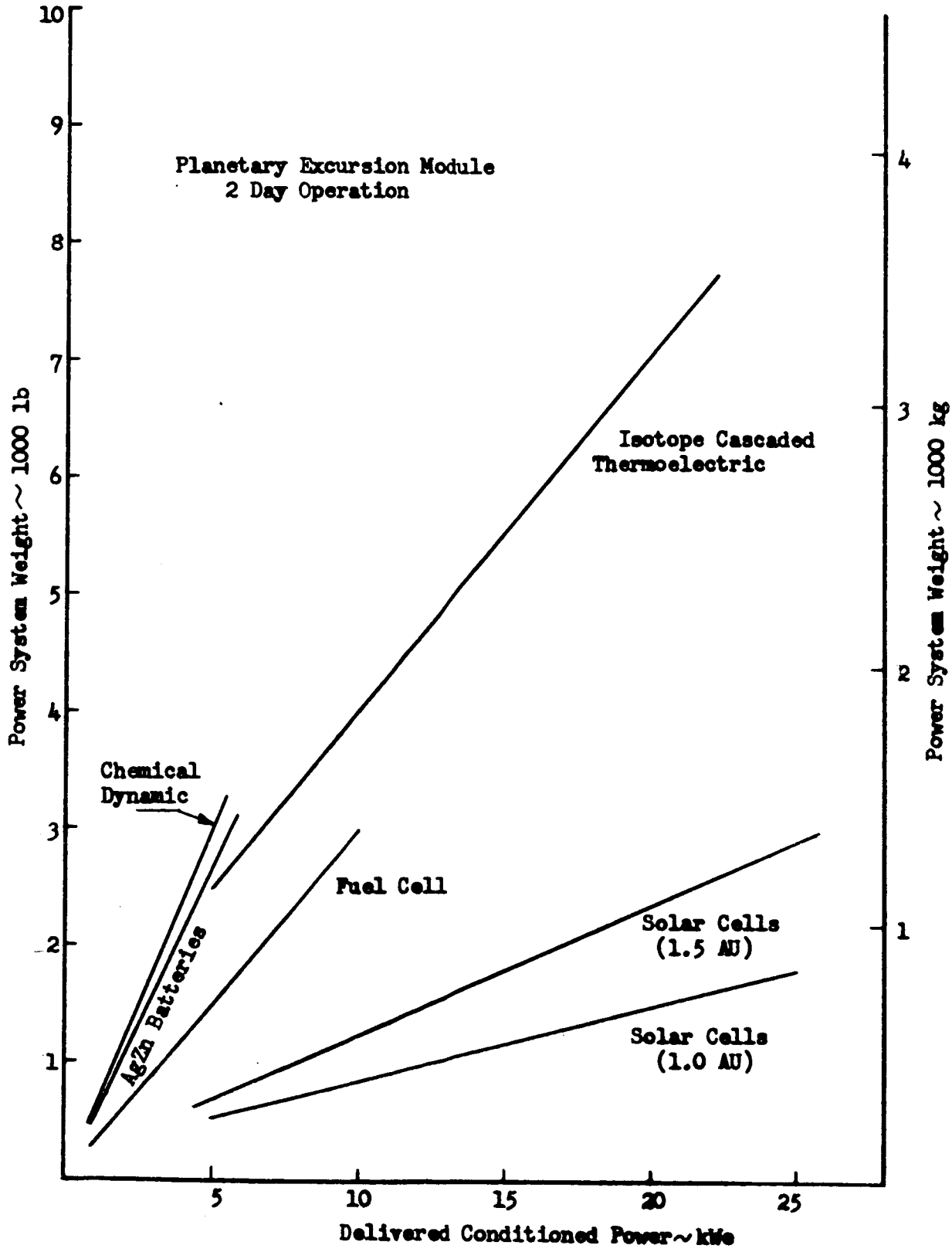

Figure 37. Power System Weight for Planetary Excursion Module, 2-Day Operation

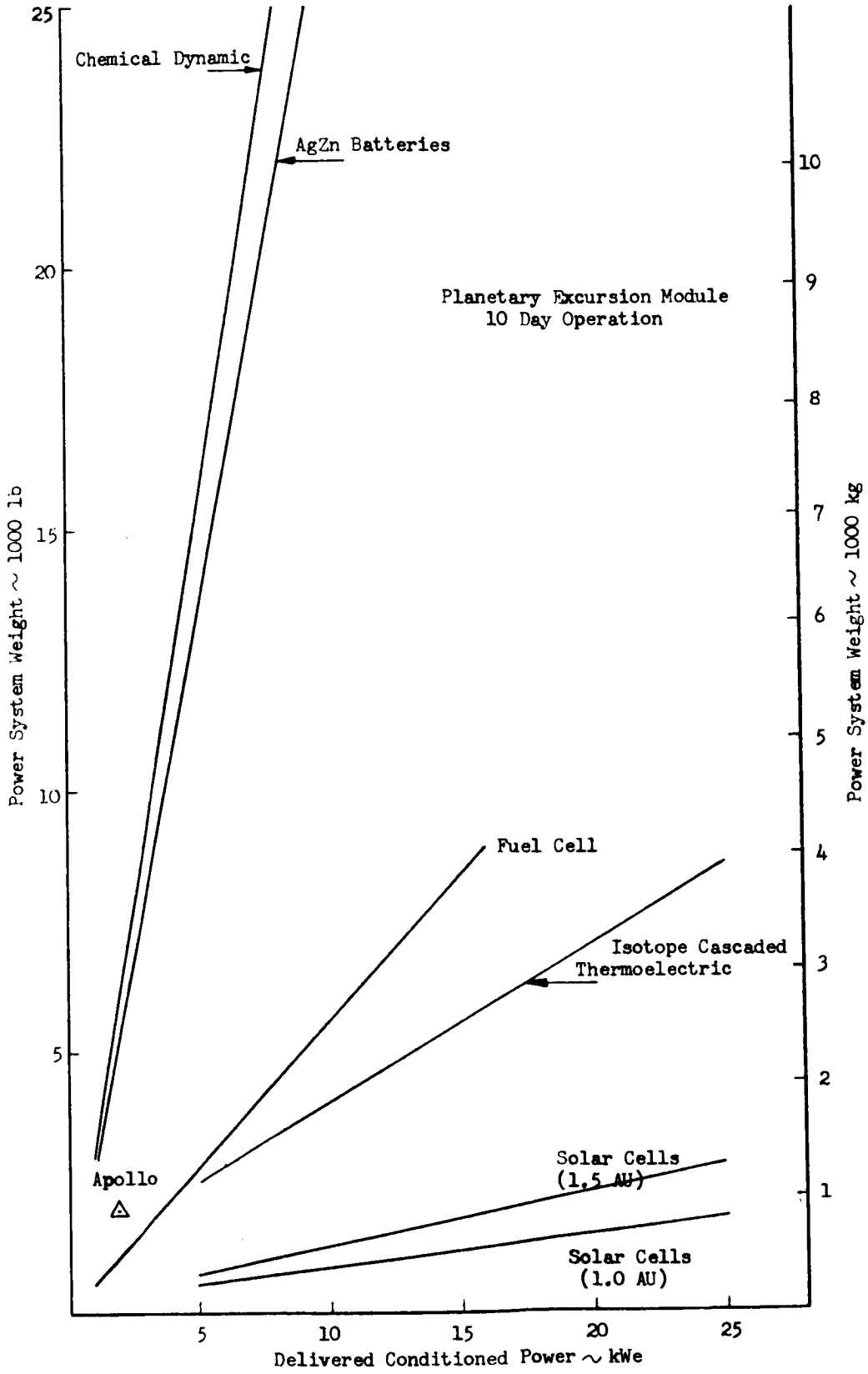

Figure 38. Power System Weight for Planetary Excursion Module, 10-Day Operation

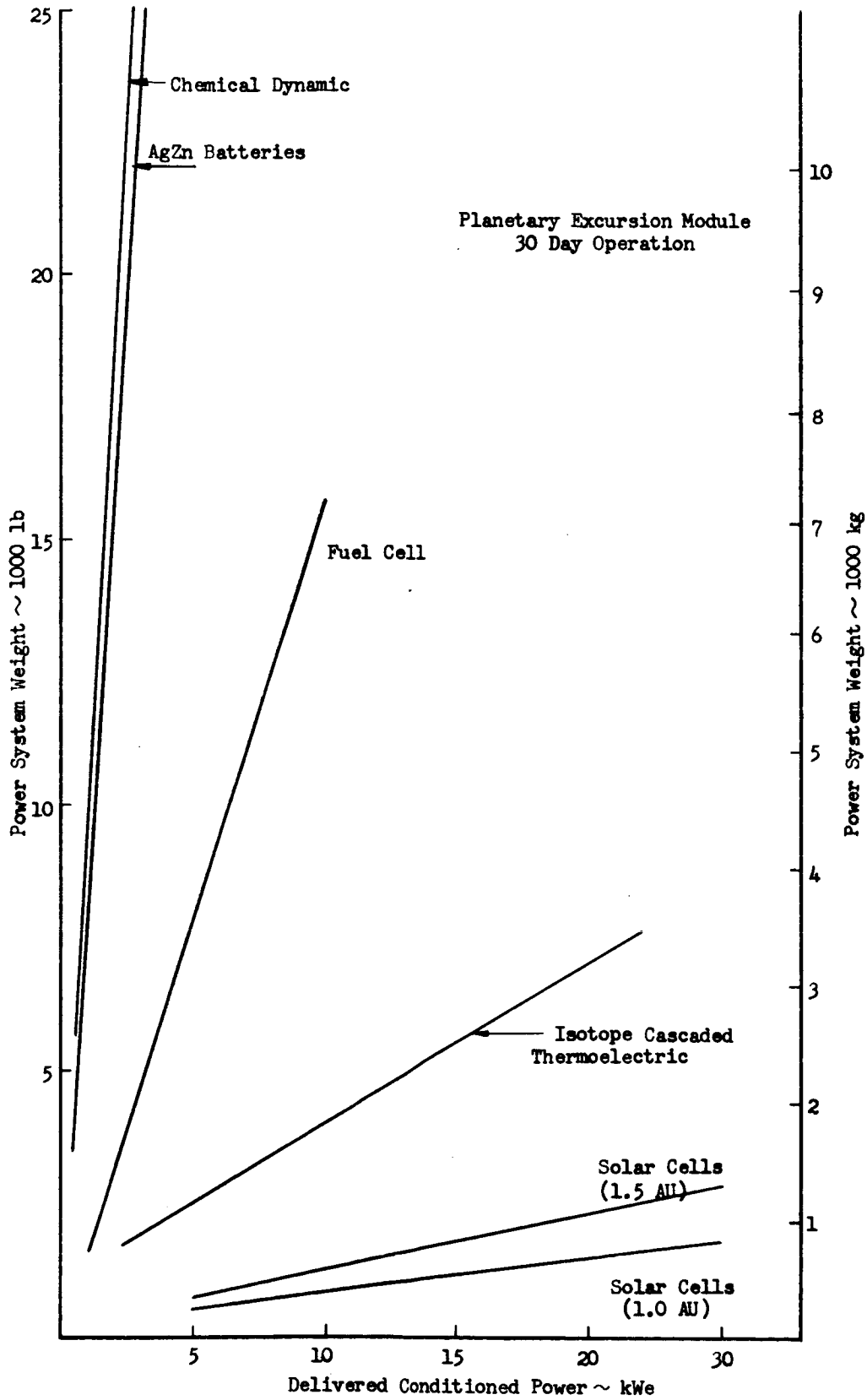

Figure 39. Power System Weight for Planetary Excursion Module, 30-Day Operation

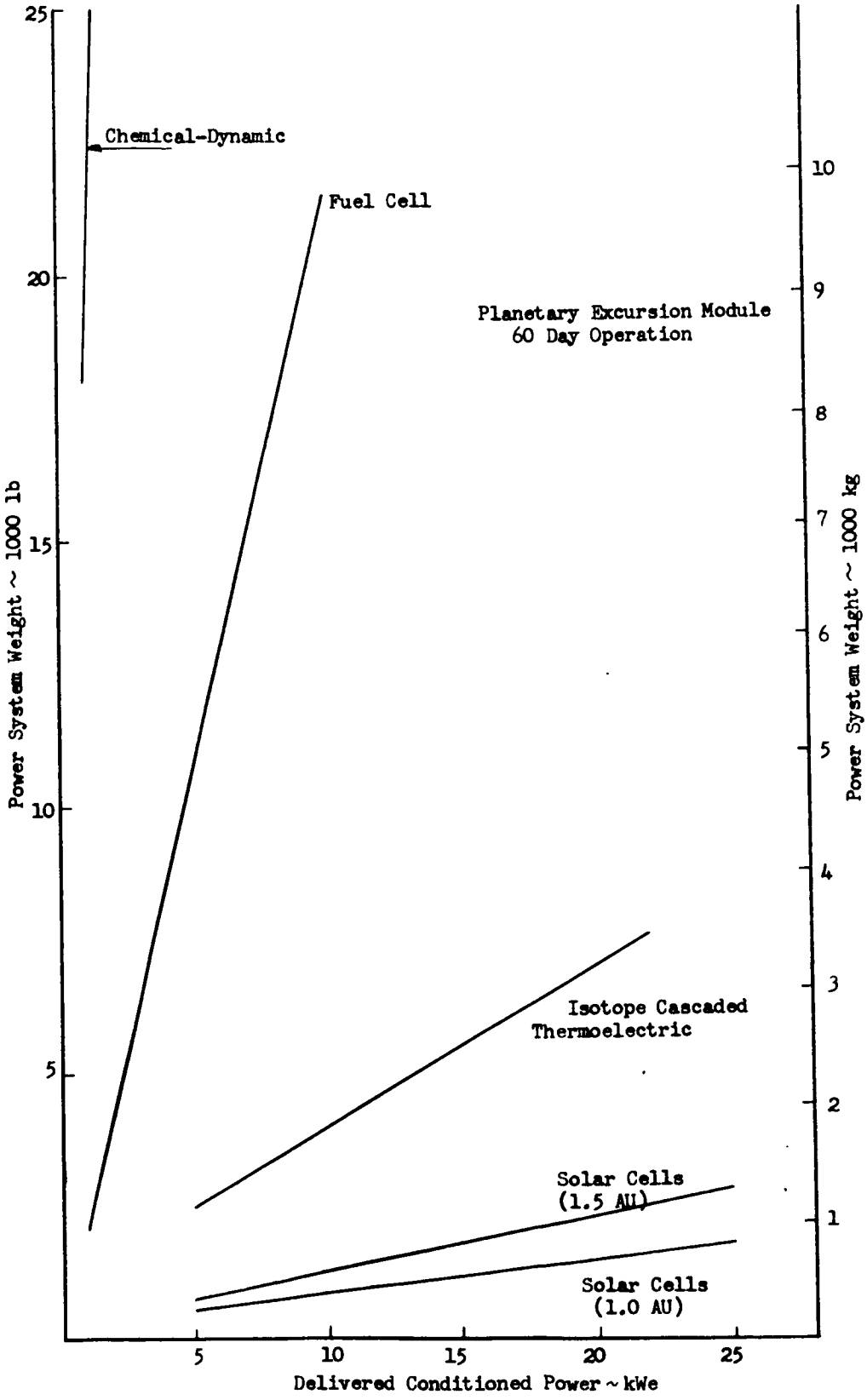

Figure 40. Power System Weight for Planetary Excursion Module, 60-Day Operation

GROUND RULES

Reliability and Maintenance Philosophy

A power subsystem reliability goal of 0.999 was assumed for this study, reliability being defined here as the probability of providing the required power for the duration of the mission. Since no known power system can achieve a reliability of 0.999 for all missions unassisted, maintenance and/or redundancy is utilized for system synthesis.

No attempt was made to distinguish between total load and essential load requirements since these levels vary with individual mission objectives. In this respect, then, some of the power system weights are conservative. For example, a 30-kWe power level total design requirement could be met by utilizing six 5-kWe systems in parallel and, thereby, permitting failure of one or more system to deliver a reduced essential load level. Although there would be a weight penalty associated with the parallel system, an overall weight saving may be effected through a reduction of redundant systems and spare parts. Smaller systems are combined, however, when total power requirements exceed practical size limitations of particular systems.

Since reliability forecasts are generally not available, failure rates of dynamic conversion equipment operating in the post-1980 period are assumed to be one-tenth that of present-day demonstrated values. For those systems having no suitable failure rate history at present, failure rates are projected based on the demonstrated values of similar type equipment.

The 0.999 reliability was assumed to be met through redundancy and maintenance except where it is not practical due to hazards, complexity, or inaccessibility. For example, high speed turbo-alternators and compressors were assumed to have a one-year life, would be replaced as a unit, and would require redundancy for each additional year of operation. Additionally, 5 percent of the electrical power conversion system weight is allowed for power conditioning system spare parts.

Environmental Effects

Temperature (Heliocentric Radius)

The effect of temperature was found to be critical only for solar power systems (radiators excepted) wherein power output is directly a function of local solar photon flux density, which establishes equilibrium temperature. Compensation was provided for the decreased performance of solar power systems with increased heliocentric radius. Although weight is a function of heliocentric radius, no advantage was taken for distances of less than one AU (0.38 AU being the smallest heliocentric radius of concern). This was based

on the assumption of meeting a constant power requirement from earth orbit, although in practice the requirement would likely be tailored for a given mission.

Space Radiation

The effects of space radiation are critical only for photovoltaic cells at flux values $\geq 10^{10} \frac{\text{Protons}}{\text{cm}^2}$. Space fluxes of electrons and protons cause defects by knocking atoms out of their equilibrium lattice positions, thereby forming recombination centers for electron-hole pairs prior to collection. Thus, the cell power output is inversely proportional to total intercepted flux and must be compensated for. Figure 76 (Page 179) shows power degradation for different values of proton flux.

Several methods of reducing space radiation effects have been established. These include the use of a fused silica shield over the exposed surface of the cell, providing additional cells to achieve an end-of-life power level, and using more radiation resistant crystals. For this study, advantage is taken of all three methods based on dendritic crystal growth with weight allowances for additional cells of projected epitaxial (lithium doped) and drift-field systems.

Meteoroid Impact

The meteoroid environment has a pronounced effect on the design of solar cells, solar mirrors, and radiators. Meteoroid flux density is considered to be a strong function of heliocentric radius; therefore, the prediction of total flux interception quantities must be approached through trajectory integration. The projected influence of meteoroid impact on future developed solar cells and mirrors is nebulous at best. For these reasons, the estimated weights are the result of judgment, and an earth orbit baseline for radiator design. These establish baseline parameters that may be modified for a given mission for promising systems.

For solar mirrors, the assumption of a five-year life was made with a weight allowance of 20 percent increase per year duration of mission. The weight allowance for solar cells is included in an overall degradation of 5 percent per year.

For radiator design, data exists for an earth orbit (Reference 3) and was used herein for sizing purposes. Incremental weights must be added to match specific mission profile requirements.

Occultation Effects

Solar power systems in planetary orbit require secondary energy sources during shadow periods. With photovoltaic power systems, secondary batteries are normally used. Power systems utilizing solar heat could use either secondary batteries or thermal energy storage devices. Use of thermal storage devices is restricted to solar concentrator type power systems such as thermoelectric, thermionic and dynamic systems. Cycle efficiency of all these latter systems is dependent on heat source temperature. They are designed to operate at the maximum permissible equipment temperature. A thermal energy storage device used to augment these systems must maintain this operating temperature for best efficiency. Use of the latent heat of molten material while allowing a few hundred degrees of temperature change was surveyed for this application. Even with thermal energy storage, secondary batteries may be required to compensate for fluctuations in generator output and to supply peak loads. The materials considered for thermal energy storage are corrosive in the molten state and their containment is not yet possible. They also shrink considerably during solidification (for example, 16 percent for LiH) and, therefore, present difficult heat transfer problems.

Depending on the material used, 210 to 730 Whr/kg can be stored. Estimating 20 percent additional weight for containers and 10 percent for converter efficiency, the usable stored energy will be between 18 and 60 Whr/kg. In this study, thermal energy storage was not considered in the subsequent mission/system analyses since the availability of systems of this type is not certain for the time period considered and system reliability has not been established.

The approach for determining additional required capacity for solar power systems augmented by secondary batteries is discussed in the following paragraphs.

Silver-cadmium secondary batteries have a discharge-charge efficiency of 70 percent to 75 percent. This efficiency is a function of battery discharge rate, depth of discharge, temperature, and rate of charge. With the assumption of a one-hour discharge rate, the plateau voltage per cell is 1.05 volts. Maximum voltage at start of discharge is 1.25 volts and, declines to the plateau voltage after 20 percent discharge of total capacity. Until maximum depth of discharge is less than 66 percent, the charge voltage will also be constant at about 1.45 volts during constant current charging. This voltage will rise when 85 percent to 90 percent charge is reached. The end of charge voltage should be kept below 1.55 to 1.60 volts per cell for maximum life. This corresponds to approximately 95 percent of full charge. Based on this data, a 72 percent discharge-charge efficiency was used to determine the

required increase in solar panel size. The battery charger efficiency is assumed to be 85 percent. Thus, the overall charge-discharge efficiency becomes 0.72 x 0.85 = 0.61.

Figure 41 provides the necessary relationships to size the required primary system output to accommodate secondary battery charging during eclipse. An example of its use is provided for clarification since these weights must be added to the projected solar power system weights presented in the Weight Summary for particular missions.

Example:

Hypothesis;

Primary system - Photovoltaic power system
Mission - Planetary orbit, three months duration
Orbit period - 100 min (1.67 hr)
Dark period - 40 min (0.67 hr)
Solar panel normal load - 10 kWe
Battery load during darkness - 5 kWe

Solution:

Number of charge-discharge cycles (2175-hr mission)

$$= \frac{2175 \text{ hr}}{1.67 \text{ hr/cycle}} = 1310 \text{ cycles}$$

Silver-cadmium battery energy density = 20 Whr/kg

$$\text{Battery weight} = \frac{5 \text{ kWe}}{20 \text{ Whr/kg}} = 250 \text{ kg}$$

(see also Figure 86, Page 205)

$$\frac{\text{Shadow duration}}{\text{Illumination duration}} \times \frac{\%\ \text{Normal load}}{\text{while dark}} = \frac{0.67 \text{ hr}}{1.00 \text{ hr}} \times 50\% = 33.3\%$$

Ratio of required solar panel output to rated load (from Figure 41) = 1.55

Required solar panel output = 1.55 x 10 kWe = 15.5 kWe

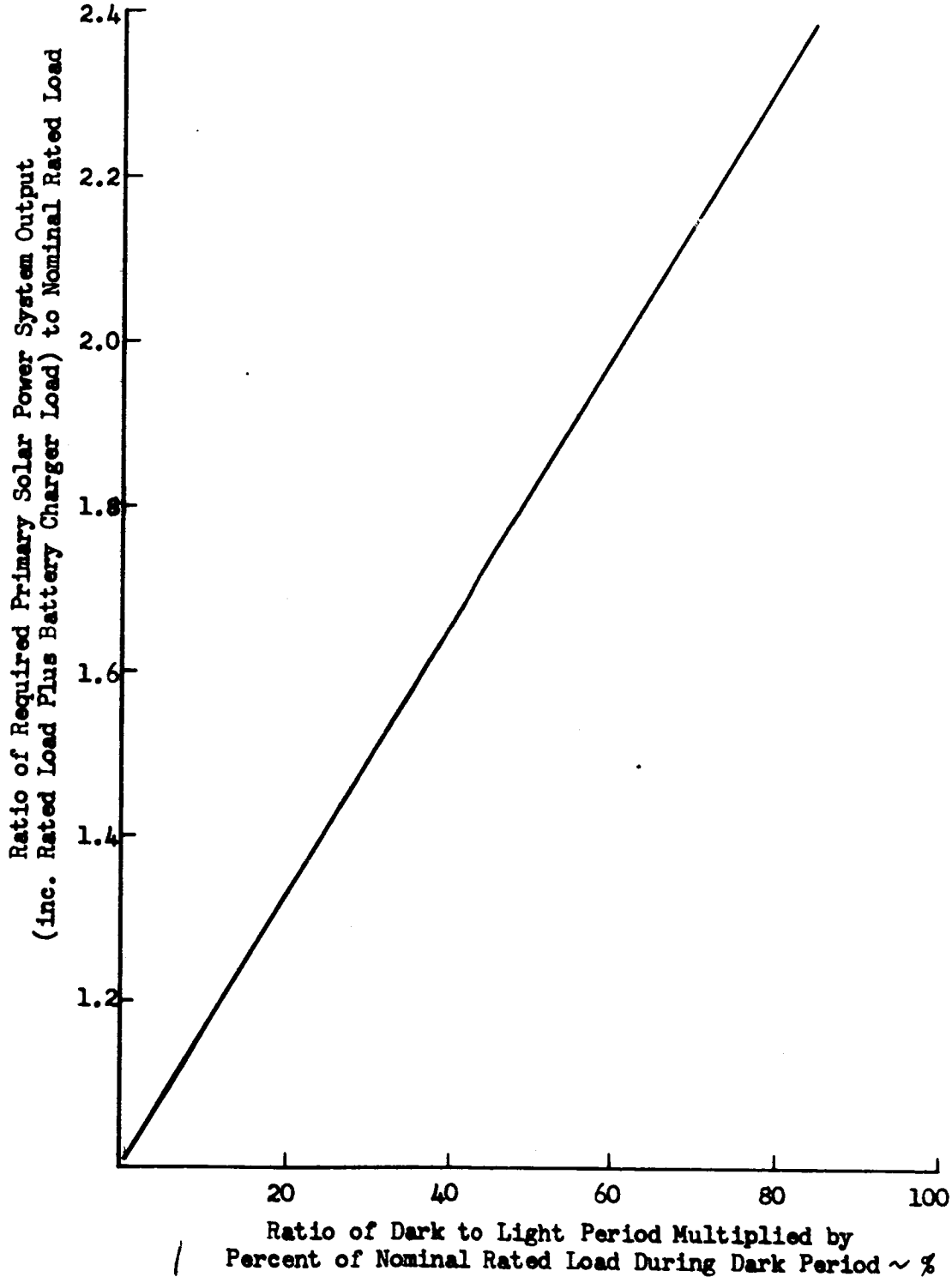

Figure 41. Required Primary Solar Power System Output Increase to Accommodate Occultation Effects Requiring Charging of Secondary Batteries

Special Considerations

Secondary Systems

Nominal power only was used in sizing the candidate systems. It was assumed that all selected systems would be able to supply small overload power demands (10 to 15 percent) for short periods (≈15 minutes) but large peak loads (≈200 percent nominal) and/or emergency power would have to be accommodated by secondary systems whose weights have not been included in the Weight Summary compared values. The methodology for sizing these secondary systems is included in this report and can be used when specific vehicles are tailored to given missions.

Similarly, to satisfy occultation needs, the required increase in power systems is not included in the baseline solar panel system weights. The methodology to determine the added weight requirements is included in the Occultation section and the weight penalties can be assessed for selected mission profiles.

A minimal battery for initial nuclear reactor start and for downtime less than two hours is included in power conditioning weights. For extended reactor downtime, battery allowances of 110 lb/hr (each module) and gas bottles of 7 pounds/restart (each module) must be added to Table 22.

Radiation Shielding

For this study, radiation shielding is based on a dose rate of 10 rem per year. This accumulates to a total dose of 50 rem for the five year missions, 25 percent of the acceptable dose limit of 200 rem to the blood-forming organs (bone marrow). For shorter missions, the dose rate could be increased but the added complexity of varying shield weight (second-order effect) with mission duration is not merited until the spacecraft is better defined.

Shadow shielding is assumed for both the reactor and isotope systems. For the reactor designs, the shield weights are predicated on a reactor/mission module separation distance of 125 feet, consistent with the MORL studies. The dose plane diameter is taken as 60 feet*, a compromise between the ~35 feet used in some studies (Reference 6) and the 80 feet diameter considered for MORL. Further dimensional scaling and power source positioning (location with respect to the mission module) is possible but unnecessary in the light of the uncertainties inherent in conceptual design. No allowance is

*Subsequent analysis indicates that the mission module diameter need not exceed 33 feet.

made for a 4 π shutdown shield, rendezvous and docking (thereby requiring approach within the shadow cone), or retraction and shutdown of the reactor prior to vehicle mateup. Weight allowances have been included for retraction mechanisms but not for restart capability since the number of restarts is not defined.

Radiation shields for the isotope systems for the mission module are based on an effective distance of 25.4 feet, determined by residence time/distance integration. This allows for separation distances of approximately 200 feet between the mission module and the isotope heat source during the majority of the mission and for much smaller distances when retraction of the system is required.

CANDIDATE POWER SUBSYSTEMS

Nuclear Reactor System

Nuclear Reactor Sources

Thermal nuclear reactor systems only have been considered for this application. The associated power conversion systems considered include Brayton, Rankine, and thermoelectric cycles. For each of these systems/reactor combinations, projected efficiency data are available for the post-1980 era and require no further extrapolation. Rankine and thermoelectric cycle data have been established for a range of power levels and are directly referenced. For the Brayton cycle, the baseline data are based on the 20-kWe MORL system which is comprised of two 10-kWe power conversion systems (PCS). Weight scaling as a function of power level for the post-1980 era is augmented by Figure 42, which accounts for (i.e., includes) power conditioning and a thermal shield. Figure 42, resulted from examination of available data defining applicable power system to the 1975 to 1985 period. The information generally described systems in a 4- to 15-kWe range with the majority of the data at 6.0 kWe. Therefore, this point was used as a reference. The shape of the curve represents an extrapolation to 35 kWe output relative to 6.0-kWe for power conditioning and thermal shield weights. Shielding is based on a common configuration for all systems (125-foot separation, 60-foot dose plane), and has a direct influence on the shield, extension boom, and cables weights evolved.

A weight penalty for startup and restart batteries is required for more than one hour delay or down-time. This weight penalty is estimated to be 110 pounds per module per hour of continuous down-time; however, no weight allowance has been made for this condition at this time.

The reactor with the PCS is separated from the mission module by a boom to accomplish radiation attenuation. The power transmission cables

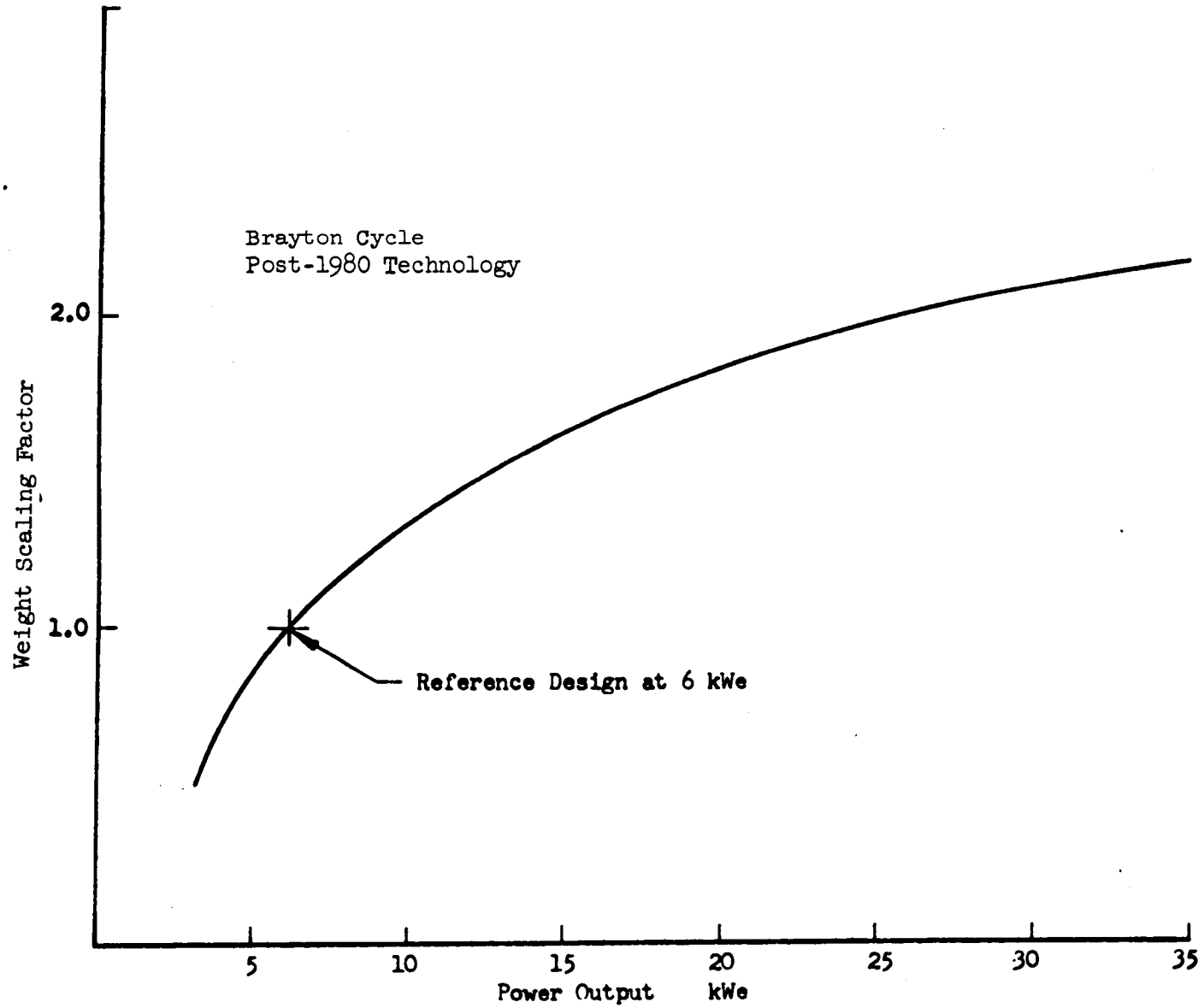

Figure 42. Combined Power Conditioning Unit and Thermal Shield Scaling Factor vs Power Output

leading to the power conditioning system are housed inside the boom. Parametric weights of boom and transmission cables are shown in Figures 43 and 44.

All power systems considered consist of a nuclear reactor fueled by uranium with a zirconium hydride moderator and are controlled by beryllium reflectors. The basic technology and design of these reactors were developed by the Atomics International Division of North American Rockwell Corp. for SNAP 10, 2, and 8 reactors (Reference 5).

The fast neutron spectrum nuclear reactors presently under study/development are concentrating on power levels considerably above 30 kWe; it is felt that this power level exceeds that for the application considered in this study. The associated power conversion systems being considered are based on Brayton, potassium, Rankine, and thermionic cycles. Even though the efficiencies of fast reactor systems appear attractive, a direct comparison between fast and thermal nuclear reactors was not undertaken because:

1. The projected long-life reliabilities of fast spectrum nuclear reactors is uncertain because of the requirement for presently undeveloped materials to withstand extremely high operating temperatures.

2. Available data consider power levels in the range of 300 to 3000 kWe, thereby, making extrapolated results doubtful.

Thermal Nuclear Reactor/Brayton Cycle Power System

The reactor is cooled by an eutectic mixture of sodium and potassium (NaK), forming a primary loop to a heat exchanger located between the primary and secondary radiation shield (Figure 45). This feature attenuates activated primary coolant gamma rays. An intermediate NaK loop connects the primary heat exchanger with a NaK-to-gas heat exchanger. Heated argon drives the turbine, flows through a recuperator, gas cooler, compressor and returns via the recuperator to the heat exchanger. A NaK radiating loop conducts the waste heat from the gas cooler to the radiator. Temperatures, efficiencies, and corresponding weight breakdown are given in Table 28.

The radiation shield designed to attenuate both neutron and gamma radiation behind the dose plane of the payload to a maximum level of 10 rem per year is split into two sections. The upper section is located below the reactor, while the lower section is located below the primary loop, forming a gallery for the primary heat exchanger. Both shield sections provide gamma and neutron shielding and are fabricated from spent uranium and

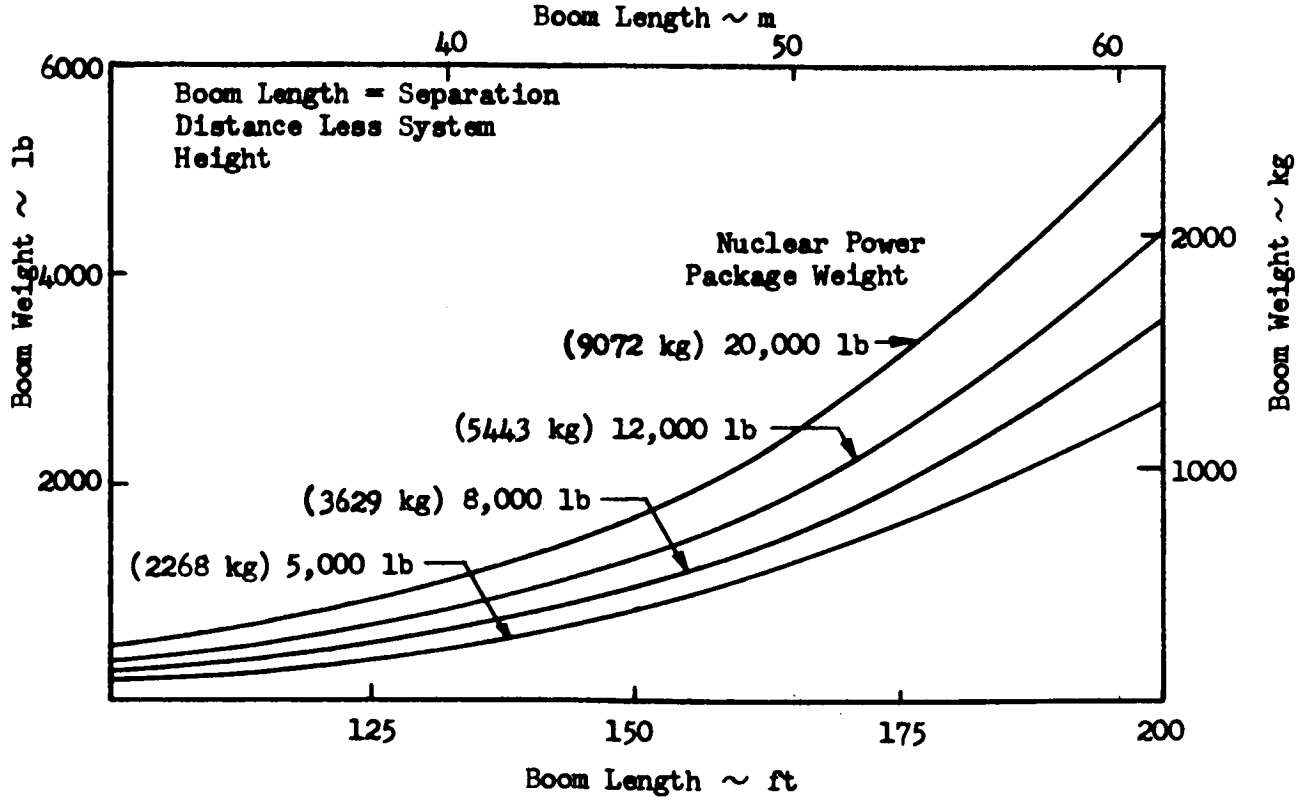

Figure 43. Boom Weight for Nuclear Reactor Subsystems

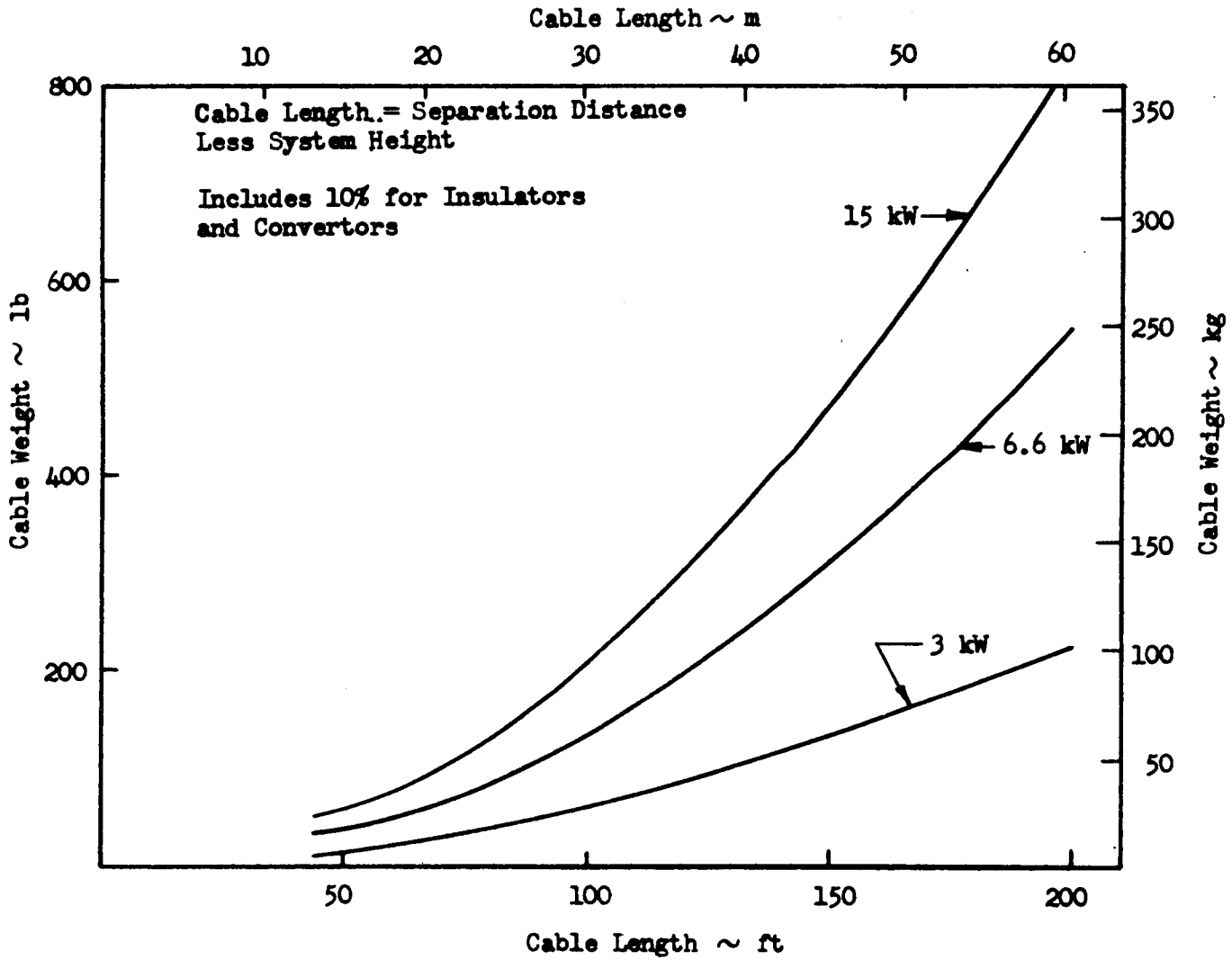

Figure 44. Cable Weight Versus Length for 1800-Cycle, 3-Phase, 115/200 Volts

Table 28. Parametric Data for Reactor/Brayton PCS
(Based on 10-kwe System, Reference 3)

Item	Characteristic
Reactor outlet temperature	1300 F
Turbine inlet temperature	1250 F
Turbine outlet temperature	970 F
Radiator inlet temperature	413 F
Compressor inlet temperature	200 F
Turbine efficiency	0.9
Cycle efficiency (E_C)	0.18
Alternator efficiency (E_A)	0.95
Power conditioning efficiency (E_{PC})	0.83
Compressor efficiency	0.83
Recuperator efficiency	0.9
Losses (L)	0.923
Gross system efficiency (E_C) (E_A) (E_{PC}) (L)	0.131
Power source (reactor)	388 lb
Radiation shield	2980 lb
Primary loop	79 lb
PCS (1 active, 2 redundant)	2519 lb
Radiator	885 lb
Boom and cable	575 lb
Power conditioning system	1500 lb
Thermal shield	1118 lb

lithium hydride. The shield weight reflects several governing parameters, and the breakdown for several thermal power ratings and system configurations is shown in Table 29.

The reactor and power conversion systems are separated from the mission module by an extension boom to complement shield attenuation. A thermal shield surrounds the reactor and the radiators during launch and

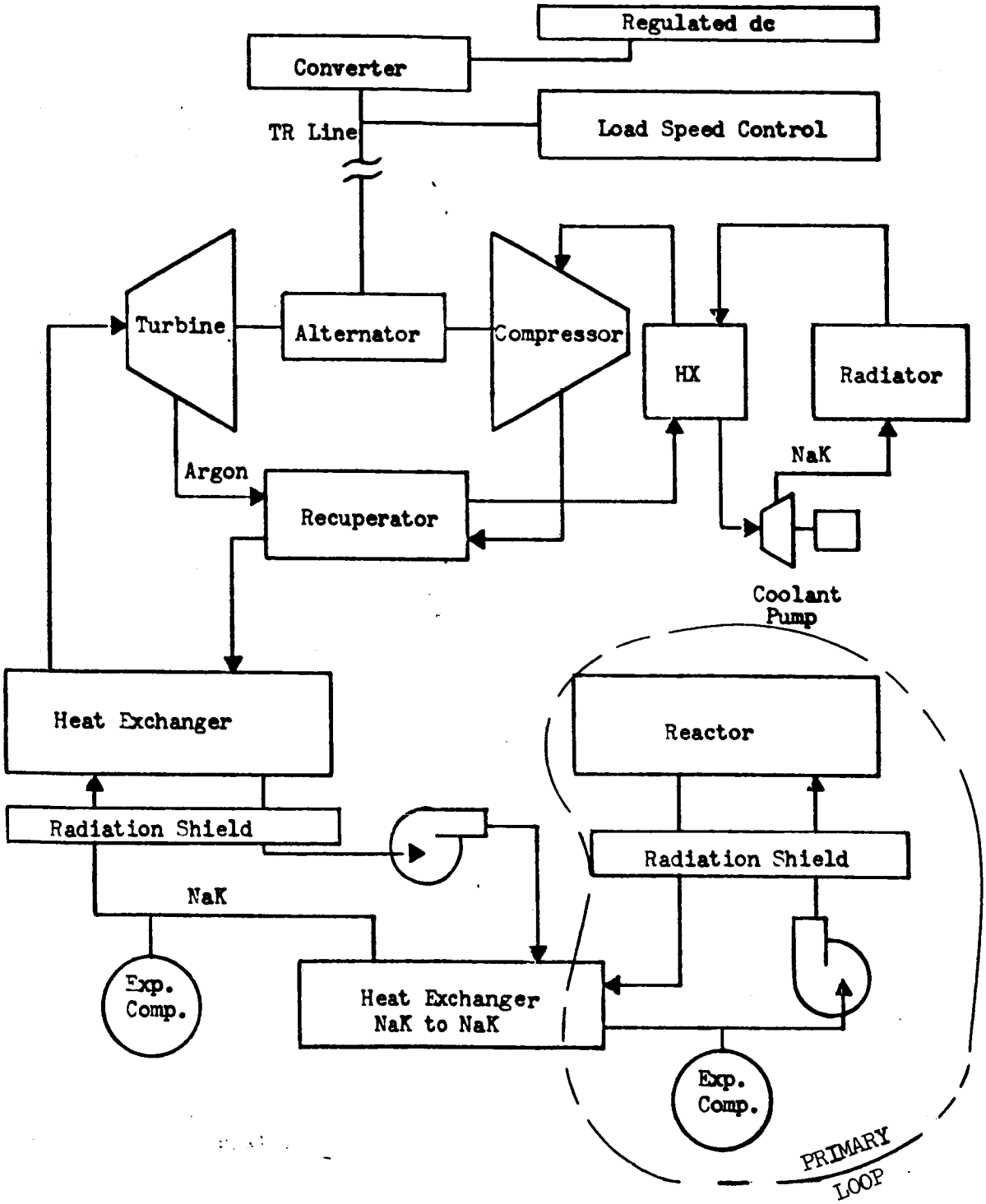

Figure 45. Nuclear Reactor Brayton Cycle System

Table 29. Radiation Shield Parameters for Nuclear Reactor/Brayton Cycle System

Parameter	Reference System					
	SNAP 10B (10 kwe)		SNAP 8 (20 kwe)		SNAP 8 (35 kwe)	
	Basic Weight Influencing Parameter	Correction Factor*	Basic Weight Influencing Parameter	Correction Factor	Basic Weight Influencing Parameter	Correction Factor
Dose plane diameter (ft)	60	1.0	60	1.0	60	1.0
Separation distance (ft)	125	1.3	125	1.3	125	1.3
Reactor power (kwt)	76	0.75	152	0.82	226	0.89
Shadow cone diameter (in.)	14.6	0.8	23.5	1.15	23.5	1.15
Fuel element length (in.)	13.8	0.92	24	1.17	24	1.17
Core diagram (in.)	8.9	0.99	9.7	1.0	9.7	1.0
Dose rate (rem/yr)	10	1.06	10	1.06	10	1.6
Gallery height (in.)	14.5	0.87	15.5	0.9	20	0.95
Total (product) correction factor		0.65		1.13		1.29
Shield weight (lb)		2980		5190		5820

*Correction factor is compensation for deviation from nominal value (see Reference 7)

reactor shutdown operations. This thermal shield prevents fluid freezing in the radiator tubes. After reactor startup, this thermal shield is deployed around the boom. Prior to earth reentry, the reactor power system is jettisoned by a release mechanism at the end of the boom attaching structure. After separation of the attaching structure from the mission module, deorbit action is effected by firing rockets attached to the boom structure. An elementary guidance system and an RCS system are used to supplement the main rockets. The weight (511 lbs) of this disposal system is included in the weight of the thermal shield and reactor disposal system.

The information for this system was derived from the MORL studies, which were based on an overall life expectancy of two and one-half years, with a design reliability of 0.95, approximately equal to 0.98 for one year since:

$$R_2 = e^{-\lambda t_2} = 0.95; \lambda t_2 = 0.05$$

$$t_2 = 21250 \text{ hours (2-1/2 years)}$$

$$\lambda = \frac{0.05}{t_2} = \frac{0.05}{21250} = 2.355 \times 10^{-6}, \text{ failure rate per hour}$$

$$t_1 = 8500 \text{ hours (1 year)}$$

$$\lambda t_1 = 2 \times 10^{-2}$$

$$R_1 = e^{-0.02} = 0.98$$

The MORL study is based on a power level of 20 kwe, with two active and four standby power conversion systems. The reliability figures presented in this study are based on a Poisson distribution (Reference 3).

$$R = e^{-N\lambda t}\left[1 - N\lambda t + \frac{(N\lambda t)^2}{2!} + \ldots \frac{(N\lambda t)^n}{n!}\right]$$

where

N = Number of operating units

n = Number of standby units

λ = Failure rate per hour

t = Operating time, hours

The preceding equation directly applies to thermoelectric system designs where component and system lifetimes are assumed to be equal. For systems where component or subsystem lifetimes equal one-half the system lifetime, an equation was developed for a total of three such subsystems. Failure density and success density were combined for each of the three possible paths to successful operation for system lifetime. These functions were combined to provide the required reliability formula for both the Brayton and Rankine power conversion systems (PCS).

$$R = e^{-2\lambda t}\left[1 + 2\lambda t + \frac{(2\lambda t)^2}{8}\right]$$

where

t = One-half system life, hour

λ = Single power conversion subsystem failure rate per hour

A complete failure rate diagram of this 20-kwe Brayton cycle system is shown in Figure 46.. For the 10-kwe Brayton system, one active and two standby PCS are assumed with a one-year reliability of 0.98. Failure rate improvement associated with advances in technology should achieve the desired reliability of 0.999 by 1980. In general, the Brayton cycle power conversion has higher cycle efficiencies than other power conversion systems. Also, its working fluid is noncorrosive. Problems, such as zero-gravity boiling and condensing, inherent in other working fluids are nonexistent. One disadvantage of this PCS is the requirement for larger radiators, since heat is neither added nor rejected isothermally as in a Rankine cycle PCS. Also, Brayton cycle performance is very sensitive to system pressure losses. The radiator for the PCS consists of one active and two redundant loops. Each of the loops comprises straight radiator tubes that make a single pass along the inside of the radiator wall between the inlet and outlet manifolds. The tube and shell are fabricated of aluminum, with a stainless steel liner bonded to the inside of the aluminum tube to prevent NaK corrosion. Armor is provided for bumper meteoroid protection. The alternative radiator coolant considered is FC-75, which requires a slightly larger radiator area, but results in considerable weight saving due to elimination of the corrosion protective stainless steel liner. However, there is the possibility of long-term thermal decomposition at upper system temperatures, and film temperatures in the heat-sink heat exchanger are near the critical temperature for the FC-75 coolant. These

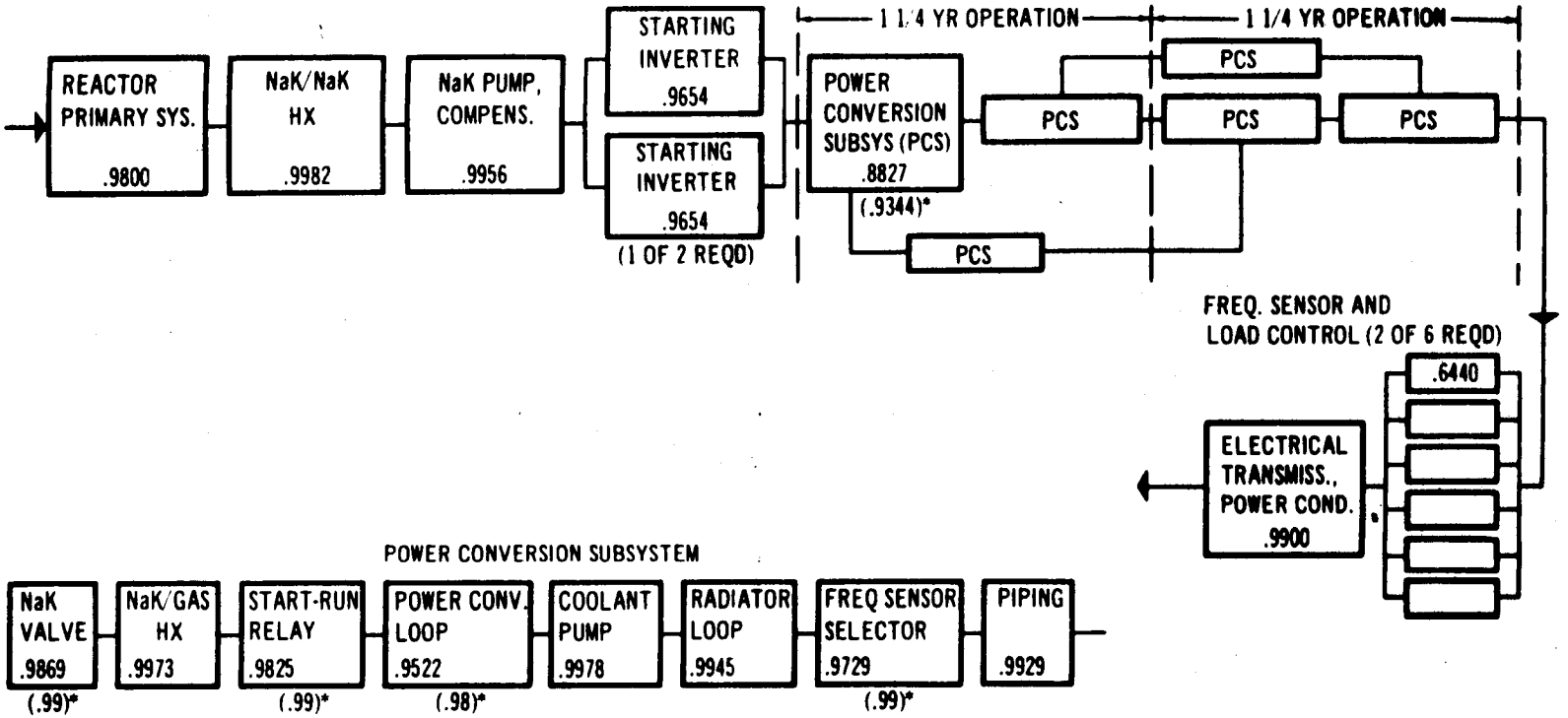

RELIABILITY CALCULATION:

R (STARTING INVERTERS) = $e^{-\lambda t}(1 + \lambda t) = .9654\,(1 + .0352) = 0.9994$

R (POWER CONVERSION SUBSYS, 1 1/4 YRS) = (.9869) (.9973) (.9825) (.9522) (.9978) (.9945) (.9729) (.9929) = 0.8827, AND $\lambda t = .1248$,
ALTERNATELY (0.9344, AND $\lambda t = .0679$)*

R (FREQ SENSOR, LOAD CONTROL) = $e^{-N\lambda t}\left(1 + N\lambda t + \ldots + \frac{(N\lambda t)^n}{n!}\right) = 0.4148\left(1 + .88 + \frac{(.88)^2}{2} + \frac{(.88)^3}{6} + \frac{(.88)^4}{24}\right) = 0.9978$

WHERE N = OPERATING UNITS (2)
n = STANDBY UNITS (4)

R (REACTOR POWER SYS, 2 1/2 YRS) = (.9800) (.9982) (.9956) (.9994) $\left[e^{-2\lambda t}\left(1 + 2\lambda t + \frac{(2\lambda t)^2}{8}\right)\right]^2$ (.9978) (.9900) = 0.9227; (ALTERNATELY 0.9482)*
P.C.S.

*REFLECTS REVISION OF COMPONENT RELIABILITY VALUES TO GENERALLY CONFORM WITH BASIS FOR OTHER POWER CONVERSION SYSTEMS)

Figure 46. 20 kwe Brayton Cycle System Reliability Diagram

characteristics of FC-75 have resulted in marginal use of this coolant at this time. Meteoroid nonpuncture probability of 0.99 for two and one-half years used in the MORL study compares to approximately 0.999 for one year nonpuncture probability, which is the basis for the radiator weights used. Additional meteoroid shielding may be required, however, for missions which extend toward the asteroid belts.

Thermal Nuclear Reactor/Mercury Rankine Cycle Power System

The heat source description for this power system is the same as for the Brayton cycle power conversion system previously described. Thermal power levels are different due to differing overall cycle efficiencies, for specific electrical output ratings.

The power conversion system consists of a mercury boiler, a combined rotating unit consisting of mercury pumps, turbine and alternator, and a radiator-condenser, as shown schematically in Figure 47. Efficiencies, temperatures, and component weights are given in Table 30. This power system is considered for mission module application for lifetimes of from one to five years. For power conversion, a 5-kwe unit is assumed as the basic building block of this system, and multiples of this unit are used to arrive at higher power ratings. There is hope of developing a 25-kwe combined rotating unit. At present, however, this is only a matter of concept. For one-year operation, present day studies show an overall system reliability of 0.98, using multiples of 5-kwe active loops up to four total units (equivalent to 20 kwe) with one redundant unit, as indicated in Figure 48, with two redundant units used for ratings up to ten active loops. It is expected that by 1980 the target reliability may be achieved with improvement in failure rates of components.

Shield weights for this power system are shown in Table 31.

Advantages of this power conversion system are the lower power conversion system and radiator weights. Disadvantages are based on the corrosive qualities of mercury, uncertainties connected with the possibility of zero-gravity boiling and condensing, and lubrication and bearing problems.

The power conversion system is housed below the shadow shield, and the radiator-condenser forms a cone around the PCS components subtending the shadow shield (Figure 49). The reactor and power conversion systems

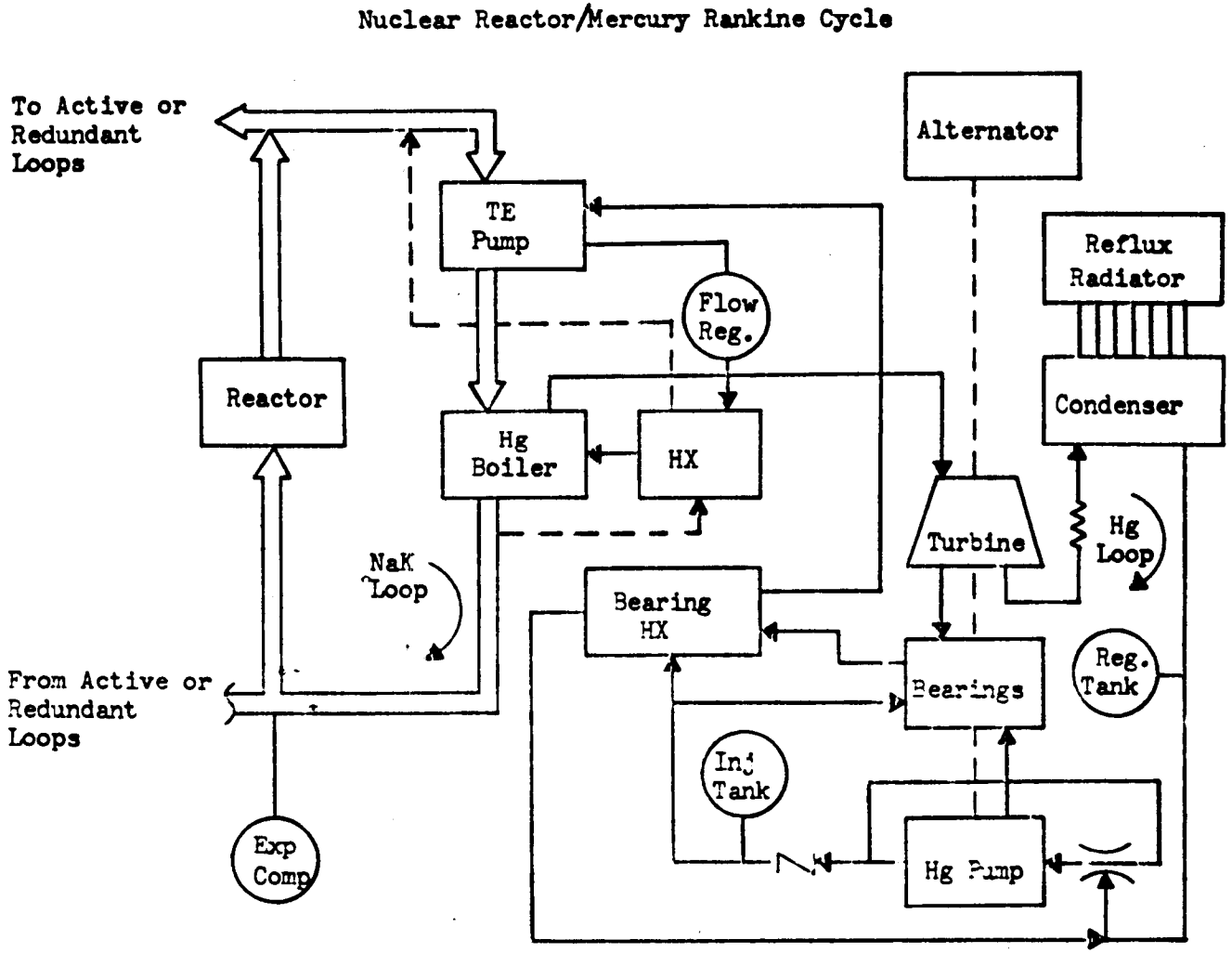

Figure 47. Nuclear Reactor Mercury Rankine Cycle System Schematic

Table 30. Parametric Data for Reactor/Rankine PCS
(Based on 10 kwe System, Reference 4)

Item	Characteristic
Reactor outlet temperature	1300 F
Turbine inlet temperature	1250 F
Radiator/condenser inlet temperature	622 F
Turbine efficiency	0.6
Mercury pump efficiency	0.36
Machine efficiency	0.48
Cycle efficiency (E_c)	0.084
Alternator efficiency	0.9
Power conditioning efficiency (E_{pc})	0.83
Gross system efficiency (E_c) (E_{pc})	0.07
Power source (reactor)	388 lb
Radiation shield	3215 lb
Primary loop	298 lb
PCS (2 active 5 kwe modules, 1 redundant)	1282 lb
Radiator	558 lb
Boom and cables	545 lb
Power conditioning system	1900 lb
Thermal shield	921 lb

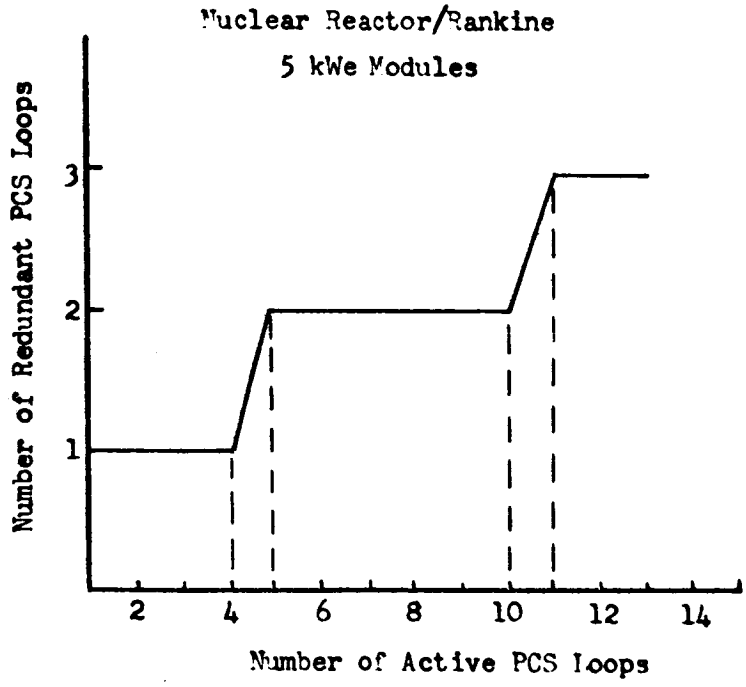

Figure 48. Power Conditioning System Redundancy Versus Number of Active Loops (Nuclear Reactor Systems)

Table 31. Radiation Shield Parameters for Nuclear Reactor/Rankine Cycle System

Parameter	Reference System					
	SNAP 10B (5 kwe)		SNAP 10B (10 kwe)		SNAP 8 (20 kwe)	
	Basic Weight Influencing Parameters	Correction Factor*	Basic Weight Influencing Parameters	Correction Factor	Basic Weight Influencing Parameters	Correction Factor
Dose plane diagram (ft)	60	1.0	60	1.0	60	1.0
Separation distance (ft)	125	1.3	125	1.3	125	1.3
Reactor power (kwt)	71	0.73	143	0.8	286	0.9
Shadow cone diameter (in.)	14.6	0.8	14.6	0.8	23.5	1.15
Fuel element length (in.)	13.8	0.92	13.8	0.92	24	1.17
Core diameter (in.)	8.9	0.99	8.9	0.99	9.7	1.0
Dose rate (rem/yr)	10	1.06	10	1.06	10	1.06
Gallery height (in.)	14.5	0.87	14.5	0.87	18.5	0.93
Total (product) correction factor		0.63		0.7		1.25
Shield weight (lb)		2895		3215		5740

*Correction factor is compensation for deviation from nominal value (see Reference 7).

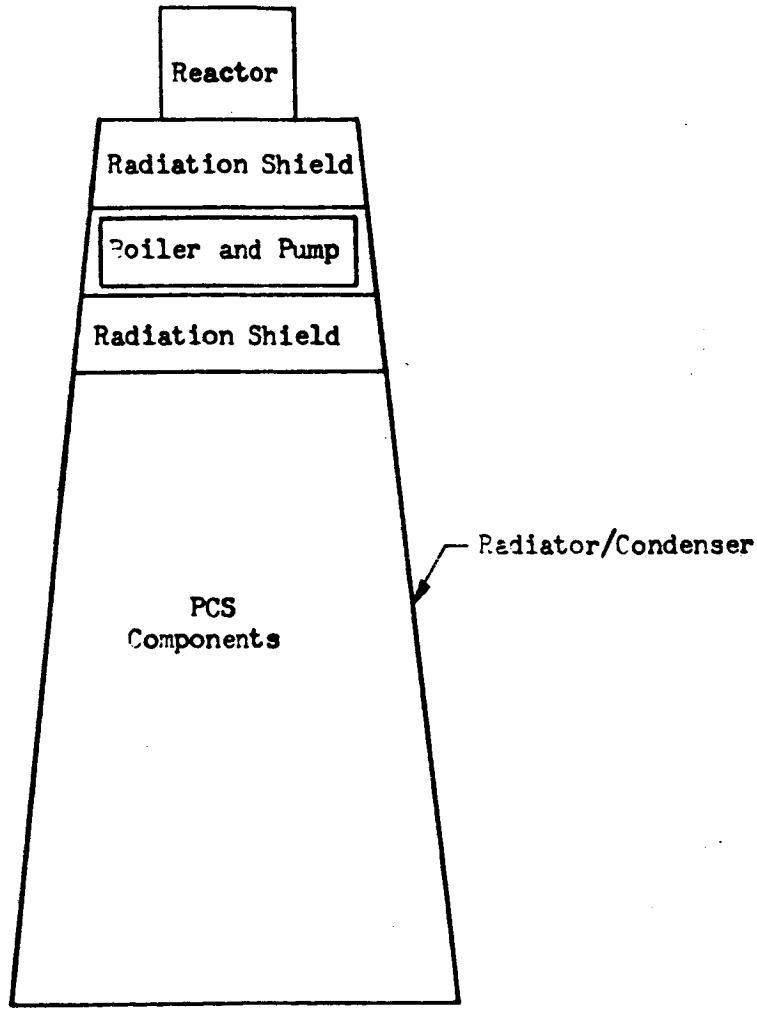

Figure 49. Typical Arrangement of Nuclear Reactor Mercury/Rankine Power System

are separated from the mission module by an extension boom, designed to attenuate radiation levels. This boom is retracted during launch operations and is extended after reaching a designated orbit. For orbit insertion and aerobraking, provisions must be made to retract the reactor. This will involve reactor shutdown and later restart. Detailed analysis of these operational requirements was beyond the scope of this particular study.

The mercury Rankine radiator-condenser is a hollow truncated cone made of a material with high thermal conductivity characteristics, which constitutes the set of radiating fins. The condensing and subcooling of the mercury is accomplished in tubes brazed longitudinally to the inside of this shell. The radiating outer surface of this shell is coated with a material of high emissivity and low solar absorptivity. An armor strip provides meteoroid puncture protection, located on the outside of the fin opposite the tube.

Parametric data were compiled to determine the minimum weight influenced by cone area, fin thickness, and number of tubes, corresponding to a given cone angle and diameter. Optimization studies for this design utilize aluminum-steel combinations, using rectangular tubes of Haynes-25 alloy. The study shows a specific weight of 1.39 pounds per square foot for a one-year nonpuncture probability of 0.97. Figure 50 shows the weight increase to achieve a nonpuncture probability of 0.999, i.e., to a specific weight of 1.55 pounds per square foot. The area utilized is 120 square feet per 5-kWe module, resulting in a weight of 186 pounds of radiator per module.

For lifetimes greater than one year, nonpuncture probability is achieved by adding redundant radiator loops, consisting of tubes, manifolds, and armor. This weight increase amounts to 78 pounds per 5-kWe module per year extension of lifetime.

The reactor with the PCS system is separated from the mission module by a boom to accomplish radiation attenuation. The power transmission cables leading to the power conditioning system are housed inside the boom. Parametric weights of boom and transmission cables were shown in Figures 43 and 44.

The electrical power conditioning subsystem consists of the alternator load control, d-c and a-c control and conditioning unit, load control, and the bus and distribution system.

The parasitic load control assembly, parasitic load resistors, and generator load control breakers are incorporated in the alternator load control systems. The d-c control system consists of a transformer and voltage

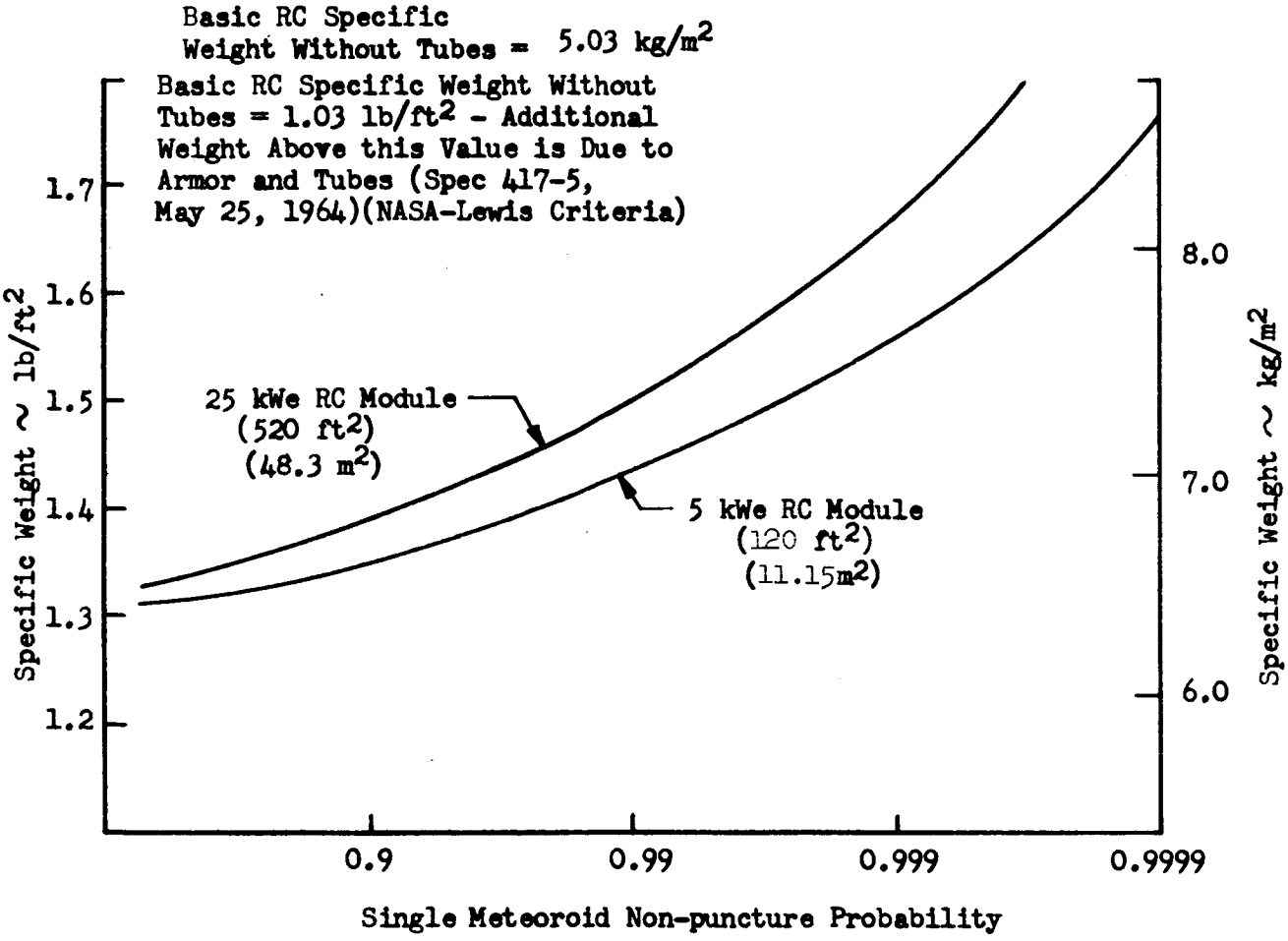

Figure 50. Radiator Condenser (RC) Specific Weight Versus Meteoroid Nonpuncture Probability

regulator. The a-c control system incorporates high-voltage rectifiers, square-wave inverters, sine wave inverters, and variable frequency start and emergency inverters. Load control consists of switches, circuit breakers, and relays.

Thermal Nuclear Reactor/Thermoelectric Power System

Thermoelectric power systems convert thermal energy directly to electrical energy without rotating or moving parts. The reactor heat source design considerations are the same as for dynamic systems.

Semiconductors are used for thermoelectric energy conversion. To date, two types of semiconductors have been developed for this application, based on lead telluride alloys and silicon-germanium alloys. The lead telluride alloy semiconductor is currently limited to operate at temperatures below 860 K, while the silicon-germanium alloy semiconductor operates most efficiently around 1100 K. Due to temperature limitations in the nuclear reactors, only lead telluride thermoelectric systems were considered in this study.

The lead telluride thermoelectric materials have an efficiency up to 50 percent higher than the silicon-germanium materials. Converters using these two thermoelectric materials in a cascaded arrangement are considered in connection with isotopic heat sources, and will be attractive when higher reactor temperatures can be achieved. Based on material improvements forecast in recent studies, a 1000 K operating temperature for lead telluride will be feasible in the next decade. A 20,000 hour life is projected with a 0.999 reliability. A degradation of thermocouples of 5 percent per year is expected. Overall system efficiency will be approximately 6.5 percent. A block diagram of this power system is shown in Figure 51. Efficiencies, temperatures, and component weights are given in Table 32. Shield weights are shown in Table 33.

Radioisotope Power Subsystems

Radioisotope Power Sources

In radioisotope power sources, the kinetic energy of the particles emitted by the decay process is converted into thermal energy. Heat must be transferred from the fuel capsules to the power conversion system. This heat transfer can be accomplished either by conduction, convection, or radiation.

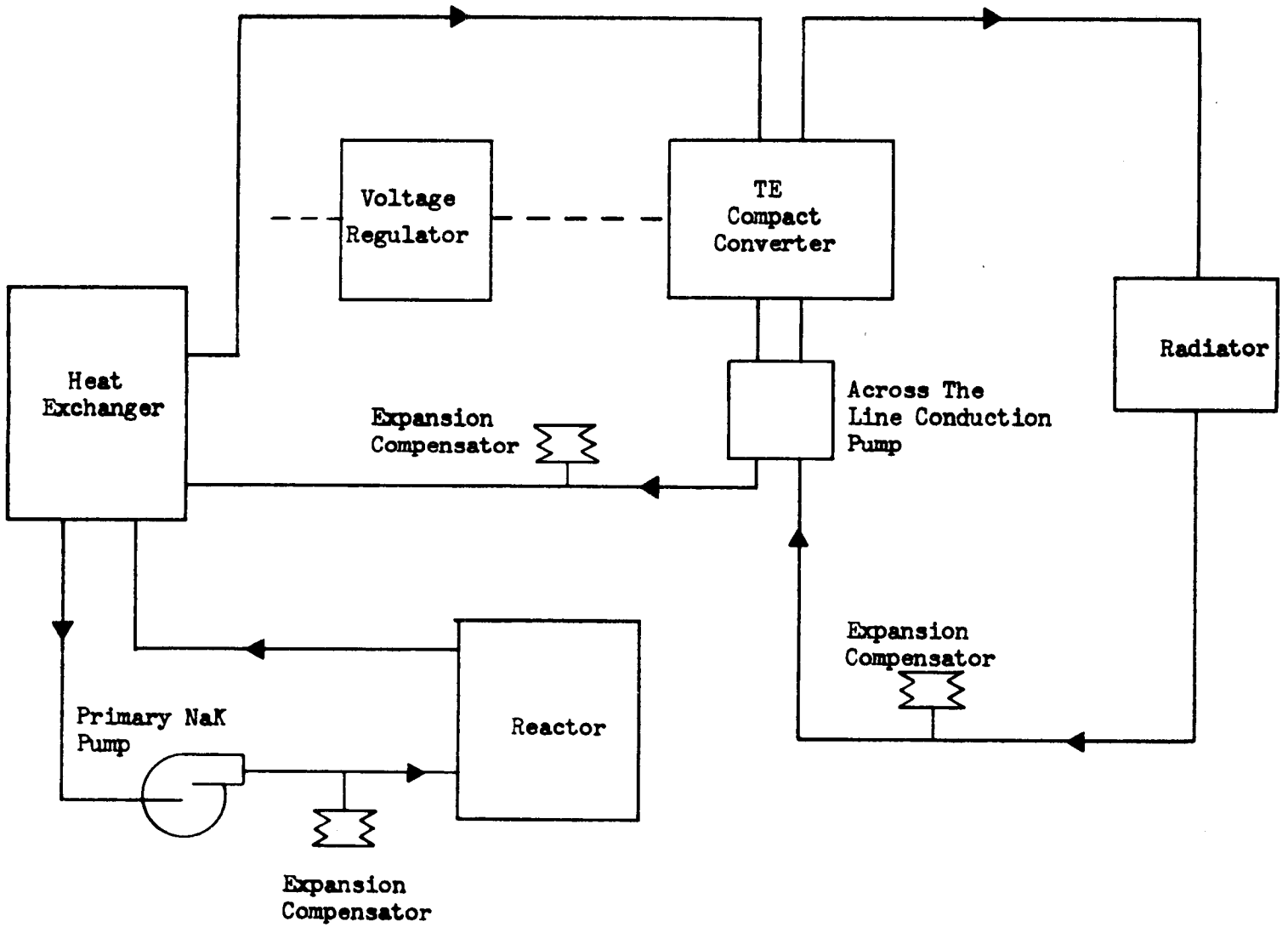

Figure 51. Reactor Thermoelectric Power System

Table 32. Parametric Data for Reactor/Thermoelectric System (Based on 10 kwe Systems, Reference 5)

Item	Characteristic
Reactor outlet temperature	1340 F
Converter hot side inlet temperature	1300 F
Converter hot side outlet temperature	1100 F
Converter cold side inlet temperature	325 F
Converter hot side outlet temperature (radiator inlet temperature)	525 F
Cycle efficiency	0.065
Power conditioning efficiency	0.83
Gross system efficiency	0.054
Power source (reactor)	388 lb
Radiation shield	3500 lb
Primary loop	153 lb
PCS	1457 lb
Radiator	1294 lb
Boom and cables	980 lb
Power conditioning system	861 lb
Heat shield	1581 lb

Table 33. Radiation Shield Parameters for Nuclear Reactor/Thermoelectric System

Parameters	Reference System					
	SNAP 10B (5 kWe)		SNAP 10B (10 kWe)		SNAP 8 (15 kWe)	
	Basic Weight Influencing Parameters	Correction Factor*	Basic Weight Influencing Parameters	Correction Factor	Basic Weight Influencing Parameters	Correction Factor
Dose plane (ft)	60	1.0	60	1.0	60	1.0
Separation distance (ft)	125	1.3	125	1.3	125	1.3
Reactor power (kWt)	94	0.76	188	0.86	282	0.9
Shadow cone diameter (in.)	14.6	0.8	14.6	0.8	23.5	1.15
Fuel element length (in.)	13.8	0.92	13.8	0.92	24	1.17
Core diameter (in.)	8.9	0.99	8.9	0.99	9.7	1.0
Dose rate (rem/yr)	10	1.06	10	1.06	10	1.06
Gallery height (in.)	14.5	0.87	14.5	0.87	15.5	0.88
Total (product) correction factor		0.67		0.76		1.32
Shield weight (lb)		3080		3500		6050

*See Reference 7.

The heat transfer and NaK flow design and technology for a compact isotope heat source is similar to that of SNAP reactor cores. In addition to the NaK loop, the source must also contain the reentry and emergency cooling loop. The reentry and emergency cooling loop is required to recover the isotope heat source following the mission in order to conserve a national resource. This cooling loop could also be used when the subsystem is retracted during an aerobraking maneuver. The source is composed of tubes containing isotope fuel capsules. Concentric tubes around the source tube provide passages for a two-pass NaK flow. The two-pass NaK system is not necessary from the standpoint of heat transfer, but it does place the NaK inlet and exit manifold at the same end, allowing the other end to be opened and closed for launch pad loading of fuel capsules without breaching the NaK system. The reentry coolant, in this case water, flows in the interstices between the NaK tubes. Several alternative possibilities for the NaK and water coolant passages are possible. If the heat exchanger is designed with radial conduction paths, the reentry coolant passage could be a jacket around the source, and the internal design would be simplified.

Another approach to the compact isotope heat source design is to have rows of isotope capsules transferring thermal energy by radiation to NaK tubes. The optimum heat source design will be a strong function of the size and shape requirements resulting from the isotope power system integration concept selected.

Shielding. The weight of the nuclear shield required to protect the crew from the isotope source radiation is a major consideration in the utilization of radioisotope heat sources.

The radiation from heat-producing isotopes can emanate directly from the natural decay scheme of the radioactive nuclide, or it can result from the interaction with other materials. Direct radiation is in the form of gamma rays, alpha particles, beta particles, and neutrons, with each radioisotope having a typical spectrum of each radiation form. The direct radiation from many nuclides is primarily restricted to only one or two forms, while in others, there are significant contributions from three or more decay modes. The radiation that results from interactions with other materials is usually from Bremsstrahlung and from the alpha neutron reactions with light nuclei. The presence of materials that cause this secondary radiation usually cannot be completely avoided since they are present as fuel compounds, impurities, or fuel cladding.

Uranium is used for gamma shielding (density = 18.8 gm/cc) although materials such as tungsten, lead, mercury, and others may be used.

Lithium hydride was chosen for the neutron shield (density = 0.74 gm/cc). The thicknesses considered in this study do not account for the effect of the uranium on neutron attenuation. The effect of lithium on gamma attenuation is neglected since this is a second-order effect on shield weights. Also, the gamma ray dose buildup factor was neglected. Figure 52 shows shield weight requirements for various residence times with allowable dosages of 20 rem per year and 10 rem per year.

Heat Rejection. With mercury-Rankine power conversion systems, it has been the practice to design the system at worst-case environmental conditions, and to maintain constant electrical output by sacrificing efficiency during intervals of lower sink temperature. Thermoelectric conversion systems are more permissive toward cycle parameter variations and, consequently, are designed on the basis of a hypothetical 0 R sink temperature.

Shutdown Heat Rejection Subsystems. During shutdown, isotope heat will be removed by the secondary NaK loop consisting of the heat exchanger, a high-temperature heat rejection radiator, a finned thermoelectric pump, and an expansion compensator. In addition, a water boiloff heat rejection loop will provide one hour reentry cooling of the source while the primary radiator is inoperative. Heating water to approximately 1500 F at 1 to 10 psia will remove approximately 1700 Btu per pound water.

Single-Phase Indirect Radiators. From the standpoint of radiator analysis, the single-phase indirect radiator is probably the simplest type of radiator. It is filled with fluid and usually operates in a secondary or tertiary loop. Substantial temperature gradient exists over the radiator, resulting in an effective radiating temperature well below the inlet temperature (Figure 53a).

The design of this radiator is relatively free of system interaction considerations, and may be separately optimized for vehicle integration. As a zero-void system, it is also especially attractive for zero-gravity applications. It was, therefore, selected as the type for use in the NASA/SNAP 8 system during the period when the final application was unknown. Disadvantages, when used in an indirect loop, include the requirement of additional expansion compensators, circulation pumps, and pumping power. Meteoroid puncture probability is determined only by tube, fin, and armor thicknesses.

Condenser-Radiators. This radiator is applicable to Rankine cycle systems. Condensation of the turbine exhaust takes place in the radiator

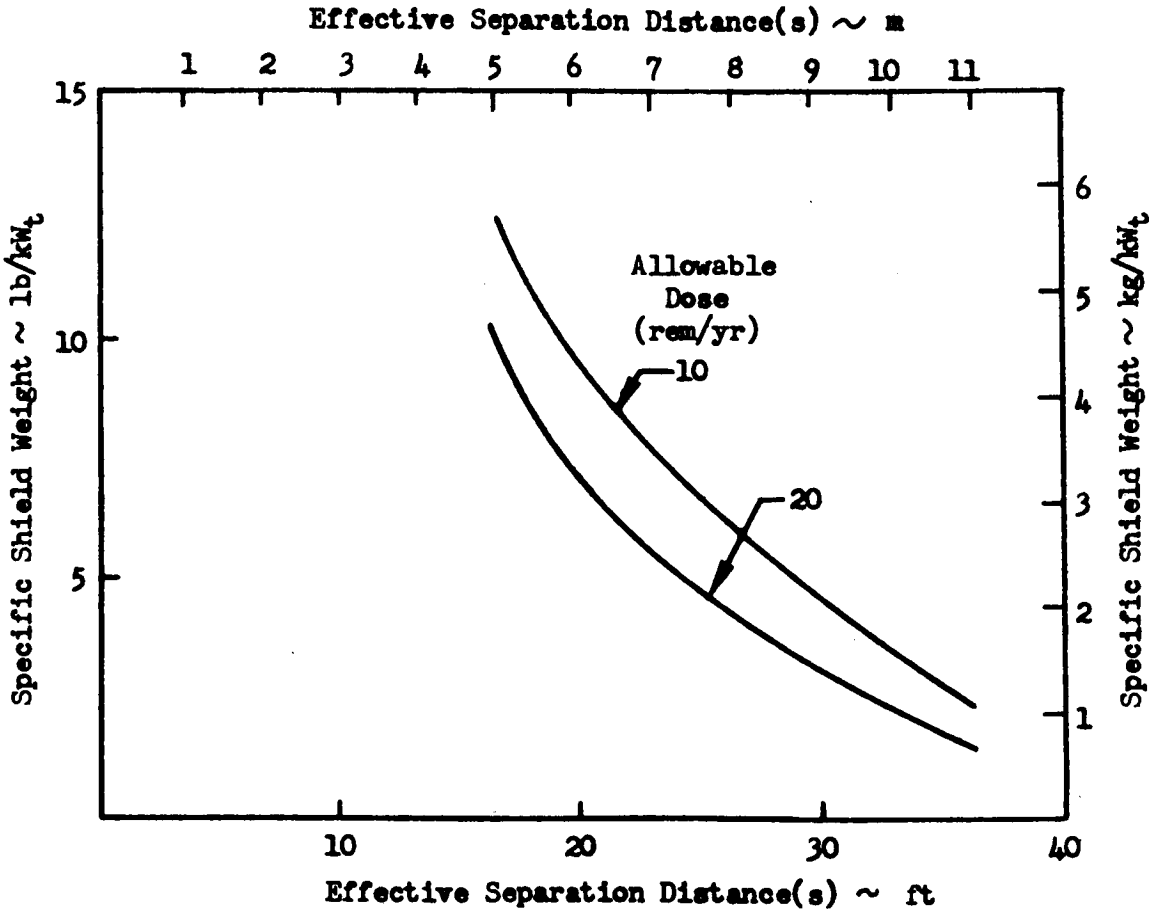

Note: Applicable to the isotope and configuration assumed in this study.

Figure 52. Specific Shield Weight for Pu238 Isotope Power Systems Versus Effective Separation Distance

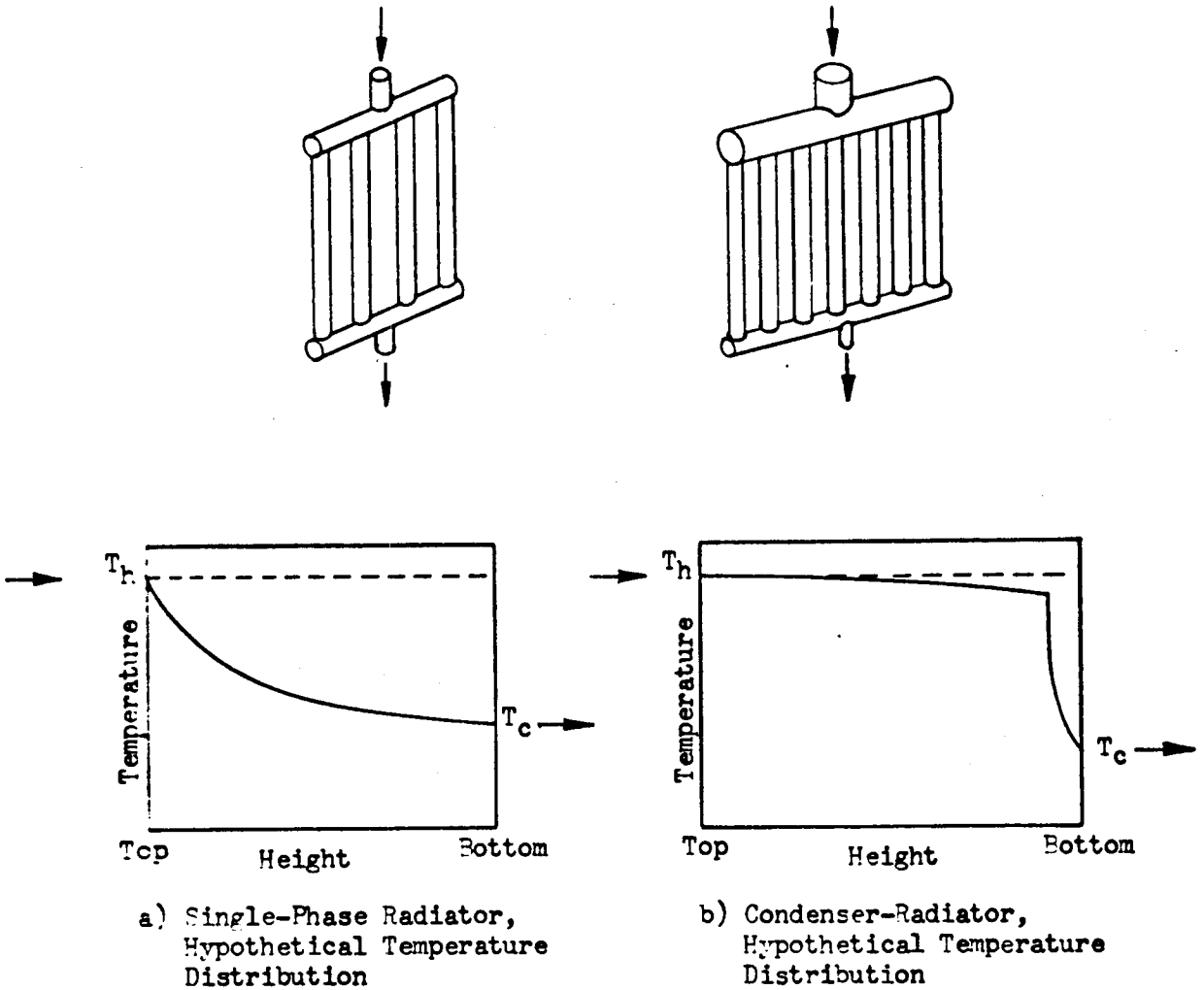

Figure 53. Radiator Temperature Distribution

tubes at nearly constant temperature (Figure 53b). The effective radiating temperature thus approaches the radiator inlet temperature. Relatively large tubes and headers are required, however, to prevent excessive vapor-phase pressure drop.

Use of a condenser-radiator completely eliminates any tertiary loop and the additional complexity, weight, and losses associated therewith. Therefore, a radiator system is used in this study with the Rankine cycle systems.

The radiator area requirements for the different conversion systems considered are shown in Figure 54. The variation in the Brayton cycle requirements are due to variations in the design criteria. The upper curve represents the area that results from the assumed operating conditions, i.e., turbine inlet temperature of 1111 K (1540 F) and compressor inlet temperature of 300 K (80 F). The area can be reduced by raising the compressor outlet temperature; i.e., by minimizing radiator area at the expense of efficiency.

Electrical Control. The power distribution concept is shown in Figures 55 and 56 for the isotope dynamic systems. Figure 55 illustrates the fundamental difference in delivered conditioned power and alternator power in rating systems and comparing weights. Nuclear reactor system conditioning equipment efficiencies can be taken as the same, for preliminary estimates. The active and standby CRU's are interconnected to a common bus so that only one can operate or be on the line at a given time. The frequency of the system is maintained by controlling the shaft speed. A constant load is kept on the alternator as the demand for useful power varies by application of a parasitic load.

The alternator uses dc excitation to maintain line voltage under load. The regulator is a three-phase, half-wave, silicon-controlled rectifier which is activated by signal from a circuit that senses alternator line voltage.

Radioisotope/Brayton Cycle Power System

The Brayton cycle power generation system takes advantage of the fact that the work of compression or expansion of a gas is directly proportional to its initial absolute temperature. Thus, the expansion of a gas at high temperature produces more work than that required for compression of the same gas at lower temperature resulting in a generation of usable

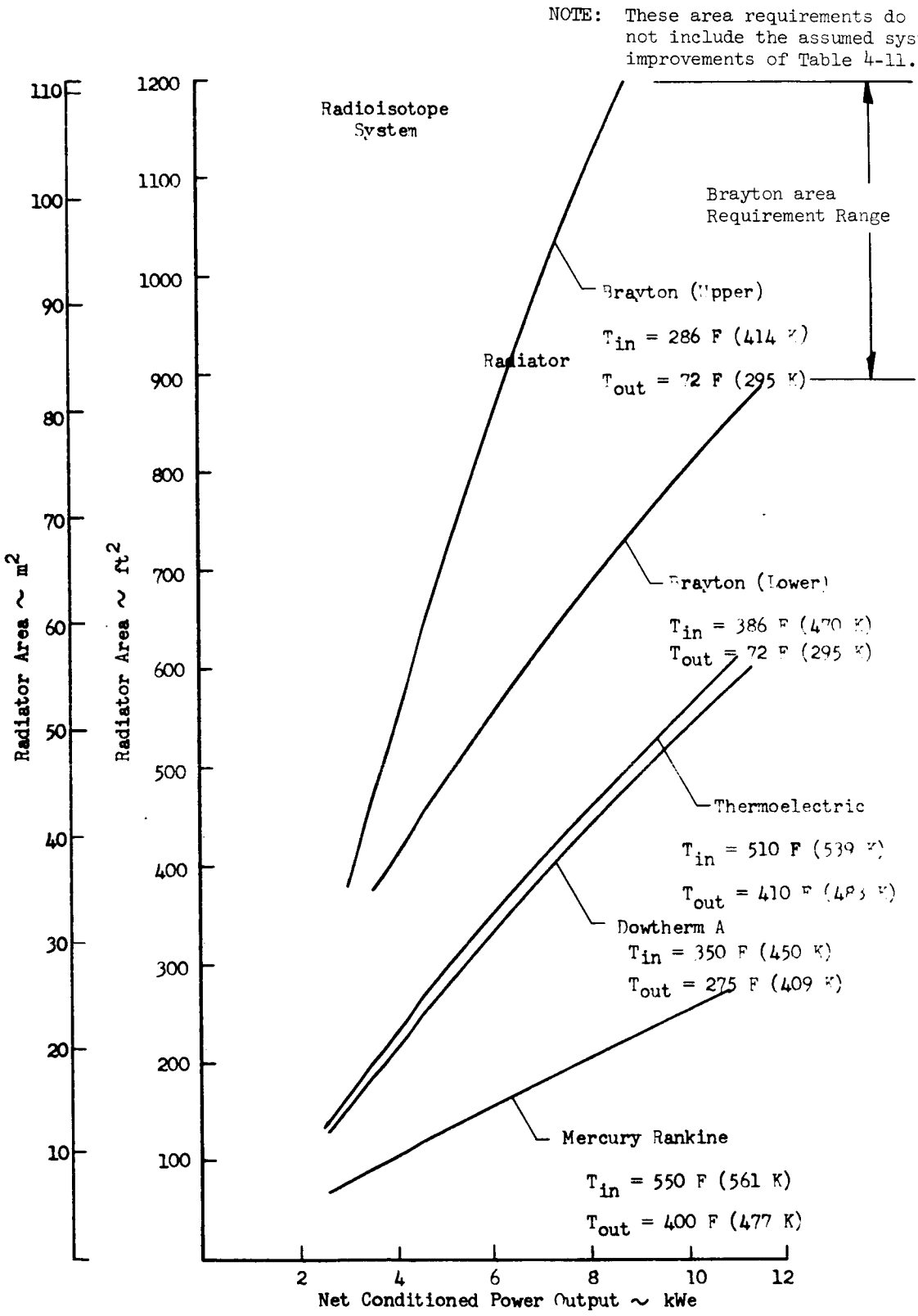

Figure 54. Radiator Area Versus Power Output for Various Power Conversion Cycles

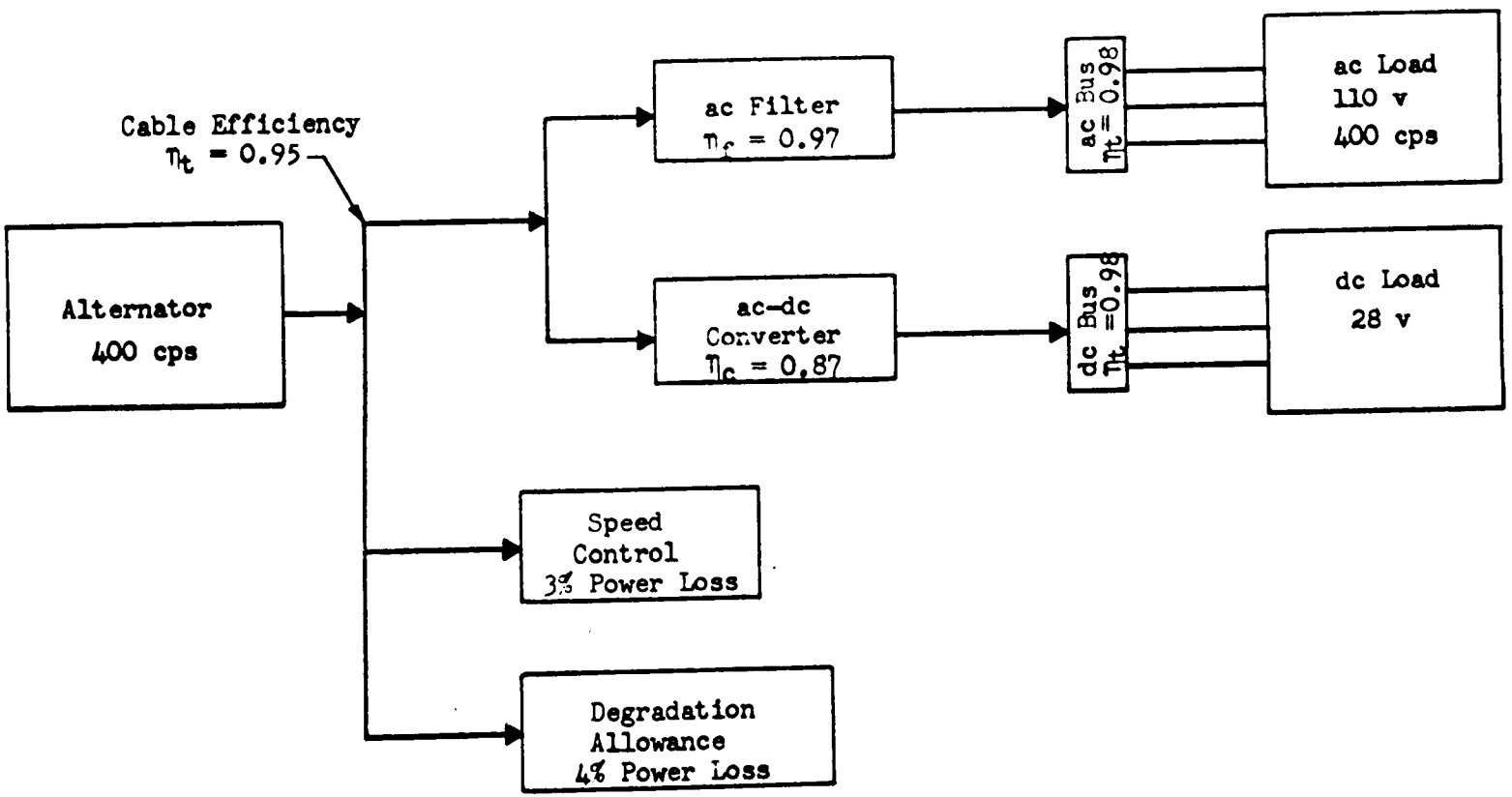

Figure 55. Power Distribution Schematic, 400 cps Alternator

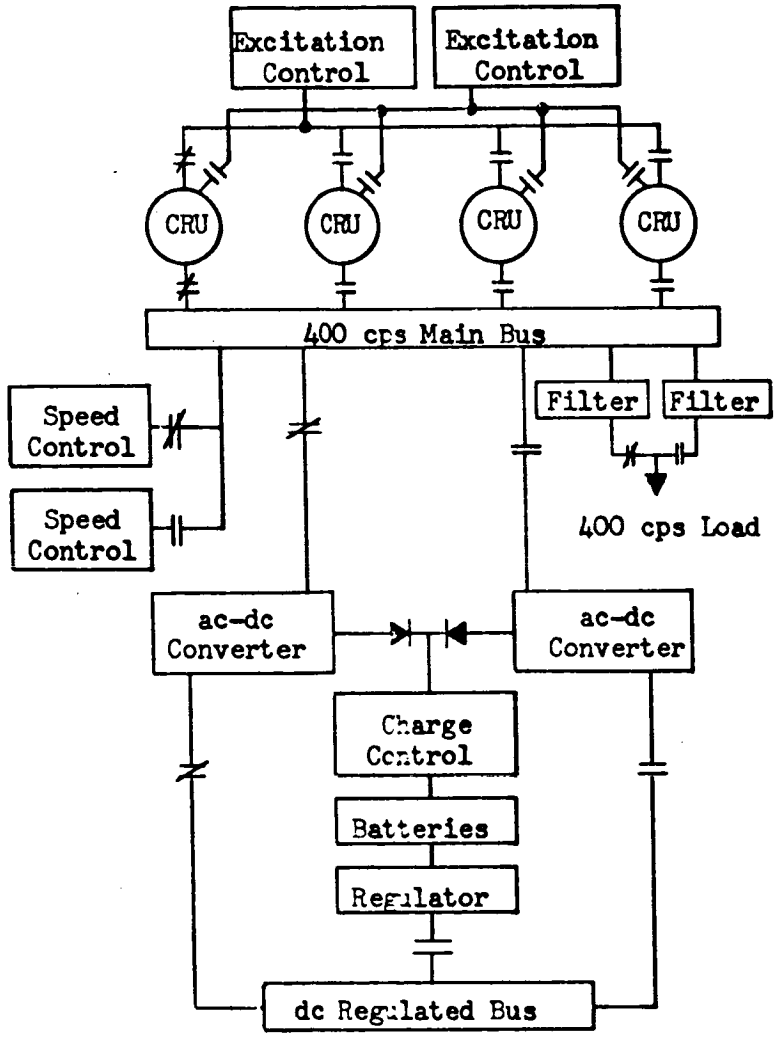

Figure 56. Power Distribution Block Diagram, Dynamic Conversion System

mechanical power. In this study, the turbine and compressor inlet temperatures were assumed to be 1111 K (1540 F) and 300 K (80 F), respectively.

A flow schematic is shown in Figure 57. Preheated gas enters the isotope heat source where it is heated to the turbine inlet temperature and expanded producing mechanical power. The gas then flows through the recuperator, where it is cooled by preheating the incoming gas stream. The gas then transfers the cycle reject heat to an organic coolant (FC-75) in the heat exchanger, where it is cooled to the compressor inlet temperature. The gas is compressed, preheated in the recuperator, and finally returned into the heat source. A bleed stream from the compressor outlet provides the CRU lubrication and cooling. From the heat exchanger, the FC-75 flows through the heat rejection radiator and then completes its loop. Brayton cycle systems exhibit high overall efficiencies and by the use of an inert gas (single phase), reduce many of the problems of corrosion caused by other working fluids.

Brayton Cycle. Maximum cycle temperature is limited by material and design facets of the isotope source and rotating machinery.* The optimum lower-cycle temperature for a given upper-cycle temperature is largely a function of design criteria and vehicle constraints. If weight is the prime factor, one optimum lower temperature exists; minimum radiator area yields another optimum value (these two may be the same for missions requiring heavy meteoroid protection); maximum cycle efficiency (minimum isotope inventory) gives another value. Table 34 shows relative values for radiator area, system weight, and cycle efficiency for typical systems with constant peak temperature optimized to different criteria. As indicated the Brayton cycle system will vary considerably in radiator area requirements, depending upon the selection of an optimizing parameter. This effect was shown in Figure 54 for the upper and lower range of area requirements for this system. The upper curve represents the area that results from operating conditions listed previously, i.e., the reference design used in the study. The area can be reduced by raising the compressor inlet temperature; i.e., by minimizing radiator area at the expense of efficiency.

Figure 58 shows the effect of compressor inlet temperature on radiator area for the same component parameters. Figure 59 shows the effect of regenerator effectiveness, machinery efficiency, and useful pressure ratio on relative cycle efficiency with constant upper and lower cycle temperatures.

*Present isotope encapsulation material technology limits isotopes to ~ 1250 F as a heat source. It is expected that this technology will be improved to permit 2000 F isotope heat sources for missions in the 1980 to 2000 period.

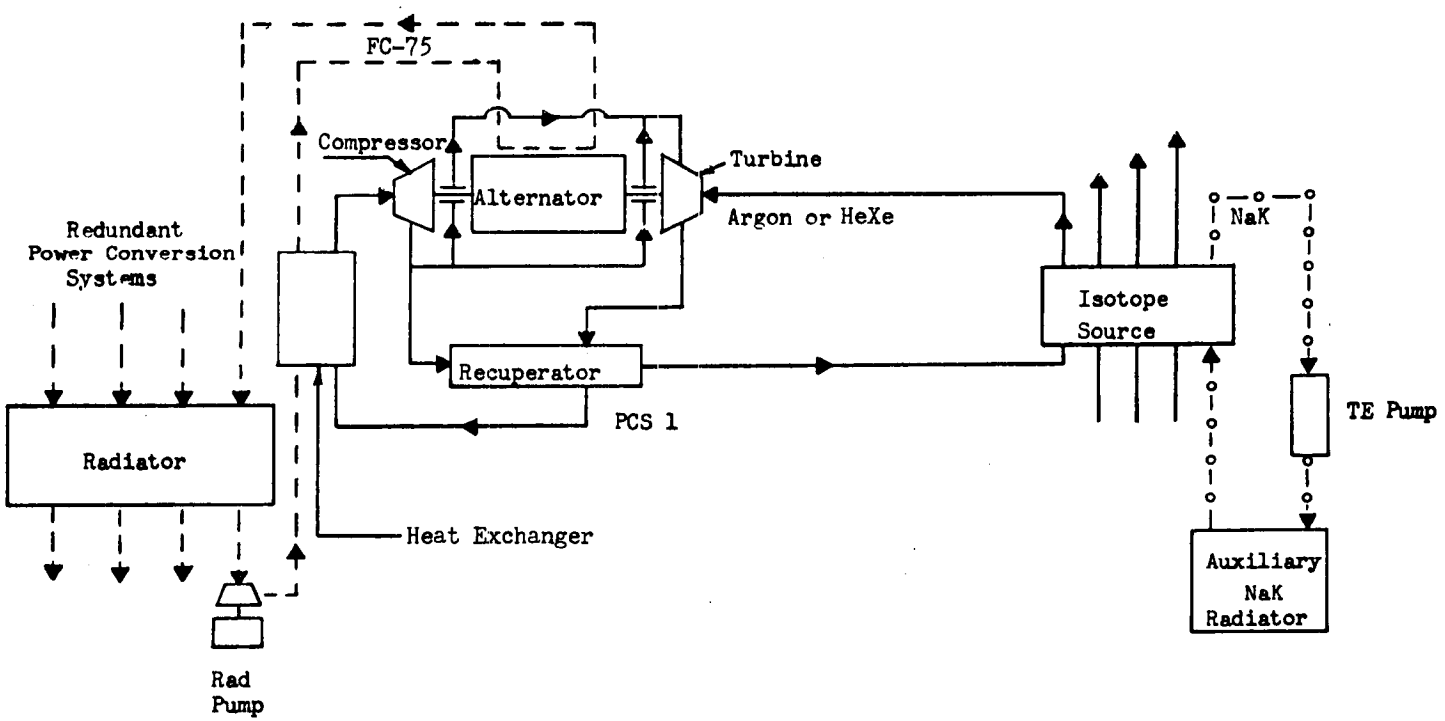

Figure 57. Isotope Source/Brayton-Cycle Conversion System Schematic

Figure 60 shows peak cycle efficiency as a function of compressor inlet temperature with the constant conditions: 80 percent compressor efficiency, 80 percent regenerator effectiveness, 90 percent turbine efficiency, and 10 percent pressure loss ratio.

Table 34. Effect of Brayton System Optimization Criteria

Optimizing Parameter	Radiator Area	System Weight	Cycle Efficiency
Area	1.0	1.30	0.30
Weight	1.31	1.00	0.77
Efficiency	1.36	1.22	1.00

Vehicle and system configuration, in conjunction with the specific mission and type of system, imposes constraints on system performance design. There is nothing inherent in an isotope system which requires orientation of the complete system, however, the changing environment of space must be considered.

Radioisotope/Rankine Cycle Power System

The Rankine cycle for space application is similar to that used in steam turbine power systems and is a two-phase system. A liquid is evaporated and superheated in a boiler. The vapor is then expanded through a turbine which drives an electrical generator. The working fluid is then condensed and subcooled by a radiator-condenser with the liquid then pumped back to the boiler by means of a boiler feed pump. Among working fluids that might be used in space Rankine power cycles are potassium, mercury, Dowtherm A, and water. The principal advantage of the Rankine cycle is the high cycle efficiency and the isothermal heat rejection that allows minimum radiator area for a given source temperature. Principal disadvantages are the inherent corrosion and erosion characteristics of the applicable working fluids.

A superheat mercury Rankine cycle is shown in Figure 61. Liquid mercury enters the boiler through a flow regulator. In the boiler, the mercury is preheated, boiled, and superheated. The mercury vapor is then expanded through an impulse turbine, providing power to drive the permanent magnet alternator and the mercury centrifugal pump, all mounted on a common shaft-CRU. The turbine exhaust vapor flows through the alternator housing for cooling purposes and then enters the radiator-condenser where the mercury is condensed and subcooled. The subcooled condensate then

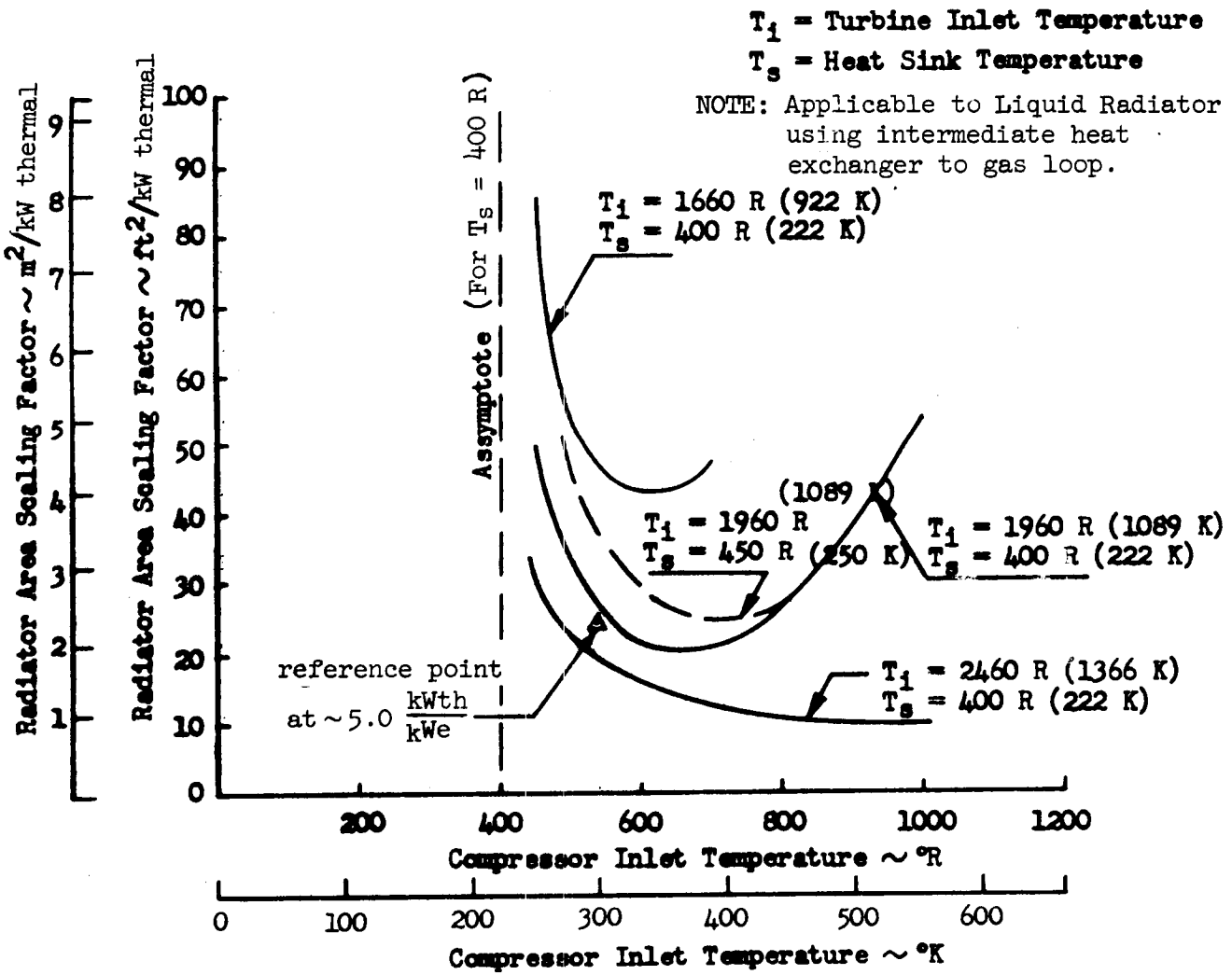

Figure 58. Radiator Specific Area Versus Compressor Inlet Temperature, Isotope Brayton Cycle

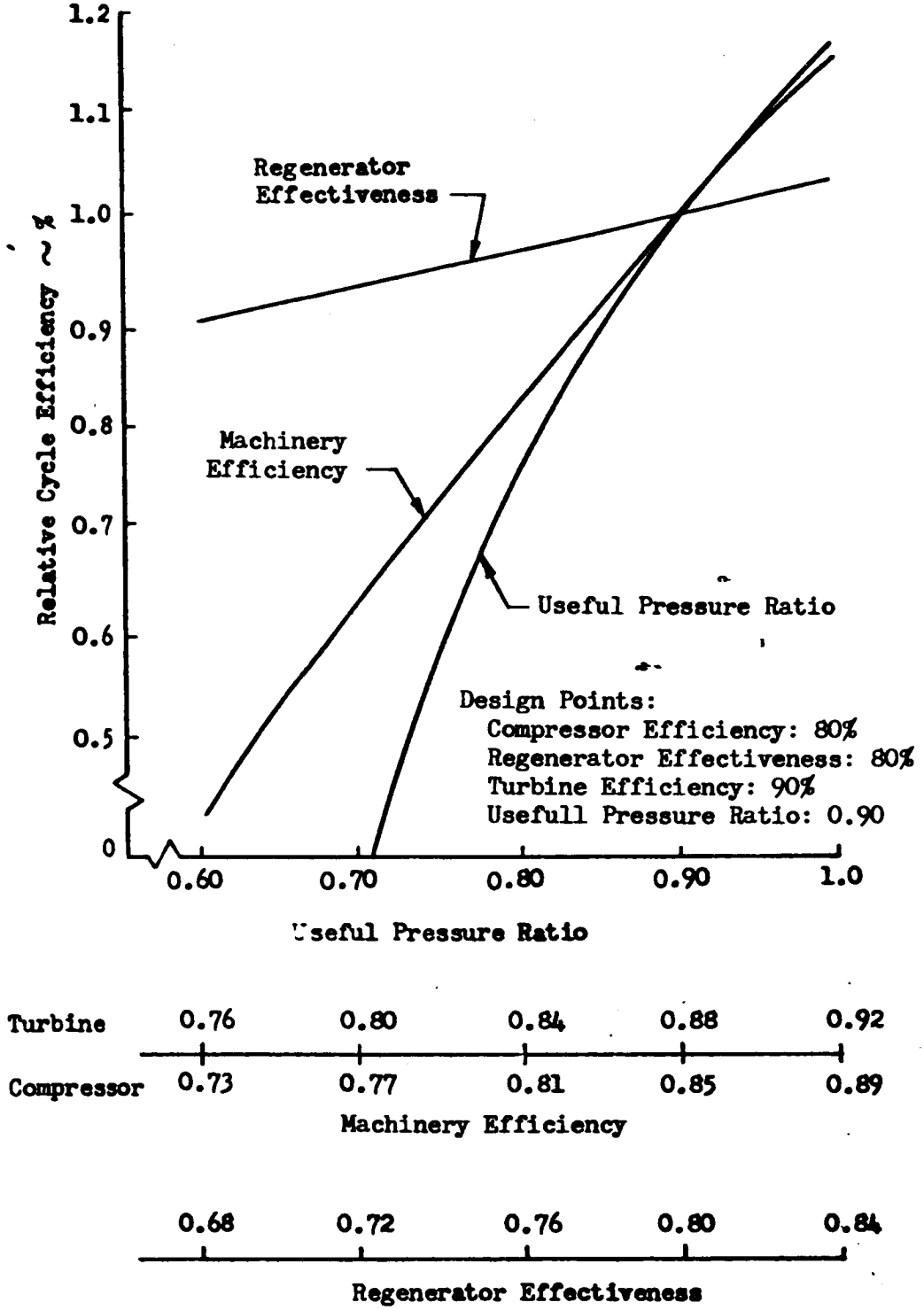

Figure 59. Effect of Design Point Variation on Cycle Efficiency, Brayton Cycle

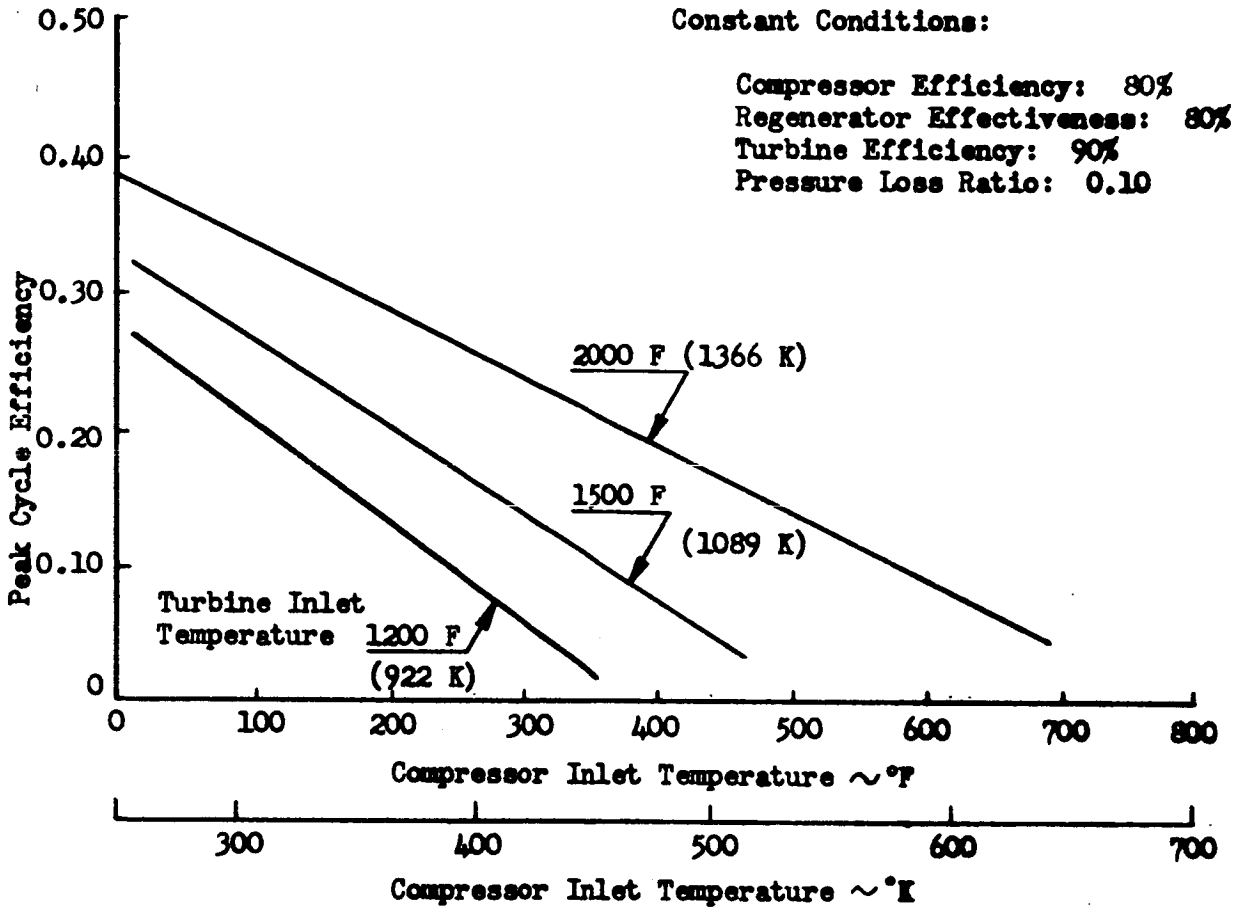

Figure 60. Peak Brayton Cycle Efficiency (Theoretical) Versus Compressor Inlet Temperature

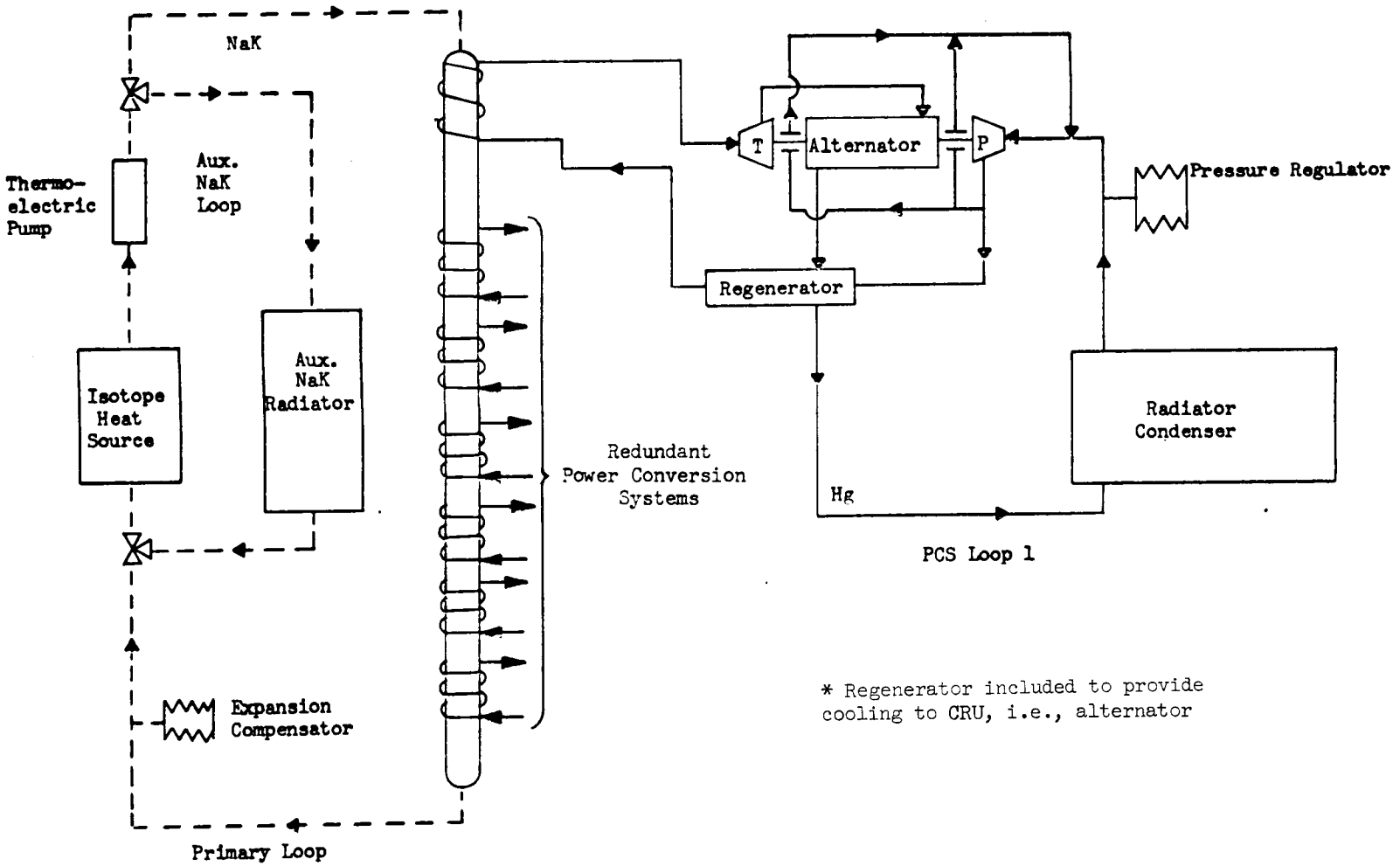

Figure 61. Isotope Mercury Rankine System Schematic

mixes with a higher temperature bearing effluent stream and enters the jet-boosted centrifugal pump. A portion of the high-pressure pump discharge flows through the CRU, providing lubrication and cooling. Provision for dissipation of the excess isotope power and total isotope power dissipation in event of shutdown is included in the form of a separate liquid coolant loop and high-temperature radiator.

Since the weights of the organic (e.g., Dowtherm A) Rankine system are comparable to the mercury Rankine system, it was concluded that only the mercury Rankine system be included in the Weight Summary and that the mercury Rankine be considered as typical of Rankine conversion systems. The primary advantage of using mercury as a working fluid over Dowtherm A is that this fluid results in less radiator area requirement for the system due to higher heat rejection temperatures. Another major advantage is that this fluid has been used in the SNAP nuclear reactor development program and its characteristics are fully understood with a vast background of experience available, i.e., design technology directly applicable to the power conversion system of interest here.

Potassium and water were considered in the weight analysis but did not show any advantage in overall weight. A major advantage of potassium is in savings in radiator area requirement, which may be a decisive parameter for missions into the asteroid belt.

Performance limitations result from considerations of structural strength, corrosion, pump cavitation, condensing stability, and heat-rejection capability. The design strength limit is based on creep, fatigue, and stress applicable to the hardware. As temperature increases, corrosion becomes more pronounced. Figure 62 illustrates some of the constraints considered in projecting conceptual design performance to the 1980-2000 time period.

Turbine Efficiency. Experience with the design of small mercury turbines indicates that over the power range of interest to this study, the turbine efficiency will vary with shaft power, but that the effect on overall weight should be small. The SNAP 2, CRU-V turbine, for example, is a two-stage subsonic-transonic design running at 36,000 rpm at pressures of 115 psia inlet and 9 psia outlet. Its shaft power is 5,610 watts and its efficiency is 54.3 percent. This data, combined with analysis of higher power output designs, has lead to the curve of turbine efficiency versus shaft power (Figure 63). Reference design is at a turbine efficiency of 55 percent with an assumed increase of 3 percent added for system improvement (Table 35).

Overall Efficiency. It is apparent from Figure 64 that significant gains are available if the pump can be run at very low inlet pressures. Almost 1 percent improvement (e.g., 0.75) can be made on a 4 kWe system, for example, if the turbine back pressure is lowered from 4.5 to 3.5 psia.

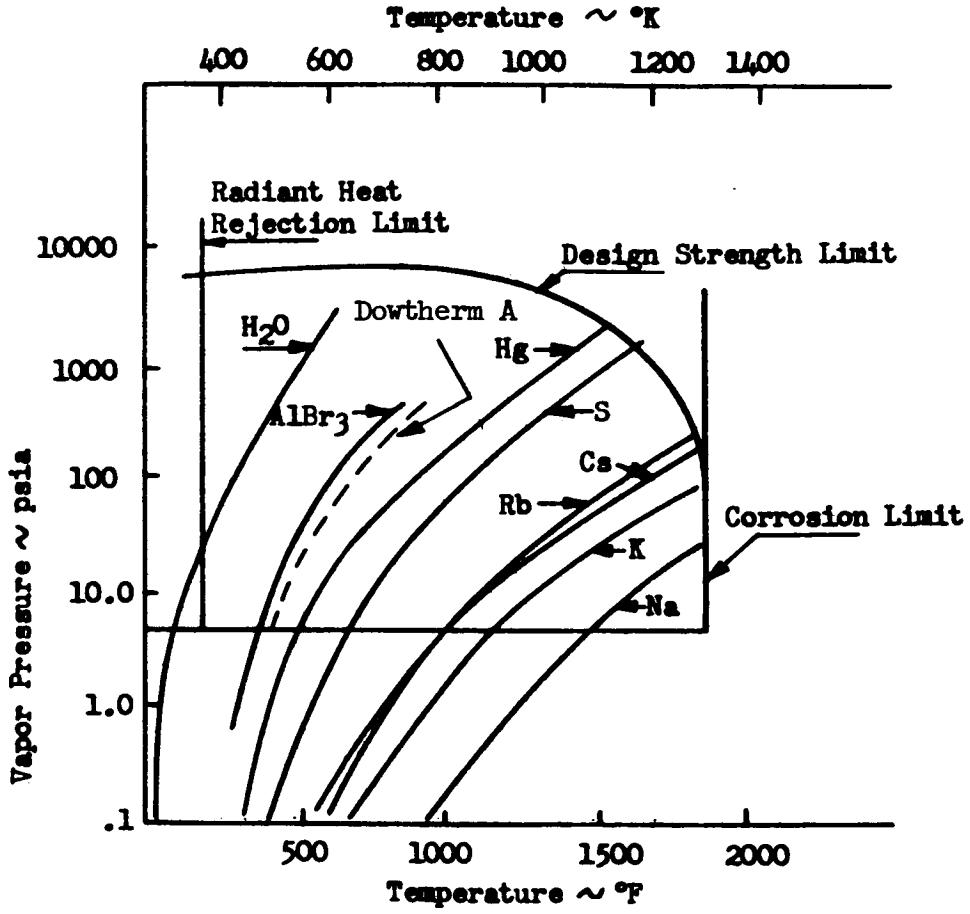

Figure 62. Vapor Pressure Versus Boiling Temperature, Working Fluids for Rankine Cycle

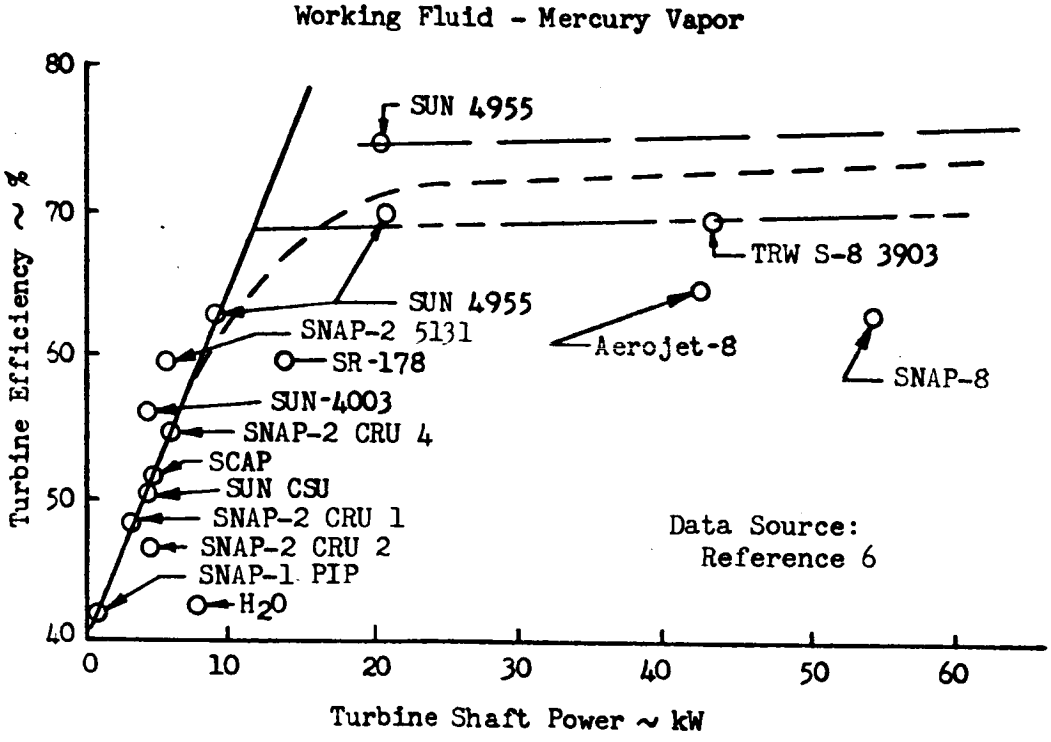

Figure 63. Turbine Efficiency Versus Shaft Power, Comparative Systems

Table 35. System Improvements and Weight Savings Assumed to Calculate Data in Weight Summary - Isotope Power Source

System	Boiling Temperature (°F)	Turbine Inlet Temperature (°F)	Turbine Exhaust Pressure psia	Regenerator Effect (percent)	Compressor Effect (percent)	Turbine Efficiency (percent)	Net Overall (percent)	Net Weight Savings (percent)
Rankine mercury	+100	+100	-1.0			+3	+2.55	20
Dowtherm A	+0	+25	+0			+5	2.5	20
Brayton	+0	+100	+0	+2	+5	+4	8.6	35
Thermoelectrics (cascaded)	(200 degree increase in hot junction temperature)						1.3	23

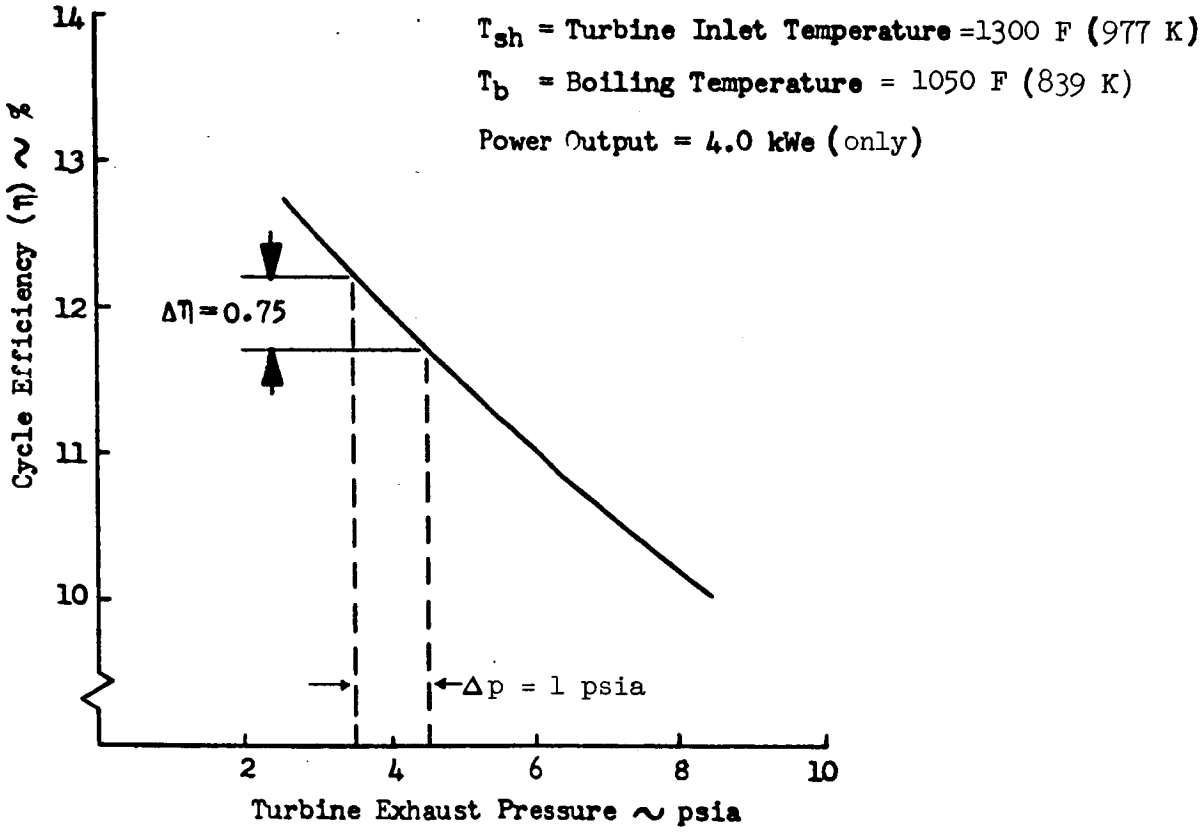

Figure 64. Cycle Efficiency Versus Turbine Exhaust Pressure, Mercury Rankine Cycle

Another possibility is an increase in boiling temperature. An increase from 1050 to 1150 F shows an improvement of 1.75 percent. If refractory or coextruded refractory boiler tubes were developed, it would be reasonable to consider boiling temperatures of 1200 to 1300 F. Figure 65 shows the effect of mercury boiling temperature on cycle efficiency. The reference design was at 1050 F boiling temperature; for the weight summaries this temperature was increased to 1150 F (Table 35).

Radioisotope/Thermoelectric Power Systems

Several thermoelectric power conversion systems are currently under development by the Atomic Energy Commission which can be utilized with radioisotope heat sources for the production of electricity. These programs are based on the utilization of SiGe or the family of PbTe materials for direct conversion of thermal energy into electrical energy. These materials exhibit different mechanical, thermal, and electrical characteristics. PbTe devices, because of their higher materials efficiency, exhibit slightly higher overall conversion efficiencies. A comparison of system weights (based on present designs) is shown in Figures 66 and 67.

Since the performance of either type of device is dependent on the temperature difference between the thermoelectric hot junction and cold junctions (Carnot efficiency), overall system efficiency and radiator area tradeoffs can be accomplished over a broad range without incurring a system weight penalty. Efficiencies as a function of these temperature differences are shown in Figures 68 and 69. In the weight summaries, it was assumed that improvements in temperature would be achieved by the 1980-2000 period, and that overall efficiency would be improved as shown; e.g., a 100 degree increase in hot junction temperature for the SiGe system results in 1.3 percent increase in overall efficiency.

SiGe devices are currently under development by RCA's Thermoelectric Products Engineering Division. Two separate development efforts are proceeding: one based on the direct radiating approach similar to the SNAP 10A converter design, and one based on a compact converter arrangement utilizing two liquid metal coolant loops. In the compact converter approach, one loop supplies high-temperature liquid metal to the thermoelectric hot junction and the second loop removes waste heat from the cold junction at a reduced temperature.

PbTe devices are under development by several companies, including the 3M Company's Electrical Products Division, Westinghouse Astronuclear Laboratory, and Martin Marietta Nuclear Division. These development efforts are oriented toward a compact converter design. The Westinghouse effort is specifically oriented toward a compact converter design which utilizes two liquid metal coolant loops.

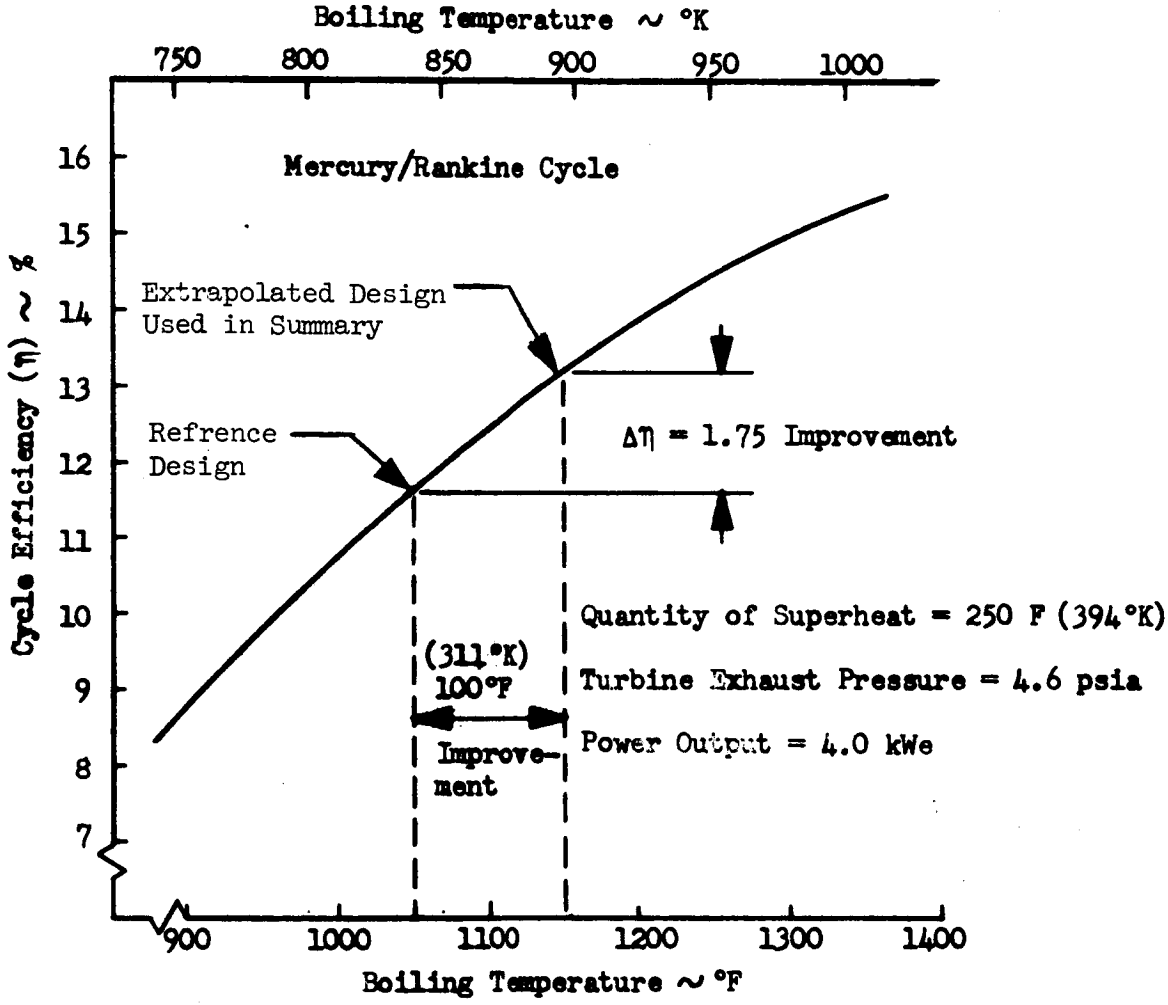

Figure 65. Cycle Efficiency Versus Boiling Temperature, Mercury Rankine Cycle

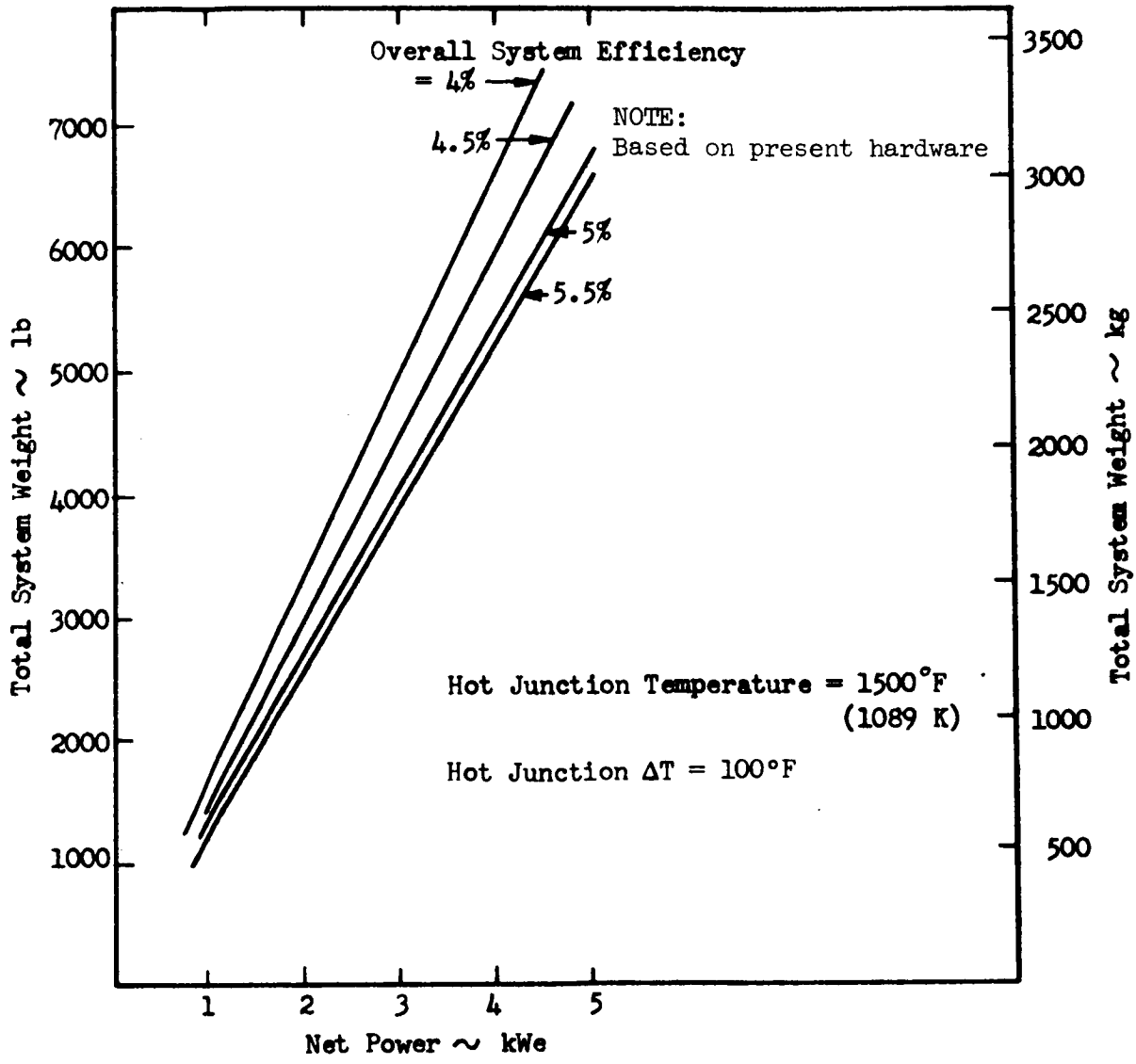

Figure 66. Total System Weight Versus Net Power, Isotopic (Pu238) Thermoelectric System (Silicon-Germanium)

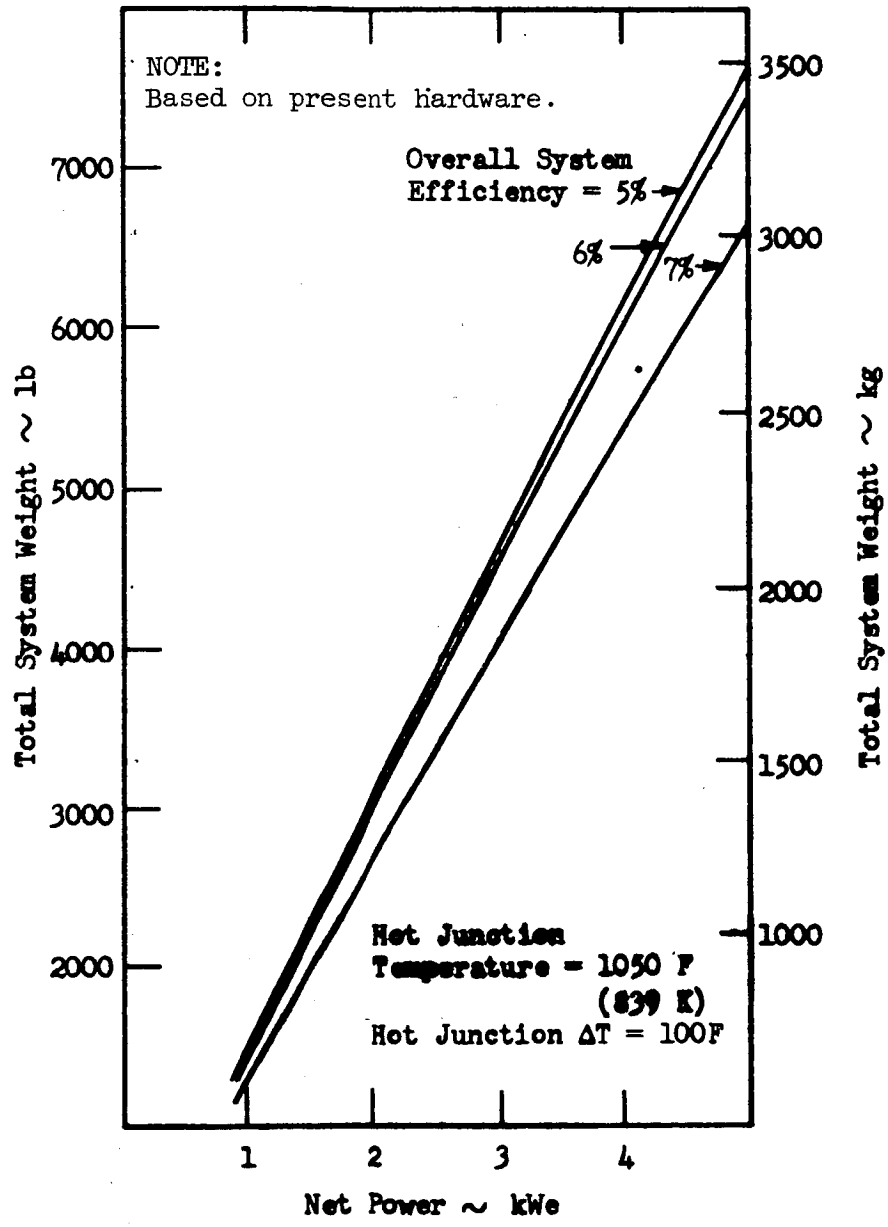

Figure 67. Total System Weight Versus Net Power, Isotope (Pu238) Thermoelectric System (Lead Telluride)

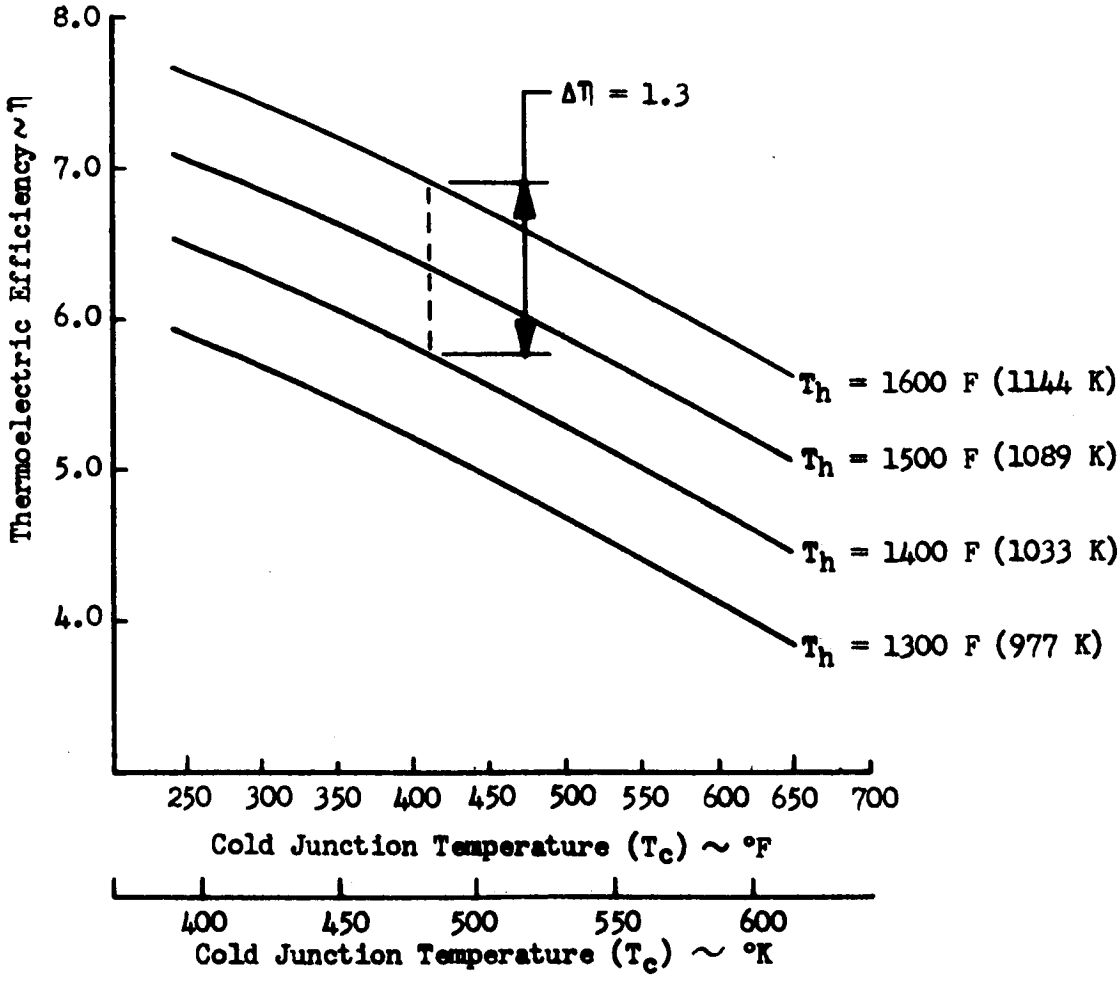

Note: Operating temperature differential is taken to be T_h-T_c.

Figure 68. Thermoelectric Efficiency (Germanium-Silicon Thermoelectric System)

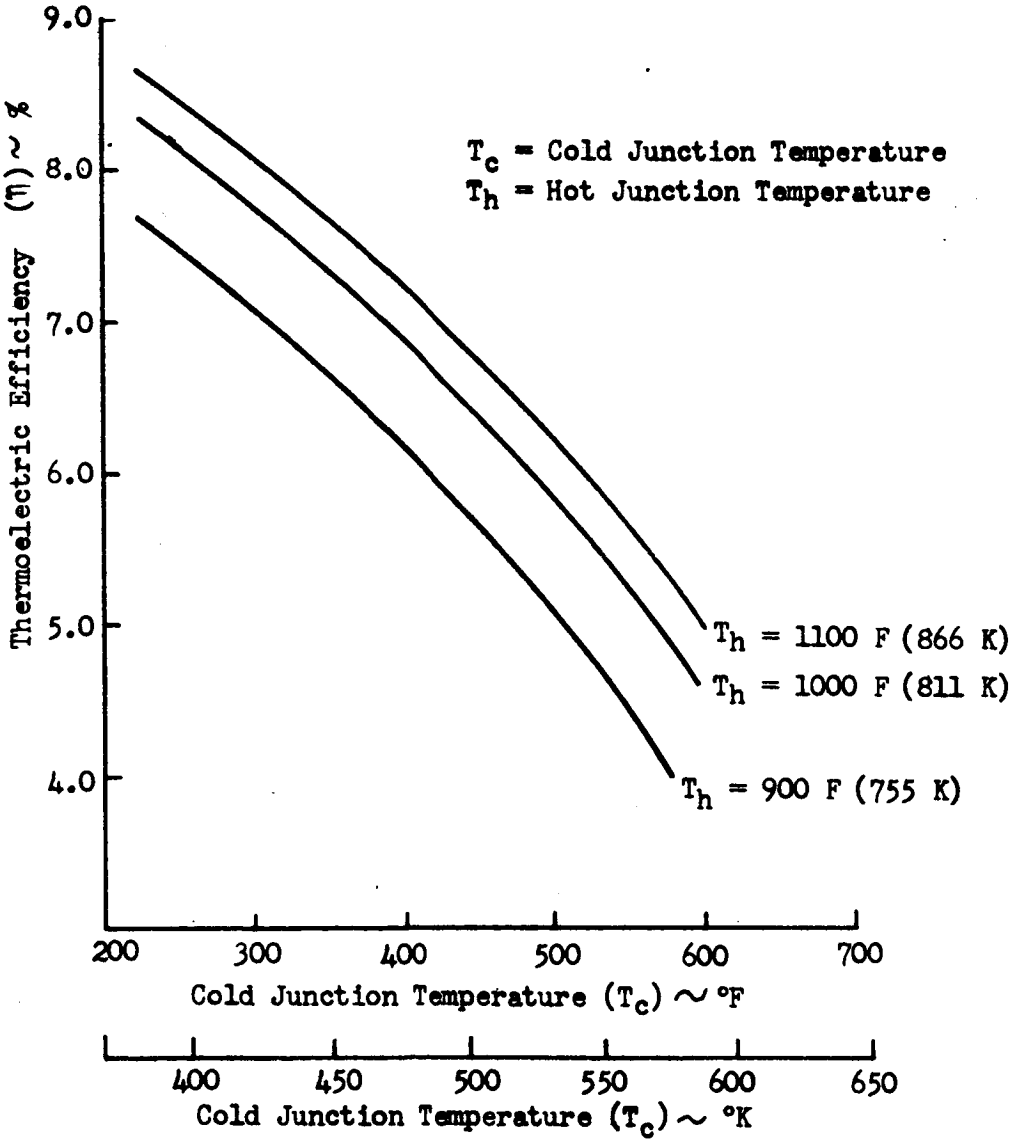

Note: Operating Temperature Differential is taken to be $T_h - T_c$.

Figure 69. Thermoelectric Efficiency Versus Operating Temperature Differential, Lead Telluride Thermoelectric System

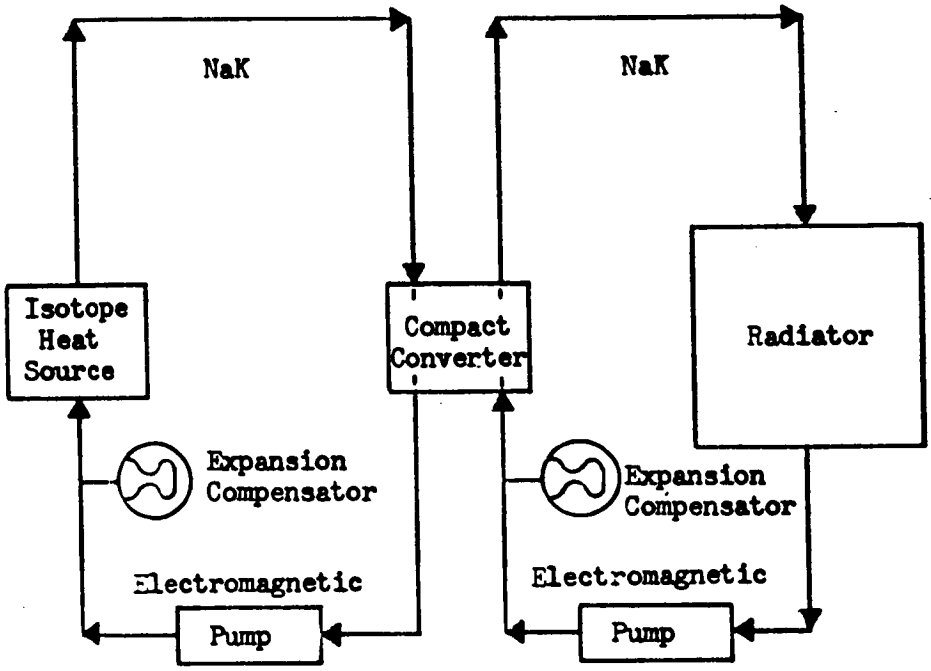

Figure 70. Compact Thermoelectric System Schematic

The compact thermoelectric converter consists of a closely packed array of SiGe or PbTe thermoelectric elements confined between a heat source and a heat sink. The heat source could be a hot NaK channel or radiation directly from isotope fuel capsules. A coolant loop removes waste heat from the converter and transports it to a space radiator. The thermoelectric elements are electrically connected in series and in parallel to provide the desired voltage and power. Interconnections between the series modules are used to provide the high reliability against open circuit failure. The isotope thermoelectric power systems considered in this study are based on the flow schematic shown in Figure 70. An isotope source, fueled with Pu^{238} is used to heat NaK in the primary loop. The NaK is circulated by an electromagnetic pump and maintains the hot junction temperature of the thermoelectric converter. Thermal energy passes through the thermoelectric elements in the compact converter to a second NaK loop which rejects waste heat by means of a space radiator. Isotope thermoelectric systems may also be designed with direct radiating power converters. The weights and performance shown for compact thermoelectric converters are also representative for direct radiating power systems.

SiGe converter operation at 1500 F and PbTe operation at 1100 F are believed to be attainable with operational systems during the 1975-1985 periods. Converter state of the art for either SiGe or PbTe is estimated to be approximately the same at the preceding temperatures, i.e., compact thermoelectric design state of the art.

Cascaded Thermoelectric System. The two thermoelectric systems discussed are based on the use of single converter units. The different thermoelectric materials have different optimum operating temperatures and the use of both the Pb Te and SiGe converters in the same system yields a higher system efficiency and, hence, lower fuel inventory, lower system weight, and lower radiator area requirement. Coupling between converters is accomplished by a pumped liquid metal loop, similar to the normal system loop previously discussed. The use of a cascaded system is dependent on the development of both compact converter designs. The system flow schematic is shown in Figure 71. Assuming continuation of current AEC programs, an application in the 1970's is within reason. Additional information can be found in many sources, including Reference 4. Figure 72 shows the variation of radiator area required and efficiency as a function of Carnot efficiency.

The Weight Summary data (Table 23) are based on the cascaded imp compact converters assuming a 23 percent improvement in weight based on higher temperatures, i.e., an increase in the hot junction temperature of 200 F. This assumption is based on the premise that 2000 F isotope heat sources will be available. No change in the cold junction temperature was included, since this affects radiator area requirements. The data shown in Table 23 was obtained by considering present conceptual system weights proposed in the studies for 1975 to 1985 flyby missions and allowing for the anticipated system performance improvements.

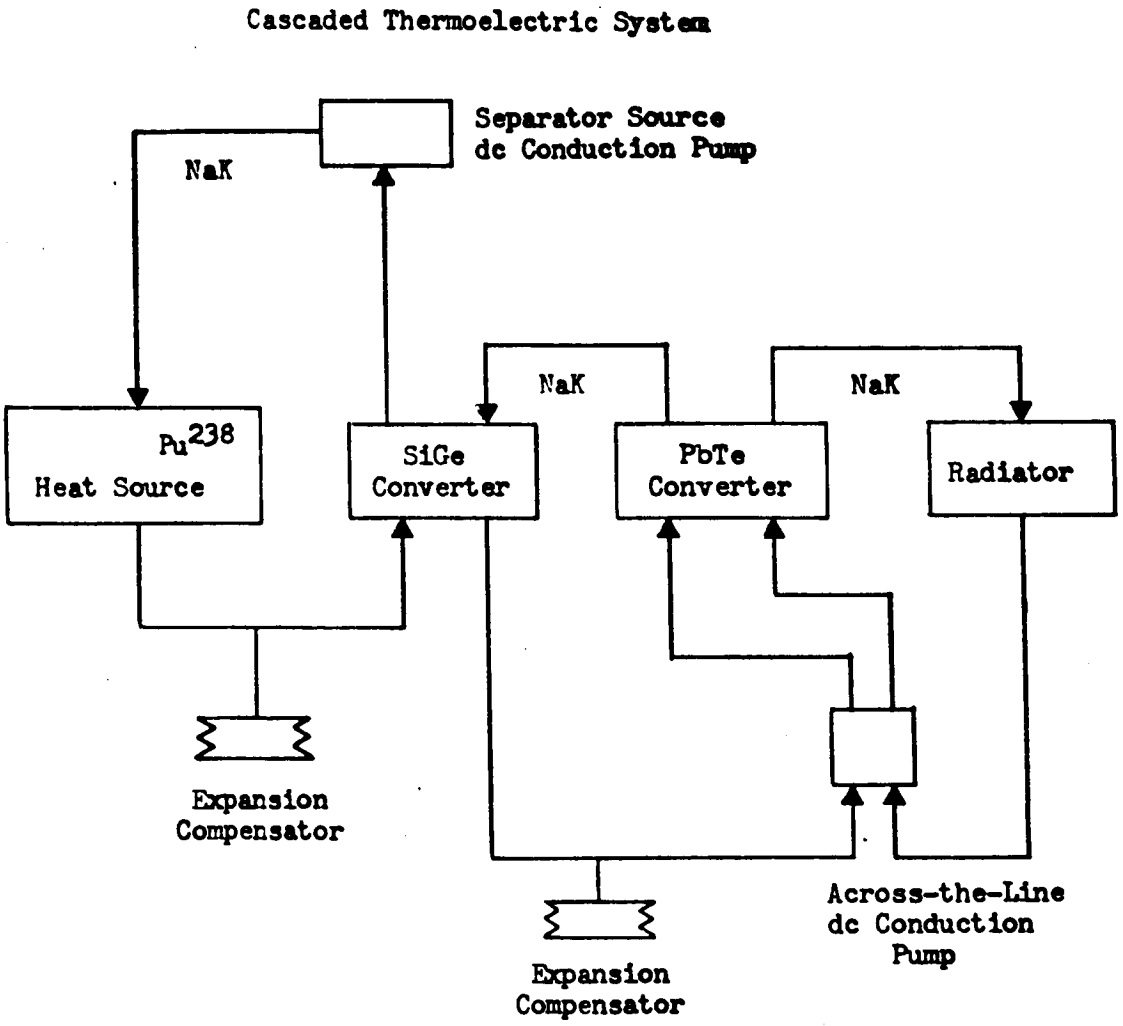

Figure 71. Cascaded Thermoelectric System Schematic

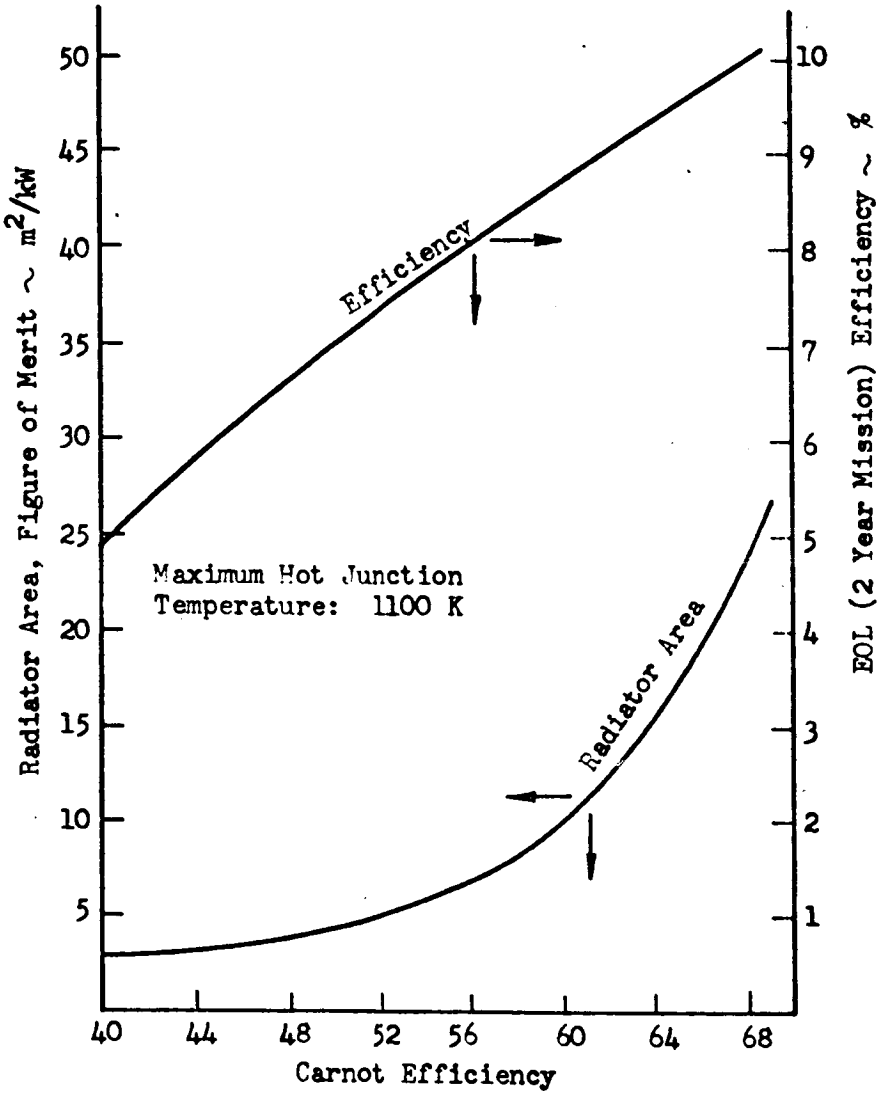

Figure 72. Pu238 Fueled Cascaded Thermoelectric Generator System Performance

Single element thermoelectrics were not shown in the Weight Summary since they result in additional weight, i.e., approximately 1.28 times the weight of cascaded systems. For example, the isotope thermoelectric cascaded system shown in Table 23 totals 4920 pounds for an electrical output of 10 kilowatts (0.49 lb/watt). Reference 7 shows a total weight of 2450 pounds for a 3-kWe output single SiGe element design. Using the 23 percent improvement in performance, the following results:

$$\frac{2450 \text{ lb}}{3000 \text{ watt}} \quad \frac{1}{1.28} (1 - 0.23) = 0.49 \text{ lb/watt}$$

This value will differ from Figure 66 since new study has shown reduced isotope fuel block weight by allowing helium venting and it is reasonable to project these weight savings. Weights shown in Figures 66 and 67 apply only to existing hardware design, which does not allow for helium venting.

The isotope thermoelectrics were selected for comparison to solar photovoltaic and chemical energy systems for the planetary excursion module descent stage (Figures 37 through 40). A summary of weight savings, as compared to longer missions, is shown in Table 36. These savings are not excessive since redundancy in the thermoelectrics was figured at 5 percent per year rather than by additional converters because of the inherent reliability resulting form series-parallel arrangements of the thermoelectrics.

Table 36. Weight Reduction for Isotope Thermoelectric Power Systems at Missions Less Than One Year

Component	Weight Savings
Converter	5 percent (no redundancy)
Electric and Control	50 percent (no redundancy)
Radiator	33 percent (less meteoroid protection)
Auxiliary radiator	35 percent (less meteoroid protection)
Shield	31 percent (increased allowance to 20 rem/yr)
Total overall savings	16.5 percent (system weight)

Note: For the nuclear isotope systems only the thermoelectric system was shown for use with the planetary excursion module descent stage (Figures 37 through 40).

Weight Scaling Assumptions and Methods Applicable to Isotope Systems

The shield weights are based on a spacecraft concept which permits the source location separate from the mission module (assuming a recoverable source). Isotope shield weights are a function of effective separation distance were shown in Figure 52.

The assumptions used to determine the major component and subsystem weights are:

1. Levels of redundancy required to meet the mission reliability goals. All system configurations were assumed to require one active PCS loop plus two redundant loops as a minimum to produce the desired electrical power.

   Each redundant PCS loop is inactive until required to take over the load-sharing duties of an active loop. An alternative approach is to assume two active PCS loops plus several redundant loops. This criterion would preclude shutting down the entire dynamic power system in event of PCS loop failure. This latter approach results in some weight increase. For purposes of this study, it was believed that only one active loop should be considered. A summary of the redundancy criterion used in this study is presented in Table 37. Table 37 differs from Figure 48 because isotope systems are assumed to be most applicable at low power demands, which will allow satisfying total power by one active power conversion system. This assumption does not apply to the higher power output of nuclear reactor systems.

2. The meteoroid armor protection required to meet the specified "0" puncture probabilities. In the interest of evaluating each system on a common basis, a weight penalty for radiators was assessed per square foot. The radiator weights used in the study are summarized in Table 38 . These weights were obtained by providing sufficient armor for P(0) = 0.999 (one year) based on reference weights for MORL systems and adding one redundant radiator loop per year of additional operation.

The Rankine cycle system weights are based primarily on weight data obtained from the Mercury Rankine Program (MRP), including temperature, pressure, volume, geometry, etc. considerations for each component. The Brayton cycle system weights are based primarily on the studies and programs conducted at AiResearch and TRW. These data were generated by Atomics International and applied within mission constraints of the manned Mars flyby mission (References 4 and 8). Beginning with established design for 1975-1985 manned planetary flyby missions for range 2 kwe to 8 kWe, it was possible to estimate improvements and show final weights based

Table 37. Redundancy of Isotope Dynamic Power Conversion Systems (Used in Weight Summary)

Mission Duration (years)	Number of Power Conversion Systems*		
	Active	Redundant	Total No.
1	1	2	3
2	1	3	4
3	1	4	5
4	1	5	6
5	1	6	7

*Based on the assumption that rotating machinery will be designed to achieve a minimum of one-year life.

Table 38. Radiator Weights (lbs/ft^2) Used in the Weight Summary For Isotope and Nuclear Reactor Power Systems*

Auxiliary NaK - All Systems (lbs/ft^2)	FC-75 - Brayton; Dowtherm A (lbs/ft^2)	NaK and Radiator-Condenser Rankine; Thermoelectric (lbs/ft^2)	Mission Duration (year)
6.2	1.06	1.61	1
9.8	1.46	2.56	2
13.4	1.86	3.51	3
17.0	2.26	4.46	4
20.6	2.66	5.41	5

Notes: *Total weight is a function of fluid tube vulnerable area i.e., power level. These weights are to be taken as average values most applicable to the power level of isotope systems. See Figure 56 for variations.

Radiator weights were based on:

1. Meteoroid thickness to give P(0) = 0.999 (one year-based on reference weights for MORL systems)
2. One redundant loop added per year starting with the second year

on these estimates. A summary of the assumed improvements in system performance and the relationship to overall weight reduction as reflected in the weight summary is shown in Table 35.

The following discussion describes the methods used in the Atomics International study to determine the weights of key components or subsystems in each cycle.

Boiler-Heat Exchanger. The Rankine cycle boiler weights were calculated from the sizes resulting from the Rankine cycle analysis. The Brayton cycle heat exchanger weights were obtained by adjusting the referenced heat exchanger weights (as shown in Table 23) according to power level, fluid flow, and heat transfer capabilities.

CRU. The CRU weights were calculated by adjusting the referenced CRU weights according to piping sizes, turbine diameters and stages, and alternator sizes.

Regenerator. The regenerator is required only in the organic and Brayton systems. It is shown in the schematic of the Rankine Mercury system (Figure 61) primarily as a heat exchanger, providing a method to cool the alternator. Its weight was obtained by ratioing the flow rate and ΔT between the PCS working fluid at the turbine exhaust and the boiler inlet for each cycle to those for the referenced regenerator weights.

Inventory. The Rankine cycle working fluid inventory is based on the steady-state operating condition, and twice this quantity is required for each module for restart capability. The inventory weight is dependent on:

1. Quantity and size of the boiler tubes
2. Length and size of piping to and from the boiler
3. Size of liquid manifolds in the radiator condenser (R-C)
4. Quantity and condensing height of the R-C tubes

These values were ratioed to those for the Mercury Rankine Program steady-state weights to obtain the inventory weight for each Rankine cycle fluid. The Brayton cycle inventory weight was adjusted according to volume.

Regulator Tank (Rankine Cycle). The size and weight of the regulator tank are dependent on the working fluid volume and the anticipated fluctuations in system performance, along with the working pressure. The weight was assumed uniform for all systems since the tank volume is essentially constant between fluids. For a reference design at 4.0 kwe output, the total

start system components are assumed to weigh 80 pounds and to occupy 1.6 cubic feet. Fluid inventory estimates vary from 2.5 pounds (Dowtherm A) to 30 pounds (Hg) for steady state operation.

Injection Tank (Working Fluid). The injection tank weights (part of start system) were obtained by adjusting the MRP weight by ratioing the PCS working fluid volume and injection pressure.

Heat Rejection System. The heat rejection system is a radiator condenser or radiator sized physically on the heat rejection requirements of the system. Materials were selected on a compromise basis between the thermal and structural requirements to minimize weight. The system is composed of the items discussed in the following paragraphs.

Tubes and Meteoroid Armor. The quantity of tubes was determined by the thermal requirements. The tube material was selected considering (1) compatibility with the PCS working fluid, (2) structural capability, and (3) meteoroid armor effectiveness. The tube thickness was held constant at 0.025 inch, which was considered the minimum for the strength and fabrication requirements. The tube lengths are a function of the required area.

Fin. The fin area and thickness are directly related to the thermal requirements. Material selection was based on conductivity, density, and strength. A shared fin concept was used in which one tube from each module (active—passive) shares one common fin, i.e., area is not duplicated for inactive module.

Manifold. The length of the vapor and liquid (not in the Brayton cycle) manifolds are a function of the R-C or radiator width. The diameter is dependent on the allowable pressure drop in the system. Thickness is determined from structural and meteoroid armor requirements. The material is the same as for the tubes.

Structure. Additional structure to that already enumerated is required to satisfy structural requirements. This structure includes frames for structural stability, rings for attachment, and brackets and doublers for component attachments.

Deployment. No radiator deployment was considered. It was assumed that radiator area availability is sufficient to satisfy requirements. The deployable R-C's or radiators require twice the meteoroid armor shown since both sides are considered vulnerable to meteoroid exposure without the aid of any structure to act as a bumper for meteoroid bombardment. However, deployable R-C/radiators radiate from both sides, thus, requiring only one-half of the conventional R-C/radiator required area.

Miscellaneous. These weights include all miscellaneous items not previously covered, such as brace, mechanical fasteners, emissivity coatings, joints, clips, intercostals, etc. This weight was estimated from the referenced R-C/radiator designs and apportioned according to area.

Electrical and Control. The weights used are based on the power conditioning schematic (e.g., Figures 57, 61, and 70) and on weights of similar available equipment where possible. When typical weights were not available, such as was the case for excitation control, an estimate was made based on the typical material that would be found in such an item.

Source. The source weight was obtained as a function of thermal power required based on typical isotope fuel capsule designs using Pu^{238} microspheres.

Shield. A comparison of shield weights for the isotope systems reveals small difference. The largest influences are the source location in the vehicle and flight configurations. Shield weights were calculated using typical crew duty cycles and distances from the source as found in Reference 1. The shield configuration was determined by its location and line-of-sight geometry and the boiler-heat exchanger configuration.

Further description of these components and the parametric curves that influence their weights are presented in References 4 and 6.

Solar/Dynamic Power System

The solar dynamic power system considered included both the Rankine and Brayton conversion cycles. Both of these cycles were described in the Radioisotope Power System section of this report, and since the flow schematics are similar, they will not be repeated here. Weights have been determined for solar-powered systems assuming the same conversion equipment as for the radioisotopes. Solar concentrator-absorber weights are used to replace those of the isotope, shield, reentry boiloff, and isotope auxiliary radiator. Characteristics of the conversion cycle are assumed to be the same, thereby, resulting in identical conversion component weights and radiator area requirements. Meteoroid protection of the radiator, cycle improvement, and redundancy philosophy were considered to be identical.

The solar concentrator-absorber combination was sized for constant efficiency, i.e.,

$$\eta_{concentrator} = 0.85 \text{ (assumed constant)}$$

$$\eta_{absorber} = 0.70 \text{ (assumed constant)}$$

Figure 73 shows area utilization used in the weight determination. Specific weight variations for different concentrator designs are shown in Figure 74. For this study, concentrator weights were based on paraboloid mirrors of either the petal construction or the inflatible construction. A specific value of 0.4 pound per square foot was used, which includes a 20-percent penalty for orientation. A comparison of orientation requirements for various systems is shown in Table 39.

Figure 75 shows the combined collector-absorber efficiency as a function of absorber temperature for six collector concepts based on experimental data assuming an ideal cavity absorber. Four concentrator types (inflatable, inflatable rigidized, petal, and Fresnel) fall within the same range of concentrating ability but with widely varying efficiencies. The failure to approach the near-theoretical value of the one-piece design can be attributed to material and fabrication problems. Future developmental efforts should narrow this gap. Future collector capabilities may be summarized as follows:

Table 39. Allowable Misorientation for 10-Percent Power Reduction

System	Misorientation
Turbogenerator system (1170 F)	1 deg - 8 min.
Thermionic generator (2390 F) (4900 F)	16 min. 5 min.
Photovoltaic	
(a) Flat panel (50 F)	26 deg
(b) 2 to 1 concentrator (85 F)	6-1/2 to 15 deg

1. Reflectivity (silver or aluminum freshly deposited) ranges from 90 to 93 percent on metallic surfaces and from 85 to 87 percent on mylar substrates. Silicon monoxide coatings will probably retain this reflectivity for ground applications, however, little is known of the long-time integrity of the reflectivity in the space environment

2. Concentration ratios (projected area of concentrator to optimum area with cavity opening) vary from approximately 2000:1 for metallic types to 800:1 for inflatable units

3. Specific weights (reflecting surface only) are 0.2 to 0.5 pounds per square foot for metallic and 0.15 pounds per square foot for inflatable types. Based on current state of art, concentrators can

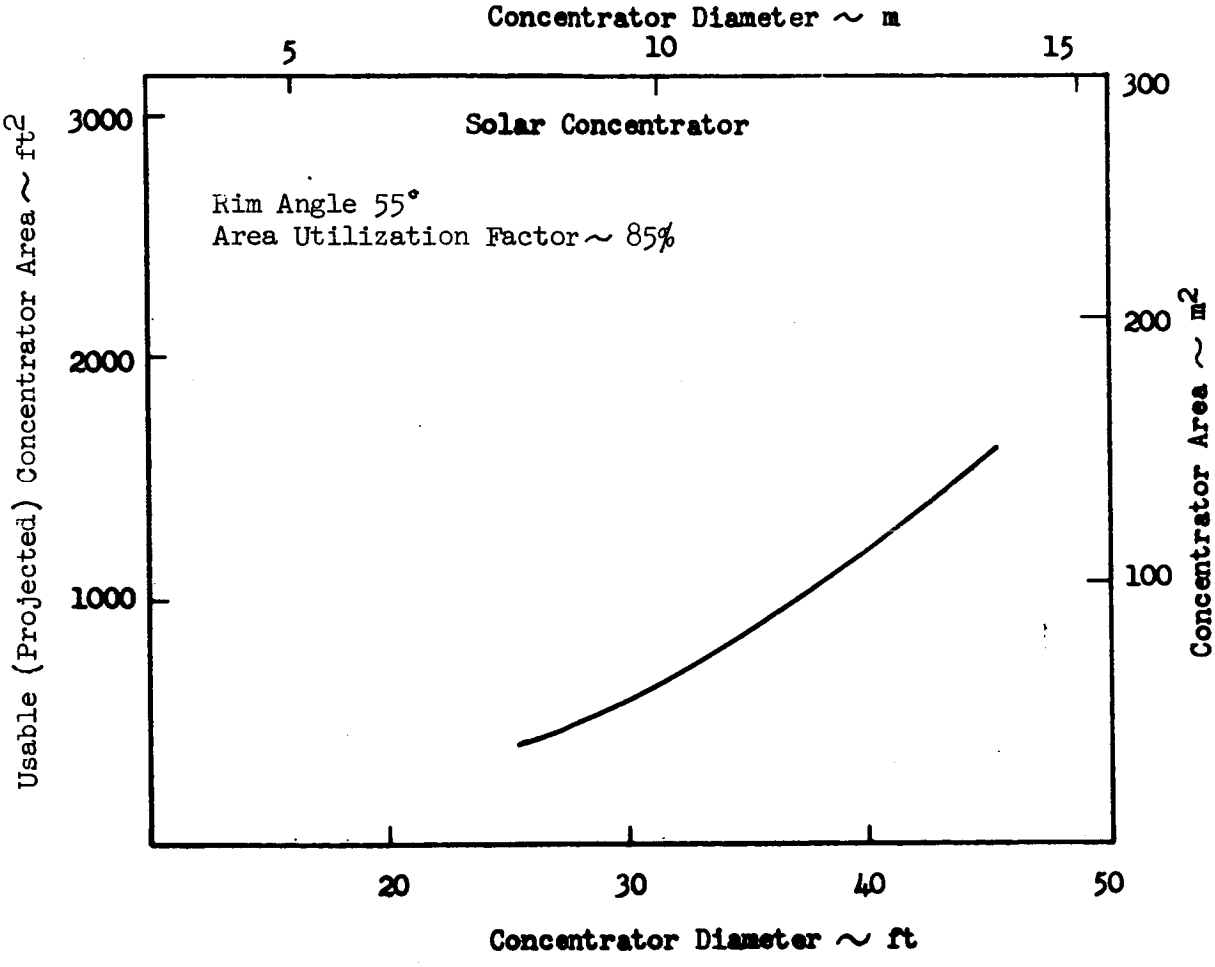

Figure 73. Concentrator Area Versus Diameter Solar Dynamic Power System

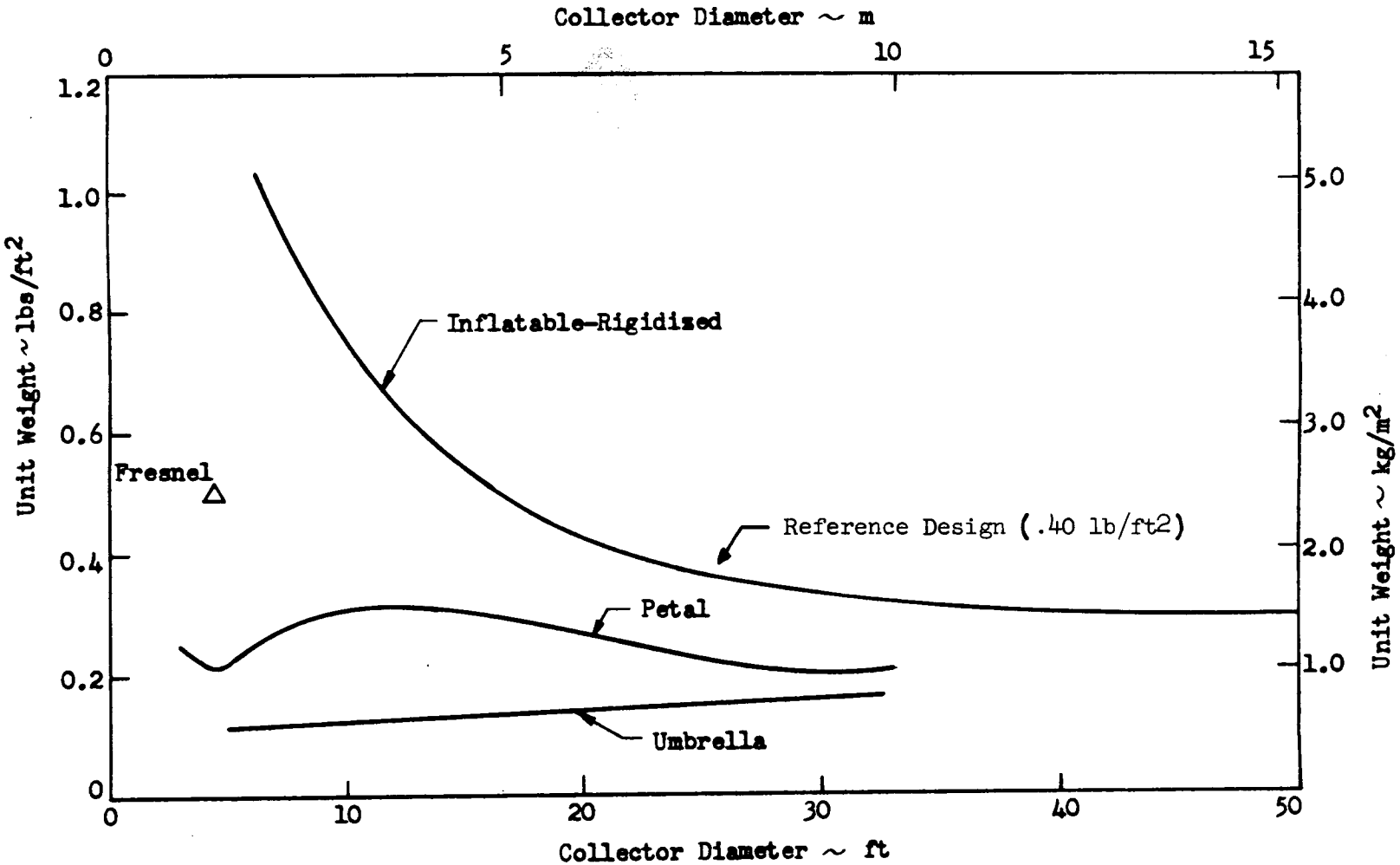

Figure 74. Collector Unit Weight Versus Collector Diameter
(Reference-Manned Mars Mission Study)

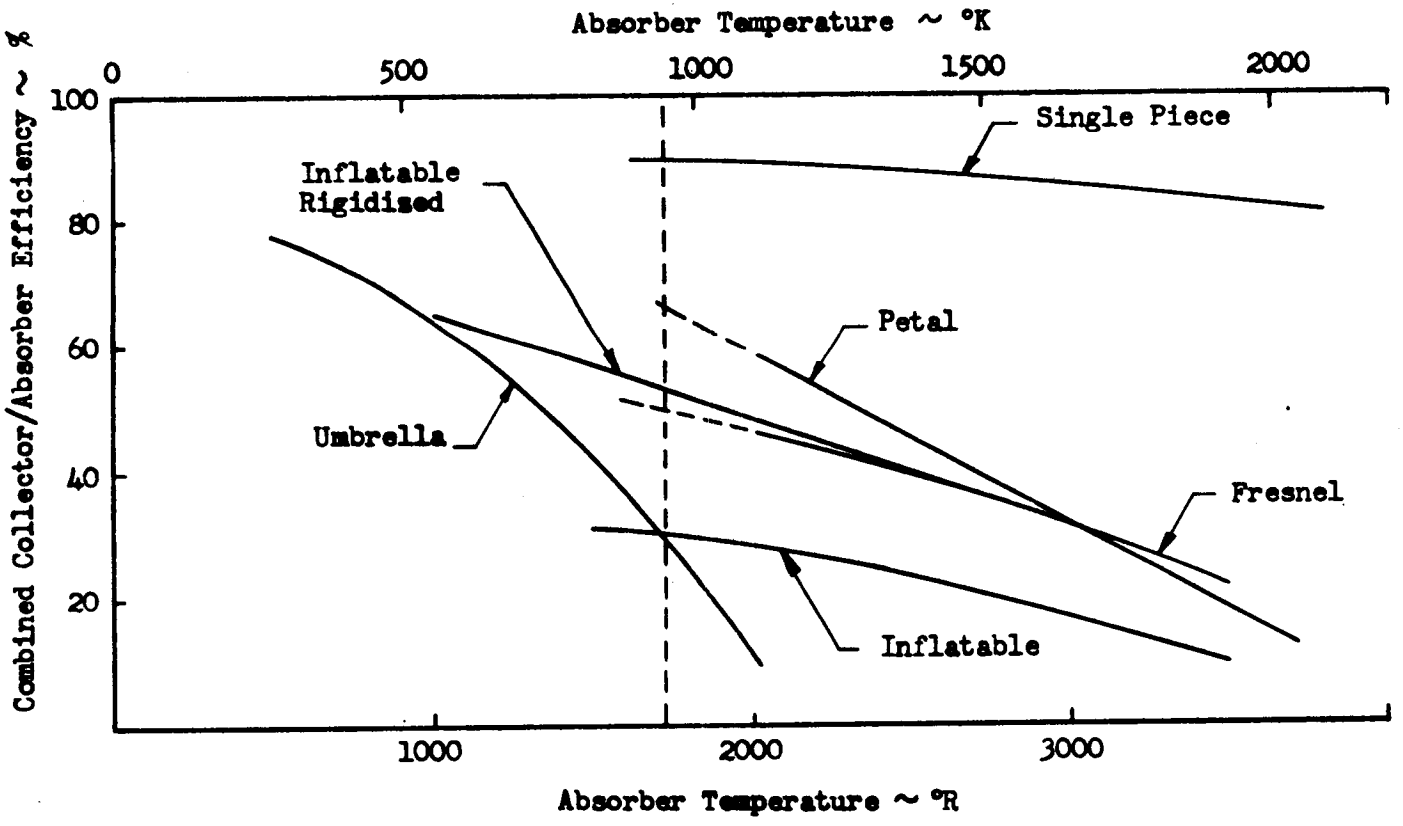

Figure 75. Combined Collector-Absorber Efficiency Versus Absorber Temperature

be considered of the petal, inflatable-rigidized, and Fresnel types for collector diameters up to 50 feet. The inflatable-rigidized type is preferred because of its lower prelaunch storage volumes and minimum problems of ground handling and launch structural stresses.

Photovoltaic Power System

The use of solar cell systems must be considered as either a primary power source or a back-up source for the majority of the missions considered during this study. These systems have been the primary power source on the majority of the unmanned systems launched to date which has resulted in a backlog of information regarding their operational use. There are, however, recognized problems associated with the large arrays which would be required for the systems considered in this study, e.g., deployment, retraction, orientation, structural design, etc.

A solar cell system based on projecting the present state-of-the-art hardware was used for the solar cell system basepoint weights (References 1 and 8). The solar array consists of oriented panels constructed of replaceable electrically interconnected modules of solar cells. Each solar cell module is made up of N/P, 1 ohm cm, 11 percent AMO, 2 x 2 cm silicon cells formed from parallel groups of cells having a fixed number of series cells. Each module weight is based on using beryllium substrates and aluminum backup structure. The backside of the substrate has a thermal control coating with an emissivity of 0.82 or greater and an absorptivity no greater than 0.20. These modules are connected in matrix to give the required array output power and voltages.

Power Transfer

Sun sensor signals and power will be transferred from rotating solar cell panels to a stationary control system through a slip ring assembly on the drive shaft. Electrical leads are integral with each slip ring with the shields for the signal wires allowed to float at the slip rings.

Array Deployment

The deployment scheme is based on a lazy tong mechanism consisting of a number of connecting links. The erection mechanism is considered as the heart of the deployment sequence, and as a result, uses ultimate simplicity for maximum reliability. It is a simple slider-crank device that rotates under the action of a single liquid dampened spring actuator, extending and angularly positioning the array in one single continuous cycle. The mechanism consists of a frame, an adjustable liquid dampened spring actuator, a bell-crank, a slider, and a support assembly. The actuator is used to control the extension rate and complement the array arm forces when they are approaching their minimum output. Rate control adjustment is accomplished by throttling the fluid flow with a needle valve located within

the piston rod. A compression spring surrounding the actuator, sided by the mechanical advantage of the mechanism is used to complement the forces built into the arm assembly. Table 40 shows typical structural configurations that may be considered.

A direct drive assembly is used where the meter shaft is coupled directly to the solar array axle through a simple spring and damper mechanism. It is designed to transmit constant torque to the solar array at a rate of rotation maintained by a controller which senses the sun and modifies the rate of rotation to correct for such factors as orbital eccentricity, programming, errors, etc. The basepoint drive assembly is based on the experience and development test parameters generated and utilized during the SNAP reactor control drum drive development program.

Design Considerations

There are three possible ways of designing a solar cell system for a particular mission. The first method involves utilizing a developed system or a system in development, exhibiting comparative performance characteristics requiring only minor sizing modifications. The second approach uses a proven system as a submodule in a building block process for higher power requirements. The third method is to design a completely new system based on advanced technology.

Table 41 relates the present and future solar cell panel trends for large area panels. Of the arrays now being developed, Boeing is developing the largest array of 4590 square feet. Both TRW and RCS are studing panel sizes in the area of 1000 square feet, and Hughes is developing a flexible roll-up array using dendritic cells for areas of approximately 500 square feet. It appears that modification of existing hardware will not be possible, however, modification of the Boeing advanced design may prove feasible. The other solar cell arrays may be considered as submodules for system sizing.

If a new panel is completely redesigned for optimum mission requirements, solar cells other than that of the N/P; 12 mil, 1 ohm-cm silicon, single crystal cell may be considered. Major emphasis was placed on the utilization of large area thin film cells, resulting in a large reduction in panel weight. The lighter-weight panel stems from the fact that only very thin layers of silicon (100 microns) are required to convert solar photon energy to electrical power. Most of the remaining 10 to 20 mils of material used in conventional single crystal cells serves as structural support. At present, thin film cells of Cadmium Sulfide (CdS) and Cadmium Telluride (CdTe) are receiving major attention. These materials have diffusion lengths considerably less than that of silicon. The processing of high efficient arrays is quite expensive and probably will require several years to perfect.

CONCEPT	Load Conditions					
	Boost - Static	Boost Dynamic	Deployment	Roll-Up	Maneuver	Meteoroid Environment
①  RYAN'S OPEN -SECTION BEAM	Good characteristics - Requires protection of cell from next rolled layers	Good characteristics expected. Requires dynamic dampers in between layers for cell protection	Limited operation. Highly stressed material - Poor torsional and bending rigidity	Limited number of cycles - Possibility of buckling and crack development	Low torsional and bending rigidity because of open beam sections and thin gauges	Poor - highly susceptible to crack development and propagation
② 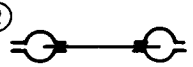 RYAN'S CLOSED-SECTION BEAM	Same as 1	Same as 1	Same as 1 with improved bending and torsional characteristics	Same as 1	Improved bending and torsional rigidity	Same as 1
③  DE-HAVILLAND ROLLED-UP BEAM	Same as 1	Same as 1	Same as 1	Same as 1	Same as 1	Same as 1
④ 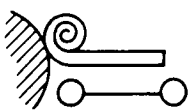 ROLLING-OUT INFLATABLE	Same as 1. Cell protection may be avoided by use of multiple folding cell modules	Same as 1. Cell protection may be avoided by use of multiple folding cell modules	Unlimited operation - Meteoroid sensitivity may be reduced by dividing beam into airtight compartment	Unlimited number of uses	Good bending and torsional characteristics. Possible array-sun alignment	Poor to good - Meteoroid sensitivity may be reduced by partitioning the beam section into tight compartments
⑤ 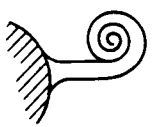 OUTWARD "ROLL-OUT" INFLATABLE	Same as 4	Same as 4	Same as 4. Simplified array/vehicle structural and electrical interface	Same as 4. Simplified structural and electrical interface	Same as 4	Same as 4
⑥ 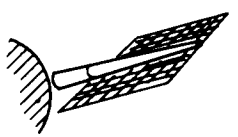 MAST AND SAIL	Good - Multiple folding may be used to obtain extremely high volumetric efficiency in packing	Good -	Mast may be retracted or not. Deployment of array is highly simplified - unlimited operation	Array may be rolled up without disturbing support structure - Low power operation -	Good characteristics - Structure may also be used to support experiments	Good. Mast structure may be partially destroyed without affecting ability of array to deploy or be rolled-up
⑦ 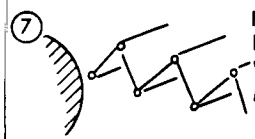 FOLDED RIGID PANELS AND "LAZY TONG" MECHANISMS	Good	Dynamic response of individual panels to sound & vibration must be evaluated	Mechanism design to assure even & constant rate deployment may be complicated	Reliability of operation is reduced by number of working parts	Good load carrying characteristics - Relatively heavy members	Good

Table 41. Solar Cell Performance Scaling Factor

Solar Cell Thickness (mils)	Present		1975		1980-2000	
	Efficiency (percent)	Power Output Scaling Factor	Efficiency (percent)	Power Output Scaling Factor	Efficiency (percent)	Power Output Scaling Factor
12	10.5	1.0	11.7	1.1	13.0	1.235
8	9.5	0.905	11.0	1.045	12.0	1.145
4	7.5 - 8.5	0.715-81	9.5 - 10.5	0.904-1.0	11.7	1.1*
*Used in Weight Summary						

Table 42 relates the solar panel specific weights for both the present and future single crystal silicon cells. These weights do not include any environmental degradation factors, and make use of the lightest beryllium substrates. For this portion of the study, solar cell panel weights were based on the values shown in Table 42.

Temperature is a primary variable in the efficiency of operation of a solar array. The steady-state thermal balance equation for a unit area solar array operating in space yields the curve shown in Figure 76. This was obtained by selecting values for the parameters from Reference 9 shown in Table 43.

Radiation Damage

Several silicon cell modifications have been investigated for reducing cell damage due to radiation exposure. One of the most significant changes has been the use of a 10 ohm-cm base resistivity cell in place of the conventional base resistivity of 1 ohm-cm. A factor of 2 to 3 in resistance to electron damage has been realized. The main disadvantage to this approach, however, is that the 10 ohm-cm cell is inherently a lower efficient cell, exhibiting a lower output voltage.

Another type of cell, the drift field cell, has been given considerable attention. In this cell, a drift field is added to a conventional cell where the base region contains an impurity gradient to provide an accelerating field for minority carriers towards the junction. Improvements in radiation degredation of a factor of 2 to 5 may be achieved, although these results are not yet final.

Table 42. Weight Breakdown of Solar Array, 2x2 cm Cells

Solar Cell Array Assembly Components	1 kW Array				10 kW Array			
	Present		1980-200		Present		1980-200	
	Thickness (in.)	Weight (lb/ft^2)	Thickness (in.)	Weight (lb/ft^2)	Thickness (in.)	Weight (lb/ft^2)	Thickness (in.)	Weight (lb/ft^2)
Cover	0.006	0.075	0.001	0.012	0.006	0.075	0.001	0.012
Cover adhesive		0.027		0.016		0.027		0.016
Cell	0.0125	0.167	0.008	0.086	0.0125	0.167	0.004	0.043
Interconnections		0.005		0.004		0.005		0.004
Substrate adhesive		0.019		0.019		0.019		0.019
Skin		0.138		0.108		0.138		0.108
Beams		0.046		0.032		0.048		0.038
Reinforcing		0.016				0.018		
Storage and deploy		0.380		0.250		0.142		0.120
Subtotal		0.873		0.527		0.639		0.360
Orientation								0.079
Structure		0.427		0.256		0.312		0.112
Total		1.300		0.783		0.951		0.541

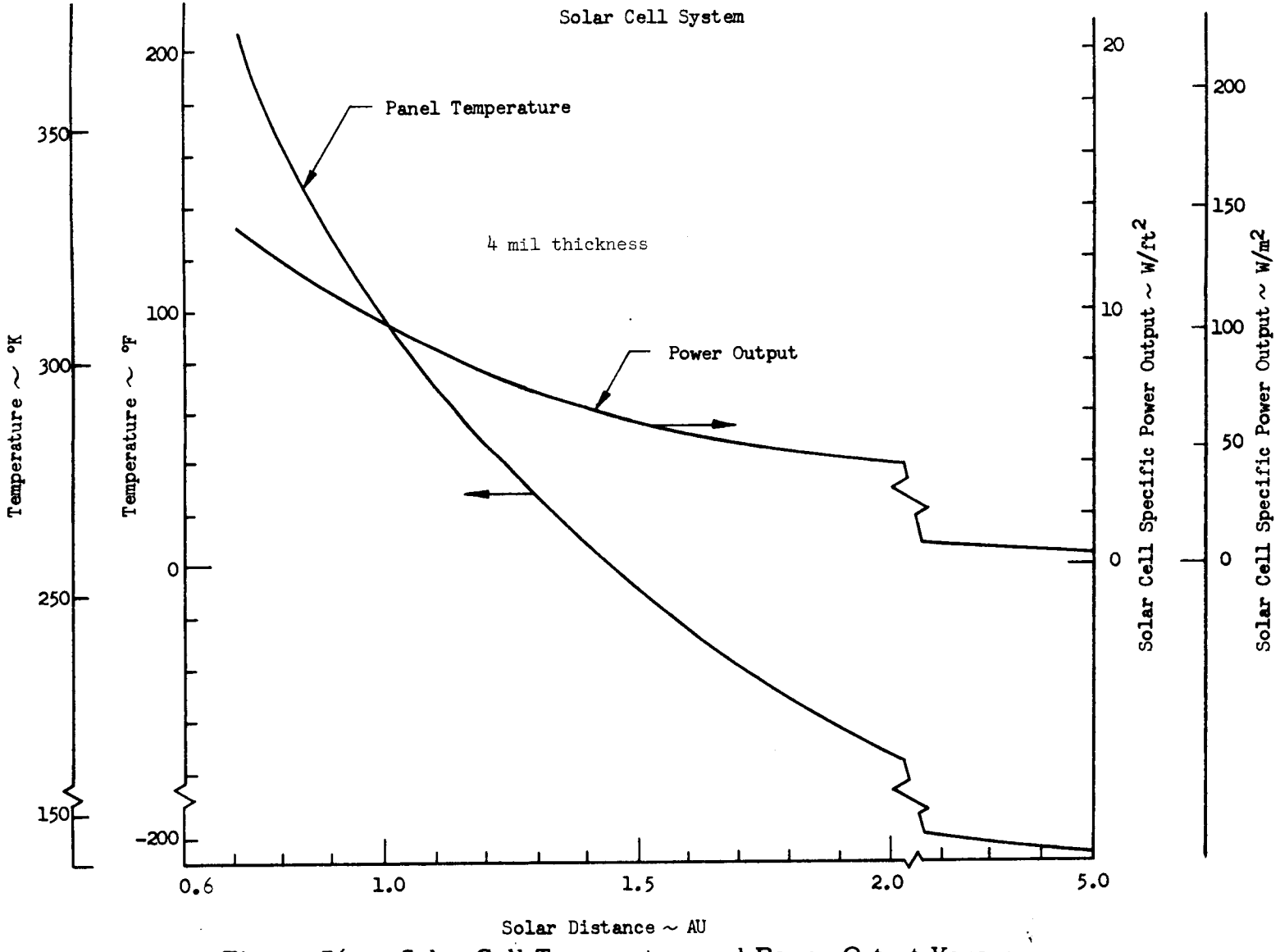

Figure 76. Solar Cell Temperature and Power Output Versus Solar Distance

Table 43. Solar Array Scaling Factor

Solar Cells Parameter	Present Consideration	Anticipated By 1980-2000
Area utilization factor	0.85	0.90
Degradation factor	25 percent	25 percent
N/P silicon solar cells	10.5 AMO: 12 mils	12.0 AMO: 8 mils
Absorptivity: 0.83 (solar cell)	0.25 (inactive)	Same
Emissivity: 0.835 (solar cell)	0.85 (inactive)	Same
Specific heat capacity	0.250 Btu/ft^2 °F	$\frac{0.151 \text{ Btu}}{\text{ft}^2 \text{ °F}}$ (8 mils) $\frac{0.105 \text{ Btu}}{\text{ft}^2 \text{ °F}}$ (4 mils)

The most recent result in the reduction of radiation damage to solar cells has been the use of lithium as the n-type dopant in a P/N silicon cell. It has been found that with a lithium doped P/N cell, the output of the cell in a radiation environment is much higher than that of the best N/P cell. Lithium is quite mobile in silicon at room temperature. When radiation causes a vacancy, lithium can diffuse to the vacancy, look into the substitutional site, and eliminate it as a recombination center. The major problem with this type cell, at present, is the shelf life. It has not yet been determined how long the lithium will stay in the silicon.

To determine the degradation of panel output power as to a radiation environment, certain factors must be considered. There is no ideal way to present the data defining radiation damage to solar cells, partly because there are so many measurable parameters which are sensitive to radiation, e.g., efficiency of energy conversion, maximum power point, short circuit current, open circuit voltage, minority-carrier-diffusion length, spectral response, junction capacitance, dark current, and curve factor. In addition, damage is different for the various types of cells and cover slides. It can be seen, therefore, that certain limitations had to be set.

The following assumptions were used:

1. Cell:
   a. Type - N/P Silicon
   b. Resistivity - 1 Ohm Cm
   c. Thickness - 12 Mil
2. Cover Slide
   a. Type - Quartz

Power Degradation

Figure 77 depicts the degradation to the maximum power output of bare 1 ohm cm resistivity N/P cells due to varying proton fluxes at increasing energies. As can be seen from the curves, the cell is most sensitive to low energy protons. For the missions considered in this study, the proton flux from solar flares will be the predominate factor for system sizing.

Radiation Shielding

Figures 78 and 79 relate the quartz slide thickness required to shield proton fluxes below a required energy range (mev). For instance, in order to shield for all proton flux below 10 mev, a quartz thickness of approximately 24 mils is required. The other ordinate depicts the increase in panel weight per square foot of panel size due to the use of quartz shielding. If 10 mev is the design shielding line, an increase in panel weight of 0.275 pound per square foot is required. However, for this study, it was assumed that radiation-hardened cells would be available, and that no allowance would be made for radiation shielding.

The curves of Figures 77 through 79 were included to show that present solar photovoltaic power systems suffer considerable degradation in power output due to solar proton radiation effects. An optimum cover slide thickness exists for each cell design and anticipated radiation level. However, it is beyond the scope of this power systems study to define the space environments accurately enough to be of use.*

It is reasonable to assume that improvements will permit radiation resistant cells. It may be that a differential between 1980 and say 1990 should be made with some radiation shielding allowed. However, this was not part of the study. In figure 78 the lines labeled 3, 6, 12 and 20 mils are perpendicular to a constant lb/ft^2 since a given thickness will shield out energy levels independent of total flux quantity considering the same energy distribution.

Typical System

A functional schematic of a solar cell system for this application is shown in Figure 80. Two isolated cell panels are connected to the main distributing dc bus through motor switches. Unregulated panel power is then distributed to the secondary battery subsystem, unregulated and regulated load buses. Since the output of the solar panels has a wide voltage swing, additional voltage regulation must be imposed to satisfy most dc subsystem load requirements.

* Only a nominal degradation allowance of 5 percent per year in power output was assumed (Table 44).

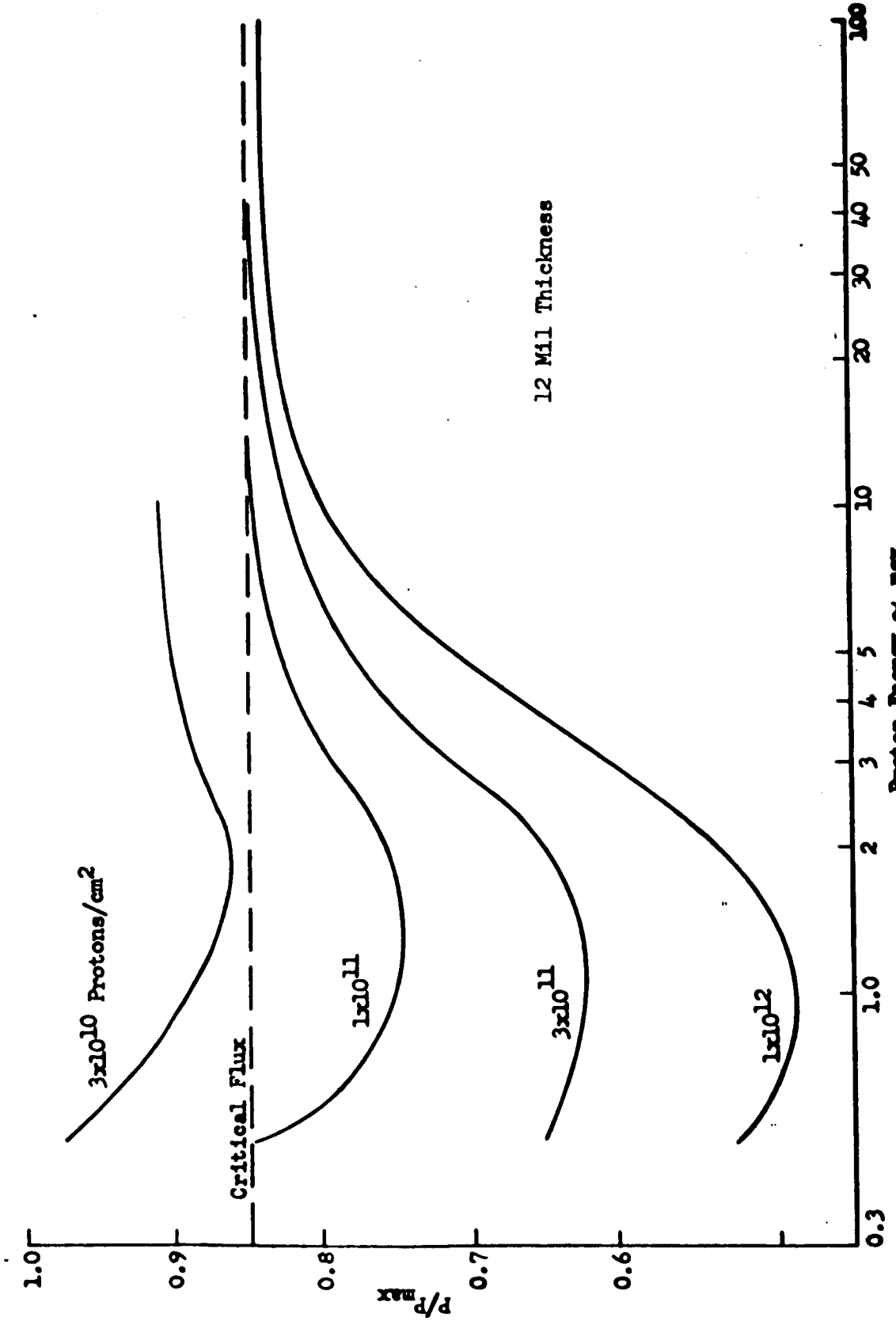

Figure 77. Relative Power of Solar Cell Panel Versus Proton Energy

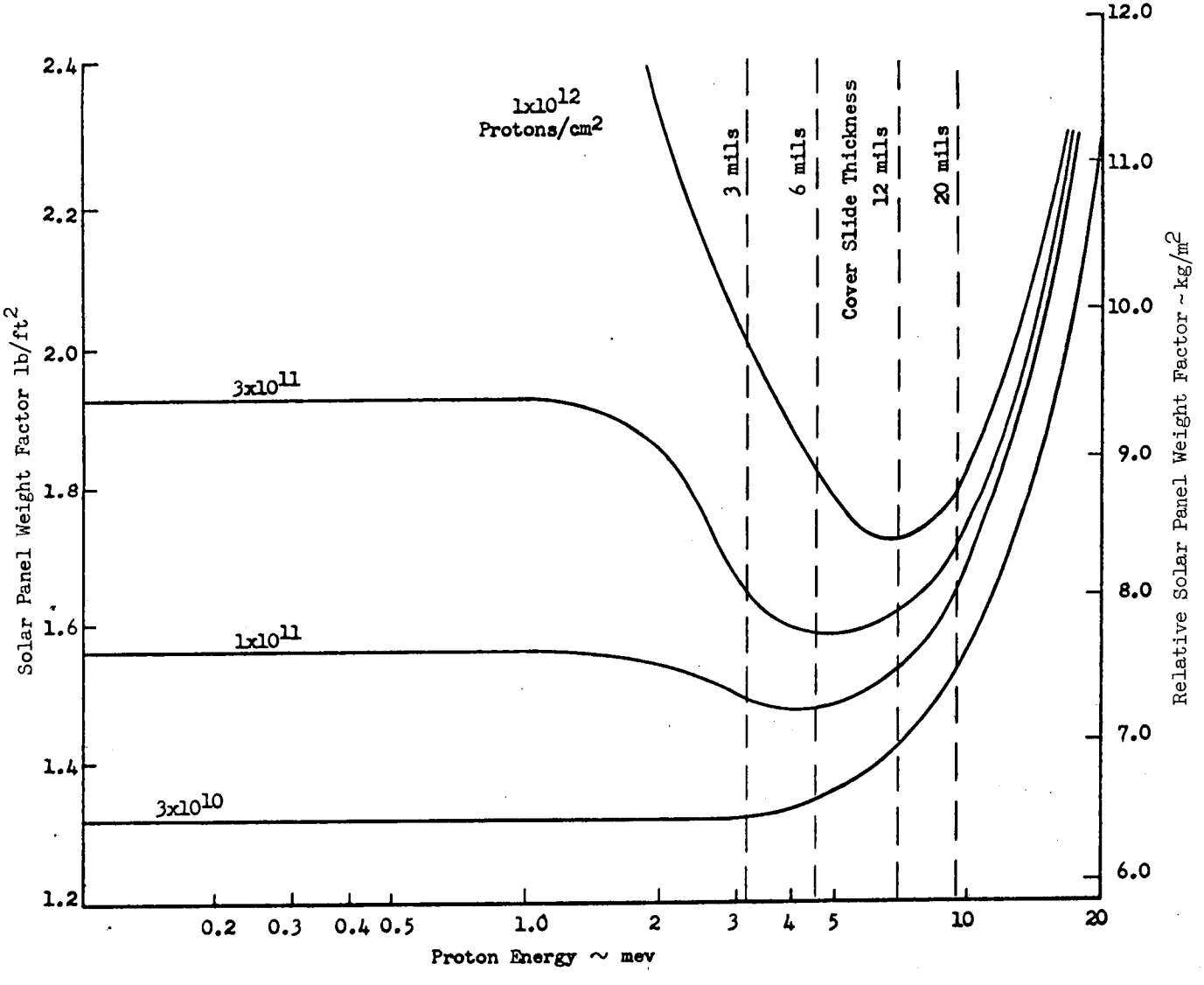

Figure 78. Specific Solar Panel Weight Versus Proton Energy Level and Flux

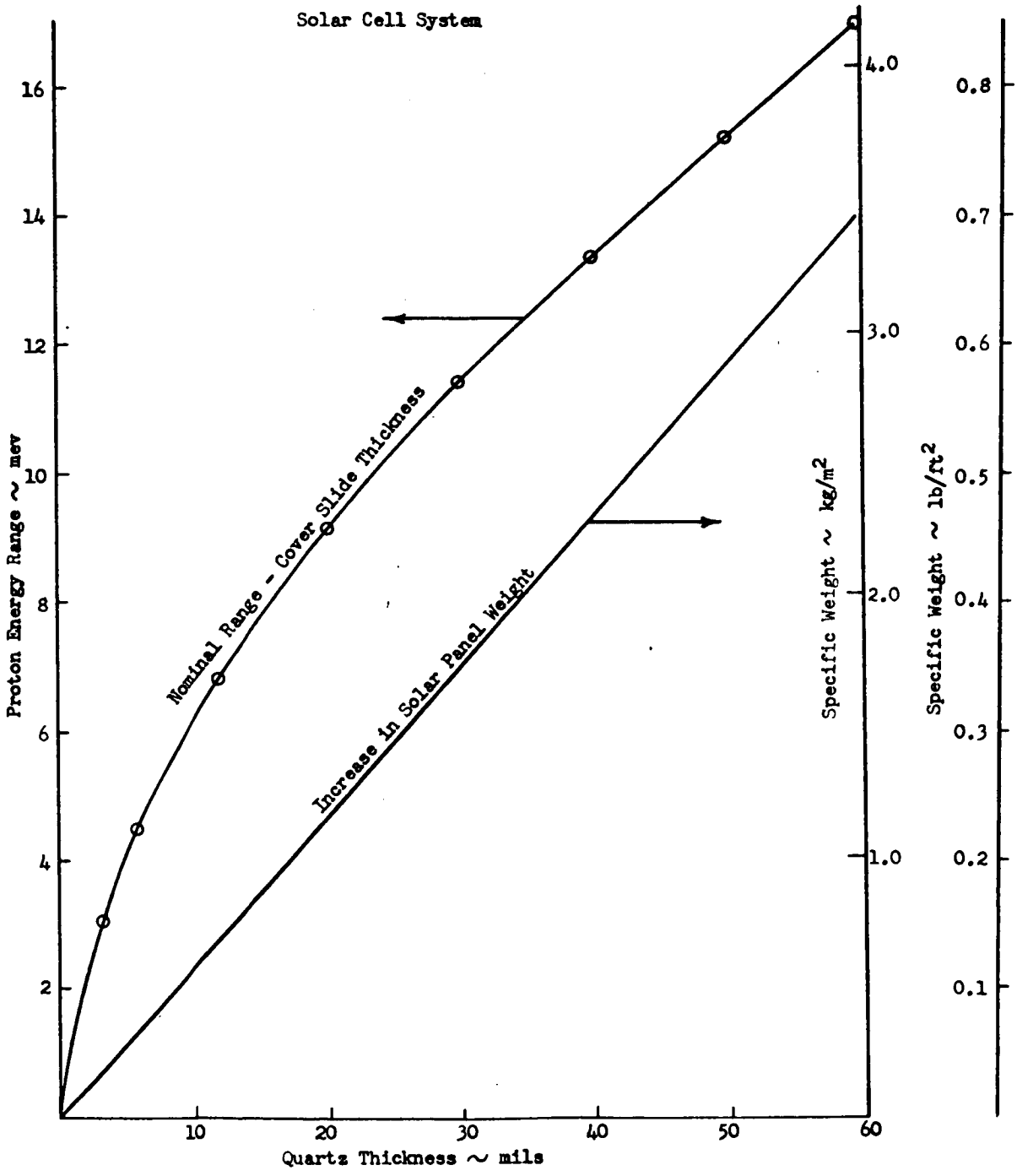

Figure 79. Panel Specific Weight and Relative Proton Energy Cutoff Versus Cover Slide Thickness

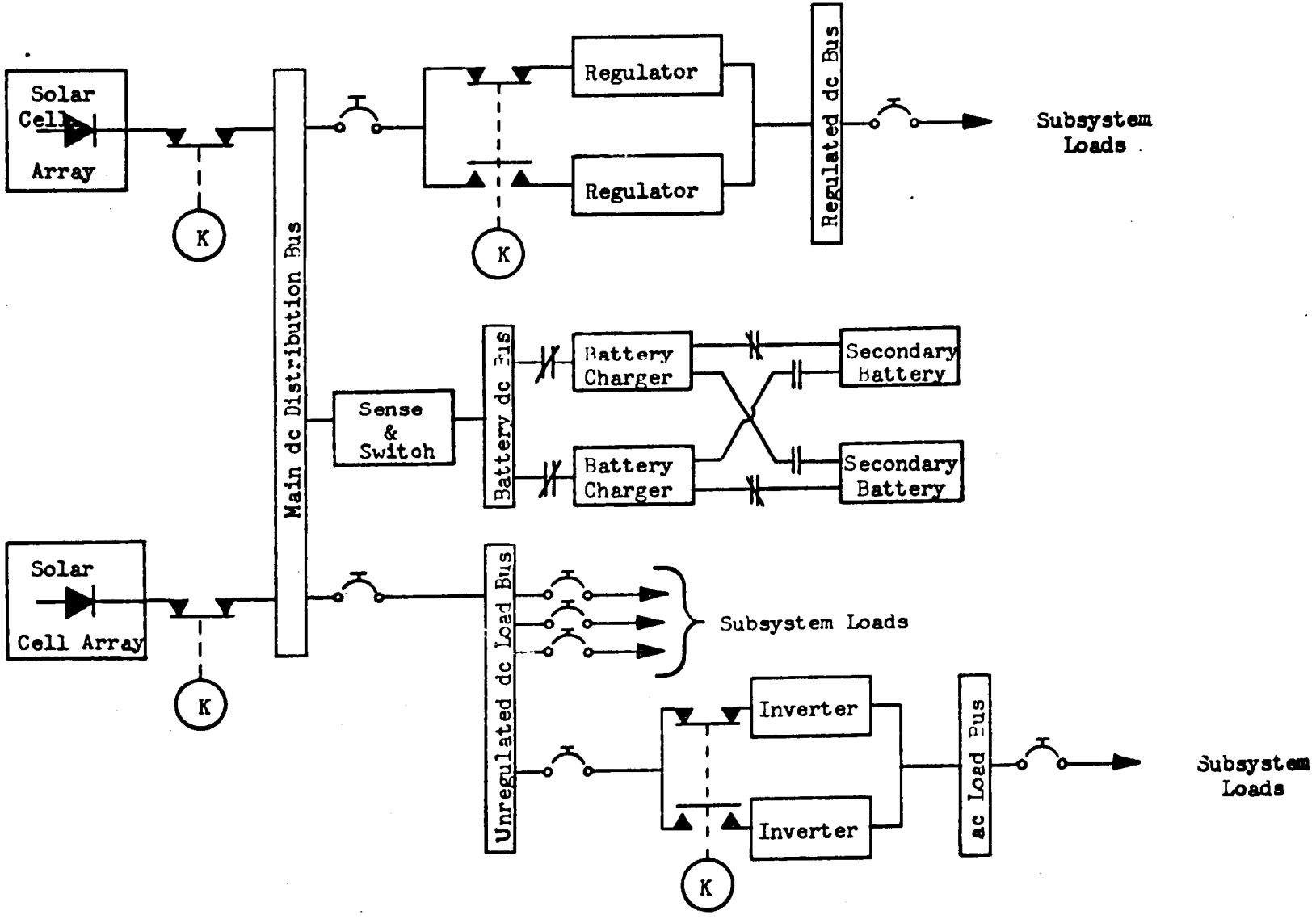

Figure 80. Solar Cell System Functional Schematic

During most of the mission, primary power is supplied by the solar cell panels, and the secondary batters are on a controlled charge cycle. The output of the array will maintain a 24 to 32 volt dc to the unregulated bus. To meet the requirement of the regulated loads, the panel voltage is regulated by a non-dissipative d-c voltage regulator to within 27.5 ± 2.5 volts. During this period, the unregulated panel bus also furnishes input power to the battery charging and control system. This system furnishes a controlled charge to the battery and provides control for applying the battery output to or removing it from the unregulated bus during periods of peak loading, shadow eclipse, and eclipse to light cycles. A weight allowance for the latter peak loads and occultation effects is not included in the Weight Summary data (Table 24 and Figures 32 to 36) since they are mission dependent. Methodology for accommodating these conditions is presented in the Ground Rules section.

Weight Scaling

Solar cell array weights are based on data shown in Table 42 which provides the component breakdown. A 4-mil cell was assumed with improvements as shown in Table 41. The resulting improvements are as given in Table 43; i.e., a 4-mil cell with 11.7 percent efficiency results in 1.1 times the power output of the 12 mil cell at 10.5 percent air mass zero (AMO). Table 44 provides a power output summary for different solar distances and associated temperatures.

Fuel Cells

Many types of fuel cells are possible. The present stages of development range from theoretical systems, through demonstration models, to practical systems. The fuel cell electrochemical system which was evaluated and analyzed for this study is hydrogen-oxygen, with alkaline electrolyte and passive or inert separation material. It is clearly the most advantageous system for general spacecraft use since hydrogen/oxygen is very nearly the most energetic of all electrochemical systems and its chemical product is a continuous stream of fresh drinking water. Although several electrochemical systems can potentially provide more electrical energy per unit weight of reactants, disadvantages have limited the extent of research with such systems. A typical example is the hydrogen-fluorine system which has potentiality far greater electric energy output on a weight basis; however, its chemical product is hydrogen fluoride, a hazardous chemical requiring special handling procedures.

Reference System

The Allis-Chalmers 200 watt and 2.0 kilowatt fuel cells represent the second generation Bacon-type (or modified Bacon-type) porous electrode-alkaline electrolyte-cryogenic hydrogen and oxygen fuel cell. These fuel cells are expected to be fully qualified for general spacecraft use before 1970.

Table 44. Power Output Summary

A.U.	Panel Equilibrium Temperature (°F)	Power Output Present (12 Mils) Watts/ft^2	Watts/ft^2 1980 - 2000	
			8 Mils	4 Mils*
0.70	209	14.1	16.2	15.5
1.0	96	9.7	11.1	10.65
1.2	46	7.5	8.6	8.22
1.5	-10	5.2	5.95	5.72
1.65	-33	4.2	4.81	4.61
2.2	-84	3.0	3.44	3.3

*Used in Weight Summary

Redundancy:

Meteoroids; ≤1.8 AU; no allowance

>1.8 AU; 100 percent replaceable panel

Radiation Degradation; 5 percent total degradation per year based on:

a. 1.5 percent/year reliability allowance

b. 5 percent/year having been used in previous studies and which may be conservative for lithium doped cells

Power Conditioning; 100 percent redundancy for one year missions and 5 percent/year increase for mission > 1 year.

Since power ratings considered in this study are in the 1 to 20 kilowatt range, (PEM), the 2.0 kilowatt cell is more applicable, and is selected as representative of the best state-of-the-art system for the 1970 period. It is expected that modifications and improvements of this type fuel cell will represent the best state-of-art system in the post-1980 period. Therefore, estimated improvements resulting in lighter cells, accessories, and fuel tanks are based on this second-generation system.

Interrelated subsystems comprise the Allis-Chalmers 2.0-kilowatt fuel cell power plant (FCP):

1. Fuel cell stack (FCS)

2. Reactant conditioning and control subsystem (RCCS)

3. Thermal conditioning and control subsystem (TCCS)

4. Moisture removal subsystem (MRS)

5. Water recovery subsystem (WRS)

6. Electrical monitoring and control subsystem (EMCS)

7. Instrumentation

8. Canister and support

Operation and Construction of Basic Cell

In any fuel cell system, the power producing element is the individual cell. The fuel cell is a static energy converter which produces dc electrical energy, with water and heat as by-products, by the electrochemical combination of hydrogen and oxygen. The simplified fuel cell reactions are as follows:

Anode

$$H_2 + 2\ OH^- \longrightarrow 2\ H_2O + 2e$$

Cathode

$$1/2\ O_2 + H_2O + 2e \longrightarrow 2\ OH^-$$

Overall reaction

$$H_2 + 1/2\ O_2 \longrightarrow H_2O + \text{electrical energy} + \text{heat}$$

Electrical energy is produced and reactants are consumed only when current flows in the external load.

The Allis-Chalmers cell consists of two porous electrodes separated by an asbestos capillary matrix which contains an aqueous potassium hydroxide (KOH) electrolyte. The anode (H_2 electrode) is constructed of porous nickel activated with a platinum-palladium catalyst, while the cathode (O_2 electrode) is constructed of a high-surface area silver. The active area of each electrode is approximately 0.20 square feet. Slotted magnesium electrode support plates, adjacent to the electrodes, provide the cavities for distribution of the hydrogen and oxygen reactant gases over the surfaces of the electrodes and for removal of the water vapor. In addition, the support plates serve as electrical current collectors and as thermal cooling fins for removal of waste heat.

Fuel Cell Stack

The fuel cell stack (FCS) is constructed by connecting cell sections in series to provide the nominal 29 volt dc terminal voltage for the desired average power. Figure 81 is a schematic diagram of the FCM. The complete fuel cell electric power system is shown in Figure 82.

System Design

Established design practice is to form fuel cell systems from standard modules. The main advantages are good predictability of performance for the intended system and accurate cost planning, since mass production techniques can be used. The design of a typical fuel cell entails postulation of a logical matrix of combinations and then determination of voltage regulation and system reliability. Table 45 illustrates this practice.

Table 45. Design Configuration Matrix; Voltage Regulation and Reliability of Alternative Fuel Cell Configurations

System Configuration of 200 Watt Cells in Electric Parallel	Required Active	Redundant		Voltage Regulation (dc)	Reliability
		Active	Inactive		
A	2		1	22-26.5	0.9928
B	2	1		25-28	0.9933
C*	2	1	1	25-28	0.9993
D	2	2		26-28.5	0.9998

*Configuration used as baseline for weight estimates

Specific Weight

Design aspects of fuel cells and cryogenic fuel storage have been examined to determine where expected improvements will result in lighter weight in the post-1980 period. The Allis-Chalmers 2.0-kilowatt fuel cell and the Apollo Block II cryogenic fuel storage subsystem were used as the reference design. From these subassemblies, specific weight parameters have been obtained, representing a state-of-the-art design for the 1970 period. By examining each subsystem in detail, weight-saving improvements have been estimated for post-1980 and are summarized in Table 46. Weight saving can be expected with improvements in temperature, voltage and current sensors, ampere-hour purge controllers, electric and electronic controls;

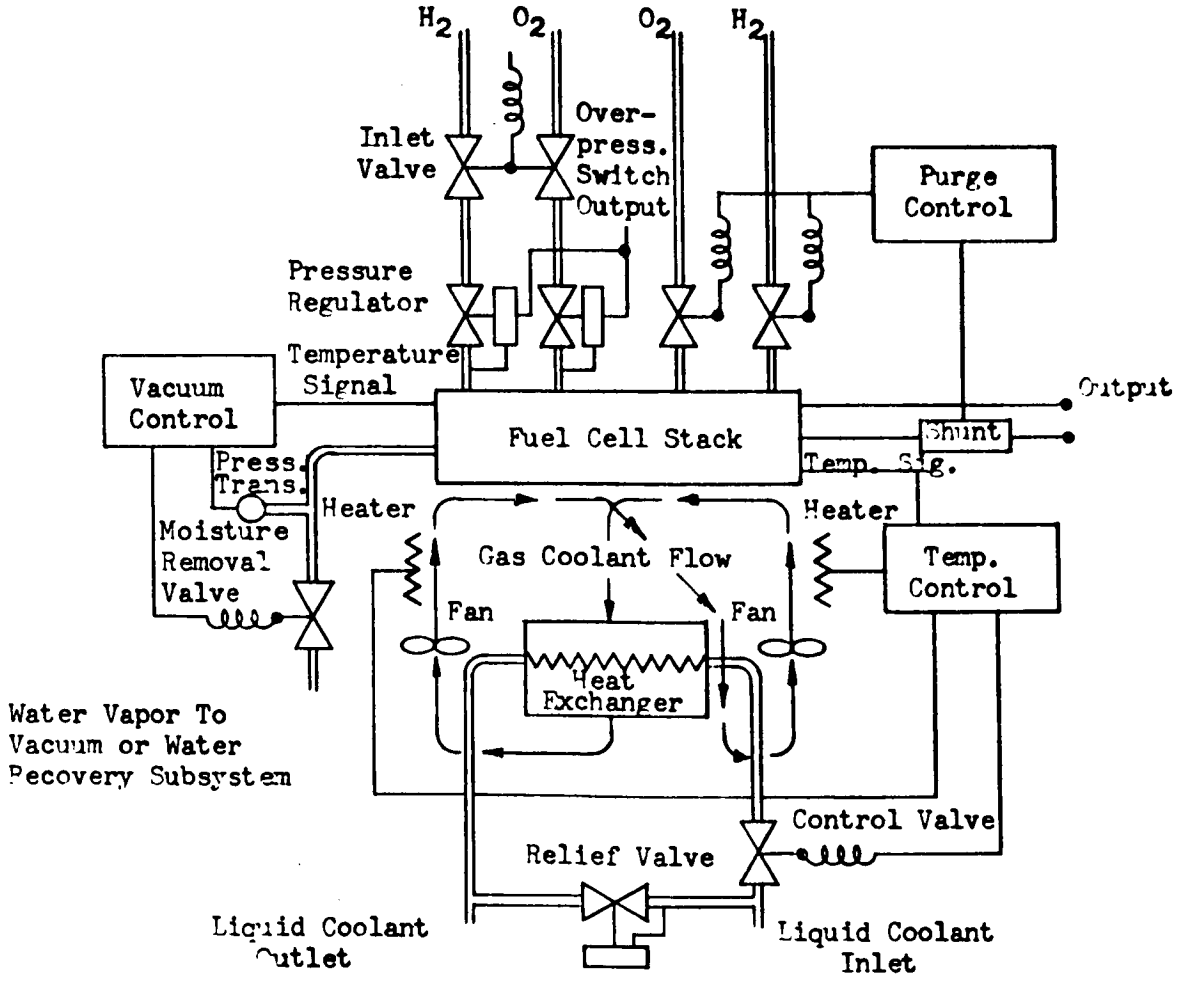

Figure 81. Fuel Cell Module Schematic Diagram

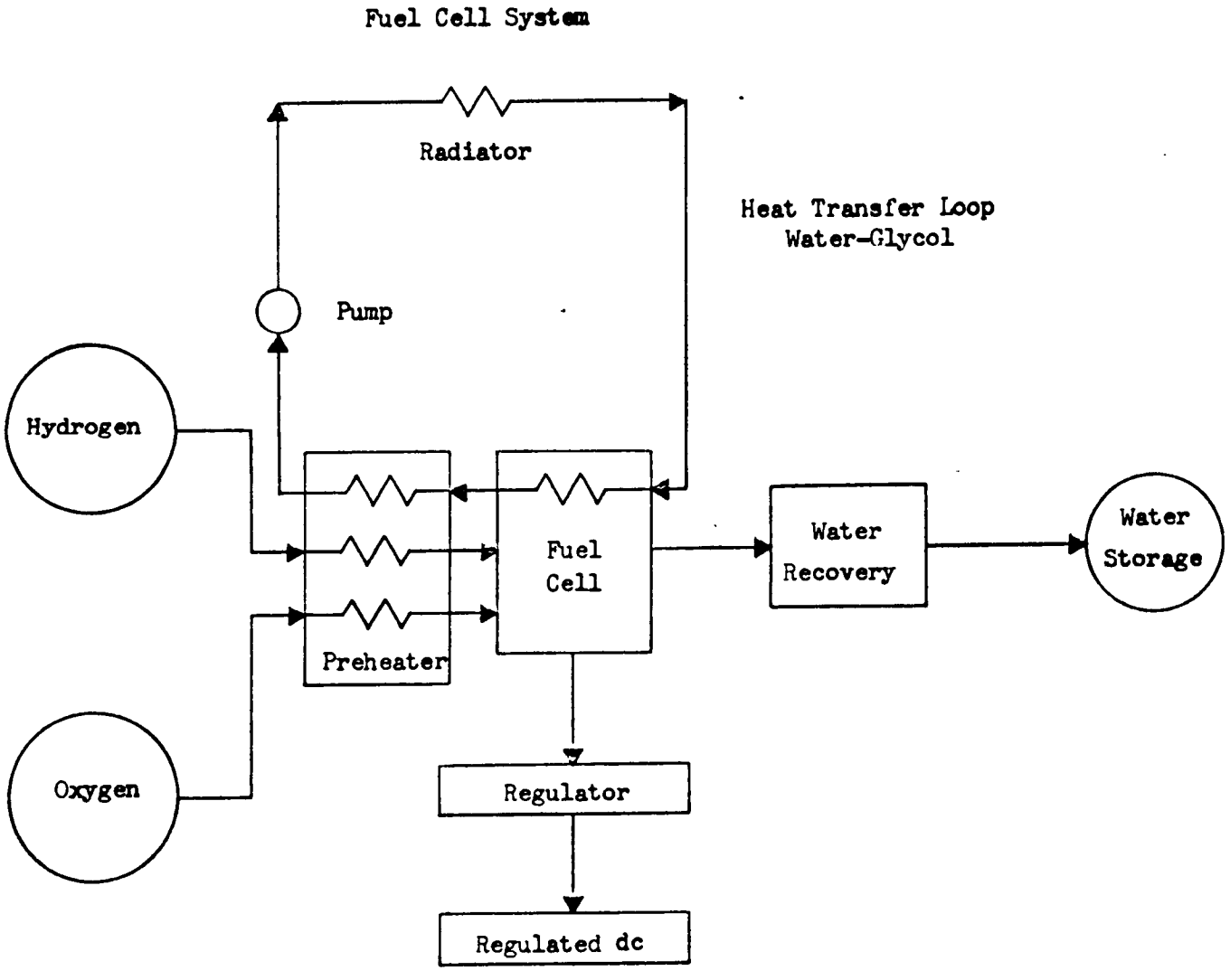

Figure 82. Fuel Cell System Schematic

Table 46. Fuel Cell Specific Weights

Item	1970	1980	1990+
Power output basis for calculations (kW)	1.0	1.0	1.0
Weight of module and accessories as rated (lb) Basis: Allis Chalmers 2.0 kW fuel cell	75	75	75
Weight of module (and accessories) configuration required (lb) to meet reliability criterion of 0.999	225	149	140
Specific weight of hydrogen tanks and accessories. Basis: Apollo Block II tank system (lb/kWe hr)	0.27	0.25	0.23
Specific weight of oxygen tanks and accessories. Basis: Apollo Block II tank system (lb/kWe hr)	0.24	0.22	0.20
Reactant consumption (lb/kWe hr)			
Hydrogen	0.10 ± 0.02	0.10 ± 0.02	0.10 ± 0.02
Oxygen	0.80 ± 0.16	0.80 ± 0.16	0.80 ± 0.16
Peaking battery and charger (postulate 800 Whr/kWe system rating)	100	95	90
Specific weight of reactants, tanks and accessories (lb/kWe hr)	1.41 ± 0.18	1.37 ± 0.18	1.33 ± 0.18
Constraints Relating to No Boiloff Conditions i.e., Insignificant Boiloff			
Fuel tank system maximum ambient temperature °F)	40	40	40
Active service minimum H_2 flow rate (lb/hr tank)	0.06	0.05	0.04
DESIGN GOALS			
Design goal fuel tank redundancy to meet 0.999 reliability criterion (%)	200	100	100

Table 46. Fuel Cell Specific Weights (Cont)

Item	1970	1980	1990+
Average minimum allowable power (sustained 3.0 hr or more), kw	1.2	0.7	0.6
Inactive subcritical storage time duration, days (minimum)	60	90	120
Reliability design goal of fuel cell module configuration	0.999	0.999	0.999
Reliability design goal of fuel cell cryogenic storage system	0.999	0.999	0.999

increased use of integrated circuitry; improved metals and alloys; more highly resistive insulating materials; lighter capacitors; and lightweight design supports and fasteners. Also, expected improvements in module and accessories include increased voltage stability and efficiency with service time; however, these changes will not affect weight.

Expected improvements in cryogenic fuel storage and delivery systems leading to reduced weight are metallurgical improvements in tank shell materials, mechanical design techniques relating to mechanical stress and control of thermal gradients, and improved sealing and welding techniques. Improvements expected to significantly increase cycle life but reduce weight only secondarily are improvements in peaking batteries and chargers; better construction materials for separators, electrolytic combinations, wetting agents; refined production processes relating to all parts; and integrated circuitry in voltage sensing and control devices. Also, projected improvements that will have a still smaller effect on weight include reduced fuel storage heat leak and increased mechanical resistance to thermal and mechanical shock.

All constraints governing the fuel cell system specific weight projections are given in Table 46 for a "no boiloff" system (including tank insulation weights).

Weight Scaling Factors

Specific weight parameters as summarized in Table 46 can be fitted into an analytic linear expression as:

$$\frac{M_s}{P} = (M_o + B) + M_T T$$

M_s = Fuel cell system weight (lb)

P = Power demand average (kWe)

T = Time duration of active service (may be intermittent) (hr)

M_o = Specific module (and accessories) weight (lb/kWe)

B = Peaking battery and charger specific weight (lb, kWe)

M_T = Specific weight of reactant tankages (lb/kWe hr)

For the time periods listed, and based on Table 46, the weight scaling function becomes

$$1970; \quad \frac{M_s}{P} = 325 + (1.41 \pm 0.18)\ T$$

$$1980; \quad \frac{M_s}{P} = 244 + (1.37 \pm 0.18)\ T$$

$$1990+; \quad \frac{M_s}{P} = 230 + (1.33 \pm 0.18)\ T$$

For the post-1990 time period, system weights are projected for active service durations of 2, 10, 30, and 60 days and are used as nominal values for the 1980-2000 time period (Table 47).

Table 47. Fuel Cell Weight

Active Service Days	1 kWe	10 kWe	20 kWe
2	295 lb 135 kg	2,950 1,350	5,900 2,700
10	550 250	5,500 2,500	11,000 5,000
30	1,185 540	11,850 5,400	23,700 2,370
60	2,150 975	21,500 9,750	43,000 lb 19,500 kg

Chemical-Dynamic Power Systems

There is continuing funded support by NASA (MSC) on the pulsed turboalternator being developed by TRW, Inc. It is intended to use the power system as space emergency power and for short-time durations, typically less than one week, following a long inactive storage time. A typical example of emergency power relates to a unit which can run on fuel cell reactants while fuel cells are either shut down or only partially operative. The second typical use can be for an orbiting mission around a remote planet such as Jupiter or Saturn. Cruise time to Jupiter might be two to three years. During the cruise period, spacecraft power can be supplied by an RTG, typically 500 Watt (electrical) or multiples thereof. After orbit has been established, the turboalternator can be started to provide sufficient power to observe planet characteristics, store and compute information if necessary, and communicate results to Earth stations at a high bit rate.

Chemical-dynamic systems prototypes, including reciprocators, turbines, cryocycles, and sterling cycles, have been surveyed. Of these, the pulsed turbine is expected to be space-qualified by 1980 with characteristics essentially as described in this report. Therefore, only the pulsed turboalternator is examined in detail.

Basic Components

The power generation system shown in schematic form in Figure 83 consists of an alternator directly driven by a single stage, full-admission impulse turbine. The combined shaft assembly is supported on a ball bearing between the turbine wheel and alternator and a roller bearing on the opposite end. The bearings and seal are lubricated and the alternator is cooled with turbojet lubricating oil.

Power characteristics of the 6.0 kwe representative system design are given in Table 48.

System Operation

The turbine is driven in an open cycle by hot gas produced in the gas generator. The gas is the product of reaction of a fuel, 50-50 mixture of anhydrous hydrazine and UDMH, with an oxidizer (N_2O_4). The fuel and oxidizer are stored as liquids in pressurized tanks. During a gas pulse, metered flows of these liquids are admitted to the gas generator by opening the bipropellant solenoid valve. The liquids enter the gas generator through the injector which has been calibrated to pass the required weight flows of fuel and oxidizer. The injector causes the liquids to mix in the gas generator where they react hypergolicly.

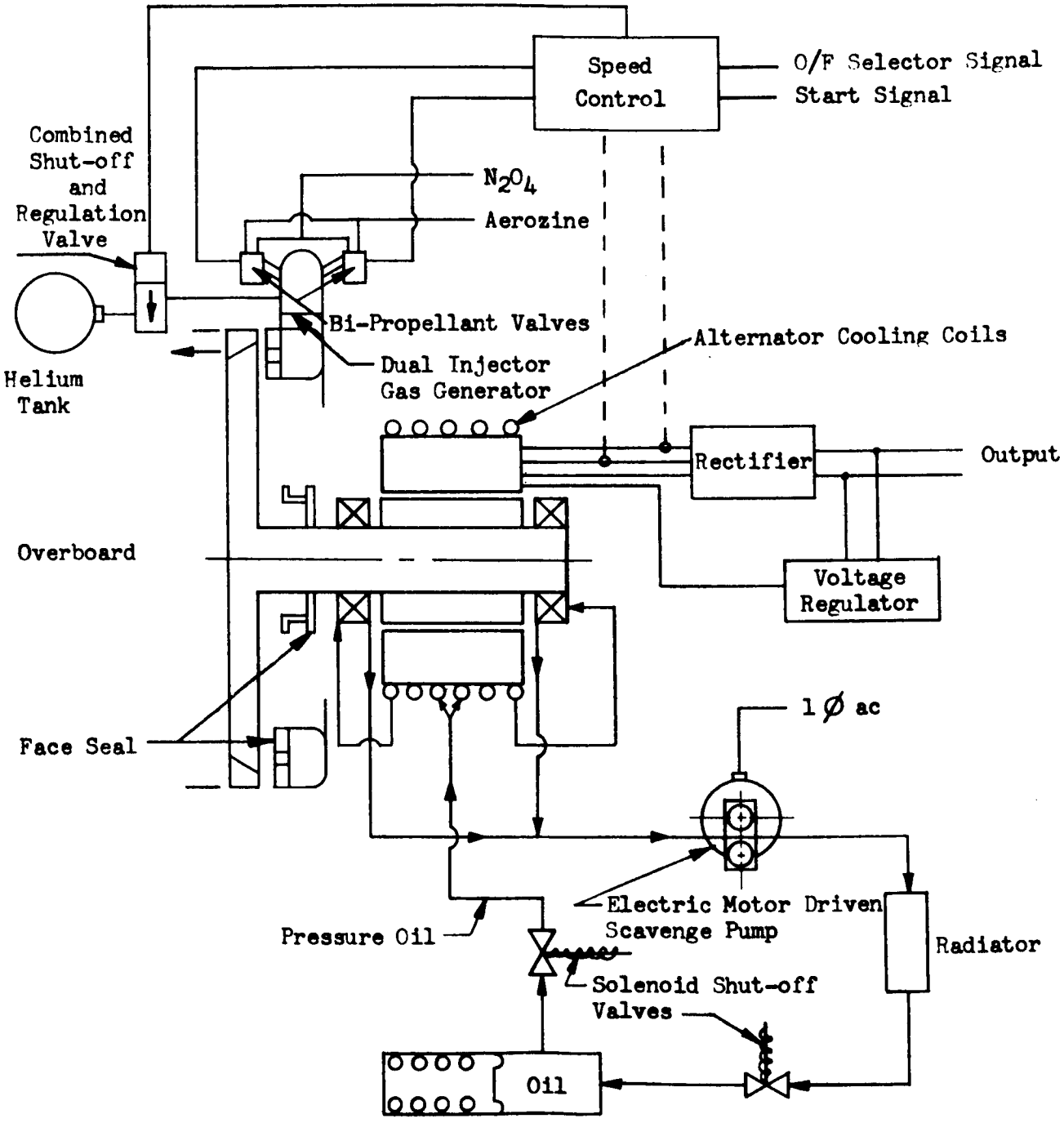

Figure 83. Turboalternator System Schematic

Table 48. TRW Pulsed Turboalternator (6.0 kwe) Power Characteristics

Power output (dc)	6.0 kWe
Time, active	100 hr
Specific reactant consumption	11.0 ± 1.0 lb/kWe hr
Reactant consumption	1100 lb/kWe (100 hr operation)
Reactant tanks, (O/F = 1.6) 6.85 ft^3 each	13.7 ft^3/100 kW hr
Reactant tanks, weight, lb ea	160 lbs/100 kW hr
Turboalternator and Accessories	235 lb (for a 6 kWe)
Turbine Blade Temperature	1300.0 ± 100°F

The injector has been designed to admit fuel and oxidizer at either of two oxidizer/fuel (O/F) ratios. This dual design permits operation at O/F = 0.9 through one set of injector orfices or at O/F = 2.7 through another set of injector orifices. Therefore, two bipropellant valves are needed, one at each O/F ratio. This two-valve design is required only for laboratory research. The reference design used for weight analysis in this study has one set of valves to operate at O/F = 1.6 so that equivalent volumes of oxidizer and fuel are required (hence, only one size of reactant storage tank is required).

The hot gas produced has a high energy level at a high temperature. The adiabatic flame temperatures at 100 psia have been calculated to be 4235 R at O/F = 0.9 and 5520 R at O/F = 2.7.

The pulsing sequence is regulated by the speed control which controls the length of coast time, or the time between pulses. The speed control senses alternator output frequency. When it senses that the speed has decreased to a predetermined set point, it causes the bipropellant valve to open for 0.2 seconds allowing combustion to take place. The turboalternator speed increases during this pulse period, then decreases during the coast period to the low speed set point.

The voltage regulator senses alternator output voltage. It controls alternator field excitation to maintain constant output voltage over the speed variation.

Lubrication and cooling are accomplished by a closed loop oil system. Bearings and seal are fed by an oil spray. The alternator is cooled by oil flowing through the annular jacket. The bearing and seal cavities and alternator jacket are scavenged by a pump which sends the oil through a radiator to a pressurized reservoir. The oil passes from the reservoir to the bearing and alternator inlets at 25 to 30 psia. A carbon face seal located between the turbine wheel, and ball bearing maintains a barrier between the alternator and bearing cavity, and the external vacuum environment.

Heat rejection from the system is accomplished in two ways. The oil system takes heat from the bearing, seal, and alternator areas as previously described. In addition, a large portion of the heat rejection is accomplished by radiation from the turbine and nozzle-scroll assembly.

The major portion of the heat removal is by direct radiation from the turbine scroll which operates at a temperature up to 1500 F. Turbine blade and disk cooling is also accomplished by direct radiation to space, or by radiation to some other surface in the case of a submerged installation.

The output of the alternator is three phase 23 volts RMS line-to-line which is rectified and filtered to 29 volts dc. The alternator is capable of delivering 6 kwe continuously at 29 volts dc.

Specific Weight

The 6.0 kwe reference design is a carefully scaled design based on a laboratory construction of 3.0 kwe rating.* Spherical reactant storage tanks for this study are scaled models and modifications of these models based on expected future improvements. Design parameters of the reactant storage and delivery system are given in Table 49. The range of storage temperatures is shown in Table 50.

Improvements in the pulsed turboalternator are expected to be primarily mechanical. Improvements in production techniques are expected to result in more reliable turbine and alternator units. Metallurgical improvements may result in stronger, more heat-resistive bearings with less clearance; more heat-resistive turbine blades with higher yield strength and greater fatigue strength; and more reliable reactant storage tanks. Advances in integrated circuitry should result in lighter electric controls and sensors. Direct current converters should become lighter as a result of advances in semiconductor technology and electrical packaging techniques. The aforementioned expected improvements have been applied to each subsystem of the reference design for the purpose of estimating specific weight parameters as given in Table 50. Turboalternator and accessories are expected to have a

*3.0 kwe and 6.0 kwe data are available and it is felt that a 1.0 kwe module can be scaled.

Table 49. Mechanical Design Parameters of Chemical-Dynamic Reactant Storage Tank System

Reactant volume (ft^3)	
Oxidizer	6.85 each
Fuel	6.85 each
Rupture strength (psi)	160,000
Safety factor	1.5
Geometrical shape of tank	Sphere
Tank material	Titanium
Expulsion system	Metal bellows
Tank configuration	Two pair (Volume = 27.4 ft^3/ 100 kw hr)
Calculated wall thickness (inch)	0.014
Selected design wall thickness (inch)	0.030
Design goal reliability (single unit)	0.999

moderate decrease in specific weight in the post 1980 time periods. Specific reactant consumption is not expected to improve, since blade and rotor design is already well advanced. Although tank reliability is expected to improve by 1990, weight of complete configurations may not be smaller since it is believed that tank configuration design is well advanced.

Constraints for the chemical-dynamic system are postulated in Table 50. Reactant storage time, reactant temperature, and turboalternator service life are covered. These postulates are based upon present state-of-art technology using the same qualitative techniques which have been applied to specific weight estimates.

Reliability criteria have been postulated for the reactant tank storage and delivery system on the basis of state-of-art technology (Table 50). Pulsed turboalternator state of art is laboratory technology. There has not been enough active service experience under real or simulated space conditions to provide a mathematical basis for determining reliability. However, there are indications that since support of pulsed turboalternator development is continuing, reliability will be sufficiently high by the post-1990 year to use them on planetary missions.

Weight Scaling

Based on a modular approach to supplying power greater than 1 kwe, a linear function can be established for weight scaling. This is consistent with the present state of the art wherein uncertainties in component design do not allow projections of specific weight improvements with power level. The scaling function is

Table 50. Chemical-Dynamic Specific Weight Parameters

Item	1970	1980	1990+
Power output (kWe)	As Required	(1-10)	
Specific weight of turboalternator and accessories, sized to peak power. Postulated as twice average power (lb/kWe)	39.0	35.0	35.0
Specfic reactant consumption (lb/kWe hr)	10.9	10.9	10.9
Specific tank and accessories weight (lb/kWe hr)	1.60 ± 0.15	1.60 ± 0.15	1.60 ± 0.15
Specific weight of reactants, tanks and accessories (lb/kWe hr)	12.5 ± 0.15	12.5 ± 0.15	12.5 ± 0.15
Constraints			
Reactant storage time max. (yr)	5.0	5.0	5.0
Allowable range of reactant storage tank temperature (°F)	40-100	40-100	40-100
Turboalternator and accessories active service life (yr)	0.1	0.5	0.5
Reliability Criteria Turboalternator (Present State of Art Technology Is Laboratory Technology)			
Reactant tank storage and delivery system	0.995	0.995	0.999

$$\frac{M_s}{P} = M_o + M_T T$$

where

M_o = Weight of turboalternator and accessories (lb)

P = Average power (kWe)

M_T = Specific weight of reactants, tanks and accessories (lb/kWe hr)

T = Active service time (while delivering power), hr

M_s = Chemical-dynamic electric power system weight (lb)

For the time periods listed,

1970; $\frac{M_s}{P} = 39 + 12.5\ T$, lb/kWe

1980; $\frac{M_s}{P} = 35 + 12.5\ T$, lb/kWe

1990+; $\frac{M_s}{P} = 35 + 12.5\ T$, lb/kWe

For the post-1990 period, system weights are projected for active service durations of 2, 10, 30, and 60 days and are used as nominal values for the 1980-2000 time period (Table 51).

Table 51. Chemical-Dynamic System Weight

Active Service Days	1 kWe	5 kWe	10 kWe
2	600 lb 272 kg	3,000 1,360	6,000 2,720
10	3,035 1,375	15,175 6,900	30,350 13,750
30	9,035 4,100	18,070 8,200	90,350 41,000
60	18,035 8,200	36,070 lb 16,400 kg	

Batteries

Primary Electric Storage Batteries

Today's silver-zinc primary battery has a typical energy density of 110 to 220 Watt-hours per kilogram depending on temperature and discharge rate. Higher specific power batteries have been produced in laboratories, but they are not yet available. The best that can be hoped for is a 20 percent improvement in specific power.

Primary batteries have short wet stand-time and have to be activated before use. In this study, manual activation by the crew is assumed. Fifteen percent of the battery weight is assumed to be electrolyte. Electrolyte storage container weight is considered negligible. Specific weight ot the assumed primary battery is 220 Watt-hours per kilogram. Primary batteries are considered only for short missions. In this study no allowance is given to storage caused degradation after activation. Also, no redundancy is considered. Projected weights are given in Table 52.

For the time period of 1990 to 2000, other primary batteries with energy densities of 500 Watt-hours per kilogram or more may become available. These are the zinc-oxygen, sodium-sulphur and other high-energy-density systems now under development. Due to lack of data, they are not considered here.

Table 52. Silver-Zinc Primary Battery Weights

Mission Mission	Component	Weight for 28-volt System (kilograms)		
		2 kWe	5 kWe	10 kWe
2-day	Battery cells	430	1,080	2,160
	Battery container	30	60	120
	Interconnecting hardware	30	75	150
	Total	490	1,215	2,430
10-day		2,430	6,075	12,150

Silver-Zinc Secondary Electric Storage Batteries

Silver-zinc electric storage battery cells presently have up to 175 Watt hours per kilogram energy density. For the time period considered, this energy density is used with the following limitations: activated battery life not to exceed 1 year; weight penalty of 15 percent to account for battery

container and interconnecting hardware; a battery charge rate of C/6 (1/6 capacity); and a battery charger weight of 7.5 kilogram/kilowatt. Based on this for a 6 kilowatt hour battery system, the weight is given in Table 53.

Table 53. Silver-Zinc Secondary Battery Weight

Component	Weight (kilograms)
Cells	34.2 (175 Whr/kg)
Connectors and Container	5.2
Battery Charger	7.5
Total Battery System	46.9 (128 Whr/kg)

With 25 percent depth of discharge, the usable energy density of a typical secondary silver-zinc battery system is 32 Watt-hour per kilogram. Such a battery will be capable of approximately 800 charge-discharge cycles. For other cycle lives, consult Figures 84 and 85.

Silver-Cadmium Secondary Electric Storage Batteries

Secondary storage batteries are considered in connection with solar power systems. They must supply power in planetary orbit while the spacecraft passes through the shadow. They also can be used to supply peak loads. The best silver-cadmium cell today can supply 88 Watt hours per kilogram energy. Allowing a weight penalty of 15 percent for container and interconnecting hardware and considering a battery charge rate of C/6, the battery system specific weight can be determined from a 6 kilowatt system with 25 percent depth of discharge, as given in Table 54.

The specific energy density of this secondary silver-cadmium battery system is 18.7 Watt hours per kilogram. This battery will last 1500 charge-discharge cycles, based on present-day technology. With increased depth of discharge, the number of discharge cycles decreases (Figures 86 and 87). These data are expected to provide a 0.999 reliability for the battery cells.

Battery energy efficiency is a function of operating temperature and charge-discharge rate. At temperatures between 60 F and 80 F, and considering a maximum of 33 percent discharge with a charge rate less than 1.5 of discharge rate, an energy efficiency of 77 percent can be expected. (This is based on tests conducted on Yardney 15 ampere-hour silver-cadmium cells.) A switching regulator type battery charger was considered. Such a charger

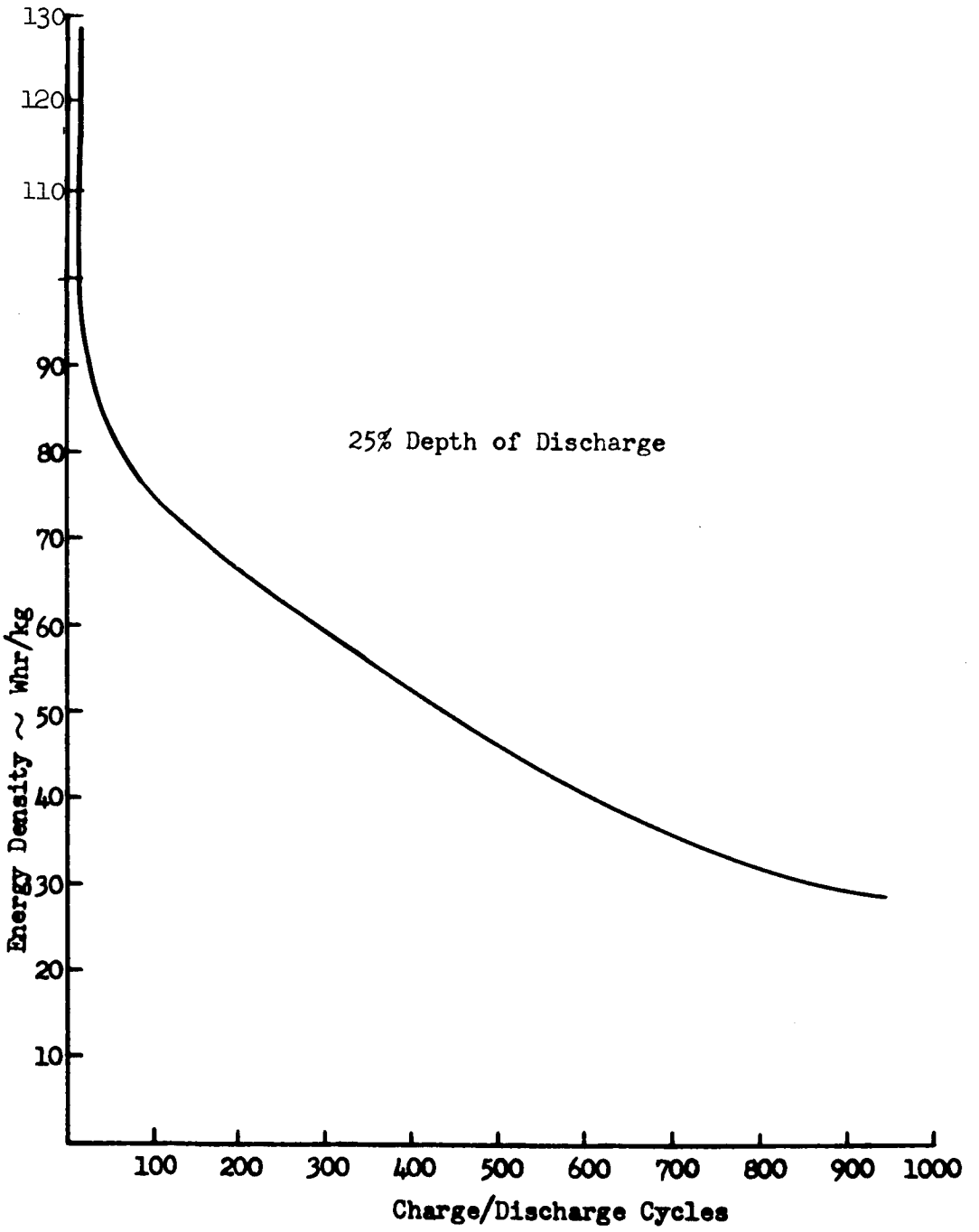

Figure 84. Energy Density for Silver-Zinc Battery Versus Cycle Life Based on Complete 28-Volt Assembly, Including Charger Weight; Battery Charge-to-Discharge Rate Ratio = 1:6

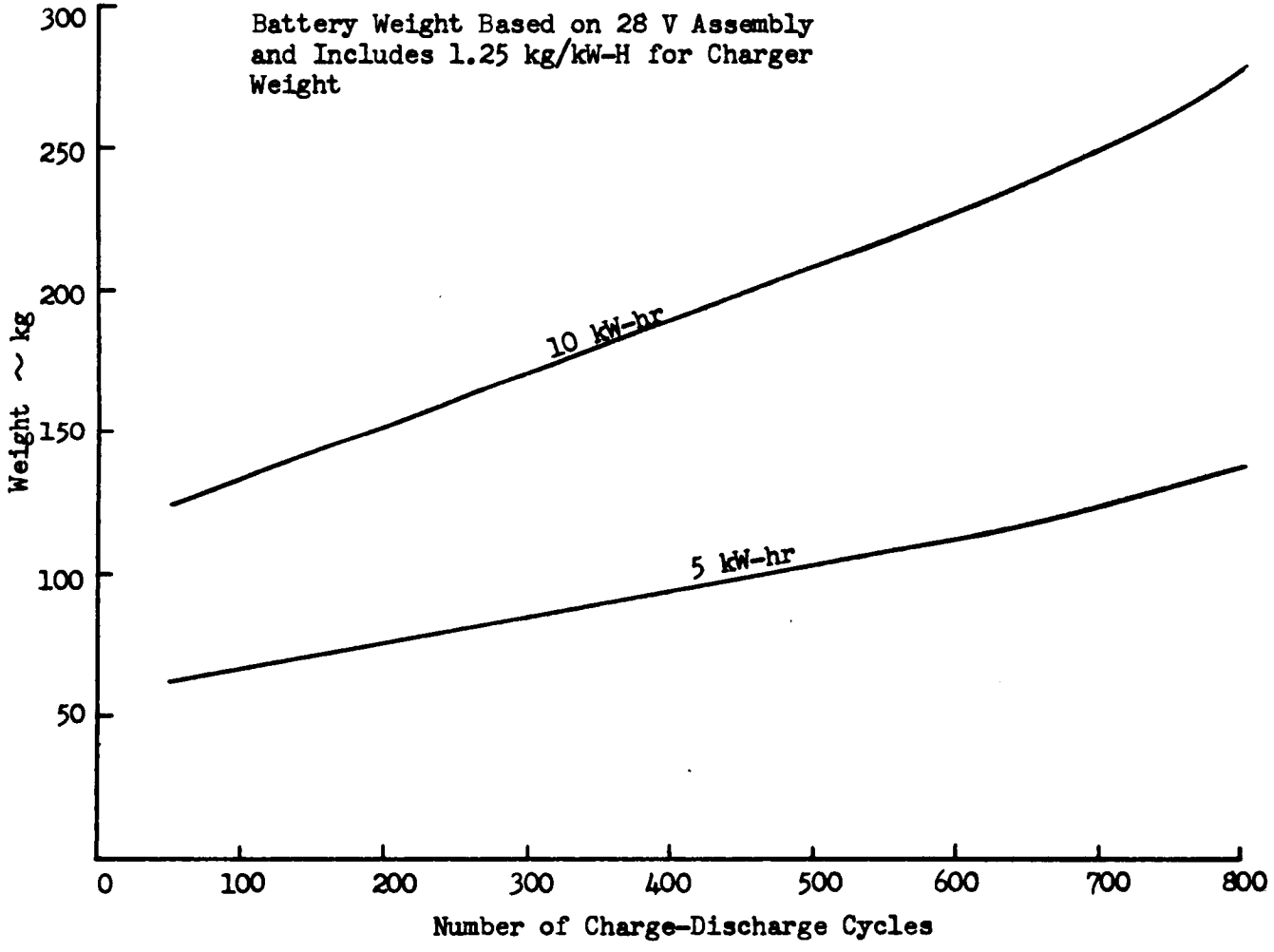

Figure 85. 28-Volt Silver-Zinc Battery System Weight Versus Charge-Discharge Cycles

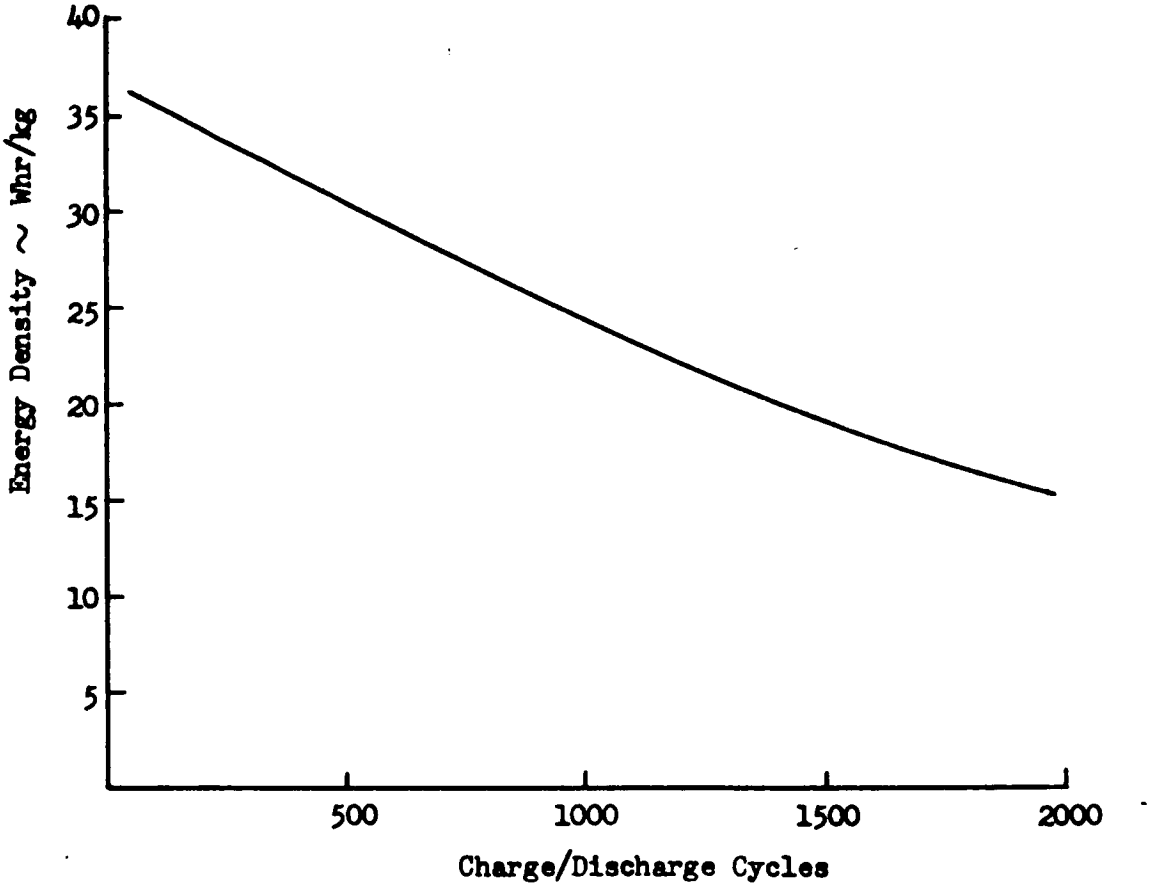

Figure 86. Energy Density for Silver-Cadmium Battery Versus Cycle Life Based on Complete 28-Volt Assembly, Including Charger Weight; Battery Charge-to-Discharge Rate Ratio = 1:6

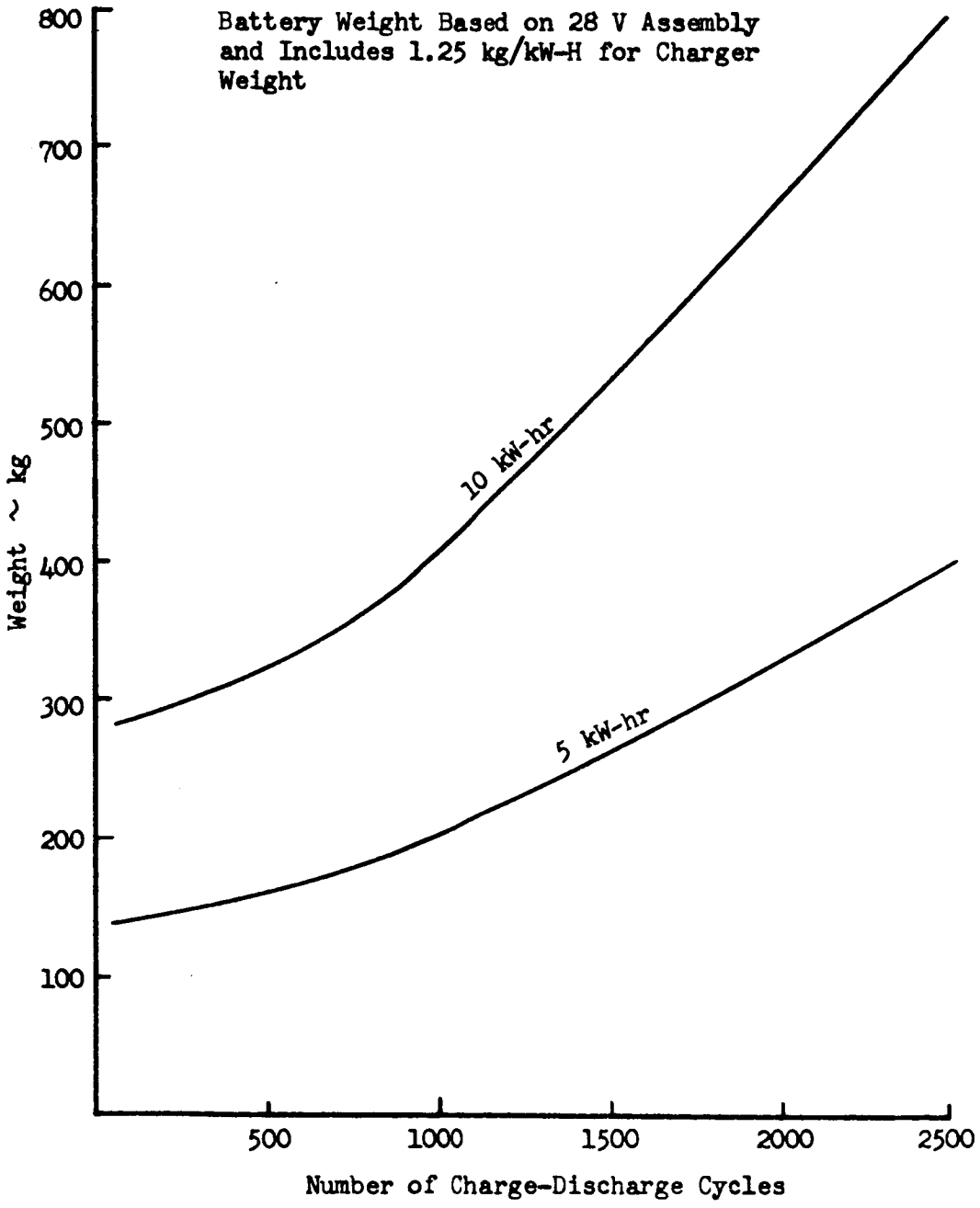

Figure 87. Silver-Cadmium Battery System Weight Versus Charge-Discharge Cycles

Table 54. Silver-Cadmium Secondary Battery Weight (6.0 KWH)

Component	Weight (kilograms)
24 kW hr Cells	273.0 (22 WH/kg)
Connectors and Container	41.6
Battery Charger	7.5
Total Battery System	322.1 (18.7 WH/kg)

can be built today with an efficiency of 92 percent or greater. Thus, the charge-discharge efficiency of the battery-and-charger system will be 71 percent or greater.

Thermionic Converters

Thermionic power subsystems offer a potential for high-performance specific weight. The cesium vapor diode used in these power converters operates efficiently at temperatures in excess of 2200 F. The high operating temperature requirement (Figure 88) is the underlying reason for current limited experience with these devices. Most promising is the solar thermionic converter which requires solar concentrators with close orientation (Figure 89). Isotope and nuclear reactor heated thermionic converters are of cylindrical design with the heat source or heat exchanger fluid surrounded by the emitter, with the converter being cooled from the outside. Development is needed of materials to facilitate containment of the reactor fuel or isotopes at high temperatures. Thermionic diodes are presently being tested to demonstrate a life expectancy of 10,000 hours. For longer missions, this life expectancy is not sufficient and redundant standby power systems with an external heat source should be considered. Based on todays state of the art and the development effort spent on these systems, their availability is not assured before the end of the time period considered.

General Electric is developing the STAR-R reactor thermionic power plant with an in-pile converter design. This power system incorporates a nuclear reactor fueled by uranium oxide or uranium carbide controlled by beryllium reflectors. Since most of these data and related publications are closely controlled, only approximate information has been obtained.

Two general GE STAR (space thermionic auxiliary reactor) systems are under consideration; STAR-R applicable to 10 to 100 kwe, and STAR-C application to 100 kwe to 100 mWe. The reactor has a fast UO_2 fueled heat source. Power conversion is effected by tubular converter diodes with Cesium gas in the 0.005 to 0.010 inch gap, and tungsten, tungsten-rhenium, and molybdenum are used as refractory metals. The approximate specific

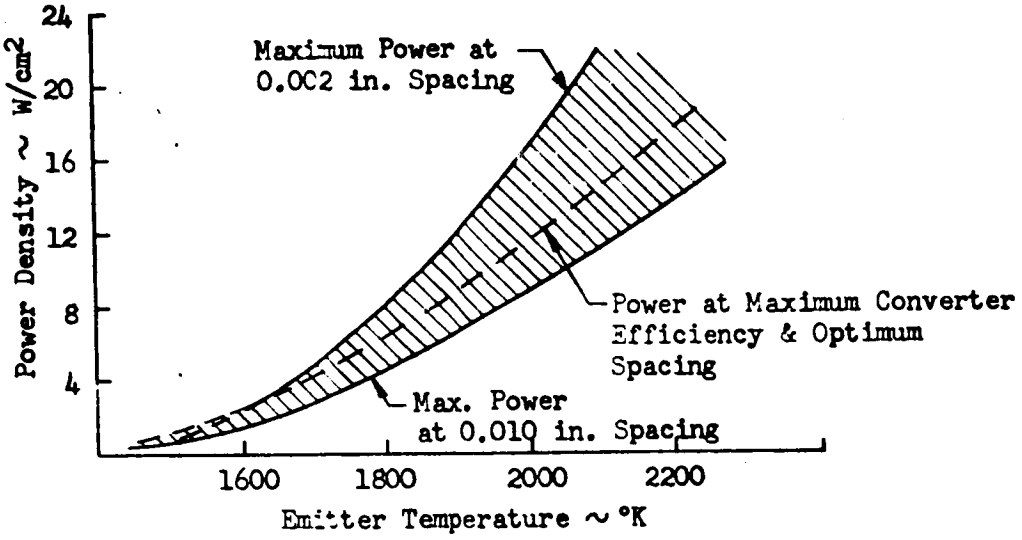

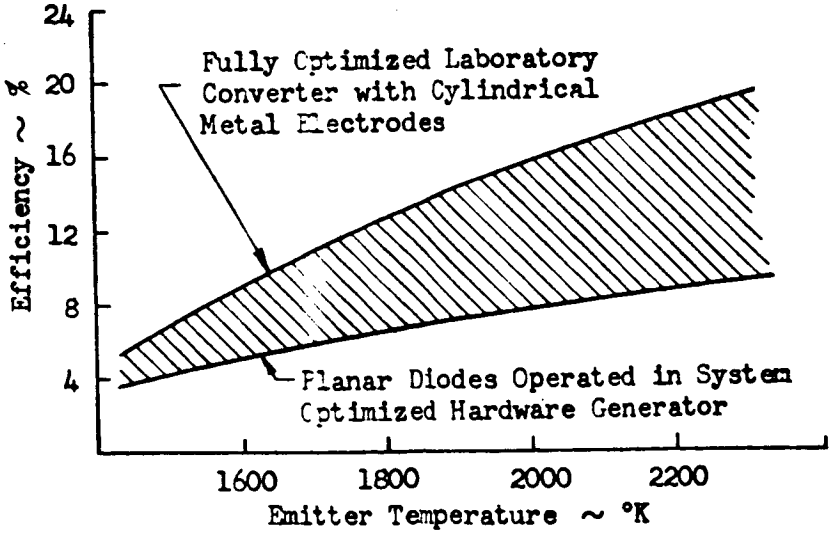

Figure 88. Thermionic Converter Power Densities and Efficiencies

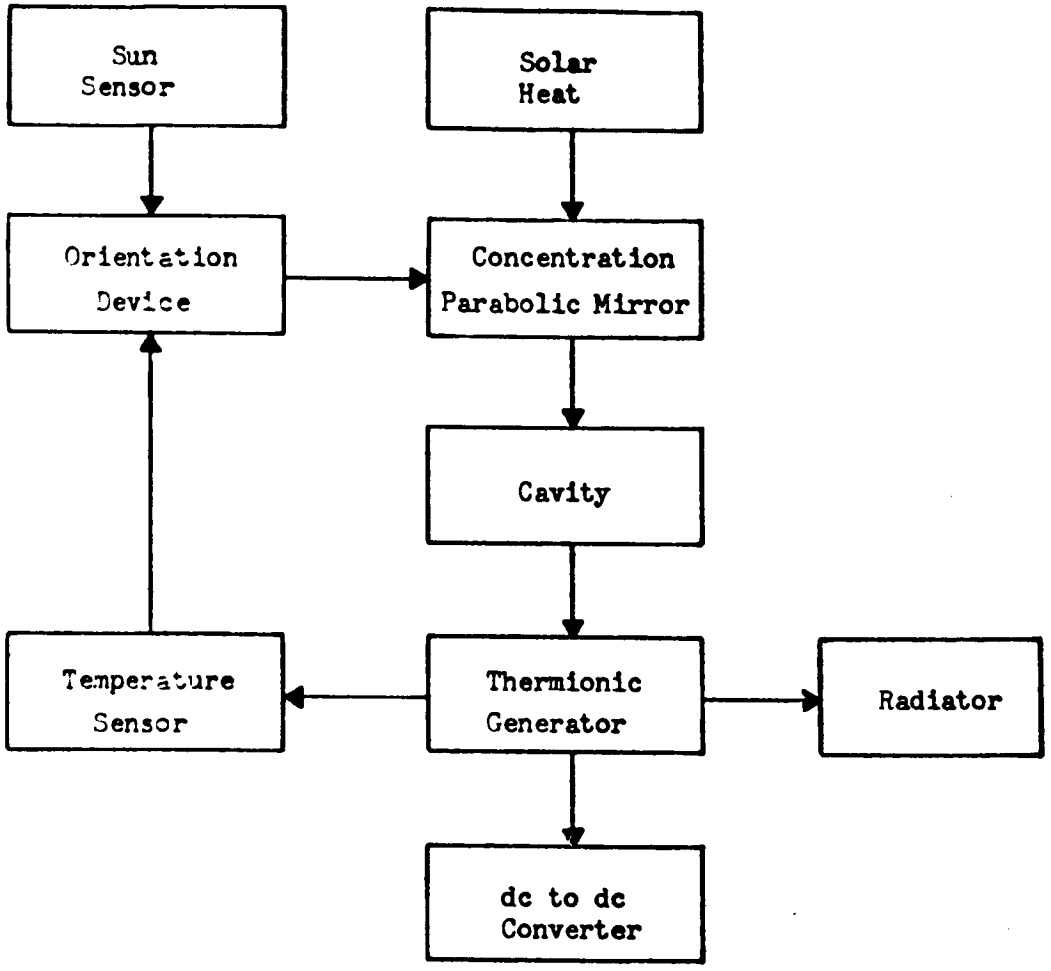

Figure 89. Solar Thermionic Power System

weight, excluding radiation shielding for STAR-R is 90 kg/kw (200 lb/kw); for STAR-C, 22.7 kg/kw (50 lb/kw). Overall efficiency is 10 percent. Emitter temperature is 1600 to 1800 C; collector temperature is 700 C. Reliability figures are not available at this time, and it appears that a large amount of development work must still be done before any confidence in this power system can be established. For this study, a reliability of 90 percent for 10,000 hours has been assumed. Since the temperatures are very high, material technology advances are required, and may not be achieved by the target dates. The power system weights based on STAR-R technology are given in Table 55.

Table 55. Thermionic Power System Weights Based on STAR-R Technology

Rating	20 kw	50 kw
System weight	1800 kg	4500 kg
Standby systems (2)	3600 kg	9000 kg
Radiation shield	5900 kg	11700 kg
Boom and cables	600 kg	1200 kg
1-year mission weight	11900 kg	26400 kg
One additional standby system for each additional year of mission		
2-year mission	12700 kg	30900 kg
3-year mission	14500 kg	35400 kg
4-year mission	16300 kg	39900 kg
5-year mission	18100 kg	44400 kg
Note: The high weight values are due to present day integrated heat source - converter design.		

While nuclear reactor and isotopic thermionic systems are not expected to be available before the end of the time period considered, solar thermionic systems may be available sooner. Diodes as shown in Figure 90 were tested for several thousand hours. As seen in Table 56, the converter weight contributes relatively little to the overall system weight. The relatively small converter modules can be easily replaced and require little redundancy for high reliability. These systems require highly accurate orientation. The maximum weight penalty for orientation using 7 kg per 10 square meter mirror area would be as given in Table 57.

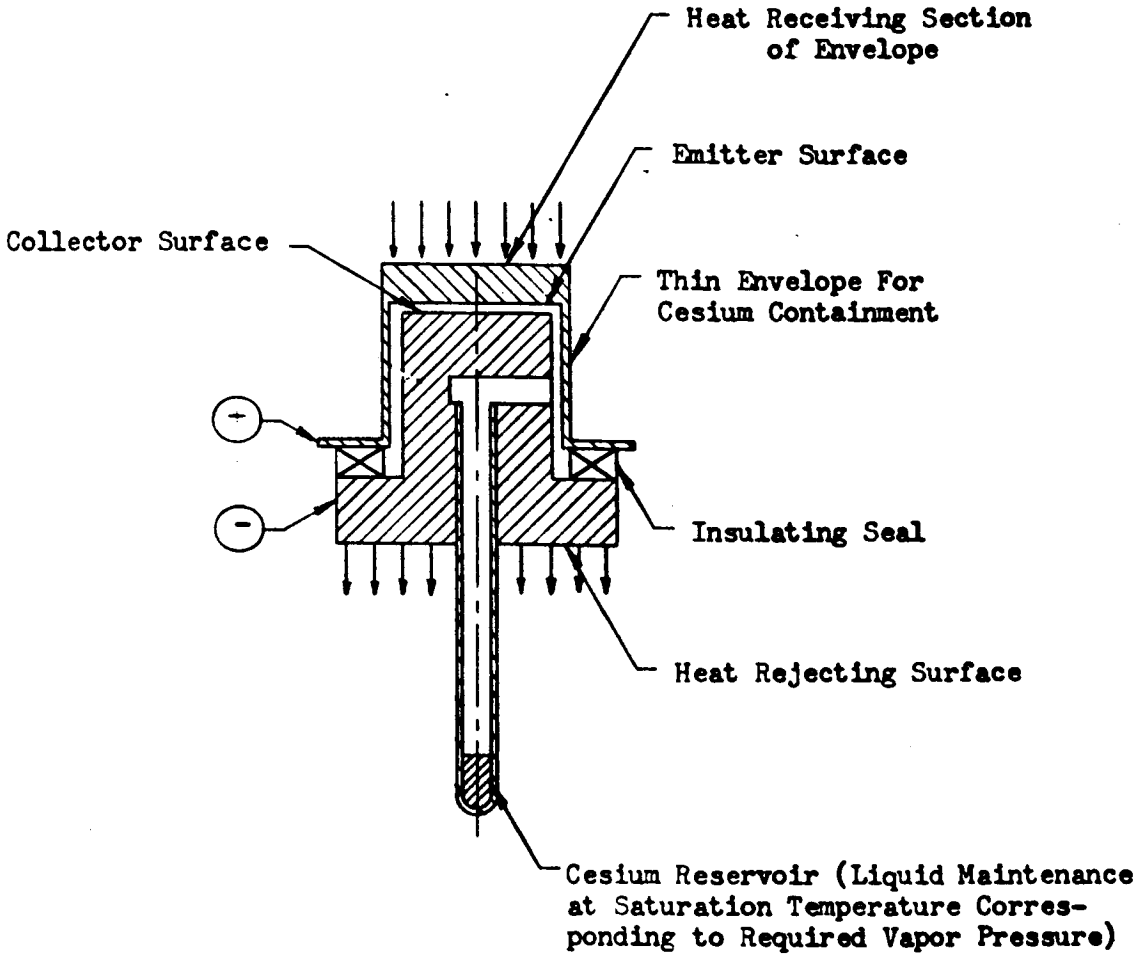

Figure 90. Basic Planar Diode Thermionic Converter Structure

Table 56. Solar Thermionic Generator at 1 AU
Consisting of 225 Watt Modules

	225 Watt	2.5 kw	5 kw	10 kw	20 kw
Mirror diameter	2.8 meter				
Weight with berillium concentrator	5.2 kg				
Support	3.6 kg				
Converter	1.3 kg				
Structure	2.6 kg				
Thermal insulation	3.4 kg				
	16.1 kg	175 kg	350 kg	700 kg	1400 kg
DC to DC converter	3	23	40	80	160
Controls	2.4	18	30	60	120
	21.5 kg	216 kg	420 kg	840 kg	1680 kg
Add 30% redundancy for 1-year mission	4.9 kg	53	105	210	420
	26.4 kg	269 kg	525 kg	1050 kg	2100 kg
Add 100% redundancy for 2-year mission	16.1	175	350	700	1400
	37.6 kg	391 kg	770 kg	1540 kg	3080 kg
Add 200% redundancy for 3-year mission	53.7	566	1120	2140	4480
Add 300% redundancy for 4-year mission	69.8	741	1470	2840	5880
Add 400% for 5-year mission	85.9	916	1820	3540	7280

Table 57. Maximum Weight Penalty for Mirror Orientation

Mission Duration (years)	Weight Penalty (percent of mirror weight)
1	15
2	26
3	34
4	40
5	45

CONCLUSIONS

Mission Module Power Sources

Applicable auxiliary power system candidates were selected for comparison. Two energy sources (nuclear and solar) were considered for the mission module with many combinations of power conversion designs. As a result, several conclusions can be made.

Nuclear reactors should not be considered at power levels below about 15 kWe. When compared to radioisotopes at low levels, the reactors prove to be heavier (because of higher levels of radiation) and more complex. Using a reactor necessitates separation of source and crew for distances in the order of 50 to 125 feet. Reactor shutdown is required for any spacecraft operations outside the protection of a shadow shield.

It can also be stated that solar concentrators should not be included in any further trade-off study. Concentrators require a higher degree of orientation accuracy when compared to solar cells for the same power degradation and have a very large area requirement. As a solar powered generator, photovoltaic systems generally can be used wherever concentrators might apply. The relative state of development and weight comparisons show a major advantage to solar cells.

Thermionics can also be excluded for 1980 missions. However, ultimately the power system converters may be thermionic in design, and present indications are that the technology will permit hardware by the year 2000.

Candidate systems which should receive major attention (for power range of 2 to 15 kWe) can be limited to radioisotopes combined with dynamic conversion (Rankine and Brayton cycle), thermoelectrics and solar cells.

Converters

Brayton Cycle

This conversion offers the highest overall efficiency. The major disadvantages are its high turbine inlet temperature and large radiator area requirements. For reference designs the highest temperature in the cycle is approximately 1600 F, which will necessitate a new technology for isotope encapsulation. Reactor Brayton systems are limited to the 1300 F reactor heat source temperature. Increasing this limit to 1600 F could only be achieved by a new reactor design from present SNAP 8 and 10B reactors.

This does not appear as likely as for an increased isotope heat source temperature. Overall development of the required conversion equipment is not as far along as that for the Rankine cycle. It is felt that additional development time will be required for this system, when compared to the Rankine cycle. Radiator area required for a 6 kWe system is approximately 850 ft^2. For higher power output, radiator area requirement may exceed available area, and deployed radiators would then be required. Meteoroid weight penalties will be great for such large radiator areas when considering missions going into the asteroid belt.

Rankine Cycle

Many working fluids were evaluated using the Rankine conversion cycle. While potassium offers the minimum weight system, its development is not sufficient for serious consideration. Only Dowtherm A and mercury appear competitive for the final selection. Dowtherm A systems operate at low enough temperatures where isotope technology is firmly established. The weights of these two systems are approximately the same and in the study mercury was taken to be representative of the Rankine cycle systems. Mercury offers a tremendous backlog of data through the SNAP 2 and 8 programs. It results in minimum radiator area. However, its temperature requirement is 1300 F, and this must compare to the 700 F of the Dowtherm A. From a development standpoint, the lower temperature system should result in minimum development risk and time. The turbine design is relatively simple to modify, since it is a single-stage design relying on nozzle inlet design for change in power output. The fluid, Dowtherm A, does suffer because of gaseous decomposition at temperatures in excess of 700 F with some decomposition down to 650 F. It is not expected that the decomposition would be in the form of "crud" as one expects in a mercury loop. The isotope development at 700 F is minimized. Existing isotope encapsulation techniques are adequate for this temperature. Final selection between these two working fluids must be made on an overall program level. Both appear to be acceptable on the subsystem level. Weight considerations will not be the deciding factor. Development cost and scheduling will have to be compared on the program level. Potential meteoroid damage to radiator areas will have to be assessed to determine the major advantage of the mercury system because of its sm~ller radiator area requirement.

Thermoelectrics

The advantages of a static conversion device cannot be overlooked. Thermoelectrics offer a relatively easy isotope hardware development for the power conversion. Unfortunately, they require high isotope temperature to maintain 1500 F on the hot junction to achieve reasonable efficiency. This high temperature imposes a major problem in the isotope encapsulation and development. The overall efficiency of this conversion will vary,

depending upon materials. Highest efficiencies can be realized by cascading GeSi and PbTe so that both operate at their best temperatures. This results in a cycle efficiency of from 7 to 8 percent compared to a single-element efficiency of 4 percent. At best the thermoelectrics will mean an increase in isotope inventory of about twice that for the dynamic conversion. This becomes a critical consideration when isotope availability and cost is considered. Radiator area requirement for the cascaded system is comparable with the Rankine Dowtherm A and is about double that required for mercury systems. Thermoelectrics represent a highly developed power conversion device and can be considered as a backup conversion to the dynamic CRU's, or for use with the planetary excursion module descent stage.

Solar Cells

Up to this point in the space program, solar cells are the state-of-the-art hardware which are both available and of possible application to the missions of this study. The major disadvantages of solar cells involve restraints on the total spacecraft configuration. For missions where zero g is adequate, the spacecraft can be pointing to the sun, and solar distances are less than 1.5 AU, solar cells are attractive candidates. Lightweight, large solar arrays needed for these missions, however, are not present-day technology.

Major problems of this system are the orientation requirement if an artificial-g configuration is chosen. Counterrotation and/or slip rings will be necessary at a reliability goal consistent with man requirements. A backup system of solar cells will be needed. Meteoroid damage assessments must be made to determine the allowable degradation of the solar array. This will then permit an evaluation of backup system designs. Earth and planetary orbital operations will be greatly complicated. Another source of power will be needed, unless deployment of the solar array is feasible prior to Earth orbit escape. Fuel cells could be included for the earth orbital phase, but this means additional weight, depending on earth orbital mission duration. This also means the complications of adding another power system and the problem of how to rid the spacecraft of this system before injection. If the array is deployed during Earth orbit, it means additional constraints on vehicle configuration. The array must be located so that there are no major interferences. In the stowed configuration, the solar array must be protected from any damage which could be caused by shock and vibration during launch. In the deployed configuration, the solar array rigidity must be sufficient so that the array can be oriented and maintained in a plane normal to the direction of the sun within ±10 degrees. The solar array

design must be compatible with the spacecraft. Spacecraft and array thermal interaction must be considered on a system basis. Structural design must be such that dynamic coupling with spacecraft guidance and control equipment is minimized and the vehicle mass center displacements are minimized. Clearances must be provided with the exhaust from attitude control jets and thrusters. No interferences can be permitted with antenna view angles and sensors and camera view angles.

Another major consideration of using solar cells will be that of changing solar intensity and panel temperature. As temperature drops, voltage of an individual cell increases. With a fixed number of cells in series to obtain required voltage, it is necessary to either continually change the number of cells in series or to accept a very wide range of voltage output from the array. Large voltage regulators will be required; fortunately, surplus power is available for the losses involved, but weight penalties of the regulators will result. The earth orbital operation will be in a 60-40 minute light/dark orbit, and larger batteries will be needed for the shadow period.

Planetary Excursion Module Power System

Fuel Cells

Fuel cells, like non-rechargeable batteries and chemical-dynamic systems, are energy limited. Wear-out mechanisms limit time of useful or active service. Chemical and electrochemical degradation limits active service time of electrodes, seals, and fuel entry ports. Heat rejection electromechanical pumps run continuously while the fuel cell is active, and malfunction and wear out as a result of electrical insulation breakdown, mechanical malfunction, and wear-out. Radiators can malfunction by loss of coolant fluid due to mechanical defects and impact by meteoroids. Fuel cells have strong advantages for short missions, typically one to three weeks, resulting in their acceptance for Gemini and Apollo missions.

Chemical-Dynamic Systems

The pulsed turboalternator chemical-dynamic system can be used most advantageously where the intended use is intermittent duty not to exceed an approximate cumulative total service time of 48 hours. The system is easily started, easily shut down, and requires very little monitoring.

If Aerozine-50 and nitrogen tetroxide are used as propellants for the reaction motors, separate storage tanks for the chemical dynamic system are unnecessary and a commonality advantage can be realized.

If the intended use is intermittent duty for short active durations not exceeding four hours each, total service time less than 48 hours, and a long space mission time of typically five years, the lightest system is chemical-dynamic.

Although the system has not reached space-qualification status, and quantitative reliability data are not available, expectations based on laboratory testing are that the system, if used intermittently, will be reliable, and complete module redundancy will not be required.

Electric Storage Batteries

Electric storage batteries are used in every space vehicle today and will be used to various extents in all future missions. Batteries can supply all spacecraft power for short missions or can provide power during emergencies, peak load conditions, or in connection with solar power source normal vehicle power during planetary occultation periods. Two basic kinds of batteries were considered in this study: silver-zinc and silver-cadmium batteries. The first type is presently used in primary batteries exclusively because of a high energy density. Silver-zinc batteries have a short activated storage life. Primary batteries require activation immediately before use. Manual activation was considered for this study. Secondary silver-zinc batteries have demonstrated activated storage life of six months to a year. Based on present-day technology, their performance is expected to be highly reliable for one-year missions by 1980.

Secondary battery life is a function of the number of charge-discharge cycles, depth of discharge, and rate of charge and discharge. For longer battery life, batteries are derated. Silver-cadmium batteries are not used as primary batteries. Their specific energy is only half as much as that for silver-zinc batteries. These batteries, however, have long activated life and are prime candidates for standby and peak power source. Nickel-cadmium batteries are not considered for this study; their specific energy is much lower. They would be applicable only for long-duration low-altitude earth orbital missions. New kinds of primary batteries now under development were also excluded due to lack of sufficient data and experience with them.

Selected Electrical Power Subsystems

An estimate of the electrical power loads was required prior to the selection of systems for use during subsequent module and system synthesis analyses. The estimated basic loads for the mission module are summarized in Table 58 based on the use of a partially closed (water and oxygen recovery) EC/LSS. The loads shown in the table do not include the requirements for

Table 58. Mission Module Load Analysis

Load Element	Crew Size			
	4	6	10	20
EC/LSS	2,500	3,500	5,000	9,000
Communications	2,000	2,000	2,000	2,000
Illumination	250	350	500	1,000
Instrumentation	150	225	350	450
Housekeeping & Misc.	500	600	750	1,000
Subtotal	5,400	6,675	8,600	13,450
Losses (Line) 3%	150	200	250	400
Total	5,550	6,875	8,850	13 850

contingencies or experiment support. Even with a crew size of twenty men, the basic loads are less that 15kWe which was considered to be within the range of applicability of the radioisotope systems.

The electrical power subsystems which were used in the manned modules during subsequent module and system synthesis analyses (Appendix D) are shown in Table 59. Reactor systems were not selected for use in the mission module since they are heavier than the isotope systems, could require shutdown and retraction during propulsive (or aerobraking) maneuvers, and present potential operational constraints (e.g., rendezvous). Solar systems were not assumed since they are not generally applicable to all missions considered in this study. Although solar systems are appropriate for some of the missions, large arrays (on the order of 170 m^2) would be required.

The isotope cascaded thermoelectric system was selected for use in the planetary excursion module descent stage since it is the most appropriate system for the range of stay times considered (0 to 60 days). Chemical-dynamic systems, fuel cells, and batteries would result in an excessive weight penalty for the longer stay times. Solar cells, although the lightest system, would impose operational constraints (e.g., landing site location), are not generally applicable, and could present significant design problems.

Only batteries were considered for use in the Earth reentry module and the planetary excursion module ascent stage. The short occupancy times (up to 24-hours) precluded the necessity of considering more exotic systems.

Table 59. Selected Electrical Power Subsystems

Module	Subsystem Type
Mission Module	Isotope/Mercury Rankine
Planetary Excursion Module Descent Stage	Isotope Cascaded Thermoelectric
Planetary Excursion Module Ascent Stage	Batteries
Earth Reentry Module	Batteries

REFERENCES AND BIBLIOGRAPHY

REFERENCES

1. Manned Mars and/or Venus Flyby Vehicle Systems Study, Contract NAS9-3499, SID 65-761 (June 1965).

2. Jagow, R. B., and R. S. Thomas. Study of Life Support Systems for Space Missions Exceeding One Year in Duration. Lockheed Missiles and Space Co., Report No. 4-06-66-6 (15 March 1966).

3. Report on the Design Requirements for Reactor Power Systems for Manned Earth Orbital Applications. Douglas Aircraft, DAC-57932 (September 1966).

4. SNAP Systems Capabilities. Atomics International, NAA-SR-11685 (December 1965), Confidential.

5. Design Study of SNAP 8 Compact Converter. Atomics International, NAA-SR-11984 (June 1966), Confidential.

6. Radioisotope Dynamic Electrical Power System Study for Manned Mars/Venus Missions. Atomics International, AI 65-6 (19 February 1965), Confidential.

7. Hedgecock, J. L., and G. E. German. Weight Scaling Factors for SNAP Reactor Shields. Atomics International, NAA-SR-TDR-11971 (June 1966).

8. Manned Planetary Flyby Mission Study, Phase II. NAS8-18025.

BIBLIOGRAPHY

Batteries

Cambridge Energy Review (Oct. 1966).

Cohn, E. M. "Toward Improved Primary Electrochemical Power Systems." Intersociety Energy Conversion Engineering Conference (1966).

Construction and Test Discharge of AgZn Pile (SYLPAK) Batteries. Yardney Electric, Report No. 414-64.

"Development of a silver-Oxide Zinc Primary "Pile" Battery for an Air Force Reentry Vehicle," Energy Conversion Digest (December 1966).

Eagle-Picher. Battery Performance Data Curves.

Eagle-Picher. Customized Batteries Pamphlet.

Lander, J. J. "Sealed Silver-Zinc Batteries." Space Power Systems Engineering. New York: Academic Press (1966).

Space Power Systems Advanced Technology Conference. Lewis Research Center (1966).

Vinal, G. W. Primary Batteries, New York: Wiley and Sonc, Inc.

Vinal, G. W. Storage Batteries, Fourth Edition, New York: Wiley and Sons, Inc.

Yardney Electric. Energy Data Book.

Chemical Dynamic Systems

Bipropellant Pulsed Energy Turboalternator Power System Development. Final Report to NASA (MSC), Contract NAS 9-4820. TRW E-R 6917 (August 1966).

Fuel Cells

Coffman, S. W., P. Fono, and C. L. Gould. "Advanced Fuel Cell Applications for Space Missions," paper reproduced in Space Power Systems Engineering, New York: Academic Press, Inc. (1966).

Cook, N.A. Allis-Chalmers Manufacturing Company, Milwaukee, Wisconsin. Hydrogen-Oxygen Fuel Cell System Design Parameters. Paper presented at the Third Annual Conference on Energy Conversion and Storage, Oklahoma State University (October 1965).

Elbel, R.E. and R.W. Jenkins, Jr., TRW Equipment Laboratories, Cleveland, Ohio Pulsed Energy Turboalternator Power Generation System. Paper presented before Intersociety Energy Conversion Engineering Conference, Los Angeles, California. (September 1966).

Fuel Cells. Allis-Chalmers (1966).

Fuel Cells. General Electric Company (1965).

Power Systems for Missiles and Spacecraft. Vickers, Inc., Bulletin A-5329 (1960).

Preliminary Definition Phase Apollo Extension System, Final Report. Allis-Chalmers, M660 1710 (January 1966).

Space Power Systems. G.C. Szego (April 1961).

Nuclear Reactor Systems

Design Study of SNAP 8 Compact Converter. Atomics International, NAA-SR-11984 (June 1966), Confidential.

Freedman, S.I. Study of Nuclear Brayton Cycle Power System, General Electric Co., GE65 SD 4251 (1965).

Gylfe, J.D. Nuclear Power Systems for Advanced High-Powered Communication Satellites. Atomics International, AI-66-305 (May 1966).

Hedgecock, J.L., and G.E. German. Height Scaling Factors for SNAP Reactor Shields. Atomics International, NAA-SR-TDR-11971 (June 1966).

Nuclear Power Systems for Lunar Exploration. Atomics International, AI-66-Memo-44 (April 1966).

Space Power Systems Engineering, Vol. 16. New York: Academic Press, (1966).

Study of Fast Nuclear Reactors, Pratt & Whitney Co., SNAP 50/SPUR.

Weisman, M., and D. Burgess. SNAP 2 Meteoroid Protection. Atomics International, NAA-SR-TDR 8098 (January 1963).

Radioisotope Systems

Effectiveness Studies - Alternate Missions, Douglas Report SM-46079 (September 1964), Confidential.

Laboratory Electrical/Electronic Systems - Alternate Power Systems, Douglas Report SM-46089 (September 1964), Confidential.

Luckow, W. K., and A.A. Nussberger. An Isotopic-Dynamic APU for the Self-Deploying Space Station. NAA S&ID, SID 62-1471 (January 1963).

Manned Mars and/or Venus Flyby Vehicle Systems Study. Final Report, NAA S&ID, SID 65-761-3-A (June 1965).

Nuclear Power Systems for Lunar Exploration. Atomics International, AI-66-MEMO-44 (18 April 1966).

Preliminary Design of a Pu^{238} Isotope Brayton Cycle Power System for MORL. Douglas Aircraft Company, Inc., MSSD (September 1965).

Preliminary Studies on an Isotope Fueled Biphenyl Power System. Denver: Sundstrand Aviation, Report No. 5652 (6 March 1964).

Solar Power Systems

Large Area Solar Array Design. 1st Quarterly Report. The Boeing Company, Aerospace Group, Space Division, D2-113355-1, Volumes I and II.

Nussberger, A.A. Power Systems Evaluation of Solar vs Isotope for Early Manned Mars and/or Venus Flyby Missions. NAA S&ID, SID 65-1115 (2 August 1965).

Power Generation, Storage, and Distribution for Manned Orbital Space Station. Lockheed California Company, Contract NAS9-1307 (December 1963).

Pietsch, A. "Solar Dynamic Power System Application to Manned Space Stations," IEEE Transactions, Vol. 2 (April 1964).

"Solar Power System Considerations," Proceedings of the Fifth Photovoltaic Specialist Conference. PIC-SOL 209/6.2 (January 1966).

Stafford, G. B., and E. T. Mahefkey, Jr. Hybrid Fuel Cell - Solar Cell Space Power Subsystem Capability. APL-TDR-64-111 (September 1966).

Sunflower Solar Collector. Thompson Ramo Wooldridge, Inc., NASA CR-46 (May 1961).

1.5 kW Solar Engine Design - Fabrication and Preliminary Testing. Denver: Sundstrand Aviation, Report No. 2-DER-64 (6 January 1964).

Thermionic converters

"An Engineering Evaluation of Advanced Nuclear Thermionic Space Power Plants," Space Power Systems Engineering. New York: Academic Press (1966).

Augrist, S. W. Direct Energy Conversion, Allyn and Bacon, Inc. (1965).

Hatsopoulos, G. N. "Thermionic Energy Conversion," Intersociety Energy Conversion Engineering Conference (1966).

Leovic, W. J. and C. Zelman Kamien. "Solar Thermionic Power Systems Development," Space Power Systems Engineering. New York: Academic Press (1966).

Rouklove, P. "Status Report on Solar Thermionic Power Systems," Space Power Systems Engineering, New York: Academic Press (1966).